DOCTOR OF PHILOSOPHY

Development of new diagnostic devices for TB

Ali, Hanan

Award date:
2015

Awarding institution:
Bangor University

Development of new diagnostic devices for TB

A thesis submitted to the Bangor University

for the degree of Doctor of Philosophy

by

Hanan M. Ali

2015

Declaration and Consent

Details of the Work

I hereby agree to deposit the following item in the digital repository maintained by Bangor University and/or in any other repository authorized for use by Bangor University.

Author Name: Hanan M. Ali

Title: Development of new diagnostic devices for TB

Supervisor/Department: Professor Mark S. Baird/ Chemistry

Funding body (if any):

Qualification/Degree obtained: PhD

This item is a product of my own research endeavours and is covered by the agreement below in which the item is referred to as "the Work". It is identical in content to that deposited in the Library, subject to point 4 below.

Non-exclusive Rights

Rights granted to the digital repository through this agreement are entirely non-exclusive. I am free to publish the Work in its present version or future versions elsewhere.

I agree that Bangor University may electronically store, copy or translate the Work to any approved medium or format for the purpose of future preservation and accessibility. Bangor University is not under any obligation to reproduce or display the Work in the same formats or resolutions in which it was originally deposited.

Bangor University Digital Repository

I understand that work deposited in the digital repository will be accessible to a wide variety of people and institutions, including automated agents and search engines via the World Wide Web.

I understand that once the Work is deposited, the item and its metadata may be incorporated into public access catalogues or services, national databases of electronic theses and dissertations such as the British Library's EThOS or any service provided by the National Library of Wales.

I understand that the Work may be made available via the National Library of Wales Online Electronic Theses Service under the declared terms and conditions of use (http://www.llgc.org.uk/index.php?id=4676). I agree that as part of this service the National Library of Wales may electronically store, copy or convert the Work to any approved medium or format for the purpose of future preservation and accessibility. The National Library of Wales is not under any obligation to reproduce or display the Work in the same formats or resolutions in which it was originally deposited.

Statement 1:

This work has not previously been accepted in substance for any degree and is not being concurrently submitted in candidature for any degree unless as agreed by the University for approved dual awards.

Signed …….. (candidate)

Date ……..

Statement 2:

This thesis is the result of my own investigations, except where otherwise stated. Where correction services have been used, the extent and nature of the correction is clearly marked in a footnote(s).

All other sources are acknowledged by footnotes and/or a bibliography.

Signed ……. (candidate)

Date …….

Statement 3:

I hereby give consent for my thesis, if accepted, to be available for photocopying, for inter-library loan and for electronic storage (subject to any constraints as defined in statement 4), and for the title and summary to be made available to outside organisations.

Signed ……. (candidate)

Date …….

NB: Candidates on whose behalf a bar on access has been approved by the Academic Registry should use the following version of **Statement 3:**

Statement 3 (bar):

I hereby give consent for my thesis, if accepted, to be available for photocopying, for inter-library loans and for electronic storage (subject to any constraints as defined in statement 4), after expiry of a bar on access.

Signed …… (candidate)

Date ……

Statement 4:

Choose **one** of the following options

a) I agree to deposit an electronic copy of my thesis (the Work) in the Bangor University (BU) Institutional Digital Repository, the British Library ETHOS system, and/or in any other repository authorized for use by Bangor University and where necessary have gained the required permissions for the use of third party material.	
b) I agree to deposit an electronic copy of my thesis (the Work) in the Bangor University (BU) Institutional Digital Repository, the British Library ETHOS system, and/or in any other repository authorized for use by Bangor University when the approved **bar on access** has been lifted.	
c) I agree to submit my thesis (the Work) electronically via Bangor University's e-submission system, however I **opt-out** of the electronic deposit to the Bangor University (BU) Institutional Digital Repository, the British Library ETHOS	

system, and/or in any other repository authorized for use by Bangor University, due to lack of permissions for use of third party material.	

Options B should only be used if a bar on access has been approved by the University.

In addition to the above I also agree to the following:

1. That I am the author or have the authority of the author(s) to make this agreement and do hereby give Bangor University the right to make available the Work in the way described above.

2. That the electronic copy of the Work deposited in the digital repository and covered by this agreement, is identical in content to the paper copy of the Work deposited in the Bangor University Library, subject to point 4 below.

3. That I have exercised reasonable care to ensure that the Work is original and, to the best of my knowledge, does not breach any laws – including those relating to defamation, libel and copyright.

4. That I have, in instances where the intellectual property of other authors or copyright holders is included in the Work, and where appropriate, gained explicit permission for the inclusion of that material in the Work, and in the electronic form of the Work as accessed through the open access digital repository, *or* that I have identified and removed that material for which adequate and appropriate permission has not been obtained and which will be inaccessible via the digital repository.

5. That Bangor University does not hold any obligation to take legal action on behalf of the Depositor, or other rights holders, in the event of a breach of intellectual property rights, or any other right, in the material deposited.

6. That I will indemnify and keep indemnified Bangor University and the National Library of Wales from and against any loss, liability, claim or damage, including without limitation any related legal fees and court costs (on a full indemnity bases), related to any breach by myself of any term of this agreement.

Signature: …… Date :

…….

Acknowledgements

To the people who they left their finger prints in my life and gives me the opportunity to continue …, with all my grateful to my supervisor Prof. M. Baird who offer me a chance to work with his group, I would like to say, Thank you…, and I would like to thank Dr. J. Al-Dulayymi with appreciate all his help and advice in the laboratory. Also, I would like to thank Dr. Chris Gwenin and his group for their cooperation in this study. Many thanks go to Dr. Alison Jones, Dr. Mark Pitts and Dr. Deiniol Pritchard for their help and advice. Thanks also to all friends in Professor Baird's research group. I am also grateful to all chemistry department staff especially my research committee (Dr. Martina Lahmann and Dr. Patrick J. Murphy). Special thanks to technicians Gwynfor, Dennise, Sam, Glyn, Mike, Nick and Secretaries Caroline, Tracey, Siobhan, Bryony. I am grateful to the government of Iraq, particularly the Ministry of Higher Education and Cultural Attaché for their support. Finally, I would like to thank my family and my kids Abdullah and Mohammed Al Mustafa for their support and patience**.**

Table of Contents

Abbreviations and Acronyms

Ab	Antibody
AFB	Acid-fast bacteria
AG	Arabinogalactan
Ag	Antigen
AIDS	Acquired immune-deficiency syndrome
BCG	*M. bovis strain bacille Calmette-Gue´rin*
BHIVA	British HIV Association
bTB	Bovine TB
CD1	Cluster of differentiation 1
CFP-10	Culture filtrate protein-10
DOTS	Directly Observed Treatment Short-course
DCs	Dendritic Cells
DMAP	4-Dimethylaminopyridine
EI	Electron impact mass spectrometry
ELISA	Enzyme Linked Immunosorbent Assay
EMB	Ethambutol
ESAT-6	Early secretory antigenic target-6
False+	False positive
False-	False negative
GC	Gas chromatography
GMM	Glucose monomycolate
GroMM	Glycerol monomycolate
HIV	Human Immunodeficiency Virus
(HIV-1) HXBc2	Full-length human immunodeficiency virus type 1
HPLC	High-performance liquid chromatography

Hsp60/lep	Heat shock protein of *M. leprae*
IFN-γ	Interferon gamma
IL-4	Interleukin-4
IL-6	Interleukin-6
IL-8	Interleukin-8
IL-10	Interleukin-10
IL-12	Interleukin-12
INH	Isoniazid
IR	Infrared spectroscopy
LAB	Lactic acid bacteria
LAM	Lipoarabinomannan
MA	Mycolic acid
MAC	*Mycobacterium avium complex*
mAGP	Mycolyl-arabinogalactan-peptidolycan complex
M. avium subsp.	*Mycobacterium avium subspecies Paratuberculosis*
MCP-1	Monocyte chemoattractant protein-1
M_D	Measured molecular rotations
MDR-TB	Multidrug-resistance TB
MHC	Major Histocompatibility Complex
MIP-1α	Macrophage inflammatory protein
M. tb	*Mycobacterium tuberculosis*
MTBC	*Mycobacterium tuberculosis* complex
MS	Mass spectrometry
NAD	Nicotinamide adenine dinuclease
NMR	Nuclear magnetic resonance
NTM	Non-Tuberculosis Mycobacteria
PG	Peptidoglycan
PIMs	Phosphatidic acid

PRA	PCR-restriction length polymorphism analysis
PZA	Pyrazinamide
RMP	Rifampicin
TB	Tuberculosis
TCH	Thiophene-2-carboxylic acid hydrazide
T1D	Type 1 diabetes
TDM	Trehalose dimycolate
TLC	Two-dimensional thin layer chromatography
TMM	Trehalose monomycolate
TNF-α	Tumor necrosis factor alpha
TST	Tuberculin Skin Test
VFA	Volatile fatty acids
WHO	World Health Organization
XDR-TB	Extensively drug-resistant TB

Abstract

The main objective of the work was to develop an analytical method for the diagnosis of human and bovine TB+ and para-TB by finding the best Ag with high Ab binding signal. This was achieved in five parts. First, the synthesis of *S,S-trans*-alkene-methoxy mycolic acid (**I**) from *M. tb* was achieved successfully. This led to the synthesis of its glycolipid derivatives (TDM, TMM, GroMM, GMM and ArM).

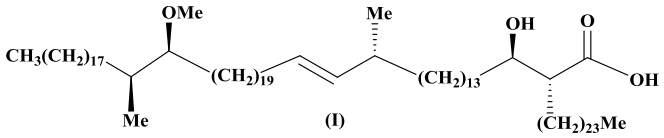

The second part was the analysis of a range of other synthetic Ags using TB+ and TB- human serum samples in ELISA assays. The best combinations of sensitivity and specificity were observed with TDM (**160**) (100 and 78%), ArM (**179**) (100 and 73%) and ArM (**158**) (100 and 86%). Combining the results from synthetic TDM (**160**), ArM (**158**) and GMM (**180**) gave 100 and 94% sensitivity and specificity. These represent very much better values than those reported with many recognised assays.

The third part involved the serodiagnostic evaluation of the sugar esters of MA (I). High biological activity was observed with TDM (**44**). This also gave high distinction between TB+ and TB- human serum samples, the best combinations of sensitivity and specificity (100, 73%) and high area under the ROC curve (0.929) in contrast with other derivatives.

The fourth part achived using four different sets of bovine serum samples, including one set of animals diagnosed with active bTB. Statistical analysis using multidimensional scaling (MDS) analysis and the Random Forest (RF) analysis showed that the ELISA assay can distinguish between different categories of serum sample. Combining the results from a set of Ags using mean decrease accuracy and mean decrease Gini illustrated that the synthetic Ags gave responses higher than the natural Ags. The best area under the ROC curves, sensitivity and specificity were observed with TDM (**156**) 0.959, 100 and 86 % respectively.

Finally, a range of antigens were studied in ELISA assays using serum from cattle infected with MAP.

Chapter 1

1. Introduction

1. 1 Tuberculosis

Tuberculosis (TB) is a chronic and ancient disease that infects humans, [1] caused by *Mycobacterium tuberculosis (M. tb).* It can be divided into two different types: pulmonary and extra-pulmonary. The first means the initial infection was in the lungs and the term extrapulmonary TB is used to describe the occurrence of TB at sites other than the lung. The most common sites of extrapulmonary TB are lymph nodes, genitourinary tract, pleura, bones and joints, meninges and the central nervous system, peritoneum and other abdominal organs. [2,3,4,5] The term TB comes from the word *tubercle*.[1] TB is a disease which kills about 3 million people annually around the world and accounts for about 25% preventable deaths and is thought to have killed more people than any other microbial pathogen[6,7] About 10 percent of people who contract TB become ill within three months. They experience chronic cough, chest pain, high fever and they expel sputum, the thick matter accumulating in the lower respiratory tract.[1] Often the sputum is rust-colored, signalling that blood has entered the lung cavity. The remaining 90 percent of victims exhibit no readily distinguishable symptoms, except malaise, fever and weight loss. In these cases, the body responds to the disease by forming a wall of white blood cells, calcium salts and fibrous materials around the organisms.[1] As these materials accumulate in the lung, a hard nodule called a *tubercle* arises and may become visible in the chest X-ray. Despite the body response, the bacilli are not killed, and the *tubercle* may expand as the lung tissue progressively deteriorates. In many instances the *tubercle* breaks apart and *bacteria* spread to other organs such as the bone, liver, kidney and meninges. The disease is now called miliary TB from the Latin milium.

1.2 Transmission

Usually, TB is transmitted through the air among people, especially those who suffer from an active infection, via coughing, sneezing, talking or spitting in their environment.[8] An infectious dose of TB is very small and the inhalation of just a single bacterium in one of these transmitted droplets can cause a new infection.[9] A big percentage of the infected population do not develop any symptoms, as the pathogen stays in a 'latent' form.[10] For those who do, the infection pattern

develops as follows; 2-4 % of patients develop the illness within a year. In the remaining patients, the infected cells will be surrounded by macrophages, B and T-lymphocytes and fibroblasts to form a granuloma, which seal in the infection.[11] This percentage of patients developing TB will rise to 33% in people that are infected with immunodeficiency virus (HIV) and the disease will develop within a maximum of 5 months.[12] HIV does, in fact, reactivate latent *M. tb* infection or facilitate TB progression in already infected patients.[13] TB is responsible for at least 25% of HIV deaths.[14] People living with latent TB infection and who are co-infected with HIV are 20 to 30 times more susceptible to developing an active TB.

1.3 The history of TB

1.3.1 The earlier period of disease

TB, one of the most prominent infectious diseases, has an ancient history in humans and animals since antiquity; it was believed that the first infected hominoid was observed in East of Africa but there was very little archaeological evidence from this period.[15] Early African hominoids began to leave Africa around 1.7 million years ago and it is thought that they took their diseases, including TB, with them. Analysis of Egyptian mummies more than 5000 years old shows evidence of the disease in early Egypt;[16] the depiction of deformities in figures as a result of contracting TB also confirms this.[16] There is evidence which shows the presence of TB in India 3300 years ago and China 2300 years ago.[17,18]It is thought that TB was established in the Americas before the arrival of European explorers, with similar evidence to that found in Egypt.[19,20] TB was also well documented in ancient Greece, where it was called phthisis and a treatment was devised by physician Clarissimus Galen of fresh air, milk and sea voyages.[18] Throughout the middle ages there is widespread archaeological evidence of TB.[20] TB was responsible for many deaths and it was not until 1819 when a group of French physicians, the most notable being Rene Theophile Hyacinthe Laennec who wrote *D'Ausculation Mediate*, outlined the physical signs of TB and its pathology.[20] During Laennec's era death rates in many Major European and American cities had reached 800-1000 in 100,000 deaths per year.[18,20,21,22]

1.3.2 The next 50 years

There were no advances in the knowledge of TB, until 1882 when Hermann Heinrich and Robert Koch gave their famous presentation on the *tubercle* bacillus and on their work to

postulate the link between a microbe and disease. More commonly known as the Koch-Henle postulates, they are still the standard explanation for how an infectious disease arises.[23,1] Koch was awarded the 1905 Nobel Prize in Medicine and Physiology for his work with TB. In 1890 Koch isolated a substance from *tubercle* bacilli which rendered the *bacteria* harmless. He named it tuberculin and in a demonstration he injected himself with it. He developed a fever and his body temperature was recorded at 39.6 °C, though he never developed TB.[24] After several years of research it was concluded that a positive reaction to tuberculin was caused by latent TB. Over the next 50 years more extensive research into tuberculin and latent TB showed that it was common for a large number of the population to be carriers of latent TB.[1,25,26] Since Koch's work a reliable vaccine has never been developed because TB immunity differs from immunity to many more common microbial` diseases.[1]

1.3.3 Effect of Bacillus Calmette-Guérin vaccine in the history of TB

It was not until 1921 that Albert Calmette and Camelle Guérin developed a vaccine from *Mycobacterium Bovis* (*M. bovis*) called Bacillus Calmette-Guérin (BCG).[27] Acceptance of the vaccine was slow as many people did not believe it to be safe, as it was based on live TB *bacteria*. The use of the vaccine took a significant blow in 1930, when there was a case in Lübeck, Germany where 240 infants under 10 days old were vaccinated and almost all developed TB, with 76 recorded deaths.[28,29,30] It was later discovered that the BCG sample used had been contaminated with a virulent strain, however this dealt massive damage to the acceptance of the vaccine and legal action was taken against the developers.[31] In the 1940's BCG had become more widespread, being used in Scandinavia, France, Spain, Russia, Latin America and some Eastern European countries.[32] Swedish Professor Arvid Wallgren[33] was one of the biggest supporters of the vaccine, and argued the case for its use in Germany. After the incident in Lübeck, the BCG vaccine had been banned in Germany and Wallgren highlighted the fact that, prior to the tragedy, regular vaccinations of infants in Gothenburg had reduced the mortality rate from 4 in 1000 to 1 in 1000.[34] However, in spite of the efforts of Wallgren and others, the vaccine was not accepted in Britain and the United States (US), with the Director of the Public Health Laboratory Service, Sir Graham Wilson, pointing out flaws in the evidence backing BCG in 1947.[35] In 1950 the opinion remained in the US that BCG was only needed in highly exposed or war-torn countries and as an emergency measure.[29] The decision whether or not to use to BCG vaccination was dependent upon how the evidence was interpreted as the data was insufficiently clear to fully accept or reject the vaccine.[28] However outside of Western

Europe and North America, the largest vaccination effort ever was undertaken by the World Health Organization (WHO) and United Nations Children's Fund (UNICEF), who decided to support BCG.[36] During the ninth UNICEF-WHO meeting in 1956 it was discussed whether the BCG vaccination efforts were actually effective and the chairman Professor Debré requested studies of the efficacy of BCG in underdeveloped areas.[37] By 1959 a report indicated that the value of the BCG vaccination was not clear. This may be interpreted as an admission that the degree of protection provided by the vaccination may not have justified such a large scale application.[38] The report included evidence from the first trials conducted by Aronson and Palmer on a population of 3000 North American Indians in 1936 which showed a reduction in mortality of 75 % over 15 years. Another study carried out in Britain on 50,000 infants showed similar success, although only in its fourth year in 1959. In contrast there were results from two trials on 200,000 Puerto Rican under 19's and on 65,000 individuals from two US communities in Georgia and Alabama, with protective success rates of 31 % and 36 % respectively.[38] The WHO suggested that the vaccine used in the trials which showed a low protective rate may have lacked potency and also that some individuals included in the survey may have had a low sensitivity to the vaccine. It was suggested that people with a low sensitivity were "associated with a considerable resistance to TB" and hence obscured the true protective properties of the vaccine. Several more reports were carried out over the next five years to justify the use of BCG, however in 1963 the WHO proposed a large-scale trial in India with the justification that although there were many anti-TB drugs available, none had been able to establish themselves and that BCG offered a cost effective method of dealing with TB.[39] In 1968, the trial in India, being carried out by the Indian Council of Medical Research in conjunction with the US Public Health Services and WHO, began. It was conducted over nine years on 360,000 people in the Chingleput district. The results were published in 1977 and to the surprise of the WHO they indicated that BCG showed no protective effects.[40] However the WHO did not abandon its policies regarding the BCG vaccine, but stated that several factors must be considered including the environmental and immunological characteristics of the population studied.[41] After the Chingleput trial, the WHO continued to back the use of BCG as a vaccine stating that "although BCG was not very effective from the epidemiological point of view, it was invaluable from the clinical standpoint for the prevention of severe and fatal forms of TB in children".[42]

1.3.4 The burden of disease

Like many other infectious diseases, TB has surged in great epidemics and then receded, where epidemics have been recorded during the 18th and 19th centuries in Europe and North America.[21] During the early to mid-19th century there was a noticeable decline in TB cases in Europe and North America; there are many hypotheses for this but none can fully explain the decline. In 2007,[43] there were an estimated 9.27 million cases of TB. As a comparison, there were 9.24 million cases in 2006, 8.3 million cases in 2000 and 6.6 million cases in 1990.

In 2009, 9.4 million new cases of TB were recorded, more than at any time in history.[44] Cases were spread throughout the world, with most in Asia and Africa, and smaller proportions in the eastern Mediterranean, the European region and the Americas, **Figure 1**. India, China, South Africa, Nigeria and Indonesia occupied the highest places in terms of the total number of cases.

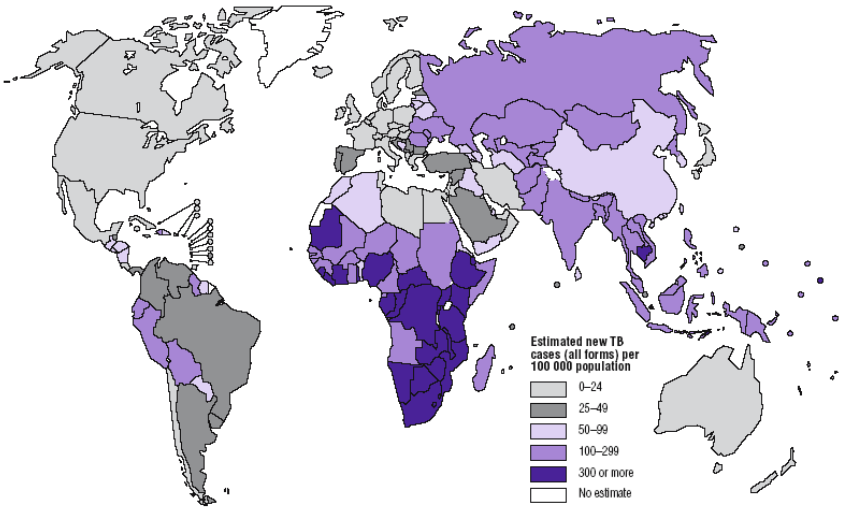

Figure 1: Estimated number of new TB cases per 100,000 population.[45]

From a recent WHO report on Global TB Control, it is estimated that in 2010 alone there were 8.8 million new cases of TB, with an estimated 1.45 million deaths.[46] An estimated 1.1 million (13%) of the 8.6 million people who developed TB in 2012 were HIV-positive. About 75% of these cases were in the African Region.

1.4 Treatment for TB

The first chemotherapy came in the form of the antibiotic streptomycin **(1)** in 1944. Streptomycin was first isolated from actinobacterium *Streptomyces griseus.*[47] The use of combination therapy to treat TB has been recommended by the WHO for over half a century. Its recommended first-line treatment for drug-susceptible (DS) TB consists of isoniazid (INH) **(2)**, rifampicin (also known as rifampin; RMP) **(3)**, ethambutol (EMB) **(4)** and pyrazinamide (PZA) **(5)**.[48] This combination is taken for two months. For the remaining four months of this Directly Observed Treatment Short-course (DOTS) regime, only isoniazid and rifampicin are taken. These drugs are used together to provide a multi-pronged sustained assault on bacteria. The aim is to kill all the bacteria infecting the host, as a single cell may give rise to drug-resistant strains. INH and EMB kill the bacteria by interfering with cell wall synthesis, while RMP, synthesised by the soil bacterium, *Amycolatopsis rifamycinica*, inhibits *M. tb* RNA polymerase.[49] PZA is able to kill bacterial cells hiding in the intracellular compartment of macrophages, see **Figure 2.**

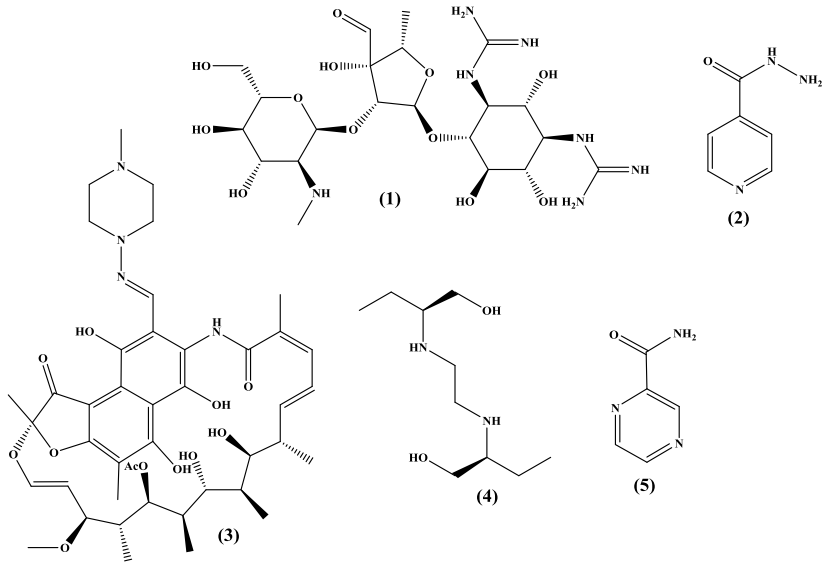

Figure 2: Molecular structures of first-line anti-TB drugs.[48]

The second-line drugs are for drug-resistant TB and for patients who cannot tolerate the first-line drugs; they are less effective, more toxic and require longer use than first-line drugs.[50] According to the WHO, in 2007 the overall success rate for TB treatment was 70 %.[51]

1.4.1 Multidrug-resistant TB (MDR-TB)

Multidrug-resistant TB shows high-level resistance to both isoniazid and rifampicin with or without resistance to other drugs.[52,53] The probability of resistance is much higher for less effective antitubercular drugs.[54]MDR-TB can occur during the treatment for fully sensitive TB, if a patient misses a dose, or does not complete the course, or if the doctor administers the wrong treatment.[55] The WHO estimates that each year 440,000 new cases of MDR-TB are emerging globally, and 150,000 patients with MDR-TB die.[56] For persons infected with *M. tb,* HIV infection is the strongest risk factor for the development of active TB, either drug-susceptible or drug-resistant, after *M. tb* infection.[1] As a result, the global HIV infection epidemic has increased the burden of TB in many countries. It has caused explosive increases in TB incidence and may be contributing to increased MDR-TB prevalence.

1.4.2 Extensively drug-resistant tuberculosis (XDR-TB)

Extensively drug-resistant TB (XDR-TB) is a form of TB caused by bacteria that are resistant to the most effective anti-TB drugs. XDR-TB is defined as TB that has developed resistance to the first line anti-TB drugs that define MDR-TB.[57] XDR-TB is associated with a much higher mortality rate than MDR-TB.[58] WHO estimates that 25,000 cases of XDR-TB emerge each year worldwide. XDR-TB has been transmitted to HIV co-infected patients and is associated with high mortality.[59] These observations warrant urgent intervention and threaten the success of treatment programmes for TB and HIV.[60]

1.5 Mycobacterium Tuberculosis

TB is mainly caused in humans by *M. tb* which can be seen in **Figure 3** below.[60,61] It is an aerobic and small rod-shaped bacillus, 1-4 x 0.3-0.6 µm in size, which divides every 16 to 20 hours. This rate of division is slower than that of most other *bacteria*.[62]

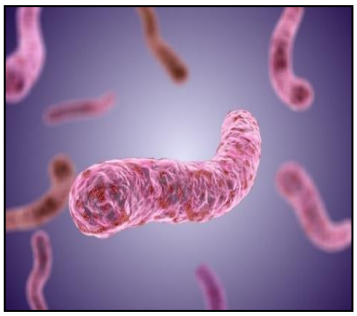

Figure (3): Scanning electron micrograph *of M. tb*. [63]

M. tb is classified as an 'acid-fast' gram positive bacterium. It is gram positive due to the lack of an outer cell membrane, and is 'acid-fast' because it does not retain methyl violet stain well.[64] The bacterium does however stain bright red in Ziehl-Neelsen stain, which is a test for acid-fast *bacteria.*[65] Since its complete genome sequence was solved in 1998, much more is now known and understood about the bacterium.[61]

1.6 Mycobacterium bovis

Mycobacterium bovis (*M. bovis*) is virulent for cattle but can infect other animals and humans causing disease; their pathology is similar to *M. tb*.[66] Both *M. tb* and *M. bovis* belong to the same complex known as the *Mycobacterium tuberculosis* complex (MTBC)[67] and their genome sequences are almost identical (greater than 99.95% similarity). *M. bovis* has a reduced genome size due to the deletion of genetic information.[68]

1.6.1 M. tb and M. bovis

Both *M. bovis* and *M. tb* are intracellular pathogens which are able to survive inside macrophages, where there is respiratory burst during infection.[69,70] Identification of *M. bovis* traditionally has been based on clear-cut differences in phenotypic characteristics and biochemical properties when compared to the other members of the MTBC.[71,72] In developing countries, information on human TB due to *M. bovis* is limited. However, human *M. bovis* infection was confirmed in African countries and recently in India.[73]There are reports describing the transmission of *M. tb* from human to cattle unequivocally confirmed by molecular typing of appropriate isolates involved in the transmission. High incidence (16/52) of cattle *M. tb* infection was confirmed in some cow herds in India. In the past decade, the cow population has been experiencing rapid expansion in China.[74]

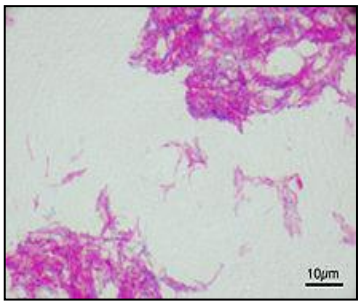

Figure 4: Attenuated strain of *M. bovis* used in the Bacillus Calmette-Guérin vaccine. [75]

M. bovis, which is seen in the **Figure 4**, infects cattle and can be transferred to humans through an infected cow's milk, raw meat or as an aerosol. [76] Bovine TB **(**BTB) is a chronic infectious disease caused by *M. bovis*, which affects cattle, [77] other domesticated species, wild animals and humans. [78,79] This disease causes economic losses in livestock farming and poses a health risk to the population that consumes products of animal origin. [80,81]

M. bovis shows a dysgonic (dysgonic bovine tubercle bacilli require for multiplication long chain fatty acids which can be supplied as oleic, palmitic or stearic acid whereas eugonic bovine strains can grow in the absence of fatty acid and can utilize glucose as a sufficient source of carbon) [82] colony shape on Lowenstein-Jensen medium, [83] is negative for niacin accumulation and nitrate reduction, is susceptible to thiophene-2-carboxylic acid hydrazide (TCH), and shows microaerophilic growth on Lebek medium. A further criterion used for differentiation is the intrinsic resistance to pyrazinamide, which is found in most *M. bovis* isolates. [84] In contrast, *M. tb* shows eugonic growth, is positive for niacin accumulation and nitrate reduction, is resistant to TCH, shows aerophilic growth on Lebek medium, and is usually not monoresistant to pyrazinamide.[84]

1.6.2 M. bovis and lactic acid bacteria

Lactic acid bacteria (LAB)[84] isolated from milk were put in milk cultures together with spiked *M. bovis*. Different LAB had different abilities to reduce *M. bovis* counts. LAB may inhibit pathogens in foods by producing antimicrobial peptides and/or acid, in addition to the competitive exclusion of pathogens.[85] Counotte and Prins suggested that there is a characteristic pattern to the changes that occur in the ruminal bacterial population at the onset of acidosis.[85] During the first few hours, excess fermentable carbohydrate causes a general increase in the growth rate of all ruminal bacteria. The production of volatile fatty acids (VFA) increases and causes a fall in ruminal pH. The decreased ruminal pH enables *Streptococcus bovis* (*S. bovis*)

[86] to outgrow other ruminal bacteria on the excess substrate that is present. Its tolerance of low pH allows this organism to proliferate, and lactate production rises. Increased lactate concentrations further depress ruminal pH and inhibit the growth of other ruminal bacteria. Then, as ruminal pH falls below 5,[85] the growth of *S. bovis* is inhibited and the very acid tolerant lactate-producing *Lactobacillus spp.*[85] predominate. Ruminal concentrations of lactate continue to rise, and the resultant low pH causes stasis of the fermentation, while absorption of D- and L-lactic acids into the bloodstream leads to metabolic acidosis and, in severe cases, death.[85]

1.7 Non-Tuberculosis Mycobacteria

Non-*Tuberculosis Mycobacteria* NTM, known as environmental *Mycobacteria*, are small, rod shaped bacilli which enter the human body through environmental sources such as natural water, soils, foods, and water pipes of the distribution system.[87] The reason for the survival of these bacteria in water pipes is their resistance to chlorine in water.[88] NTM species do not cause TB, but have the ability to cause other diseases to both humans and animals such as skin disease, disseminated disease, and pulmonary disease in HIV negative patients.[88] Unlike TB, NTM are not transmitted from one person to another, the organism being acquired exclusively from environmental sources.[89]The rate of worldwide NTM infection is increasing significantly. In the UK, the rate of all NTM reported cases increased from 0.9/100,000 to 2.9/100,000 persons between the years 1996-2006.[90] A report from Canada found an increase of pulmonary NTM cases from 9.1/100,000 in 1997 to 14.1/100,000 by 2003.[91] Similar reports also showed the prevalence of pulmonary NTM infection in other countries.[92,93] The failure to recognise NTM as pathogens of immense importance, when they are present, has resulted in slow recognition of these organisms as etiological agents of pulmonary disease. NTM are mostly identified on colony morphology, pigment production, growth rate, temperature preference, biochemical tests, serotyping and phagetyping.[94,95,96,97] These tests not only take a long time but also give unclear results because of the phenotypic variations among the different strains of the same species. Further, immunodiffusion and immuno-electrophoresis were tried but analysis was difficult because of the presence of cross reactive antigens (Ags).[98]

1.7.1 Mycobacterium avium complex

Mycobacteria included in the *Mycobacterium avium complex* (MAC) seen in **Figure 5** below, are classified as acid-fast, slowly growing bacilli that may produce a yellow pigment in the absence of light (exposure to light often intensifies pigment production).[99] MAC is a serological complex of 28 serovars (serotype) of two species, *M. avium* and *M. intracellulare*, which sometimes has been extended to include three additional serovars of a third species, *M. scrofulaceum*.[100] Therefore, the literature may include references to the complex as the *M. avium-M. intracellulare* complex or the *M. avium-M. Intracellulare-M. scrofulaceum* intermediate complex.[100] The distinction between *M. avium* and *M. intracellulare* is now well established, and Thorel *et al.*[101]have proposed three subspecies of *M. avium* on the basis of phenotypic properties and nucleic acid studies: *M. avium subsp. avium*, *M. avium subsp. paratuberculosis*, and *M. avium subsp. Silvaticum.*[101]

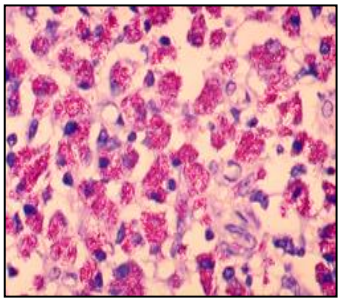

Figure 5: *M. avium* complex. [102]

Disseminated MAC disease was one of the first opportunistic infections recognized as part of the AIDS syndrome 20 years ago.[103] MAC includes both *M. avium* and *M. intracellulare*, which together account for the majority of disease-causing species of NTM in the HIV-infected patient. [104, 105] *M. avium-intracellulare* (MAI), [106] an acid–fast rod,[1] has been described traditionally as an opportunistic organism that causes disseminated disease in the HIV-positive population and acts as a pulmonary pathogen in patients with underlying lung disease such as chronic obstructive pulmonary disease (COPD) or previously diagnosed TB. [107]

Mycobacterium avium subspecies Paratuberculosis (MAP) is the causative agent of Johne's disease in cattle and may have implications for human health.[107] Johne's disease, is one of the most widespread and economically important disease of ruminants. It is a chronic granulomatous enteritis affecting primarily ruminants and many other species, [108] which is characterised by persistent diarrhoea, weight loss and a protein enteropathy, followed

eventually by death.[109] Most cattle are infected early in life by the ingestion of faeces, milk or MAP contaminated water. The relatively long incubation period is characterized by the excretion of MAP in faeces for months and years before clinical symptoms develop.[110] The exposure to contaminated faeces constitutes one of the main risk factors for MAP transmission within the herd. Infection control requires both herd management changes to limit fecal-oral infection spread and diagnostic testing to identify infectious adult cattle for segregation or removal.[111] Establishment of chronic infection by MAP depends on its subversion of host immune responses.[111] Recently, MAP has been associated with different autoimmune diseases such as Crohn's disease,[112] type 1 diabetes (T1D) and multiple sclerosis in humans.[112] Bovine paratuberculosis and TB are still a major concern in many countries and are responsible for heavy economic losses related to decreases in weight, milk production, and fertility. Additional costs include increased culling rates, diagnostic testing, and control measures.[113]

1.7.2 Mycobacterium kansasii

M. kansasii (**Figure 6**), is the second most common NTM after MAC to cause disease in HIV infected individuals.[114] It causes both pulmonary and extra-pulmonary infections.[115] In addition to chronic pulmonary disease resembling TB, the most frequent clinical presentation, *M. kansasii* can cause cervical lymphadenitis, dermatitis, osteomyelitis and arthritis.[115,116] In many ways, it is probably the easiest of the NTM pathogens to treat effectively. This stems from similarities between *M. kansasii* and *M. tb*,[117] especially the excellent activity of anti-TB drugs against *M. kansasii*. In fact, there is more data demonstrating the efficacy of anti-TB drugs for treatment of *M. kansasii* infections than for any other NTM infection.[117]

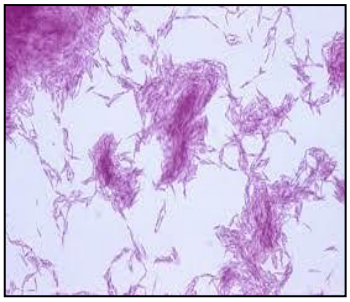

Figure 6: *Mycobacterium kansasii* (coloration de Ziehl).[118]

Infection by *M. kansasii* probably takes place via aerosols, although research has yet to confirm tap water as a major reservoir for *M. kansasii* causing human infection.[119] In fact, *M. kansasii* can be found virtually anywhere in the environment; these bacteria live in water, soil, foods and

a variety of animals. The organism has been isolated from tap water in the same communities as cases of identified *M. kansasii* disease.[119, 120,121]

M. kansasii infection of calves elicits specific responses that may confound the interpretation of BTB tests.[122] Disease management of *M. kansasii* infection is often complicated by the false interpretation of tests presumptive for *M. tb* complex, evoking further diagnostic and epidemiological investigations and action.[122]

1.7.3 Mycobacterium gordonae

M. gordonae is classed as a slow growing NTM,[123] first discovered by Ruth E. Gordon. *M. gordonae* is an acid-and alcohol-fast bacillus belonging to the II group of scotochromogenous *Mycobacteria*. [124] It is ubiquitous and commonly isolated from water, "tap water bacillus", soil and non-pasteurized fresh milk (**Figure 7**). [125] It was thought to be non-pathogenic, but recent reports showed cases of significant disease caused by *M. gordonae* infection such as pulmonary disease, disseminated infection, and genitourinary disease. [126,127,128] Infections are associated with skin, soft tissue, bone and joint and ocular diseases.[127,129,130]

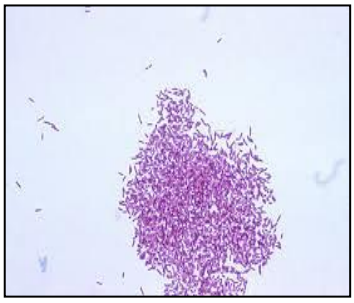

Figure 7: *M. gordonae* (coloration de Ziehl).[124]

M. gordonae in HIV-negative patients is rarely a pathogen, but in HIV-positive patients with a low CD4+ cell count, [131] it can cause significant disease and treatment is beneficial.
M. gordonae, one of the least pathogenic of the *Mycobacteria*, may infect the lungs, blood, bone marrow, and other organs.[126] Most cases of presumed infection have occurred in patients with trauma, underlying immunosuppression, or a prosthetic device.[123] Nevertheless, it is important to establish a timely diagnosis so that optimal treatment can be administered.[132] Also, reports indicate that *M. gordonae* was isolated from the blood of HIV infected patients and caused serious health complications.[133,134] Molecular-based methods for the rapid identification

of *M. gordonae* isolates have revealed genetic variability within this species. In contrast to other *Mycobacteria*, which show conservation of rDNA sequences at the species level, *M. gordonae* strains exhibit variation within a region of their rDNA; this is a common target for diagnostic species-specific probes.[135] The micro heterogeneity observed among strains of *M. gordonae* could be the reason for the hybridization problems reported by Walton and Valesco in1991 when using the Gen-Probe Rapid Diagnostic System (Gen-Probe). Studies using other molecular-based identification methods, such as PCR-restriction length polymorphism analysis (PRA), have concluded that *M. gordonae* is the most heterogenous member of the genus *Mycobacterium* studied to date.[136]

1.7.4 Mycobacterium fortuitum

M. fortuitum is a NTM, has been found in water and soil throughout the world.[137] It was first isolated from an amphibian source in 1905 and it has been considered a pathogen for both animals and humans since its first isolation from a human abscess in 1938 (**Figure 8**).[138] *M. fortuitum* group involving *M. fortuitum, Mycobacterium porcinium, Mycobacterium mageritense, M. fortuitum third biovariant complex, Mycobacterium abscessus and Mycobacterium chelonae* are species of rapidly growing *Mycobacteria* (RGM).[139]

The major types of disease caused by *M. fortuitum* include infections of postsurgical wounds, soft tissue, skin, and lung.[140] Occasionally reported infections include keratitis, endocarditis, lymphadenitis, meningitis, hepatitis, peritonitis and disseminated infections.[139,140] Deep organ involvement and disseminated infections occur in immunocompromised patients or patients with a comorbid condition and manifest both high mortality and high morbidity.[140, 141] Despite the severe degree of immunosuppression associated with AIDS, few *M. fortuitum* infections in patients with AIDS have been described in the literature.

Figure 8. Scanning electron micrograph of *M. fortuitum*.[142]

M. fortuitum is usually susceptible to most drugs used to treat TB.[143, 144] The studies of mycobacterial susceptibility testing were shown that *M. fortuitum* is a useful surrogate for *M.*

tb and the results of these studies in rapidly growing organisms correlate well with the results in *M. tb* and it has been used extensively for developing background data in structure activity analysis and computer modelling.[145]

1.7.5 Mycobacterium smegmatis

M. smegmatis as seen in **Figure 9** below, is a fast growing non-pathogenic *Mycobacterium* frequently used as a model system to study its pathogenic counterpart *M. tb. M. smegmatis* becomes dormant in low oxygen concentration conditions[146] and remains viable for over 650 days when it suffers carbon, nitrogen and phospho-starvation.[147] *M. smegmatis* was first discovered and isolated in 1884 by Lustgarten, and lives in aggregate layers of cells attached to each other in a community called a biofilm. It is found in water, soil and plants.[148]

Study of biofilms in *M. smegmatis* can aid in understanding biofilm formation in other pathogenic *Mycobacteria* like *M. tb*.[149] They may contribute to therapeutic failure by protecting the bacteria from effective penetration and action of antimicrobial agents and immune factors, consequently leading to inefficient clearance of pathogens, relapse of infection, and selection and propagation of drug-resistant *Mycobacteria*.[149]

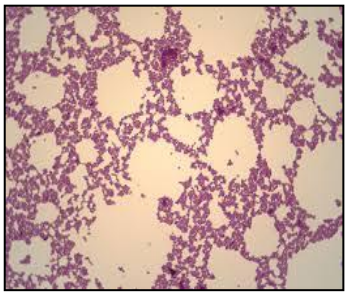

Figure 9: *M. smegmatis*.[150]

M. smegmatis has a number of properties that may make it an effective vaccine vector.[151]

1.7.6 *M. smegmatis,* BCG and HIV-1

Some *M. smegmatis* strains are non-pathogenic and (commensal) in humans.[151] Many bacteria live within our gastrointestinal tract, on our bodies or in the environment with which we come into daily contact without there being any resulting disease. In these situations, they are non-pathogenic and are called commensal bacteria, which means "eating at the same table."[152] Unlike other strains such as BCG that survive in host cells for months by inhibiting

phagosome maturation, *M. smegmatis* is rapidly destroyed by phagolysosomal proteases in the phagosomes of infected cells.[151] Nevertheless, it can induce cytokine production by macrophages better than pathogenic mycobacteria and can activate and induce the maturation of dendritic cells (DCs) better than BCG by up regulation of major histocompatibility complex (MHC) class I and costimulatory molecules. *M. smegmatis* can also access the MHC class I pathway for presentation of mycobacterial Ags more efficiently than BCG. Studies were initiated to assess the ability of recombinant *M. smegmatis* to elicit human immunodeficiency virus type 1 (HIV-1) envelope specific $CD8^+$ T-cell responses. Therefore, it was engineered as a vector expressing full-length (HIV-1) HXBc2 envelope protein.[151] Immunization of mice with recombinant *M. smegmatis* led to the expansion of major MHC I-restricted HIV-1 epitope-specific $CD8^+$ T cells that were cytolytic and secreted IFN-γ. Effector and memory T lymphocytes were elicited, and repeated immunization generated a stable central memory pool of virus specific cells. Importantly, pre-existing immunity to *M. bovis BCG* had only a marginal effect on the immunogenicity of recombinant *M. smegmatis*. This *Mycobacterium* may therefore be a useful vaccine vector.[151]

However, some studies have shown that *M. tb* and *M. smegmatis* have genomic similarities and, therefore, *M. smegmatis* has also been proposed as an appropriate model for studying the properties of these *Mycobacteria* in general.[153,154] Even though *M. smegmatis* is sometimes pathogenic to animals and humans under, it is generally considered to be a non-pathogenic species for the frog and the tissue culture model of infection. It is very useful for the analysis of other species in the genus *Mycobacteria* in cell culture laboratories.[153,154]

1.8 TB, HIV/ AIDS

It has been documented that patients who have contracted TB have an increased susceptibility to HIV, which is associated with proinflammatory cytokine production by TB granulomas.[155] One subset of CD4 T-lymphocytes is important in the control of intracellular bacterial infections.[1] The major cell infected by HIV is the helper T-lymphocyte that bears the CD4 receptor site (the helper T-lymphocyte is also called a CD4+ cell because it has the receptor site).[1] One HIV has attached to the CD4 receptor site and incorporated into the T- lymphocyte cytoplasm, the viral genome is released and, as with other retroviruses, a proviral state may occur since the person who is infected with HIV is probably infected forever. However, HIV

may infect other cells; these include certain cells in the central nervous system, megakaryocytes and the macrophage/ monocyte cell.[156] These cells also possess the CD4 receptor sites. The macrophage/ monocyte is thought to be an important reservoir for HIV. Findings from several studies suggest that active TB may accelerate HIV-induced immunologic deterioration.[157] The active TB is associated with transient CD4+ T-lymphocyte depression. Also, TB results in immune stimulation and the increased production of cytokines such as tumour necrosis factor (TNF) which increase HIV replication *in vitro*.[1] Moreover, HIV-infected patients with TB appeared to have a higher risk of opportunistic infections and death than HIV-infected patients with similar CD4+ T- cell counts but TB-.

In the conjunction between the two diseases HIV and TB,[1] each increases the rate of the other. HIV associated TB remains a major global public health challenge, with an estimated 1.4 million patients worldwide. Co-infection with HIV leads to challenges in both the diagnosis and treatment of TB.[158] In these patients the T-lymphocytes that normally mount a response to *M. tb* are being destroyed and the patient cannot respond to the bacterial infection.[1] HIV-infected patients face a mortality rate from TB of between 70 and 90 percent, usually within one to four months of developing symptoms. Unlike most other TB patients, those with HIV usually develop TB in the lymph nodes, bones, liver and numerous other organs.[1] It has been demonstrated that a person suffering from HIV and TB has a life expectancy of approximately two weeks and is about 20-40 times more likely to die from TB than a person who is infected with *M. tb* but is HIV-negative. [159,160,161] Also, TB is often the first disease to happen in the AIDS patient, before any often opportunistic diseases appear and it is generally more stubborn than in non-AIDS patients. The WHO estimates that 4.4 million people are co-infected with HIV and TB worldwide.[1] The dual epidemic is largely fuelled by the biological synergy that takes place between both pathogens, HIV and *M. tb*, within the infected human hosts.[162]

1.9 The Mycobacterial cell envelope

The cell envelope of *Mycobacteria* (**Figure 10**) is mainly composed of three structural layers: the plasma membrane (the internal layer), [163] the cell wall and the capsule (the external layer). The plasma membrane composition is typical of other types of living organisms. The capsule mainly consists of polysaccharides, proteins and lipids.[163] The composition of the plasma membrane remains similar to other living organism's lipid bilayer. It is composed of phospholipids derivatives from phosphatidic acid (PIMs). Other associated compounds are polyterpenes. The inner layer, overlaying the lipid bilayer is composed by peptidoglycan (PG),

consisting of long polysaccharide chains that give shape and rigidity to bacteria. N-Glycolylmuramic acid is linked in *β1→4* to N-acetyl glucosamine in alternating positions and cross linked to a four chain amino acids L-alanine, disoglutamine, meso-diamino-pimelic acid and D-alanine. The PG is linked to arabinogalactan (AG) by a phosphodiester bridge. The AG layer is composed of arabinose and galactose.[164]

The cell wall skeleton is composed of three covalently linked substructures: PG, attached to AG which in turn is attached to mycolic acids (MAs).[165] The junction of these three motifs is commonly known as mycolyl-arabinogalactan-peptidolycan complex (mAGP).[166] Most of these lipids assemble producing an asymmetric bilayer which is very thick. This reduces fluidity in the inner part of the bilayer, gradually increasing toward the outside.[167]

The Mycobacterial cell wall has a complex nature and very high lipid content. The cell walls contain between 30-60% (weight) lipids, including waxes, C-mycoside glycopeptidolipids, phenol glycosides, trehalose-containing lipopolysaccharides, sulfolipids, lipoarabinomannan (LAM), and MAs.[168] It is difficult to know the exact inner structure of the wall but the model proposed by Minnikin in 1982 and modified thereafter is usually accepted.[168]

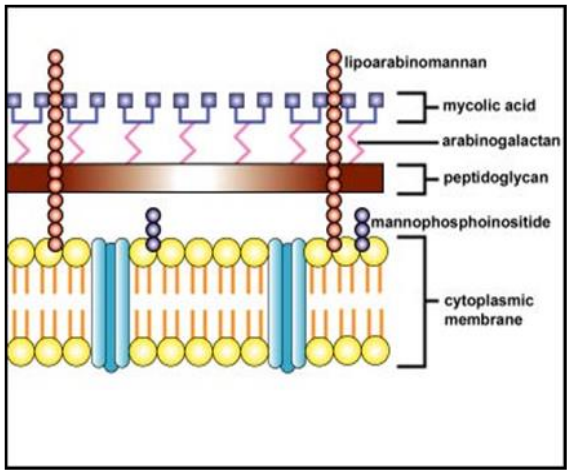

Figure 10: Schematic representation of the Mycobacterial cell wall.[169]

In particular, the *M. tb* cell wall, which plays a critical role in its intracellular survival, persistence, and pathogenicity, provides a rich source of diverse lipid Ags for immune recognition.[170,171,172] MAs, high-molecular-mass lipids, are presented as a components of the mycobacterial cell envelope, most of which are esterified to cell wall penta-arabinosyl units.[170,171,173]

1.10 Mycolic acids

1.10.1 Overview

MAs are long chain α-alkyl, β-hydroxy fatty acids, and were first isolated from *M. tb* by Anderson *et al*. in 1938. Anderson defined the 'mycolic acid' as the "ether-soluble, unsaponifable, hydroxy acids of the human tubercle bacillus".[174] Advances in analytical techniques have shown that what was once considered to be 'mycolic acid', a single component of *M. tb*, actually consists of a family of over 500 different MAs, which have closely related chemical structures.[175] MAs are now known to be characteristic of all *Mycobacteria*; however, these present in the different *Mycobacteria* vary in both the number of carbon atoms and also the functional groups present.[168] This made the isolation of a single component and the determination of its real structure extremely difficult. However, MAs have been the focus of constant study since their discovery, not only because they are unique to this type of organism but also because of their importance for the survival and virulence of the *Mycobacteria*.[170]

The first MA structures were published by Minnikin *et al* in 1967.[176,177,178,179] MAs consist of two characteristic parts; a saturated carboxylic acid part called the mycolic motif and a long fatty alcohol part called a "meromycolate" chain (**Figure 11**). The meromycolate chain of pathogenic *Mycobacteria* normally has two intra chain functional groups that vary in type, stereochemistry and spacing. Structures of various MAs from representative *Mycobacteria* have been characterized.[180,181] In models of the mycobacterial cell envelope proposed,[170, 182] MAs covalently linked to pentaarabinosyl residues of cell wall AG are arranged perpendicular to the cell wall, forming a highly structured monolayer. Computer simulations supported an arrangement of MAs as proposed in the model.[183] This outer leaflet of the mycobacterial cell envelope is considered to provide the cells with a special permeability barrier responsible for various physiological and pathogenic features.[184] Various other lipids in the mycobacterial cell envelope may also take part in the permeability function of the cell envelope as suggested.[170,185]

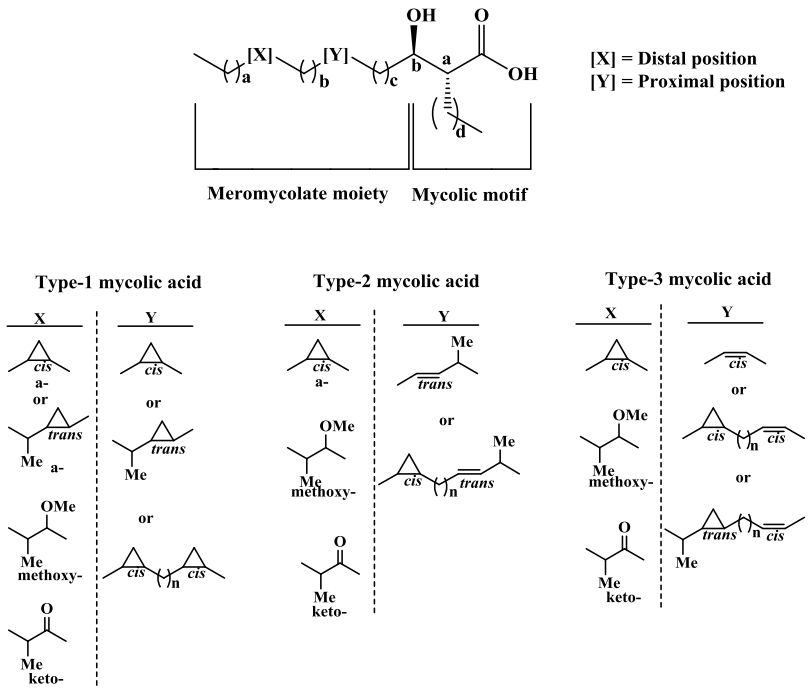

Figure 11: Typical Mycolic Acids.[186]

In the meromycolate moiety, the position labelled [X] is called the distal position and for MAs from *M. tb*, can contain double bonds, cyclopropane rings, methoxy or carbonyl functional groups while the position labelled [Y] is called the proximal position and can be either a double bond or a cyclopropane ring (**Figure 11**).[170,186] Two-dimensional TLC,[187,188,189] and subsequently GC[190] and HPLC,[191,192,193] in association with MS, IR, and NMR techniques, have permitted the identification of several kinds of MAs present in each *Mycobacterium*. HPLC patterns are also characteristic and have been used as a rapid tool for speciating *Mycobacteria*.[193]

Based on the nature of the functional group in the meromycolate chains, MAs from *M. tb* are categorized into three major groups: α-MA (**6**) with no oxygen-containing intra-chain groups, methoxy-MA (**7a** and **7b**) in which the distal group has a methoxy group and keto-MA (**8 a** and **8b**) in which the distal group has a carbonyl group. Methoxy-MAs and keto-MAs have methyl branches next to the oxygenated functional group and natural mixtures have both *cis*-cyclopropane and α-methyl *trans*-cyclopropane rings, as shown in **Figure 12** below.

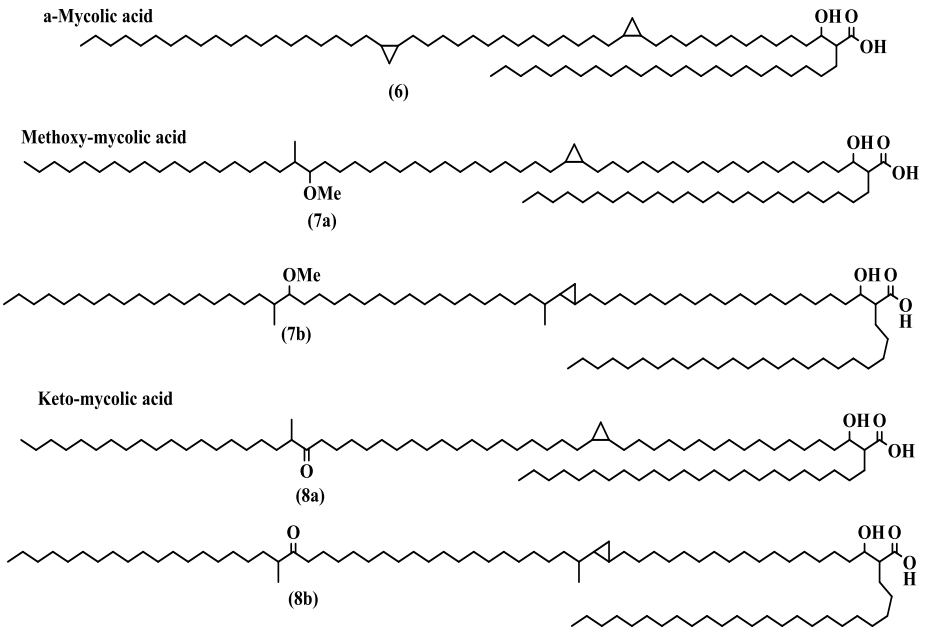

Figure 12: ***Major types of MAs from M. tb***

Other types of MA (**Figure 13)**, have been found in other species of *Mycobacterium*. *M. smegmatis* contains *α`* and α-MAs **(9)** and **(10)** with either one or two double bonds, either in the *cis* or the *trans* configuration.[194] *M. chelonae* contains α′-mycolates with a single *cis*-double bond and a small molecular size.[195,196] The epoxy-MAs **(11)**, with an epoxy ring were isolated from *M. fortuitum.*[175] ω-Carboxy-MA **(12)** have been isolated from *M. phlei*,[197] while ω-1-methoxy-MA **(13)** has been isolated from *M. alvei*.[198] *M. avium* contains a different oxygenated MA, called a wax ester **(14)**.[199] Hydroxy-MA **(15)** is a new type of MA which has been found in small amounts in *M. bovis* BCG, *M. smegmatis* and *M. tb.*[200,201]

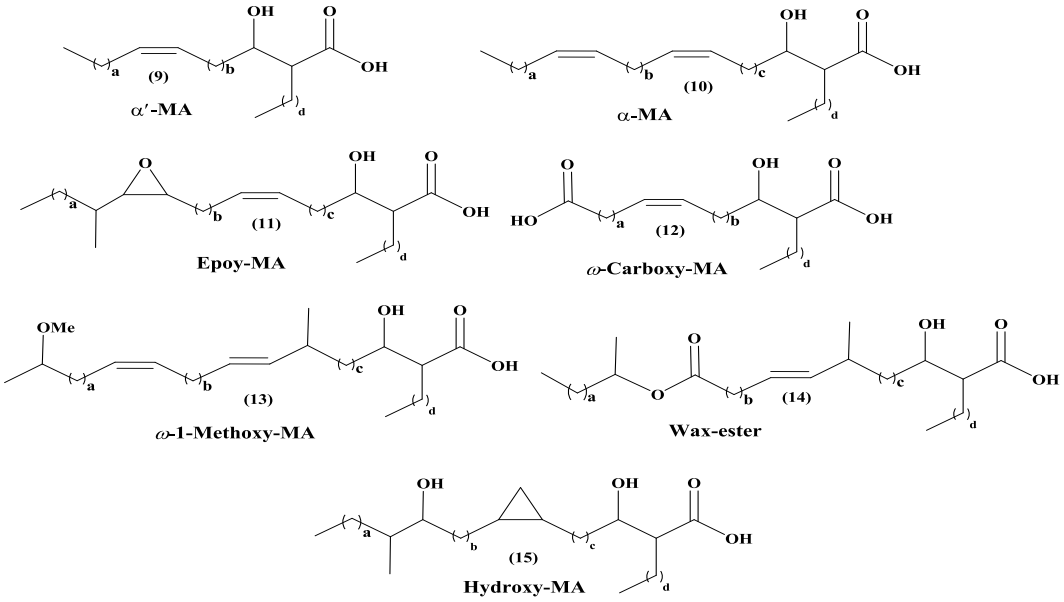

Figure 13: Types of MAs from other ***Mycobacteria***

In the past decades, electron impact (EI) mass spectrometry has been exhaustively used for the determination of the chain length of MAs and the location of functional groups.[201, 202,203] In particular, the positions the cyclopropane rings within mycolates were established.[181,202] However, EI MS studies on non-derivatized homologous mixtures of MAs do not give reliable information on the location of double bonds, cyclopropane rings and methyl branches.

Recently, MALDI-TOF spectroscopy has provided a rapid and highly sensitive analytical technique for analysis of MAs and other lipids. Initially, Laval *et al.* used MALDI-TOF spectroscopy to analyse the length of the total carbon chain of the major types of MAs of different *Mycobacteria*.[204] The nature and the location of the groups in the meromycolate chains of MAs from representative *Mycobacteria* have been studied extensively by ^{1}H NMR and MALDI-TOF spectroscopy by Watanabe *et al*.[204] Firstly, they separated the saturated, *cis* and *trans* methyl esters of the MAs into different types by argentation chromatography, according to the method of Krembel and Etémadi.[204]

The meromycolic acids were prepared by pyrolysis of the methyl ester, which was heated at 300 ˚C under a vacuum to give meromycolaldehydes and carboxylic acid methyl esters. Then, the meromycolaldehydes were oxidised to the corresponding meromycolic acids by using silver oxide, see **Scheme 1** below.

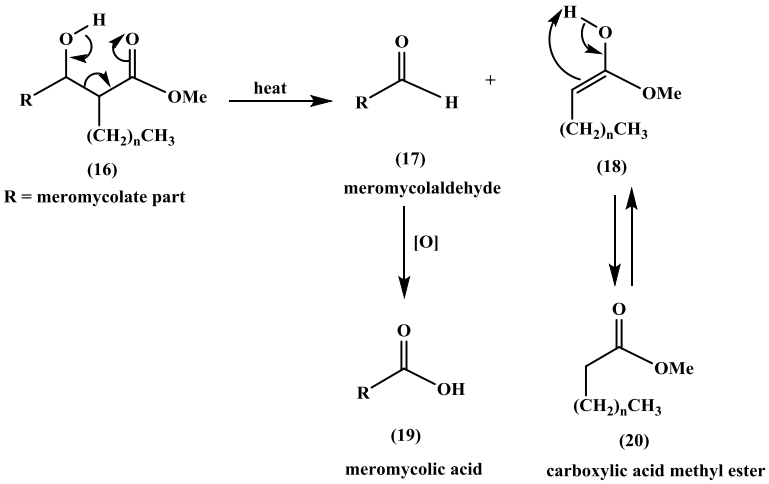

Scheme 1: Degradation of MA

The MAs were analysed using collision-induced dissociation mass spectrometry (CID MS) and over 50 different ones were found, divided into α-MA, methoxy-MA and keto-MA.[204]

1.10.2 Stereochemistry of MAs

The stereochemistry of the chiral centres in MA has still not been completely clarified. The α- and β-positions have been found to be both in the *R*-configuration for all MAs examined, irrespective of the groups in the meromycolate chain.[186,205,206] The (*R,R*)-configuration was confirmed first for the corynomycolic acids, see **Figure 14** below.[207] The formation of a hydrogen bond between the hydroxyl group and the carboxylic group has a stabilising effect for the aligned configuration between the two long chains.[208]

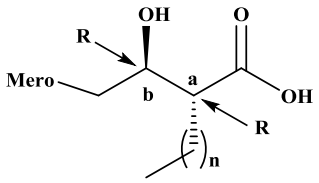

Figure 14: The chiral centres in the β-hydroxy fatty acid moiety

The configuration at these two chiral centres plays an important role in T cell recognition,[209] and the generation of an immune response by the host organism against pathogenic *Mycobacteria*; the same is true for the antitumour properties of MA derivatives.[210] Methoxy- and keto-MAs, the oxygenated series, are critical for the virulence of *Mycobacteria*.[211,212,213] It has been determined that slow-growing pathogenic *Mycobacteria* can manipulate the ratios between keto- and methoxy-MAs in order to adapt better to the environment. Dubnau *et al*,[213] using a mutant unable to produce oxygenated mycolates, verified the importance of these compounds for the permeability and fluidity of the cell wall.[213] Keto-MAs have an essential role in the growth of the organism within the natural host cell.[213]

In the case of *M. tb*, the exact role of each type in the pathogenesis of disease remains to be confirmed, but the oxygenated MAs have a particular influence on macrophage growth; strains lacking ketomycolates have a reduced ability to grow within THP-1 cells.[213,214] Moreover, the absence of keto and methoxymycolates leads to attenuation of *M. tb* in mice; the vaccine strain *Mycobacterium bovis* BCG-Pasteur lacks methoxymycolates.[213]

Recent studies suggested that, in the hydroxy (**21**), methoxy (**22**), and keto (**23**) groups in the MAs, the methyl branch adjacent to the oxygenated functions is in the *S*-configuration (**Figure 15**). The formation of the wax ester (**24**) is also believed to be via an enzymatic oxidation of the *S*-keto-MA.[215,216]

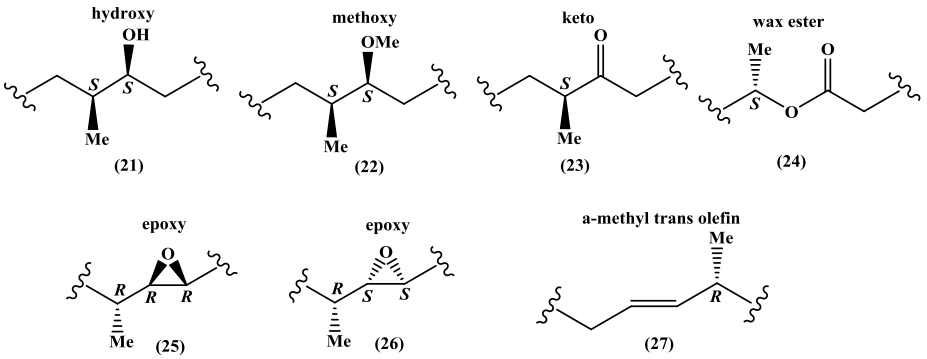

Figure 15: The stereochemistry of some chiral centres of the MAs

Reports identify the three stereocentres of the α-methyl-*trans*-epoxy MAs (**25**) as in the *R*-configuration.[217] Furthermore, the methyl branch next to the *trans*-double bond (**27**) is in the *R*-configuration in *M. aurum,*[218] *M. marinum* and *M. ulcerans.*[218,219]

The determination of the chiralities of this functional group has been derived through comparison with a simpler, established compound, and subsequent modelling of the extent to which additional chiral centres would have changed the degree of optical rotation of the entire molecule.[218] The configuration (*R* or *S*) of the functional groups in natural MA cannot be distinguished by using the many techniques, therefore, only polarimetry is available to determine specific rotations and relate these to particular stereoisomers. The stereochemical results have also been obtained by fragmenting MAs into smaller sub-units which could be compared with known compounds.[218]

Little is known regarding the non-oxygenated functionalities of MAs, particularly in the case of *cis*-cyclopropanes. The α-methyl of the *trans*-alkene unit, present in the MAs of the MTBC, is known to be in the *R*-configuration, see **Figure 16** below.[218]

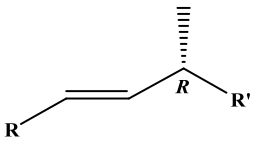

Figure 16: α-Methyl-*trans*-alkene mycolic acid configuration

However, a report discussed a synthetic strategy targeting multiple diastereomers of the α-methyl-*trans*-cyclopropane unit. After analysis of the optical rotation, ^{1}H NMR and ^{13}C NMR, in comparison with work carried out by Anderson *et al.*, Baird *et al.* deduced that the α-methyl-*trans*-cyclopropane unit is found in the *S,R,S*-configuration (**Figure 17**).[219,220]

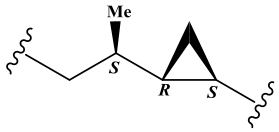

Figure 17: α-Methyl-*trans*-cyclopropane MA configuration

The configurations discussed above were deduced using measured molecular rotations (M_D), where M_D can be calculated from measured optical rotation and molecular weight of a compound. Interestingly, it is possible to calculate a theoretical value for a complete MA by adding the contributions from each chiral centre.[218]

The functionality present in the mycolate plays a role in the fluidity of the cell wall and its permeability.[221, 222] It is also known that α-mycolates occur in higher amounts than any other subclass of mycolate in *M. tb*, and that the presence of a cyclopropane ring plays a significant role in its pathogenesis.[223] The cyclopropanes of MAs are able to withstand oxidative environments better than their olefin counterparts, which would explain why they are in high abundance within *Mycobacteria*.[224] In the biosynthsis of *trans*-cyclopropane containing mycolates a higher proportion of oxygenated mycolates is recorded, which suggests that *trans*-cyclopropanes and oxygenated functionalities are biosynthetically related.[225]

Keto-mycolates have been shown to play key roles in the virulence and in regulating the fluidity of the cell wall of *M. tb*.[213] It is also known that slow-growing pathogens, such as *M. tb*, are able to manipulate the proportions of methoxy and keto-mycolates. This enables the pathogen to control the permeability of the cell wall; it is believed that it does this so that it is better adapted to its environment.[214] It is also known that keto-mycolates behave differently to α-mycolates when subjected to changes in pressure; where the α-mycolates are seen to be fully extended at high pressure, keto-mycolates do not extend to the same extent. Therefore it is believed that keto-mycolates play an important role in the permeability of the cell wall.[226] Loss of the methoxymycolates does not have an adverse effect on the pathogen's permeability and hence its resistance to therapeutic agents.[227]

The presence *cis*-olefins in the meromycolate chain has an effect on the packing of the mycolates in the cell wall, causing "a permanent elbow of about 120°", whereas *trans*-olefins do not cause as much disruption in the chain, leading to tighter packing of the mycolates.[197] Higher content of *trans*-olefins is seen if the *Mycobacterium* is grown at increased temperatures; this also suggests that the *Mycobacterium* regulates the production of olefins to favour a more rigid cell wall for additional protection from the external envinronment.[224] Further

understanding of the effects that functionality has on the fluidity and permeability of the cell wall may give an insight into possible anti-mycobacterial agents.

1.10.3 Biosynthesis of MAs

The biosynthesis of MAs has been investigated in great detail.[226,228,229] This work identified that most major functionalities in the meromycolate are derived from a common intermediate. This intermediate is generated using *S*-adenosyl-*L*-methionine (SAM) **(28)**. Methylation of a *cis*-olefin **(29)**, using SAM, gives the carbocation intermediate **(30)** (**Figure 18**).

Labelled SAM has been used so that the methylation and any subsequent reactions can be tracked. This has shown that the methyl group introduced occurs as a bridging methylene in *cis*-cyclopropanes, as methyl branches of *trans*-olefins and cyclopropanes, and the α-methyl branches of hydroxy, keto and methoxymycolates.[217,218, 230,231]

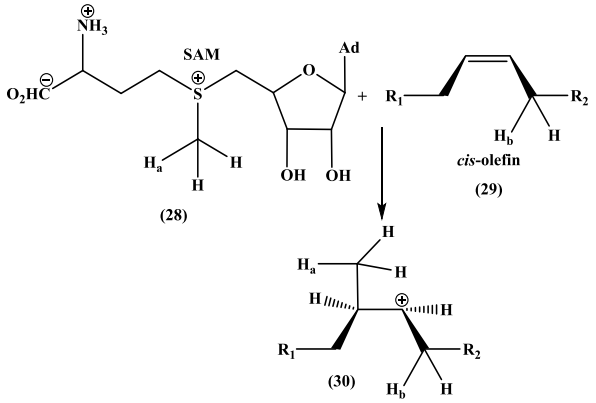

Figure 18: Formation of carbocation intermediate (30)

Deprotonation of the carbocation intermediate **(31)** may occur at two different positions, yielding two different products. If deprotonation of H_a occurs, a *cis*-cyclopropane **(32)** will result; conversely if deprotonation of H_b occurs then the *trans*-olefin **(33)** is formed. Further methylation of the *trans*-olefin, involving SAM, gives the *trans*-cyclopropane **(34)**. If the carbocation intermediate **(31)** undergoes a hydration reaction, the hydroxymycolate **(35)** is formed, which is a precursor for the biosynthesis of the corresponding keto **(36)** and methoxy-mycolates **(37)**, see **Figure 19** below.[175,214]

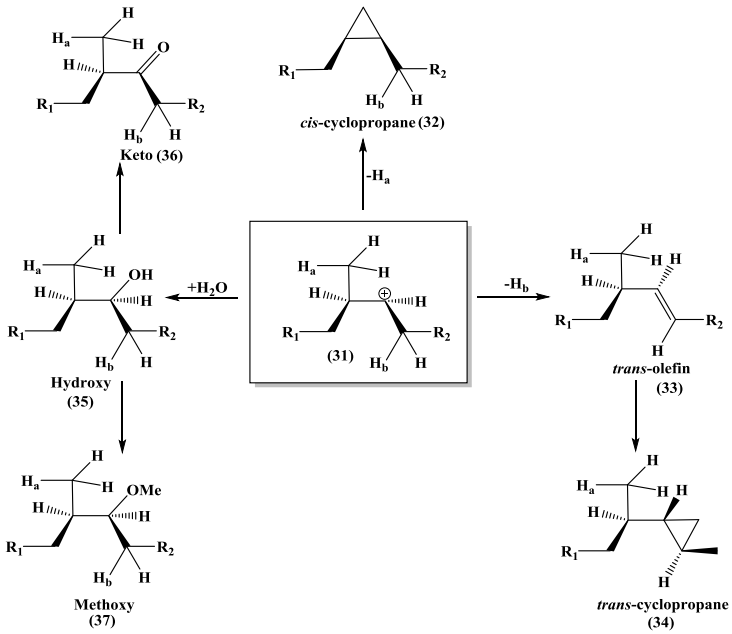

Figure 19: Biosynthesis of meromycolate functionality

In *M. tb*, the gene which is required for the biosynthesis of *trans*-cyclopropyl mycolates is active in the production of both keto and methoxy *trans*-cyclopropyl mycolates.[232] This confirms the hypothesized biosynthetic link between the different functionalities. As previously discussed, understanding the impact of individual functionality on virulence, cell wall fluidity and permeability, and how the different mycolates are naturally produced enables one to determine how to manipulate the cell wall of the pathogen, and thus provides a tool with which to combat disease.[233]

1.10.4 MA folding

Minnikin[233] and Draper[234] both stated that MAs are directly esterified to the arabinogalactan layer with the cell envelope, with the meromycolate chains in a linear configuration facing outward toward the outer surface of the cell. The MA chains are believed to be in a folded form, with the four alkyl chains occurring parallel to each other (**Figure 20**). [226,235,236]

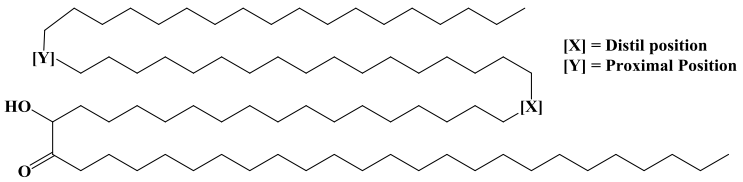

Figure 20: Proposed mycolic acid folding configuration

Watanabe *et al.*[181] and Hasegawa *et al.* [236, 237] discussed the changes which occur in the conformation of the alkyl chains when put under varying temperatures and pressure. This suggests that at low temperature and pressure the folded conformation observed above in **Figure 21**, is retained; as temperature and pressure is increased this linearity is lost. Grant *et al.*[237] suggested a possible reason for the stronger recognition by T cell receptors of oxygenated MAs. They suggested that keto and methoxymycolates fold in a way that allows the three polar functions of the lipid chain to be in proximity and to form an epitope, acting as a site for recognition within the immune system, see **Figure 21** below.

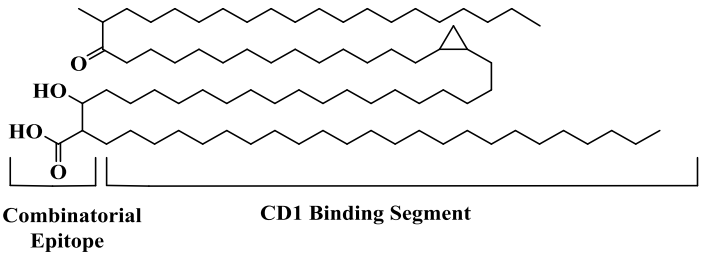

Figure 21: Modified from Grant *et al.* [238]

Villeneuve *et al.*[235, 238] discussed the changes which occur in the configuration of the alkyl chains when put under varying temperatures and pressure. This suggests that at low temperature and pressure the folded conformation observed above in **Figure 21** is retained, however as temperature and pressure is increased this folded conformation is lost.

Synthetic MAs may be utilised for the preparation of a simple model of the multi-layer structure present in the *M. tb* cell wall. This has been used to determine the relationships between monolayer properties and the chemical structures of different natural types of MA.[226,239] The importance of MA folding has been revealed by cryo-electron microscopy,[240,241] which showed the presence of a distinct mycobacterial outer membrane. To correlate with the dimensions of this outer membrane, folding of MAs is necessary.[241] MAs have been implicated in the pathogenicity and drug resistance of certain mycobacterial species.[242] They also offer potential in areas such as rapid serodiagnosis of human and animal TB. It is increasingly recognized that conformational behavior of MAs is very important in understanding all aspects of their function.[242] Atomistic molecular dynamics simulations, *in vacuo*, of stereochemically defined *M. tb* MAs show that they fold spontaneously into reproducible conformational groupings.[242] The keto-MAs behave very differently from either α-MAs or OMe-MAs, suggesting a distinct biological role.[242] However, subtle conformational differences between all the three MA types indicate that cooperative inter play of individual MAs may be important in the biophysical properties of the mycobacterial cell envelope and therefore in pathogenicity.[242] By using the

model of the W-fold,[235,238,243,244,245] and further considering structures whereby folding occurs specifically at the functional groups of the MAs, three general conformations, termed W, U and Z folds, can be defined. These conformations reflect the four-, two- and three-chain descriptions, respectively, found in monolayer studies. The innate ability of MAs to fold spontaneously into WUZ-conformations (**Figure 22**), even as single molecules in vacuum, is supportive of findings from mono-layer studies.[235,238,243,244,245]

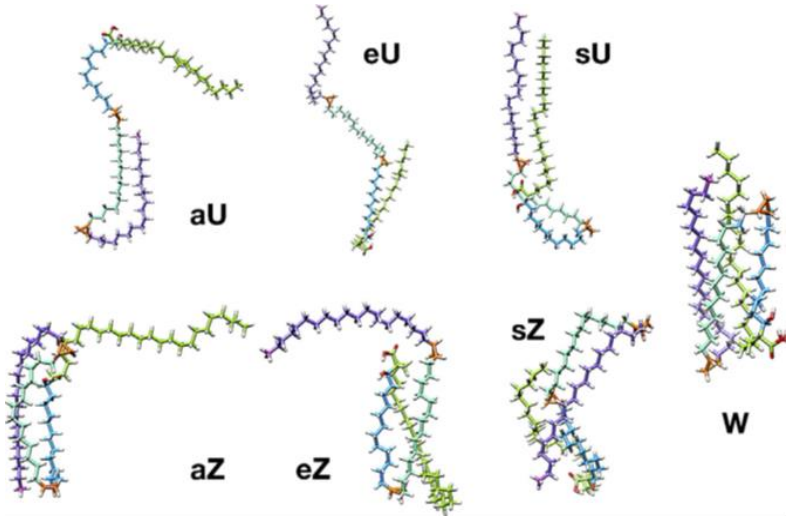

Figure 22. Representative 'WUZ' folds for α-MA 1. Prefixes "a" (aU, aZ) and "e" (eU, eZ) are used to describe conformations when a- and e-terminated chains are unfolded, while 'symmetrical' conformations have "s" as prefix (sU, sZ).[242]

The recent demonstration that MA folding is facilitated by α-methyl *trans*-cyclopropane groups rather than cis-cyclopropane units has provided a partial explanation.[242] Additional understanding of the importance of having parallel series of oxygenated MAs would be gained from the application of computational studies to a selected range of MAs, varying in chain lengths and functional group content.[242] In particular, it would be most informative to study the developing portfolio of synthetic MAs, with known absolute stereochemistry by computational methods and direct physical approaches, such as Langmuir monolayers.[242]

1.10.5 MA Derivatives

MAs are generally present as penta-arabinose tetramycolyl clusters bound to the cell wall or as non-bound species such as sugar esters, usually trehalose di- or mono-mycolate (TDM and TMM), glucose monomycolate (GMM) or glycerol monomycolate (GroMM). These species exert a number of very important immunological effects.[246]

1.10.5.1 Cord factors

Cord factor, also known as trehalose dimycolate TDM, is trehalose esterified at both primary alcohol positions with MAs (**Figure 23)**.[247] TDM, which constitutes a major part of the mycobacterial cell wall, was identified as the most immunogenic glycolipid and is produced predominantly by virulent *M. tb* as well as by atypical *Mycobacteria*.[248]

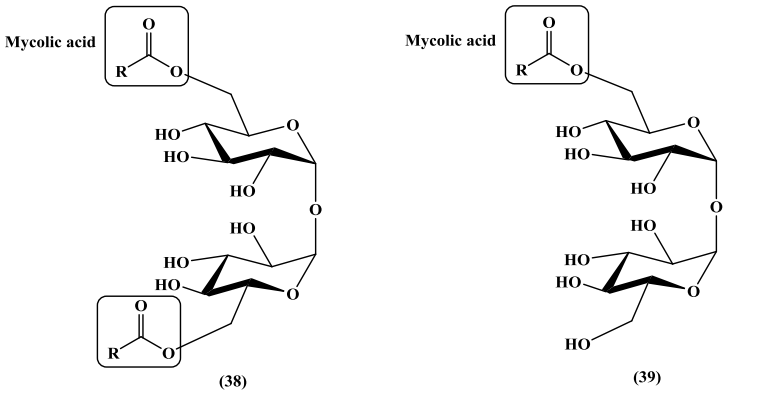

Figure 23: Generalised structures of cord factors (TDM and TMM)

MA-containing glycolipids, in particular TDM, show a number of immunomodifying effects.[249] They stimulate innate, early adaptive and both humoral and cellular adaptive immunity. Most functions can be associated with their ability to induce a range of chemokines (MCP-1, MIP-1α and IL-8) and cytokines (IL-12, IFN-γ, TNF-α, IL-4, IL-6 and IL-10). As a structural component of TDM,[250] MAs with different modifications and chain lengths can impact on its toxicity and other biological functions.

TDM toxicity is due to an increase of the tissue specific nicotinamide adenine dinuclease (NAD) activity decreasing the levels of NAD in several tissues by blocking the electron flow along the mitochondrial respiratory chain and thus oxidative phosphorylation.[166,175,251] During infection and when inside the phagosome, *M. tb* is shown to produce large quantities of TDM.[252] From many studies, it is remarkable that TDM induces lung granulomas and has immune-stimulating properties[253] that are probably at the origin of its antitumoral activity.[248,254] TDM has also been shown to have adjuvant properties generating an optimal Ab response,[255] and a non-specific immune response against bacterial and parasitic infections.[256,257,258,259] Recent studies indicate that TDM is actively participating in blocking mycobacterial phagosome maturation.[260] Inhibition of the phagosome maturation is observed after phagocytosis of virulent strains of *M. tb*, allowing the bacillus to survive within the phagocyte.[261] Recently, Mincle (macrophage-inducible C-type lectin expressed in myeloid cells)[262,263,264] on the macrophage surface, has been

shown to recognize *M. tb* TDM, and working together with the Fcγ receptor transmembrane segment induces pro-inflammation. [265,266]

A monoester of trehalose linked at the 6-position with MAs (trehalose- 6-monomycolate) was isolated from the wax D fraction of virulent human *M. tb*,[267] and its biochemical action on host-cell mitochondria was studied. TMM showed a delayed toxicity for mice. It induced *in vitro* a swelling of mouse liver mitochondria and uncoupled respiration and phosphorylation in the NAD pathway of the electron transport chain.[267] The site of functional damage was located specifically at coupling site II. Mitochondrial adenosine triphosphatase (ATPases) was slightly stimulated by TMM. These findings indicate that TMM affects mitochondrial oxidative phosphorylation in a similar manner to, but to a lesser extent than, TDM of *M. tb*.[267] The diverse immune activities of TDM and TMM indicate multiple biomedical applications. Thus they show positive effects against a range of cancers, [268,269] and may be of relevance for wound healing and hair growth.[270]

TMM (**Figure 23**) is a precursor in TDM biosynthesis and plays a role in the transfer of MAs onto the cell wall AG. AG is attached to peptidoglycan PG through a unique linker unit, and in turn is acylated at its distal end to PG with MAs.[271] Analysis of TMM by MALDI mass spectrometry has been reported.[272] Al Dulayymi *et al*. also reported the first synthetic cord factor in 2009, with the method used by the group being modifiable to produce cord factor or TMM from any MA synthesised.[251] As with MAs, the synthesis of single isomers of TDM and TMM compounds allows the antigenic properties of each of these, and any combination thereof, to be investigated.

1.10.5.2 Glucose monomycolate

It was proposed that the TDM can also be converted into GMM inside the host.[273] GMM, a glycolipid consisting of MA attached to the 6-position of glucose,[274] is present in numerous bacterial species including *Mycobacterium*, *Rhodococcus* and *Nocardia* (**Figure 24**). Environmental *Mycobacteria* express TDM on the surface of their cell wall but fail to biosynthesize GMM because of very limited availability of glucose.[275] The mechanism of reciprocal regulation of TDM and GMM involves competitive substrate selection by antigen Ag85A.[275] This is an isoform that is preferentially expressed in macrophage-resident *Mycobacteria*;[275] its catalytic potential for the TDM-GMM exchange could affect macrophage functions if TDM and GMM have differential ability to activate the cells. The switch from TDM

to GMM biosynthesis occurs near the physiological concentration of glucose present in mammalian hosts. Isamu *et al*., demonstrated that GMM is produced *in vivo* by *Mycobacteria* growing in mouse lung and establish an enzymatic pathway for GMM production.[275] They provide a specific enzymatic mechanism for dynamic alterations of cell wall glycolipid remodelling in response to the transition from non-cellular to cellular growth environments, including factors that are monitored by the host immune system.[275]

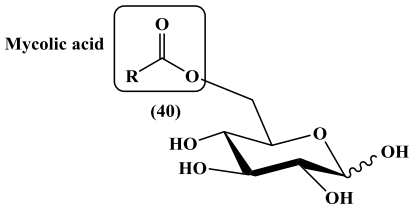

Figure 24: Example of synthetic GMM

Mycobacteria are unable to synthesise GMM outside the host cell since a non-*Mycobacterium* source of glucose is needed. Therefore, GMM is only produced by a pathogenic *Mycobacterium* after infection of the host cell.[209] T cell recognition of GMM was mediated by the T cell receptor (TCR) and was highly specific for the precise structure of natural GMM produced by *Mycobacteria*,[209] including the glucose moiety, the linkage of glucose to the mycolate, and the stereochemistry of the mycolate lipid. These results indicate that T cells are capable of extremely precise discrimination of the hydrophilic cap of the Ag that likely functions as a classical TCR epitope by directly contacting TCR variable regions.[209] Mycobacterial production of antigenic GMM absolutely required a non-mycobacterial source of glucose that could be supplied by adding it to media at concentrations found in mammalian tissues or by infecting tissue *in vivo*.[209] *Mycobacteria* synthesize antigenic GMM by coupling mycobacterial mycolates to host-derived glucose.[209] The TCR of the human T cell line LDN5 recognizes GMM of different mycobacterial species that only differ in their lipid tails.[276]

1.10.5.3 Glycerol monomycolate

GroMM (**Figure 25**), another mycolate-containing lipid species produced by *Mycobacteria*, can stimulate innate immune cells and produce inflammatory cytokines.[277] It is found among different *bacteria* of the *Corynebacterium*, *Mycobacterium*, and *Nocardia* (CMN) group.[278] Similar to TDM and LAM, GroMM also appears to directly stimulate innate immune cells to produce inflammatory cytokines.[278] A recent study pointed to a direct degradation pathway for TDM by means of enzymatic hydrolysis,[279] resulting in the accumulation of free mycolates that

was associated with the increased influx of nutrients, including glycerol.[280] Given that glycerol is ubiquitously present in host cells and *Mycobacteria* can readily utilize exogenously-derived glycerol for the production of GroMM,[281] GroMM may potentially predominate over TDM during the course of infections.

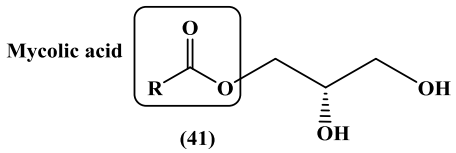

Figure 25: Example of synthetic GroMM

Recent evidence has suggested that GroMM,[281] can stimulate innate immune cells; however, its specific host receptors have yet to be identified. Yuki *et al.*, showed that cell transfectants expressing human Mincle (hMincle) reacted to both TDM and GroMM, while those expressing mouse Mincle (mMincle) only reacted to TDM and failed to recognize GroMM.[281]

1.10.5.4 Synthetic fragments from Arabinogalactan

The mycolyl-arabinogalactan complex (mAG), is the largest component structure in the cell wall of *Mycobacteria* and is located directly outside the PG. It is believed that mAG acts as a permeability barrier that prevents the passage of antibiotics.[282,283,284,285] mAGP is essential for cell wall integrity and mycobacterial survival;[286] its biosynthetic enzymes represent valid targets for several first line and second line antitubercular drugs, including INH, ethionamide, and EMB. INH and ethionamide inhibit enzymes required for MA synthesis, whereas EMB inhibits arabinosyl transferases involved in assembly of the arabinan domain of mAGP.[286] The arabinans and galactans of mycobacterial cell walls consist of D-arabinofuranose (D-Araf) and D-galactofuranose (D-Galf),[287] and the synthesis of these rare sugars alone presents opportunities for new chemotherapeutics; indeed, the mode of action of EMB, a first-line drug in the treatment of TB, involves inhibition of the synthesis of the D-arabinans.[288]

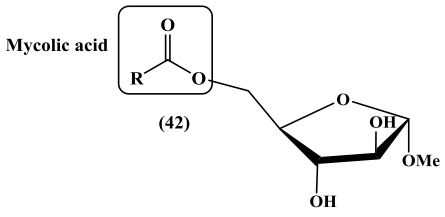

Figure 26: Example of synthetic fragment from Arabinogalactan

The chemical structure of arabinose mycolate obtained from human tubercle bacillus strain Aoyama B was established as D-arabinose-5-mycolate,[289] The glycolipid, D-arabinose-5-mycolate, was purified from bound lipids of *Mycobacteria*. The significance of this glycolipid

in the chemical structure of the cell wall and wax D was discussed. The hypothetical chemical structure of MA-AG portion of cell wall and wax D was proposed.[289]

Also, Mannose-containing glycolipids, including the phosphatidylinositol mannosides (PIMs) and their hyper mannosylated derivatives, lipomannan (LM) and lipoarabinomannan (LAM) are a major class of cell-wall glycolipids in all *Mycobacteria*.[290] The PIMs, LM and LAM are thought both to be incorporated into the plasma membrane and to be exposed on the cell surface. There is a large body of evidence to suggest that the PIMs and LAM can act as ligands for host-cell receptors and contribute to the pathogenesis of *M. tb*.[290]

1.11 CD1, T cells and Glycolipids

T lymphocytes participate in host defense against microbial pathogens, including *M. tb*, the causative agent of TB.[291, 292,293] During *M. tb* infection, both conventional and unconventional T cells are stimulated. Conventional T cells use an αβ TCR and recognize peptide Ags presented by major histocompatibility complex (MHC) II or MHC I Ag-presenting molecules on antigen presenting cells (APCs). Unconventional T cells include γδ TCR cells specific for mycobacterial phosphorylated ligands and CD1-restricted αβ TCR cells recognizing mycobacterial lipid Ags.[291,292,293] The CD1 family of proteins is made up of nonpolymorphic, transmembrane-anchored Ag-presenting molecules that associate non-covalently with β2-microglobulin.[294]

Five CD1 proteins (CD1a, b, c, d, and e) are expressed by human cells. CD1a to CD1d have Ag presenting functions, whereas CD1e facilitates glycolipidic Ag processing.[295] CD1-restricted T cells are activated in the course of *M. tb* infections.[209,296, 297, 298] Although *in vivo*[280] data in animal models are only preliminary,[299, 300] CD1-restricted T cells have been indicated to contribute to protection during infection because they kill intracellular pathogens and secrete proinflammatory cytokines, which in turn promote macrophage bactericidal activity.[297] These studies have highlighted lipids of the mycobacterial envelope as key determinants of host immune response.[280] Thus, mycobacterial lipids are now considered to be a novel class of antigens that could be used in subunit vaccine formulations.[280] Two CD1 isoforms, CD1b and CD1c, present mycobacterial lipid and glycolipid Ags to specific T cell subsets, including $CD4^-$ $CD8^-$ and $CD4^-$ $CD8^+$ T cells.[297]

Conventional CD4+ and CD8+ T cell responses recognizing peptide Ags presented by polymorphic MHC class II and I molecules, respectively, play key roles in immunity to *M. tb* and are targeted by current vaccine and immunodiagnostic strategies. [301] However, unconventional T cells that recognize non-peptidic Ags in an MHC-independent fashion are also implicated in immunity to *M. tb*.[302] Current TB vaccine strategies are largely aimed at activating conventional T cell responses to mycobacterial protein Ags. MA-specific T cells were predominant in TB patients at diagnosis, but were absent in uninfected bacillus Calmette-Guérin–vaccinated (BCG-vaccinated) controls.[302] These T cells were CD1b restricted, detectable in blood and disease sites, produced both IFN-γ and IL-2, and exhibited effector and central memory phenotypes.[302] MA-specific responses contracted markedly with declining pathogen burden and, in patients exhibited recall expansion upon Ag reencounter *in vitro* long after successful treatment, indicative of lipid-specific immunological memory. T cell recognition of MA is therefore a significant component of the acute adaptive and memory immune response in TB.[302]

CD1-restricted T cells contribute to protection during infection because they kill intracellular pathogens and secrete proinflammatory cytokines, which in turn promote macrophage bactericidal activity.[296] These studies have highlighted lipids of the mycobacterial envelope as key determinants of host immune response. Another two studies have shown that *M. tb* lipids used to vaccinate guinea pigs improve the pulmonary pathology.[300] These promising initial vaccination experiments also support the development of novel subunit vaccines priming immunity against mycobacterial lipid Ags.

Cell wall MAs from *M. tb* are CD1b presented Ags that can be used to detect Abs as surrogate markers of active TB,[303] even in HIV co-infected patients. Interestingly, a recent computational study of the binding of a model methoxy-MA glucose ester to the human MHC class I like molecule CD1b using a *R,R*-configuration for the α-methyl-*β* -methoxy unit shows a close fit to the shape of a non-functional natural mycolate.[304] The same paper reports a similar good fit for a model α-MA having a distal cyclopropane with an *S,R*-configuration. Other crystal structures give indications of the nature and geometry of the active site in related enzymes,[305,306] with no modelling of bound mycolates. A further study[307] is reported to show the fit of a putative α-mycolate containing a distal α-methyl-*trans*-cyclopropane and a proximal cis-cyclopropane to the CD1 receptor, but the actual fit appears to be with a structure having the methyl group one carbon removed from the *trans*-cyclopropane and with the second cyclopropane having *trans*-geometry.[307]

Glycolipids play a major role in biological processes such as signalling, [308] cell-cell communication, and molecular recognition. In particular, a number of the glycolipids that bind to CD1 have been identified.[308] The therapeutic role of glycolipids that modulate the immune system via interactions with CD1 and subsequent T cell activation is still in its infancy. However, much progress is being made in understanding CD1-glycolipid- T cell binding and this has the potential for use of the glycolipids in the treatment of diseases. [276]

GMM is known to be presented to human T cells by CD1b.[276] The TCR of the human T cell line LDN5 recognizes GMM of different mycobacterial species that only differ in their lipid tails. The cocrystal of human CD1b with GMM shows that both acyl chains are buried in the Ag binding groove, leaving the glucose moiety exposed on the surface of the CD1 molecule available for recognition by the TCR, explaining why one TCR can recognize GMM from different sources. Thus, GMM-specific T cell activation is not just a property of LDN5,[209,297] but is common among polyclonal lymphocytes of humans infected with *M. tb.* The biological significance of this in the context of mycobacterial infection derives from the observation that GMM is neither self nor foreign, but instead a combination of a self-carbohydrate and a foreign lipid that are coupled only after successful infection of host tissues by *Mycobacteria*. Subsequently, GMM, was also shown to be presented by human CD1b molecules,[309] and the crystal structure of the GMM-CD1b complex underscored that the acyl chain of GMM fitted tightly in pockets and a tunnel elaborated in human CD1b molecules, leading to the assumption that CD1b-bound MAs constitute a scaffold for mycolate-containing (glyco) lipids stimulating CD1b-restricted T cells.[278]

GroMM is presented by CD1b in a CD1e-independent manner,[278] by DCs infected with *M. tb*. GroMM specific T cells are detected in the circulating blood of PPD-positive healthy donors but not in that of patients with active TB. GroMM-specific, CD1b-restricted T cells have been detected in the circulation of patients with latent, but not active TB.[278]

Specific CD1b-mediated T cell recognition of an Ag produced by the interaction of host and pathogen biosynthetic pathways provides a potential immune mechanism for recognizing and responding only to those *Mycobacteria* that have productively infected host tissues.[283]

1.12 Detection of Tb

One of the biggest challenges facing clinicians is the time it takes to accurately diagnose TB.[301] Currently it takes on average 4 weeks to diagnose TB, which leads to a delay in treatment of

the disease. Two thirds of TB deaths could be prevented by early diagnosis. The diagnosis requires a high index of clinical suspicion, as detection by conventional methods is difficult. Most cases of presumed infection have occurred in patients with trauma, immune-suppression, or a prosthetic device.[301] Nevertheless, it is important to establish a timely diagnosis so that optimal treatment can be administered.[301,310] Therefore, with fast diagnosis, patients could be put on anti-TB therapy immediately and become non-infective within a few days. With the current methods of diagnosis, patients with persistent symptoms have to remain in quarantine for several weeks while awaiting the results. During this time, they can infect the medical staff, their next of kin or anyone with whom they share a closed area, such as in public transport. With MDR and XDR TB on the increase, this threatens to spread an almost incurable disease among hospital staff and the communities that can be fatal within 2 months. The need for a fast, reliable diagnostic tool for TB is therefore high, especially in high HIV incidence populations.[311] Currently, there are five main methods approved by the WHO for detecting active TB or latent TB; namely cell culture; [312,313] smear microscopy;[313] skin test;[314] interferon-γ release assay;[314] and nucleic acid amplification test.[315]

1.12.1 Cell Culture

Cell culture is considered the 'gold standard' for detecting active TB and is the only method that can definitively diagnose a patient as being TB positive (TB+).[316] It involves growing *M. tb* cultures from sputum on media. Traditionally, diagnosis was done using Lowenstein-Jensen media or Middlebrook media for culturing *M. tb*; however development in the area has led to quicker culture growth using BACTEC medium, without losing accuracy of results. Even though this method can identify whether a patient is infected with TB, it can take 3-8 weeks for the cultures to grow.[314, 317] There are three main reasons why cultivating the Mycobacteria should be undertaken:

- This method is much more sensitive than smear microscopy and has a limit of detection of approximately 10 bacilli/ml of sample.[318]
- Culturing the *Mycobacteria* allows testing for drug susceptibility.[314]
- Growth of the *Mycobacteria* is required for specific species classification.[314]

Culture is considered the 'gold standard' for detection of active TB, and has a specificity[319] of approximately 98 %; specificity is the proportion of 'true' negative samples correctly identified

by the assay, but the sensitivity is the percentage of 'true' positive samples correctly identified, see the two equation below.

$$\textbf{Sensitivity} = \frac{\textbf{Number of the } (+ve) \textbf{ detectied}}{\textbf{Actual number of } TB+ve} \textbf{x } 100 \ldots..(1)$$

$$\textbf{Specificity} = \frac{\textbf{Number of the } (-ve) \textbf{ detectied}}{\textbf{Actual number of } TB-ve} \textbf{x } 100 \ldots..(2)$$

It was reported that the cell culture method only has a sensitivity[320] of 80-85 %.[321] In real terms, this means that in 15-20% of the cases where a person does have active TB, this test diagnoses them as TB negative (TB-).

1.12.2 Sputum Smear Microscopy

Sputum smear microscopy is a rapid and inexpensive test for the detection of acid-fast bacteria (AFB) and is considered the most important method for diagnosing pulmonary TB in low-income and middle-income countries.[322] Usually, samples are stained with Ziehl-Neelsen stain and the amount of AFB present in the sample is quantified. However, in higher income regions aruamine-rhodamine staining is more common, as it increases sensitivity.[323] The staining process itself can be performed in less than an h, leading to results being available much quicker than for cell culture.[323] The main disadvantages of this method are:

- It detects all AFBs and not specifically *M. tb*, so a positive result indicates the occurrence of Mycobacteria in the sample, but not necessarily *M. tb*.[315]
- For extra-pulmonary TB, samples need to be collected from different areas of the body, such as obtaining cerebrospinal fluid (CSF). However, the sensitivity of this test, for this type of TB, can vary between 10 % and 90 %.[324]
- Another drawback is that its limit of detection is between 5,000 and 10,000 bacilli/ml of sample, compared to approximately 10 bacilli/ml for cell culture.[313]

However, sputum smear microscopy is a much quicker method than cell culture. Reports claim a high specificity of 91 – 100 % but sensitivities ranging from 50 – 80 %.[313,322]

1.12.3 The Tuberculin Skin Test

There are currently two types of Tuberculin Skin Test (TST) that are used for the detection of *M. tb* infection, the Mantoux test and the Heaf test. The Mantoux test is the most widely used,

especially after the Heaf test was discontinued in countries such as the UK in 2005. [313, 325] This method involves the injection of tuberculin purified protein derivative (tuberculin PPD), isolated by protein purification from tubercle bacilli, into the patient's skin and reading the 'lesion' in 2 to 3 days.[313]

Unlike cell culture, this method is used to detect latent TB (with is defined as a condition where a person has been infected with *M. tb*, but do not show any TB symptoms[326]); however it cannot distinguish between latent TB infection and active TB disease.[327] A major disadvantage of this method is:

- Can give both false positive (Fal.+) and false negative (Fal.-) results. Fal.+ results can be obtained for patients who are infected with *Mycobacteria* other than *M. tb*, patients who have been vaccinated with BCG vaccination and also from repeat testing with this method, while Fal.- results can be obtained for patients with compromised immune systems, such as those infected with HIV. [313,328, 329,330,331,332] The results largely depend on the interpretation by the person observing the lesion, due to it relying on the lesion size. This can lead to discrepancies from person to person measuring, which can lead to misdiagnosis of the patient.[328,329]
- AIDS patients often test negative for the TST because without T-lymphocytes they cannot produce the red welt that signals infection.[1]

These combined effects lead to reported sensitivities of between 57% and 100%,[333,334] with specificities of 93 – 100% in non-BCG vaccinated countries,[335] but specificities ranging from 35 – 79% in BCG vaccinated countries.[336 ,337] As opposed to active TB, where cell culture is used as the gold standard, and samples are compared against the results of this assay, there is no 'reference assay' for detecting latent TB, therefore no assay to which the results can be compared to determine sensitivity and specificity accurately.[327] This leads to sensitivity and specificity values generally being quoted as a range, with a set confidence interval.[327]

1.12.4 Interferon-γ Release Assays

Interferon-γ release assays (IGRAs) are a relatively new method used for the detection of *M. tb* infection, however they are quickly becoming more popular, with the QuaniFERON-TB Gold and T-SPOT.TB test kits both being commercially available.[327] This method works based on the fact that interferon-γ will be secreted from white blood cells in response to them coming into contact with TB Ags, ESAT-6 and CFP-10, if the patient is infected with *M. tb*. The interferon-

γ can then be quantified by ELISPOT or ELISA.[338,339] As with the TST, IGRAs detect both latent and active TB and cannot distinguish the two.

Although this method has some advantages over the TST, it also has some drawbacks.[327,339] The main benefits are that results can be obtained within 24 hours; no Fal.+ results occur if the patient has been previously vaccinated with the BCG vaccination, and the method does not depend on the reader's interpretation, which can lead to variability with the skin test method.[339,340,341]

The disadvantages of this method are:

- The serum samples must be properly stored and processed within 12 hours of collection, or the accuracy of the test diminishes.
- Although the method is reported to be able to detect latent and active TB,[327,339] there is some uncertainty as to its performance in detecting active TB, as it has also been reported that it is not yet certain if it can detect TB once it has become active, as it is reported that active TB is known to suppress interferon-γ (IFN-γ) response.[340]
- There is limited clinical and laboratory experience with this assay, which leads to it not being recommended for children under the age of eighteen or pregnant women due to the lack of information and insufficient data. Further studies are required in order to determine whether it can be recommended for these people.[314,339,340]

The QuantiFERON-TB Gold assay has reported sensitivities of 55 – 93%,[334,342] and specificities of 89 – 100%,[343] while the T-SPOT.TB assay has reported sensitivities of 80 – 100%,[344,345] and specificities of 85 – 100%.[334,339] As with the TST, these values for sensitivity and specificity are only approximate and do contain errors, due to there being no 'gold standard' for the detection of latent TB.[227]

1.12.5 Nucleic Acid Amplification Tests

Nucleic acid amplification tests (NAATs) are a rapid test for pulmonary TB, with one of the most common being the Amplified *M. tb* Direct Test (MTD).[315] Briefly, NAATs work by releasing nucleic acids from Mycobacteria through sonication before heat denaturing is carried out to disturb the ribosomal RNA's (in the case of MTD) secondary structure. The ribosomal RNA is then amplified and a single-stranded DNA sequence, modified to contain a

chemiluminescence marker, is added which selectively binds to *M. tb* complex-specific sequences.[346] The main advantages of this method are:

The assay can be run in approximately 2.5 to 3.5 hours once the process has commenced, which is comparable in time to sputum smear microscopy.[346,347]

Another advantage of NAATs compared to sputum smear microscopy is that they have a detection limit of less than 100 bacilli/ml of sample which associates to 1 – 10 bacilli per reaction.[348] However, these low limits of detection require great care in order to minimise contamination.[349] This method does however also have some disadvantages:

- It detects the presence of *M. tb* complex (MTBC), but cannot distinguish between the different Mycobacteria and it is stated that cell culture must be performed alongside the MTD test.[346]
- There is also limited knowledge available about this assay when samples other than sputum are used; therefore, samples containing blood may cause Fal.+ readings.[346]
- Another drawback is that the precision of the assay is much worse for sputum smear-negative patients compared to sputum smear-positive patients.[350]

NAATs have consistently been reported with specificities of greater than 95 %,[348] however the sensitivity of the test has been reported to vary between 63 – 99 %,[315,351,352] with the value of 63 % being reported for smear-negative patients and 99 % for smear positive patients.

1.12.6 Enzyme Linked Immunosorbent Assays

1.12.6.1 Methodology of an ELISA assay and antibodies binding region

An Enzyme Linked Immunosorbent Assay (ELISA) is a system to detect the presence of antibodies (Abs) in a sample, and has been used in order to detect anti TB Abs.[353,354] ELISA is a direct binding assay for detecting an antibody (Ab) or antigen (Ag) and both work on the same principle. Briefly, an ELISA assay to detect Abs is carried out as follows:

- A known amount of Ag is coated onto the surface of an ELISA plate.
- Any free non-specific binding sites are blocked.
- The sample containing the primary Ab is added to the plate.
- Any excess Abs are washed away in a washing step, leaving only the Abs that have bound to the Ag on the plate.
- A secondary Ab, labelled with an enzyme, is added, and binds to the primary Ab.

- Any excess unbound secondary Ab is removed from the plate in another washing step.
- A chemical is added which is converted by the enzyme on the secondary Ab into a detectable form.
- The signal absorbance is measured after a given time, and the magnitude of the signal is used to infer the relative amount of Abs in the sample.[355,356]

The ELISA assay can selectively measure the levels of specific Abs by varying the Ags and secondary Ab used, see **Diagram 1** below. It can be used for the detection of IgA,[357] IgD,[358] IgE,[359] IgG[360] and IgM[361] Abs.

An Ab or immunoglobulin is a glycoprotein found in plasma and extracellular fluids. It has two separate functions: one is to bind specifically to a molecule from the pathogen that elicit the immune response; the other is to employ other cells and molecules to destroy the pathogen once the Ab is bound to it.[362] All Abs are built in the same way from paired heavy and light polypeptide chains. However, the Ag-binding region varies extensively between Ab molecules and is thus known as the variable V region. The variability of Ab molecules allows each Ab to bind a different specific Ag, and the total repertoire of Abs made by signal individual is large enough to ensure that virtually any structure can be recognized.[362] The region of the Ab that engages the effector functions of the immune system does not vary in the same way and is thus known as the constant region or C region. It come in five main forms-IgM, IgD, IgG, IgA and IgE, which are each specialized for activating different effector mechanisms.[364] An ELISA assay was developed in which the glycolipid TDM Ag was purified from *M. tb* H37Rv and used as an Ag for detecting antituberculosis immunoglobulins and showed that a glycolipid was an effective Ag for serodiagnosis.[363]

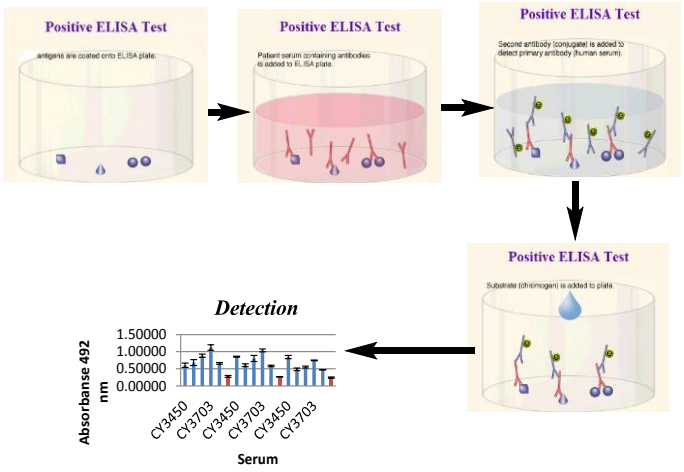

Diagram 1: ELISA assay Procedure

The ELISA assay can used as an attractive tool for diagnosing TB because it is relatively simple, cheap and quick to manage.[363] The results from this assay depend on the level of Abs detected in serum sample of TB patients depend on the type and structure of the TB Ag used.

1.12.6.2 ELISA assays and MA

The major constituents of the cell envelope of *M. tb* and other *Mycobacteria* are MAs;[168,175] their presence is thought to be linked with the resistance of these organisms to most current antibiotics and other chemotherapeutic agents.[364] Immunodiagnostic assays detecting pathogen related Abs in patient serum samples with active TB disease are an attractive alternative for rapid diagnosis. An array of Mycobacterial cell wall components have been considered as Ags for surrogate marker Abs for TB.[365] MAs provide a special opportunity due to their variability among different species of *Mycobacteria* and the unique way that they interact with the immune response of the host.[226,366,367] MAs and their sugar esters have therefore attracted great interest as surrogate markers for TB serodiagnosis.[368]

Diagnosis of TB using MA Ags in the ELISA method depends on the measurement of absorbance. A TB-positive sample is distinguished by a significantly high absorbance, while a low-absorbance sample is indicative of negative TB status. Thus, the challenge in this work is to select the best Ag, which will produce results in TB diagnosis that match those from a combination of other assays used in the current diagnostic process. The value of such Ag diagnosis will largely depend on the sensitivity and specificity with the Ag used. Both values are expressed as percentages and are determined on the basis of the selected cut-off value of the absorbance to distinguish a negative result from positive results for the test Ag. MAs occur within all *Mycobacteria*, in varying combinations of functionality type and chain length, and there are 54 reported species of *Mycobacteria*.[180, 369] Therefore, during diagnosis of mycobacterial disease, MAs can in principle be useful in predicting if the disease is tubercular or non-tubercular.

1.12.6.3 Effect of folding of free MAs and Cholesterol in an ELISA assay

In an ELISA assay, the use of mixtures of natural free MAs was not adequate for serodiagnosis of TB (accuracy = 57%).[370] An association between MAs and cholesterol was hypothesised as a possible reason for this.[371] Cholesterol may be non-specifically attracted to MAs by means of hydrophobic Van der Waals binding, or by a more specific interaction such as a hydrogen bond, arising from conformational features present in the two molecules.[371] Recently, free MAs have

been demonstrated to be able to adopt a folded conformation to give a hydrophobic surface. In particular, the "W" conformation has the alkyl chains folded to give four parallel arms, while in the "Z" conformation three folded arms provide the three-dimensional, curved hydrophobic surface.[232,372] The existence of these conformations has been suggested by analyses of Langmuir monolayers consisting of free MAs over a range of temperatures.[235,238] In an extended form, the shape and structure of a MA appears very different to that of cholesterol and does not suggest particularly strong interactions between these molecules. However, the folded conformations of MAs could be imagined to assume a shape similar to that of cholesterol (**Figure 27**).[235,303] Yolandy *et al.*[371] used an approach similar to that employed by Prendergast *et al.*[372] to suggest molecular mimicry between microbial and self-structures in autoimmune diseases. The basic assumption of this approach is that the specific molecular recognition of two substances by an established binding agent indicates resemblance in the three-dimensional structure of the two compounds.

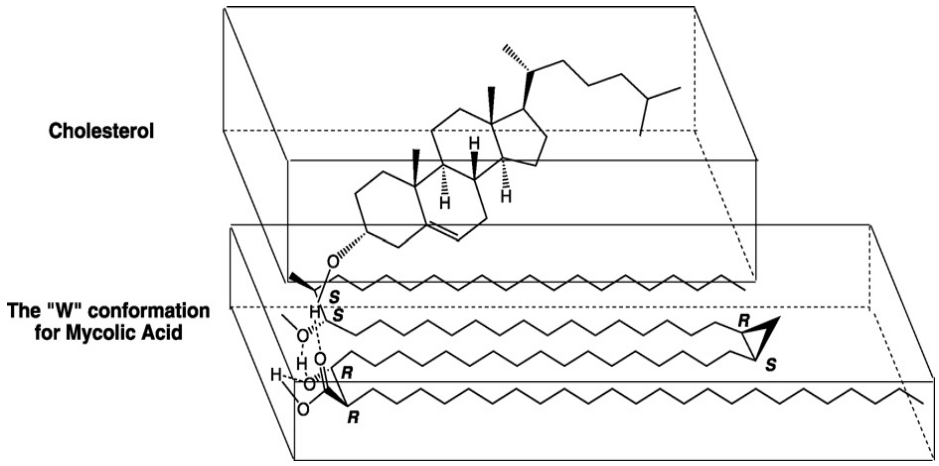

Figure 27: A pictorial representation of a hypothesised mechanism of interaction between a "W"-folded methoxy MA[235,238] and cholesterol. The absolute stereochemistry of the cyclopropane and the methoxy group are not completely clarified. Here for simplicity the *S,R* stereochemistry has been used for the cyclopropyl group and the SS for the methoxy-group. *RR* is known to be the absolute configuration of the mycolic motif. The "W" fold is drawn here in a flat plane, whereas in practice the fold shown in earlier models had a cylindrical three-dimensional structure.[235,238]

Verschoor *et al.*,[373] and Yolandy *et al.*[371] observed that Amphotericin B (AmB) recognised both cholesterol and MAs. In addition, a specific attraction was observed between the two molecules by the accumulation of cholesterol from liposomes in suspension onto immobilized MAs containing liposomes, was detected with a biosensor technique. Combined, these results suggest that MAs can assume a three-dimensional conformation similar to a sterol.[371] It is known that all humans have anti-cholesterol antibodies (ACHA), which are very specific for their

interaction with the sterol. ACHA recognise selectively 3β-hydroxy-sterols in a stereospecific manner, but they cannot distinguish between enantiomers.[374,375] Also, the interaction of MAs and cholesterol with serum samples from human TB patients, using an ELISA assay were explained by Schleicher *et. al*.[370]

The use of the complex mixtures of natural MA is thus complicated by apparent Ab cross-reactivity with cholesterol. MA structure has been experimentally interrogated to try to understand the cross- reactivity.[368] It was reported that three recombinant monoclonal scFv Ab fragments in the chicken germ-line Ab repertoire demonstrate cross-reactivity. Likewise, scFv Ab fragments to cholesterol did not necessarily cross-react with MA.[373] Whether the Ab cross-reactivity observed in human TB and control patient serum samples is due to a mixture of monospecific Abs, a true single Ab cross-reactivity, or both remains to be determined.[368]

1.12.6.4 Effect of the structure of MA in their antigenicity

There is increasing evidence of the importance of some natural free MAs.[376] Pan *et al*. in 1999 indicated that the methyl esters of homologous mixtures of natural methoxy-MAs are more antigenic than those of the keto-MA or the non-oxygenated α-MA. They estimated the titers of anti-cord factor IgG Ab in the serum samples of TB patients, and compared them with those of *M. avium*-infected patients using an ELISA assay.[368] Most of the serum samples obtained from the TB patients were highly reactive against *M. tb* cord factor isolated from *M. tb* H37Rv, a human-type mycobacterial strain, whereas they were less reactive against MAC cord factor. Similarly, most of the serum samples of the MAC-infected patients were highly reactive against MAC cord factor and less reactive against *M. tb* cord factor.[368] These results suggest that anti-cord factor IgG Ab recognizes the MA subclasses as an epitope which comprises cord factor, since *M. tb* and MAC cord factor differ in MA subclasses and molecular species composition. Furthermore, Fujiwara *et al.*[377] immunized rabbits with two kinds of cord factors isolated from *M. tb* or *M. avium* and the reactivities of the serum samples were tested against cord factors or the component MA methyl esters by ELISA. The serum from rabbits immunized with *M. tb* cord factor was highly reactive against *M. tb* cord factor, but less reactive against *M. avium* cord factor. In contrast, the serum from rabbits immunized with *M. avium* cord factor was highly reactive against *M. avium* cord factor but less reactive against *M. tb* cord factor. Moreover, the serum from rabbits immunized with *M. tb* cord factor reacted against MA methyl esters, especially methoxy MA methyl ester.[377] On the other hand, the serum from rabbits immunized with *M. tb* cord factor was less reactive against TMM and not reactive against sulfolipid

(2,3,6,6'-tetraacyl trehalose 2'- sulfate). From these results, it was concluded that the anti-cord factor IgG Ab, produced experimentally in rabbits, recognized the differences in the cord factor structures, i.e. the hydrophobic moiety rather than the carbohydrate moiety. The serum from rabbits immunized with *M. tb* cord factor was highly reactive against methoxy MA as an epitope.[382] Anti-cord factor IgG Ab could be produced in rabbits immunized with cord factor in the form of a 'water in oil in water' (w/o/w) micelle without any protein carrier and that the epitope or binding site of anti-cord factor IgG MA was MA.[382] Ab production against TDM of *Rhodococcus ruber* (*R. ruber*), a non-pathogenic species of the *Actinomycetales* group, was investigated in mice by repeated intraperitoneal injection of TDM in w/o/w micelles without carrier protein.[365] The antigenic TDM was isolated and purified chromatographically from the chloroform-methanol extractable lipids of *R. ruber*. The hydrophobic moiety of this TDM was composed of two molecules of monoenoic or dienoic α -MAs with a carbon chain length ranging from C44 to C48 centering at C46. To detect the Ab, an ELISA system was employed using plastic plates coated with TDM. The Ab reacted against the TDM of *R. ruber* and the Ab was reactive in similar fashion against glycosyl monomycolates differing in the carbohydrate moiety, such as that of glucose mycolate (GM) and mannose mycolate (MM),[365] obtained from *R. ruber*. Moreover, the Ab reacted against MA methyl ester itself when it was used as the antigen in ELISA, and trehalose did not absorb the Ab to TDM or inhibit the reaction. [365] The epitope of TDM recognized by the Ab is MA, an extremely hydrophobic part of the molecule. Also, they prepared monoclonal anti-TDM antibody (moAb) in mice myeloma cells to examine its biological activities and the role of humoral immunity in mycobacterial infection. MoAb reacted against the TDM, glycosyl mycolate, and MA methyl ester in ELISA in the same manner as polyclonal Ab did.[365] The administration of moAb suppressed granuloma formation in the lungs, spleen, and liver induced by TDM and inhibited the production of IL-1 and chemotactic factor, which is reported to precede granuloma formation.

Baird *et. al.* used single synthetic MA and their glycolipids with different stereochemistry from *M. tb* and other *Mycobacteria* in an ELISA assay. High Ab binding signals were observed with cord factors using human serum samples and the pairs of sensitivity and specificity i.e. for the three novel synthetic methoxy-, keto- and α-TDM from *M. tb* were equal to 80/87%, 75/90% and 80/84% respectively.[378]

Chapter 2

2. Results and Discussion

2.1 Project aims

This project comprises two main areas, firstly, the synthesis of a MA and secondly, the synthesis of its glycolipid derivatives. The target molecules from *M. tb* were *S,S-trans*-alkene-methoxy mycolic acid (**43**) and its glycolipid derivatives, TDM (**44**), TMM (**45**), GroMM (**46**), GMM (**47**) and the Arabino-MA fragment from AG (**48**), as seen in **Figure28**.

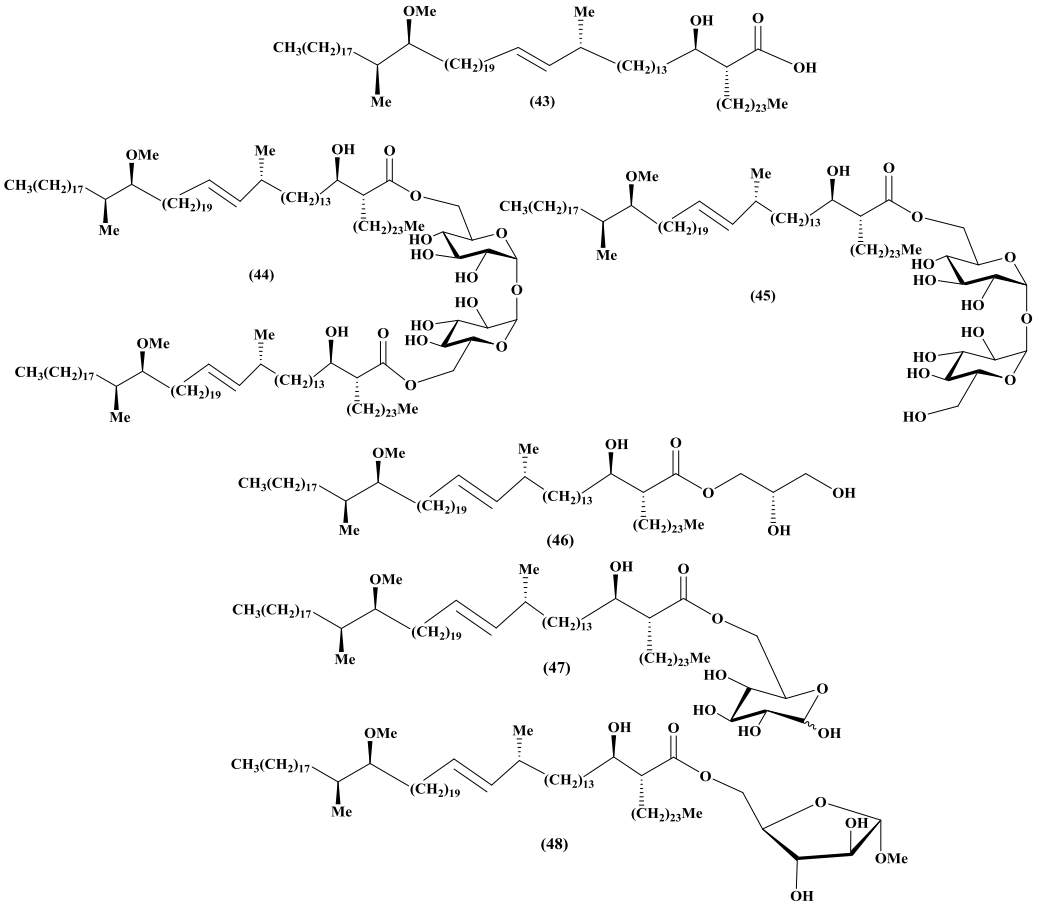

Figure 28: Target mycolic acid of *Mtb* and its derivatives.

The MA and its derivatives synthesised in this project will help towards the development of detection methods for TB, the discovery of a replacement for Freund's adjuvant, and the development of possible therapies in treating asthma and other diseases.

2.2 Synthesis of *S,S-trans*-alkene-methoxy MA (43)

It was decided to undertake the first synthesis of a *trans*-alkene methoxy-MA present in the cell wall of *M. tb*. The completed acid contains a double bond with *trans*-stereochemistry in the proximal position, and with the methoxy and methyl of the distal position in the *S,S* configuration. It was used to couple with trehalose tosylate, protected glycerol and ((2*R*,3*R*,4*S*,5*S*)-3,4-*bis*(benzyloxy)-5-methoxytetrahydrofuran-2-yl)methyl 4-methyl benzene sulfonate to prepare cord factors (TDM and TMM), GMM, GroMM, and one fragment from AG respectively. These would be used as synthetic antigens to detect Abs to MA or their glycolipids, using an ELISA assay, in order to determine if the stereochemistry of the free MA and MA present in the glycolipid antigens can affect their biological activities.

The general method of MA synthesis developed by Al-Dulayymi *et. al.*[379] entails synthesising a meromycolate moiety (**50**) and the intermediate (**51**) separately (**Figure 29)**, as the two main coupling fragments.

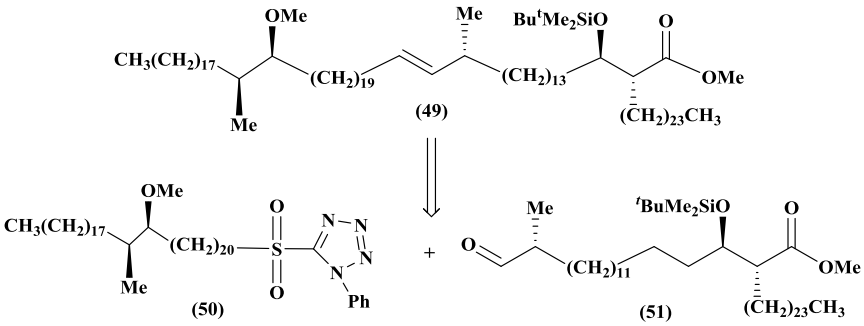

Figure 29: The distal position of meromycolate moiety and the intermediate (49)

The intermediate (**51**) can be separated further into proximal position and corynomycolate as shown in **Figure 30**.

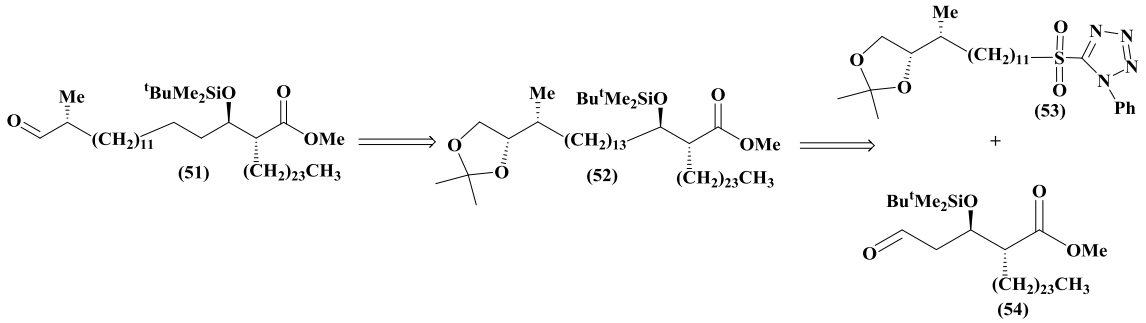

Figure 30: The proximal position and the corynomycolate disconnection

The preparation of the proximal position fragment (**53**) and corynomycolate fragment (**54**) could be carried out by the following methods (**Figure 31** and **Figure 32** respectively):

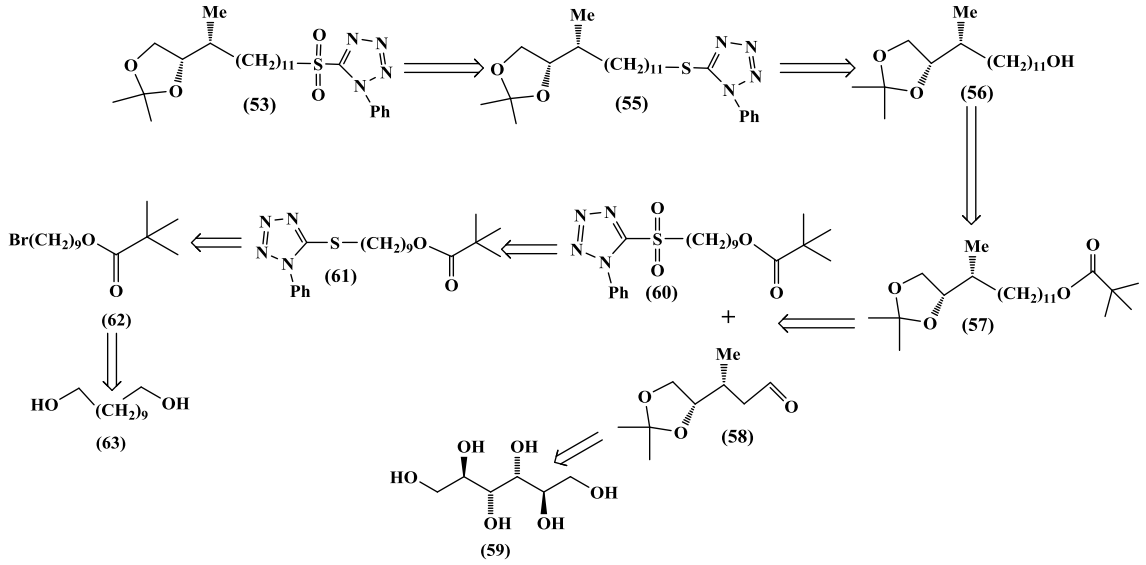

Figure 31: The proximal position of the meromycolate

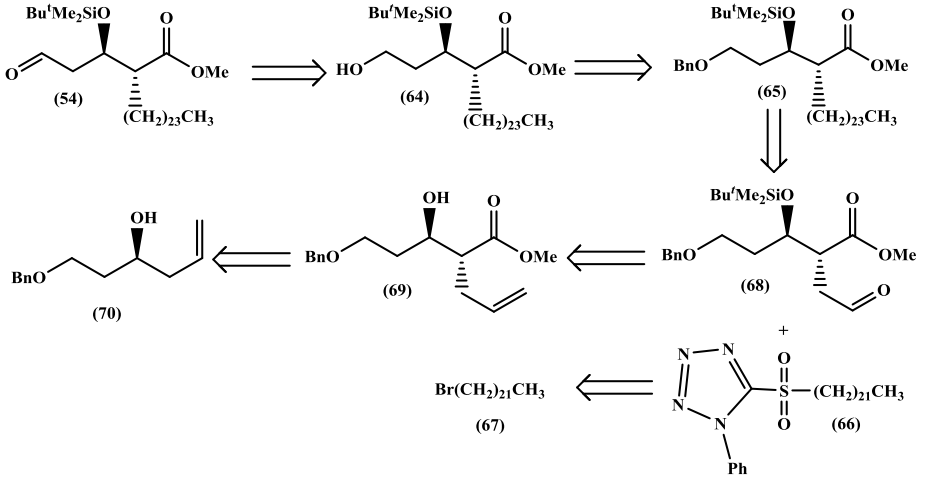

Figure 32: The corynomycolate

The *S,S* α-methyl methoxy unit at the distal position of the meromycolate (**50**) was obtainable from *L*-ascorbic acid by a multi-stage process (**Figure 33**).

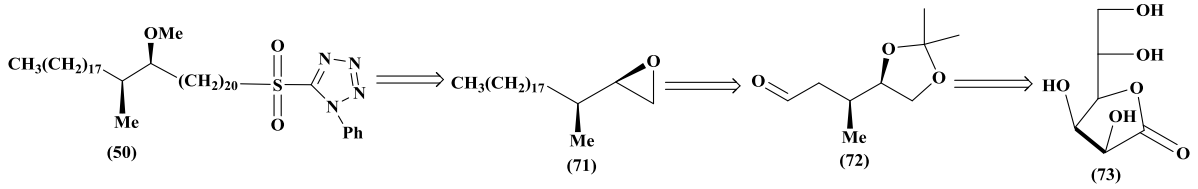

Figure 33: The retrosynthesis of *S,S* α-methyl methoxy unit

2.2.1 The preparation of distal *S,S* α-methyl methoxy unit

2.2.1.1 The preparation of aldehyde (72)

The enantiomer (**72**) was prepared from L-gulono-1,4-lactone (**73**), derived by hydrogenation of ascorbic acid.[380] In a modification of the literature procedure,[381] the lactone was protected as the acetal with 2-methoxypropene, oxidatively cleaved with sodium periodate and then reacted with methyl diisopropoxyphosphinyl acetate and potassium carbonate to give the ester (**75**) in 64% overall yield in a one-pot process. This gave the *E*-alkene rather than an *E/Z* mixture,[379] which was readily converted via three steps (**Scheme 2**) into the desired aldehyde (**72**).[186]

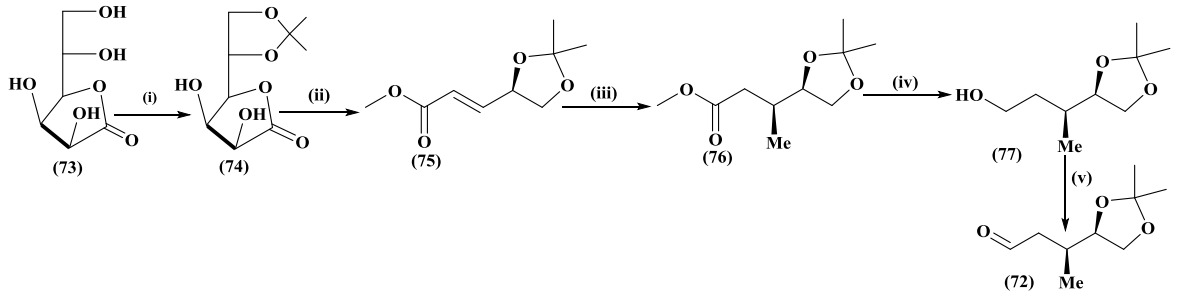

Scheme 2: Reagents and conditions: (i): *p*-toluene sulfonic acid, isopropenyl methyl ether, DMF, 96%; (ii): $NaIO_4$, NaOH aq, H_2O, methyl 2-(diisopropoxyphosphoryl)acetate, 64%; (iii): MeLi, ether, 81%; (iv): LiAlH4, THF, 82%; (v): PCC, CH_2Cl_2, 60%

The reaction of aldehydes or ketones with stabilized phosphorus ylides leads to olefins with excellent E-selectivity (Horner-Wadsworth-Emmons reaction).[382,383]

The next step entailed the diastereoselective conjugate addition of a methyl nucleophile to the α,β-unsaturated ester (**75**). The Michael addition of MeLi to the α,β-unsaturated ester (**75**) in dry ether at – 78 ^{o}C gave the *syn*-adduct, (**76**) as a single diastereomer in 81% yield. It is important to keep the temperature below –78 ^{o}C and the reaction solution dilute. The added methyl group appeared on the ^{1}H NMR spectrum as a doublet at δ 0.99 (*J* 6.6 Hz). The ^{13}C NMR spectrum showed signals at δ 173.1 for the carbonyl carbon and at δ 108.9 for the cyclic acetal carbon.[383] The ester (**76**) was reduced to the corresponding primary alcohol (**77**) by lithium aluminium hydride ($LiAlH_4$) in dry THF (**Scheme 2**) in good yield. The IR spectrum showed a broad stretch at ν_{max} 3426 cm^{-1} for the O–H group.[382,383] The alcohol (**77**) was oxidised to the aldehyde (**72**) with pyridinium chlorochromate (PCC) in CH_2Cl_2 (**Scheme 2**). The ^{1}H NMR spectrum showed a triplet at δ 9.72 (*J* 1.9 Hz) for the aldehyde proton and in the ^{13}C NMR spectrum a signal appeared at δ 201.5 for the carbonyl carbon. PCC is the ideal reagent

for this particular oxidation of primary alcohols to aldehydes, as it performs the oxidation in pH neutral conditions, and will not further oxidise the aldehyde.[382] Therefore, throughout this work, PCC was used to oxidise alcohols to the corresponding aldehydes.[379]

2.2.1.2 The preparation of C_{15} sulfone (80)

The reaction of bromo-compound (**78**) with 1-phenyl-1*H*-tetrazole-5-thiol in the presence of K_2CO_3 and acetone gave tetrazole (**79**) (95%).[379] This was then oxidised with H_2O_2 and ammonium molybdate (VI) tetrahydrate in a mixture of THF and IMS to give the corresponding sulfone (**80**),[384] which was purified by re-crystallisation from methanol to give 93% yield of product, (**Scheme 3**).

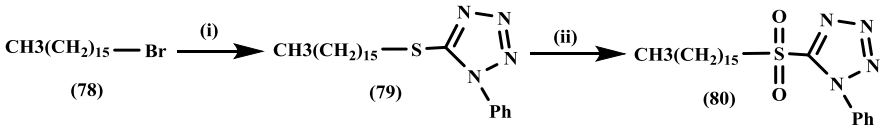

Scheme 3: Reagents and conditions: (i): 1-phenyl-1*H*-tetrazole-5-thiol, K_2CO_3, acetone, 95%; (ii): H_2O_2, $(NH_4)_6Mo_7O_{24}.4H_2O$, THF, IMS, 93%

The ^{1}H NMR spectrum of compound (**79**) showed a multiplet at δ 7.59-7.52 for the five aromatic protons, a triplet at δ 3.39 (*J* 7.6 Hz) for the (-$\underline{C}H_2$S-) and a triplet at δ 0.88 (*J* 6.9 Hz) for the terminal methyl. The ^{13}C NMR spectrum showed a signal at δ 154.5 for the tetrazole ring carbon, four signals for the aromatic carbons at δ 133.8-123.8 and signals at δ 33.4 for carbon bonded to the sulfur atom ($\underline{C}H_2$S) and at δ 14.0 for the terminal methyl.

The ^{1}H NMR spectrum of the sulfone (**80**) showed a multiplet at δ 7.72–7.68 (two protons, aromatic), another multiplet at δ 7.64–7.58 (three protons, aromatic) and a distorted triplet at 3.73 (*J* 7.9 Hz) for the two protons (H_A and $H_{A'}$) adjacent to the sulfonyl group.

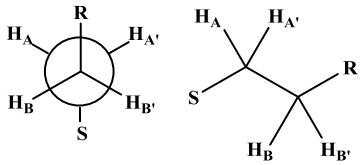

Figure 34: The diastereotopic protons (H_A and $H_{A'}$) adjacent to a sulfonyl group

The signal observed is a characteristic AA'BB' system, where the two substituents on the C–C bond mean that A and A' and B and B' respectively are not magnetically equivalent (**Figure 34**). The ^{13}C NMR spectrum showed a signal at δ 57.0 for the (-$\underline{C}H_2SO_2$-).

2.2.1.3 Extension of the chain

2.2.1.3.1 Overview of the modified Julia olefination

Formation of an alkene from a phenylsulfone and aldehyde was first published by Marc Julia and Jean-Marc Paris and called the Julia olefination.[385] The method was modified by Lythgoe and Kocienski[386] and has found use in the synthesis of many natural products.[387] It can be summarised as follows: metallation of a phenylsulfone (**81**), addition of the metallate (**82**) to an aldehyde, acylation of the resulting β-alkoxysulfone (**83**) and reductive elimination of the β-acyloxysulfone (**84**) with a single electron donor to afford alkene products (**Scheme 4**).

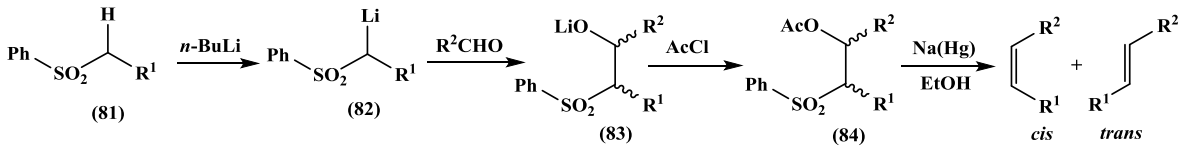

Scheme 4: Mechanism of the classical Julia olefination

Sylvestre Julia and co-workers replaced the phenylsulfone with a heteroarylsulfone, in a so-called 'modified Julia olefination'.[388] The presence of an electrophilic imine-like moiety within the heterocycle opens a new mechanistic pathway which transforms reactivity. The addition of a metallated sulfone (**86**) to an aldehyde gives *β*-alkoxysulfone (**87**). However, this *β*-alkoxysulfone is inherently unstable and readily undergoes a Smiles rearrangement.[389] This occurs *via* a spirocyclic intermediate (**88**) and transfers the heterocycle from sulphur to

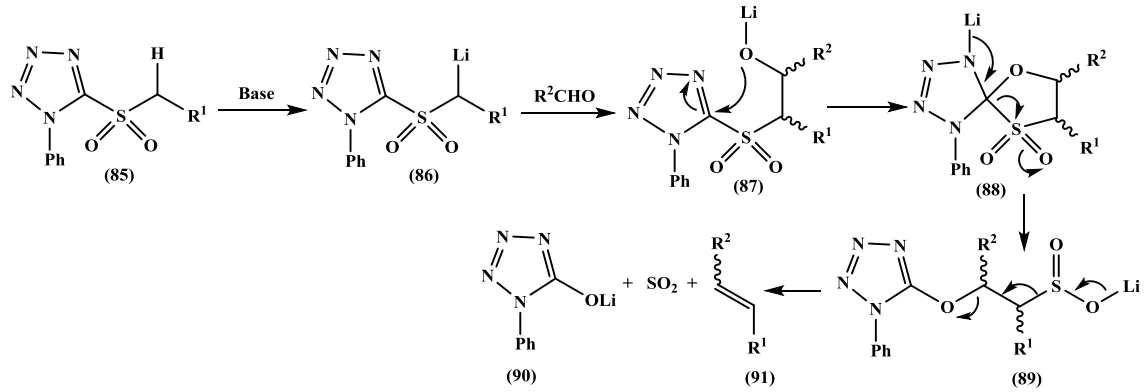

Scheme 5: Mechanism of the modified Julia olefination

Spontaneous elimination of sulphur dioxide and lithium oxygen to yield sulfinate salt (**89**). 1-phenyl-1*H*-tetrazolone (**90**) from (**89**) leads to the desired alkene (**91**) as a mixture of *E*- and *Z*-isomers respectively, (**Scheme 5**). For the modified Julia olefination, four heterocyclic activators have been found to provide useful levels of stereoselectivity in certain situations:

benzothiazol-2-yl (**BT**), pyridin-2-yl (**PYR**), 1-phenyl-1*H*-tetrazol-5-yl (**PT**) and 1-*tert*-butyl-1*H*-tetrazol-5-yl (**TBT**) (**Figure 35**).

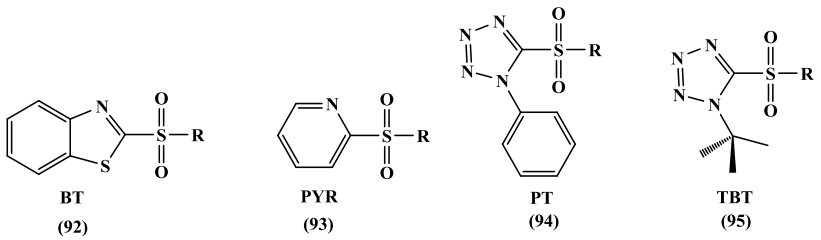

Figure 35: Heterocyclic sulfones for the modified Julia olefination

In this work, reagent (**94**) was chosen because it was easy to prepare from commercially available materials, and it has not shown problems with self condensation.[390, 391]

The Julia olefination gives mainly *E*-alkenes and it is often almost impossible to separate these from the minor *Z*-isomer by column chromatography.[392]

2.2.1.3.2 The Julia reaction between sulfone (80) and aldehyde (72)

The sulfone (**80**) was dissolved in THF and the aldehyde (**72**) was added. The coupling reaction was started by addition of the non-nucleophilic, strong base, lithium *bis*(trimethylsilyl)amide at –10 °C. Subsequently; the mixture was allowed to reach r. t. and then stirred for 2 h to give the desired alkene (**96**) as a mixture of two isomers in ratio 2.3:1 in 81% yield.[379] The alkene mixture was then saturated by hydrogenation in ethanol and methanol using Pd (10%) on carbon as a catalyst under a hydrogen atmosphere to give cyclic acetal (**97**), (**Scheme 6**). The ^{1}H and ^{13}C NMR spectra showed no signals in the olefinic region, which proved that the hydrogenation had been completed in excellent yield (99%).

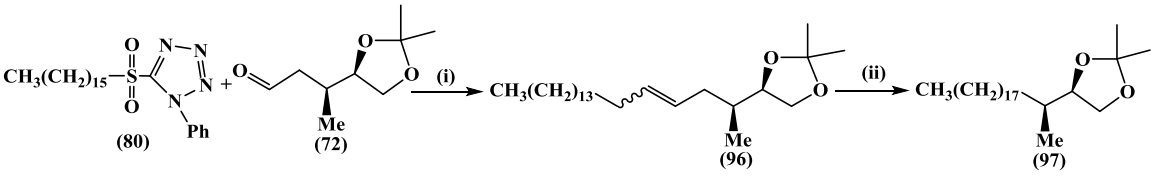

Scheme 6: Reagents and conditions: (i): $LiN(SiMe_3)_2$, dry THF, 81 %; (ii): -10 °C, H_2, Pd (10%) on C, IMS, 99 %.

2.2.1.3.3 The preparation of a chiral epoxide (71)

The cyclic acetal (**97**) was deprotected with *p*-toluenesulfonic acid monohydrate in THF, methanol and water, and refluxed for 2 h to give diol (**98**) in excellent yield (99%) as seen in **Scheme 7**.[393] The ^{1}H NMR spectrum showed the expected signals which included a multiplet at δ 3.69–3.67 (one proton) and another multiplet at δ 3.62–3.54 (two proton) for the three

protons next to the hydroxy groups. Other characteristic signals appeared as a broad multiplet at δ 1.43–1.23 for the long chain, a doublet at δ 0.94 (*J* 6.6 Hz) for the vicinal coupling of the α-methyl and a triplet at δ 0.89 (*J* 7.0 Hz) for the terminal methyl. The ^{13}C NMR spectrum showed two signals at δ 75.8 and 65.2 for the carbons next to the hydroxy groups, signals between 35.7 and 22.7 for the long chain and two signals at δ 14.6 and 14.1 for the two methyl groups. The optical rotation of the diol (**98**) was $[\alpha]_D^{22}$ = -11.5 (c 1.2, $CHCl_3$).

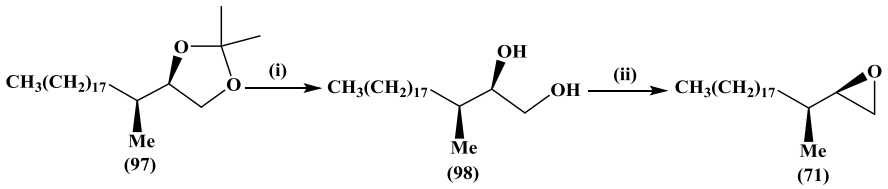

Scheme 7: Reagents and conditions: (i): PTSA, THF, MeOH, H_2O, 99%; (ii): cetrimide, NaOH, *p*-toluenesulfonylchloride, CH_2Cl_2, 59%

The diol (**98**) was converted stereospecifically into the epoxide (**71**) *via* the monotosylate which was formed *in situ*. The reaction was carried out under phase transfer conditions using (*n*-hexadecyl) trimethylammonium bromide, 50% aq. sodium hydroxide and *p*-toluenesulphonyl chloride in CH_2Cl_2 solution. It was complete after 45 min (**Scheme 7**). The ^{1}H NMR spectrum of epoxide (**71**) showed that the protons next to the oxygen atom were shifted up field and appeared as two doublets of doublets at δ 2.78 (*J* 4.1, 5.2 Hz) and 2.54 (*J* 2.9, 5.2 Hz), and a multiplet at δ 2.71–2.68. In the ^{13}C NMR spectrum, the carbons next to the oxygen atom were also shifted up-field and appeared at δ 57.2 and 47.0. The remaining signals for the ^{1}H and ^{13}C NMR were similar to those of the diol (**98**), and identical to those in the literature.[379]

2.2.1.3.4 The Grignard reaction

2.2.1.3.4.1 Preparation of Grignard reagent

Nucleophilic addition of a Grignard regent to a chiral epoxide proceeds stereospecifically. This is one of the key steps for the preparation of both the methoxy- and keto-mycolic acids.

A six carbon Grignard reagent was needed for the reaction with the epoxide (**71**). Bifunctional diols, HO–$(CH_2)_n$–OH, were used in this work to extend chain lengths as they are inexpensive, are available in a variety of different chain lengths and they can be easily desymmetrised and modified. 1,6-Hexanediol was mono-brominated with 48% HBr by refluxing in toluene for 18 h. to give 6-bromo-hexan-1-ol (**100**) in 55% yield (**Scheme 8)**.[394, 395] The NMR spectra matched those given in the literature.[396]

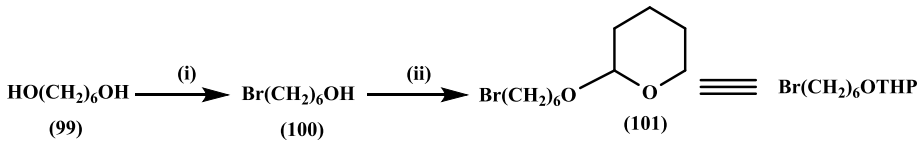

Scheme 8: Reagents and conditions: (i): HBr, Toluene, reflux, 55%; (ii): PPTS, dry CH_2Cl_2, 85%.

The hydroxy group of the 6-bromo-hexan-1-ol (**100**) was protected with 3,4-dihydro-2*H*-pyran to give 2-(6-bromo-hexyloxy)-tetrahydro-pyran (**101**) using pyridinium-*p*-toluene-sulfonate (PPTS) as a catalyst and dry CH_2Cl_2 as a solvent.

2.2.1.3.4.2 Addition of Grignard reagent to the epoxide

The Grignard reagent (**102**) was prepared from (**101**). Reaction of (**102**) (2.5 mol eq.) with epoxide (**71**) in dry THF in the presence of a catalytic amount of copper (I) iodide gave the alcohol (**103**) (**Scheme 9**).

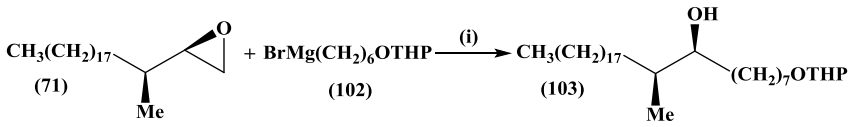

Scheme 9: Reagents and conditions: (i): Mg turnings, CuI, THF (75%)

In the IR spectrum of the alcohol (**103**), it was possible to observe the signal for the O–H stretch at 3450 cm^{-1}. In its ^1H NMR spectrum, the protecting group's protons on the ring adjacent to oxygen appeared as a broad singlet at δ 4.59 and a multiplet at δ 3.91–3.87. The protons on the chain next to oxygen appeared as a doublet of triplets at δ 3.74 showing a vicinal coupling (7.0 Hz) and a geminal coupling (9.5 Hz), and as a doublet of triplets at δ 3.40 (*J* 6.6 (vicinal), 9.5 (geminal) Hz). The proton adjacent to the secondary hydroxyl group appeared as a multiplet at δ 3.54–3.51. The long chain protons appeared at δ 1.48–1.25 and the proton adjacent to the methyl appeared as a multiplet at δ 1.21–1.14. The terminal methyl protons appeared as a triplet at δ 0.90 (*J* 7.0 Hz) and the α-methyl protons as a doublet at δ 0.88 (*J* 6.6 Hz). The ^{13}C NMR spectrum showed four signals at δ 98.9 (acetal carbon), δ 75.2 (hydroxy carbon), δ 67.7 (O<u>C</u>H_2-) and δ 62.4 (O<u>C</u>H_2-) for the carbons adjacent to oxygen. The terminal methyl carbon appeared at δ 14.1 and the α-methyl carbon at δ 13.6.

2.2.1.3.5 Preparation of aldehyde (106)

Methylation of the alcohol (**103**) led to (**104**) containing the required relative stereochemistry of the branch methyl and methoxy groups (**Scheme 10**). In the ^{1}H NMR spectrum, the multiplet of the proton adjacent to the secondary hydroxyl group at δ 3.54–3.51 was absent and, in addition, the O–H stretch at 3450 cm^{-1} had disappeared in the IR spectrum.

The deprotection of the THP group in (**104**) gave (**105**) as shown in **Scheme 10**. The ^{1}H NMR spectrum showed that there are no signals for the THP group, but there was a triplet at δ 3.65 (*J* 6.6 Hz) for the newly formed primary alcohol.

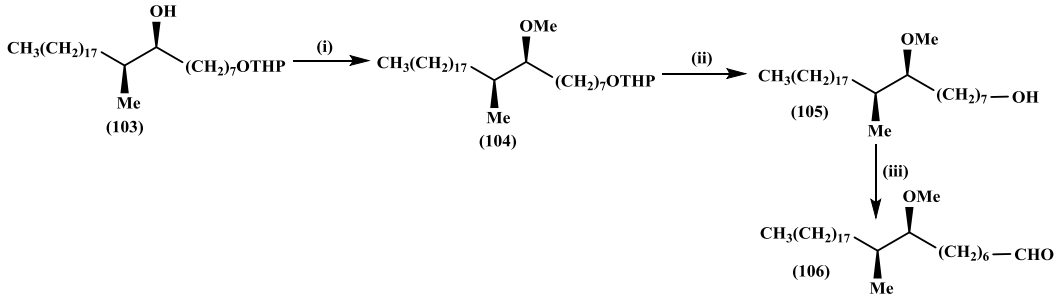

Scheme 10: Reagents and conditions: (i): sodium hydride, THF, methyl iodide (100%); (ii): PTSA, THF, methanol, water at r. t. (95%); (iii): PCC, CH_2Cl_2 (83%)

The primary alcohol (**105**) was then oxidised to the aldehyde (**106**) with PCC (1.86 mol eq.) suspended in CH_2Cl_2 at r. t. for 2 h. (**Scheme 10**). The product used on the same day to avoid the possibility of polymerisation. Its spectra matched those in the literature.[379]

2.2.1.3.6 The preparation of C_{13} sulfone (115)

PCC is the ideal reagent for the oxidation of primary alcohol (**100**)[397] to aldehyde (**107**), as shown in **Figure 36**.

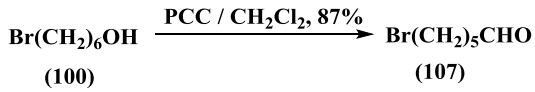

Figure 36: The oxidation of alcohol (100) by PCC

The ^{1}H NMR spectrum showed a triplet at δ 9.73 (*J* 1.9 Hz) for the aldehyde proton and in the ^{13}C NMR spectrum a signal appeared at δ 202.8 for the carbonyl carbon. The chain length of the aldehyde (**107**) is too short to couple in the next step, so it was necessary to add seven more carbons to prepare the exact length of the natural chain. Therefore, the sulfone (**111**) was prepared starting from 7-bromoheptan-1-ol (**108**), which was protected with trimethylacetyl

chloride in CH_2Cl_2 to give (**109**), followed by reaction with 1-phenyl-1*H*-tetrazole-5-thiol and anhydrous K_2CO_3 in acetone to give (**108**) (**Scheme 11**).

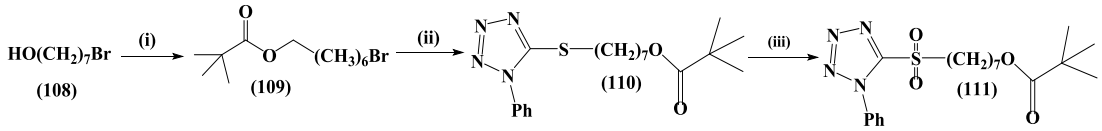

Scheme 11: Reagents and conditions: (i): trimethylacetyl chloride, triethylamine, 4-dimethylamino-pyridine, CH_2Cl_2 (98%) (ii): 1-phenyl-1*H*-tetrazole-5-thiol, K_2CO_3, acetone (90%); (iii): H_2O_2, $(NH_4)_6Mo_7O_{24}.4H_2O$, THF, IMS (83%)

Oxidation of the sulfide (**110**) with ammonium molybdate (VI) tetrahydrate and hydrogen peroxide yielded the sulfone (**111**) as shown in **Scheme 11**. Reaction of the aldehyde (**107**) with this in the presence of lithium *bis*(trimethylsilyl)amide in dry THF gave the olefin (**112**) in 58% yield as a mixture of *E*- and *Z*-stereoisomers in a ratio 2.4:1 (**Scheme 12**).

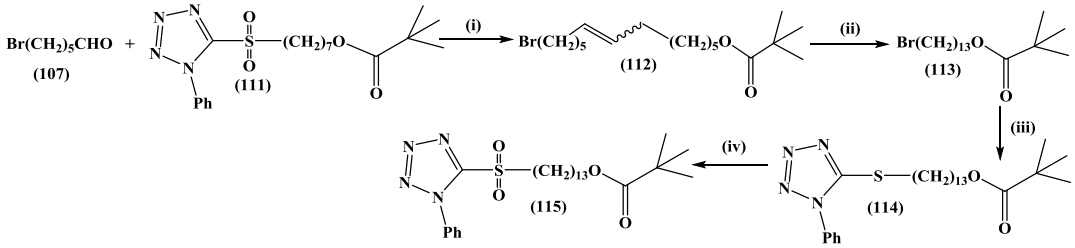

Scheme 12: Reagents and conditions: (i) $LiN(SiMe_3)_2$, dry THF (58%); (ii) -10 ºC, H_2, Pd (10%) on C, THF, IMS (88%); (iii) 1-phenyl-1*H*-tetrazole-5-thiol, K_2CO_3, acetone (86%); (iv): H_2O_2, $(NH_4)_6Mo_7O_{24}.4H_2O$, THF, IMS (95%)

The mixture of *E*- and *Z*-alkenes was then saturated by hydrogenation in a mixture of THF and IMS using Pd (10%) on carbon as a catalyst under a hydrogen atmosphere (**Scheme 12)**, to give the saturated product (**113**) in 88% yield. The ^{1}H NMR spectrum of this showed a triplet at δ 4.05 (*J* 6.6 Hz) for the protons adjacent to the carbonyl group, and a triplet at δ 3.42 (*J* 6.9 Hz) for the protons adjacent to the bromine group. The *tert*-butyl group protons appeared at δ 1.20 as a singlet. The ^{13}C NMR spectrum showed a signal at δ 178.7 for the carbonyl carbon, and a signal at δ 38.7 for the quaternary carbon of the protecting group, and a signal at δ 27.2 for the *tert*-butyl methyl carbons.

The protected bromide (**113**) was reacted with 1-phenyl-1*H*-tetrazole-5-thiol in acetone to give the sulfide (**114**) (**Scheme 12**). The ^{1}H NMR spectrum showed a multiplet at δ 7.60–7.52 for the phenyl group protons, and the ^{13}C NMR spectrum showed five signals in the aromatic region. One signal was seen at δ 154.5 for the tetrazole ring carbon, and another four signals at δ 133.7, δ 130.0, δ 129.7 and δ 123.8 for the phenyl group carbons. Finally, the sulfide (**114**) was

oxidised to the sulfone (**115**) as previously discussed. The characteristic signal of the two protons adjacent to the sulfonyl group appeared as a multiplet at 7.71–7.68.

2.2.1.3.7 The preparation of C_{20} sulfone (50)

Reaction of the aldehyde (**106**) with the sulfone (**115**) in the presence of lithium *bis*-(trimethylsilyl)amide in dry THF gave the olefin (**116**) as a mixture of *E*- and *Z*-stereoisomers in a ratio of 2.6:1 (**Scheme 13**).

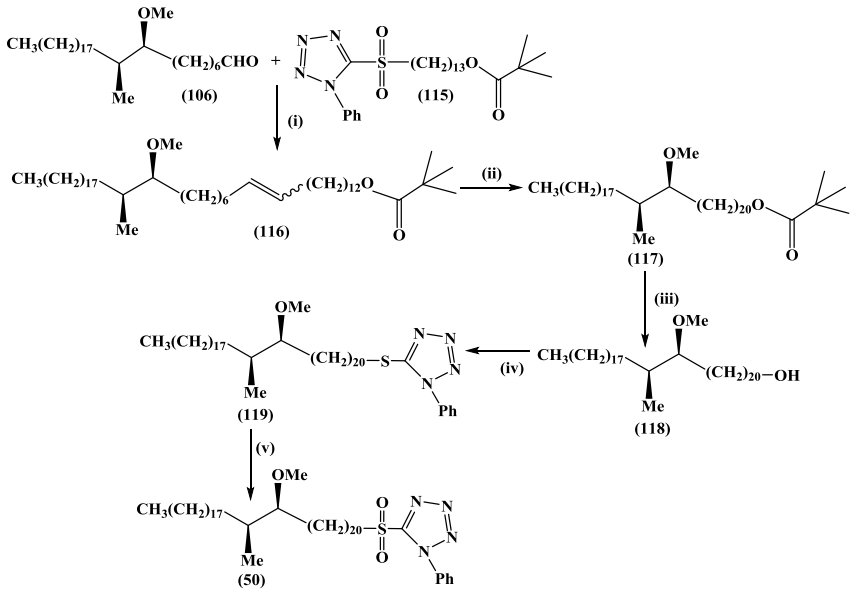

Scheme 13: Reagents and conditions: (i): $LiN(SiMe_3)_2$, dry THF (85%); (ii): -10 °C, H_2, Pd (10%) on C, ethyl acetate (100%); (iii): $LiAlH_4$, THF (98%); (iv): diethyl azodicarboxylate, 1-phenyl-1*H*-tetrazole-5-thiol, PPh_3 , THF (98%); (v): $NaHCO_3$, *m*-chloroperbenzoic acid, CH_2Cl_2 (97%)

Hydrogenation of the mixture of alkenes in ethyl acetate using Pd (10%) on carbon as a catalyst gave the saturated compound (**117**) (**Scheme 13**). The hydrogenated ester (**117**) was deprotected using $LiAlH_4$ in dry THF to give the primary alcohol (**118**) in 98% yield. The alcohol (**118**) was reacted with 1-phenyl-1*H*-tetrazole-5-thiol, PPh_3 and diethyl azodicarboxylate in dry THF to give a 98% yield of the sulfide (**119**) (**Scheme 13**). The ^1H NMR spectrum showed a multiplet at δ 7.65–7.61 for the phenyl group protons, and the ^{13}C NMR spectrum showed five signals in the aromatic region. One signal was seen at δ 153.5 for the tetrazole ring carbon, and another four signals at δ 133.1, δ 131.5, δ 129.7 and δ 125.1 for the phenyl group carbons. Then the sulfide (**119**) was oxidised to the desired sulfone (**50**). The characteristic signal of the two protons adjacent to the sulfonyl group appeared as a multiplet at 7.73–7.71, which indicated that the reaction was successful (**Scheme 13**).

2.2.2 The preparation of the proximal part of the meromycolate chain

2.2.2.1 The preparation of aldehyde (58)

D-Mannitol (**59**) was protected as 1,2:5,6-di-*O*-isopropylidene-D-mannitol (**120**) with zinc chloride and acetone as in the literature, to give the product in 86% yield (**Scheme 14**).[397]

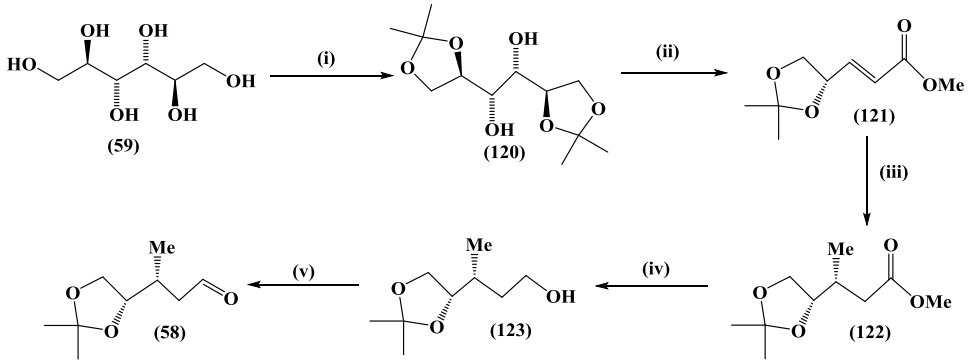

Scheme 14: Reagents and conditions: (i): $ZnCl_2$, Acetone (86%); (ii) $NaIO_4$, $NaHCO_3$, H_2O, methyl diisopropyl-phosphinyl acetate, K_2CO_3 (70%); (iii): MeLi, dry ether (77%); (iv): $LiAlH_4$, THF, (90%); (v) PCC, CH_2Cl_2 (77%)

Oxidative cleavage of the diol (**120**) with sodium metaperiodate in aqueous sodium hydrogen carbonate gave the intermediate glyceraldehyde acetonide, which was, without isolation, treated successively with methyl diisopropyl-phosphinylacetate,[398] and aqueous potassium carbonate to give the α,β-unsaturated ester (**121**) via a Horner-Wadsworth-Emmons reaction (**Scheme 14**).[399] The diastereoselective conjugate addition of a methyl nucleophile to the α, β-unsaturated ester (**121**) was conducted as reported by Leonard and co-workers.[400] Thus, (**121**) was exposed to MeLi in diethyl ether at – 78 °C to give *syn*-adduct, (**122**) as a single diastereomer. As before, it was important to keep the temperature below –78 °C. The added methyl group appeared in the ^{1}H NMR spectrum as a doublet at δ 0.98 (*J* 6.7 Hz). The ^{13}C NMR spectrum showed signals at δ 173.0 for the carbonyl carbon and at δ 108.9 for the cyclic acetal carbon. The ester (**122**) was reduced to the corresponding primary alcohol (**123**) with lithium aluminium hydride in dry THF, then oxidised using PCC gave aldehyde (**58**) in 77% yield (**Scheme 13**). The spectroscopic data were the same as those obtained before.[382,383]

2.2.2.2 Extension of the chain

The chain length of the aldehyde (**58**) is too short to couple to the corynomycolate chain in the next steps. Therefore, the sulfone (**60**) was prepared in order to extend the chain by nine carbon atoms, starting from 1,9-nonanediol **(63**). The diol was monobrominated to 9-bromononan-1-

ol (**124**) with 48% HBr refluxing in toluene. Then, the hydroxy group was protected with trimethyl-acetyl chloride. This protecting group is very common and deprotection is easy with strong base such as KOH, or $LiAlH_4$. Understanding the ^1H and ^{13}C NMR spectra is also easy compared to the THP protecting group. Consequently, compound (**62**) was obtained in 96% yield by protecting alcohol (**124**) with trimethylacetyl chloride in the presence of triethylamine and 4-dimethylaminopyridine, (**Scheme 15**).[186]

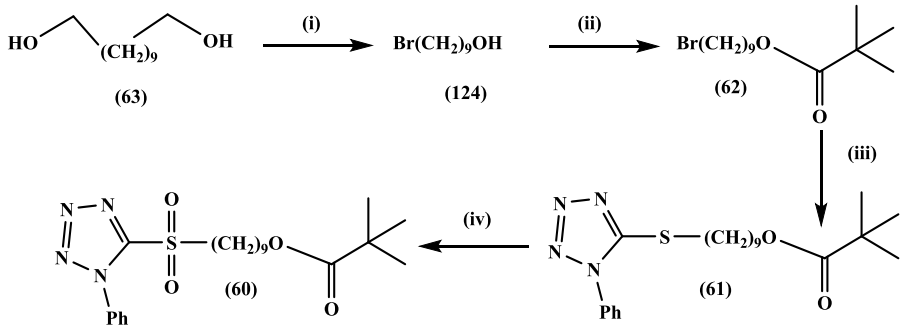

Scheme15: Reagents and conditions: (i): HBr, toluene, reflux (81%); (ii): trimethylacetyl chloride, CH_2Cl_2, trimethylamine, 4-dimethylaminopyridine (DMAP) (96%); (iii): 1-phenyl-1*H*-tetrazole-5-thiol, acetone, K_2CO_3 (91%); (iv): $(NH_4)_6Mo_7O_{24}.4H_2O$, H_2O_2, THF, IMS (97%)

The protected bromo-compound (**62**) was reacted with 1-phenyl-1*H*-tetrazole-5-thiole in acetone to give the sulfide (**61**), which was oxidised to the desired sulfone (**60**) using an excess of hydrogen peroxide and ammonium molybdate (VI) tetrahydrate (**Scheme 15**). The spectroscopic data were the same as those obtained before.[186]

2.2.2.3 The Julia reaction between sulfone (60) and aldehyde (58)

The sulfone (**60**) was dissolved in THF, and the aldehyde (**58**) was added. The coupling reaction was initiated by adding lithium *bis*-(trimethylsilyl) amide at –10 °C under nitrogen.

Subsequently, the mixture was stirred at r. t. for 2 h, giving the desired alkene as a mixture of *E*- and *Z*- stereoisomers (**125**) in a ratio of 2.3:1 (**Scheme 16**).

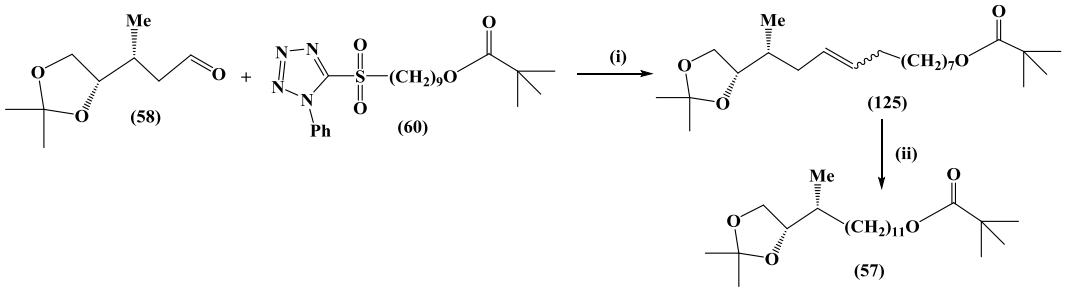

Scheme 16: Reagents and conditions: (i): $LiN(SiMe_3)_2$, dry THF (76%); (ii): -10 °C, H_2, Pd (10%) on C, IMS (92%)

The alkene mixture (**125**) was then saturated by hydrogenation in IMS using Pd (10%) on carbon as a catalyst under a hydrogen atmosphere to give the saturated compound (**57**) (**Scheme 16)**. The ^{1}H and ^{13}C NMR spectra showed no signals in the olefinic region, which proved that the hydrogenation had been completed.

2.2.2.4 The preparation of C_{11} sulfone (53)

Reduction of (**57**) by $LiAlH_4$ in THF gave the corresponding alcohol (**56**) which was converted into the sulfide (**55**) via a Mitsunobu. The ^{1}H NMR spectrum showed a multiplet at δ 7.60-7.52 for the phenyl group protons, and the ^{13}C NMR spectrum showed five signals in the aromatic region. One signal was seen at δ 154.5 for the tetrazole ring carbon, and another four signals at δ 133.7, δ 130.0, δ 129.7 and δ 123.8 for the phenyl group carbons. Lastly, the sulfide (**55**) was oxidised with hydrogen peroxide to give the sulfone (**53**) in 84% yield, (**Scheme 17**).

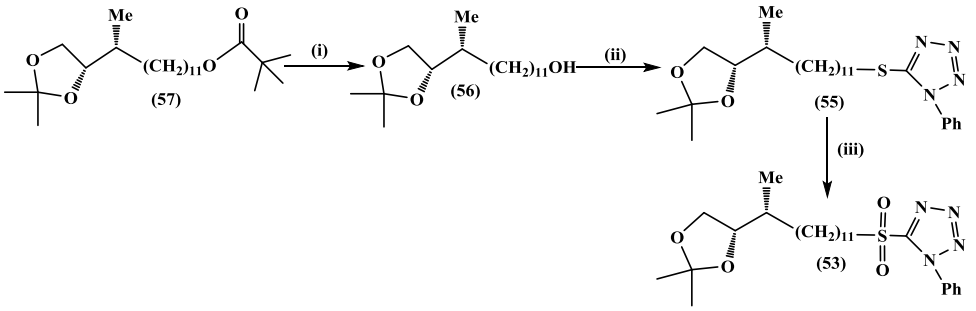

Scheme 17: Reagents and conditions: (i): $LiAlH_4$, THF (81%); (ii): diethyl azodicarboxylate, 1-phenyl-1*H*-tetrazole-5-thiol, PPh_3, dry THF (84%); (iii): $(NH_4)_6Mo_7O_{24}.4H_2O$, H_2O_2, THF, IMS (84%)

The ^{1}H NMR spectrum of the sulfone (**53**) included a broad triplet at δ 3.60 (*J* 7.9 Hz) ($C\underline{H}_2SO_2$), two singlets at δ 1.41 and δ 1.35 for the two methyls of the acetal protecting group, and a doublet at δ 0.96 (*J* 6.6 Hz) for the chiral methyl protons. The ^{13}C NMR spectrum of (**53**) showed a signal at δ 108.5 for the carbon of the acetal group.

2.2.3 The preparation of the corynomycolate chain

2.2.3.1 The preparation of β-hydroxy ester (129)

The target of this work was the β-hydroxy ester (**129**) from the epoxide (**126**).[401] The ring opening of the epoxide with vinylmagnesium bromide under Cu(I) catalysis gave the unsaturated alcohol (**70**) in excellent yield (**Figure 37**).

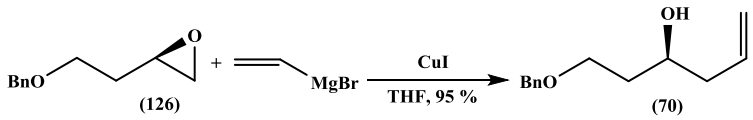

(126) (70)

Figure 37: Grignard reaction of the epoxide

Nucleophilic attack of an epoxide by a Grignard reagent is favoured at the less substituted carbon, since this is more accessible. The reaction was started at – 75 ^{o}C in the presence of catalytic copper (I) iodide in THF and then allowed to reach – 20 ^{o}C to obtain unsaturated alcohol (**70**).[402,403] The alkene group of (**70**) was to be oxidised to a carboxylic acid. Therefore, the hydroxyl group was protected to prevent further oxidation. The acetyl protecting group was chosen as it is cheap and easy to handle. The protected compound (**127**) was formed in excellent yield (99 %) by treating the alcohol (**70**) with acetic anhydride and anhydrous pyridine in toluene, (**Scheme 18**).[186,382]

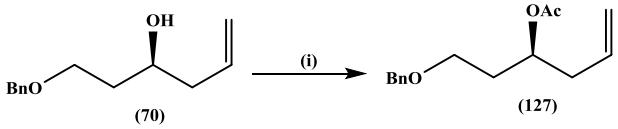

(70) (127)

Scheme 18: Reagents and conditions: (i): Acetic anhydride, pyridine, toluene (99%)

The ozonolysis of an alkene in methanolic sodium hydroxide in dichloromethane as co-solvent leads directly to methyl ester, but the desired methyl ester could not be always obtained from alkene.[383] Recently, another method was published for direct oxidation of olefins to their corresponding ketones or carboxylic acids in high yields via the carbon−carbon cleavage of an osmate ester by the action of oxone.[404] Oxone is used as the stoichiometric re-oxidant for the oxidative cleavage of olefins with catalytic OsO_4 in DMF to give the carboxylic acids (**Scheme 19**).[186,382] The desired carboxylic acid (**128**) was obtained in 78% yield by treating the alkene (**127**) in DMF with oxone (4 mol eq.) and OsO_4 (0.01 mol eq.) in 2-methyl-2-propanol at 10 ^{o}C and then 32 ^{o}C.

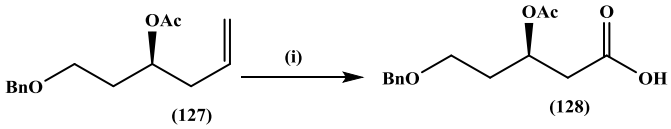

(127) (128)

Scheme 19: Reagents and conditions: (i): OsO_4, Oxone, DMF (78%)

The desired β-hydroxy methyl ester (**129**) was obtained from the acid (**128**) by refluxing in methanol (300 mL) in the presence of conc.H_2SO_4 as shown in **Scheme 20** below.

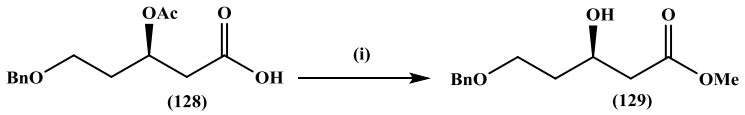

Scheme 20: Reagents and conditions: (i): Conc. H_2SO_4, methanol (78%)

The analysis of the ^{1}H and ^{13}C NMR data of **126**, **70**, **127**, **128** and **129** matched those in the literature.[186,382]

2.2.3.2 The Fräter alkylation

In the preparation of the intermediate corynomycolate moiety (**54**) for the synthesis of MAs, the key step was the *anti*-alkylation of the β-hydroxy ester (**129**). The widely utilized method is based on the use of the Fräter-Seebach alkylation.[405,406] This was chosen for the insertion of the alkyl chain at the α-position of the β-hydroxy ester, since it gives very good diastereoselectivity (95:5).[405] First, (**129**) was alkylated with a short chain, then this was extended to the required natural MA chain length, because direct insertion of the necessary long chain (24 carbons) has been found to be very inefficient. Treatment of compound (**130**) with lithium *N*,*N*-diisopropylamine (LDA) (2 mol eq.) forms the stable chelated *Z*-enolate (**131b**). The geometry of the enolate is not so important. However, the formation of a chelated species is important (**Scheme 20**).[382] The greater steric crowding of the top face of the six-membered ring intermediate (**131b**) allows for a good level of diastereoselective addition from the less hindered bottom face, resulting in the preferential formation of the *anti*-alkylated product (**132**, **Scheme 21**).

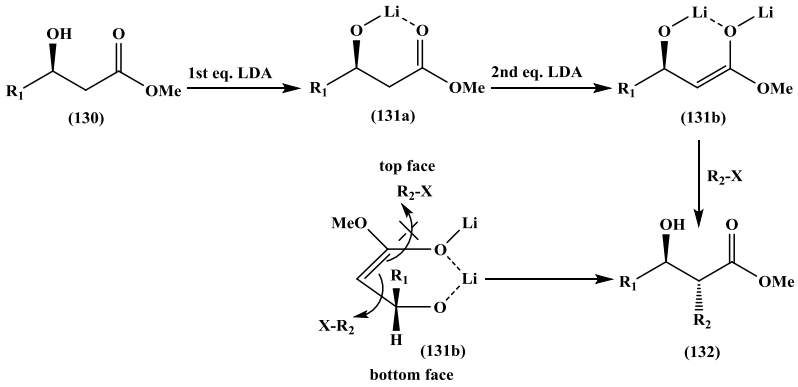

Scheme 21: The formation of the intermediate enolate (131b) and the mechanism of the anti-addition

The best yield was obtained with the method described in the experimental section (**67**, **Scheme 22**).

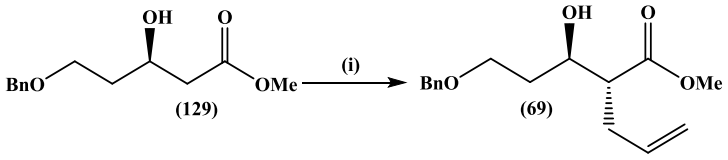

Scheme 22: Reagents and conditions: (i): diisopropylamine, THF, MeLi, allyl iodide, HMPA (76%)

To complete the chain extension of the corynomycolate moiety at the α-position, the sulfone (**66**) was prepared starting from 1-bromodocosane (**67**, **Scheme 23**).[186] This was reacted with 1-phenyl-1*H*-tetrazole-5-thiol and K_2CO_3 in acetone and the mixture was refluxed at 60 °C for 15 h to yield the sulfide (**133**). The ^{1}H NMR spectrum showed a multiplet at δ 7.61–7.54 for the phenyl group protons, and the ^{13}C NMR spectrum showed five signals in the aromatic region. One signal was seen at δ 154.5 for the tetrazole ring carbon, and another four signals at δ 133.8, δ 130.0, δ 129.7 and δ 123.9 for the phenyl group carbons.

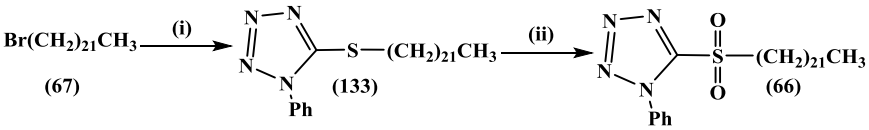

Scheme 23: Reagents and conditions: (i): 1-Phenyl-1*H*-tetrazole-5-thiol, K_2CO_3, acetone (73%); (ii): $(NH_4)_6Mo_7O_{24}.4H_2O$, H_2O_2, THF, IMS (85%)

The sulfide (**133**) was oxidised to the desired sulfone (**66**) in 85% yield using an excess of hydrogen peroxide and ammonium molybdate (VI) tetrahydrate. The characteristic signals were as before.[382]

The secondary alcohol (**69**) was treated with imidazole and *tert*-butyldimethylchlorosilane in DMF, and stirring at 45 °C for 18 h to give product (**134**) in 87% yield. The protecting group protons showed in the ^{1}H NMR spectrum as a singlet at 0.87 for the *tert*-butyl group and a singlet at 0.07 for the two methyls. By following the procedure discussed by W. Yu *et. al.*,[407] an improved oxidative cleavage of olefin (**134**) was carried out with OsO_4–$NaIO_4$ and 2,6-lutidine in 1,4-dioxane-water (3:1) to give the aldehyde (**68**) in 88 % yield (**Scheme 24**).

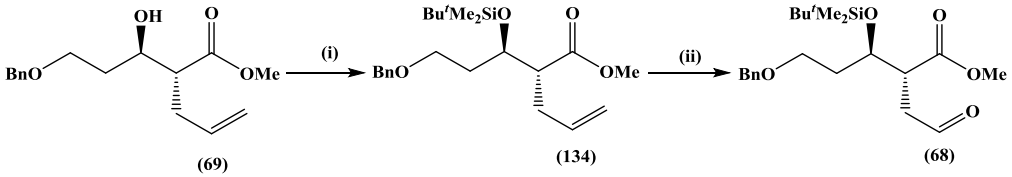

Scheme 24: Reagents and conditions: (i): imidazole, *tert*-butyldimethylchlorosilane, DMF (87%); (iii): 2,6-lutidine, OsO_4, 2-methyl-2-propanol, $NaIO_4$ (88%)

The ^{1}H NMR spectrum of (**68**) showed the appearance of the aldehyde proton as a singlet at δ 9.81 and a signal at δ 200.4 corresponding to the aldehyde carbon.

2.2.3.3 The preparation of aldehyde (54)

A modified Julia-Kocienski olefination of the resultant aldehyde (**68**) and the sulfone (**66**) in the presence of lithium *bis*(trimethylsilyl)amide in dry THF, gave a mixture of the *E*- and *Z*-alkenes (**135**) in a ratio of 3.7:1 (**Scheme 25**). The mixture was then saturated by hydrogenation in ethyl acetate using Pd (10%) on carbon as a catalyst under hydrogen atmosphere for one hour, which gave the hydrogenated benzyl compound (**65**) in excellent yield. Then, the hydrogenation and debenzylation of compound (**65**) was carried out for three days using Pd (10%) on carbon as a catalyst under hydrogen atmosphere to give the saturated compound (**64**) (**Scheme 25**). The ^{1}H NMR spectrum of alcohol (**64**) showed a multiplet at δ 3.63–3.52 for the proton adjacent to the TBDMS group and a doublet of doublets of doublets at δ 2.79 (*J* 3.8, 6.3, 10.1 Hz) for the proton at the α-position. The ^{13}C NMR spectrum showed signals at δ 71.7 for the carbon next to the silyl protecting group and δ 59.0 for the carbon next to the hydroxyl group. The IR spectrum showed a broad peak at 3449 cm^{-1} for the O–H stretch; all these data matched those in the literature.[378]

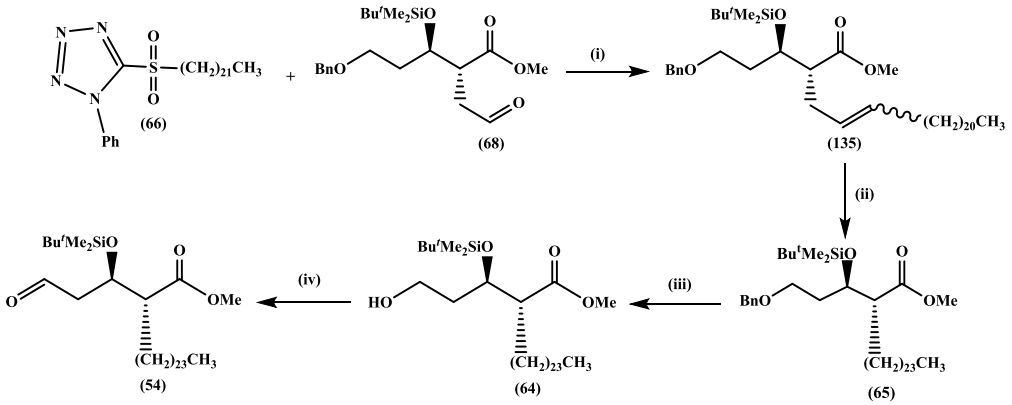

Scheme 25: Reagents and conditions: (i): LiN(SiMe$_3$)$_2$, dry THF (83%); (ii): -10 ºC, H$_2$, Pd (10%) on C, ethyl acetate (98%); (iii): Pd (10%) on C, H$_2$, ethyl acetate, 3 days (95%); (iv): PCC, CH$_2$Cl$_2$ (90%)

The primary alcohol (**64**) was then oxidised, employing PCC in CH_2Cl_2 suspension, to give the required aldehyde (**54**) (**Scheme 25**). The ^{1}H NMR spectrum of the aldehyde (**54**) showed a doublet of doublets at δ 9.81 (*J* 1.6, 2.7 Hz) for the aldehyde proton, and a very broad multiplet at δ 1.61–1.26 for the long chain protons.

2.2.3.4 The preparation of intermediate aldehyde (51)

The sulfone (**53**) was coupled with the aldehyde (**54**) using a modified Julia-Kocienski olefination with lithium *bis*(trimethylsilyl)amide at –10 °C to afford the alkene (**136**) as a mixture of *E*- and *Z*-isomers in a ratio of 2.3:1. The ^{1}H NMR spectrum showed multiplets at δ 5.46–5.39 for the two alkene protons, and a multiplet at δ 1.26–1.21 for the long chain protons. The ^{13}C NMR spectrum showed two signals at δ 132.6 and δ 127.5 for the olefinic carbons of the major *E*-isomer and another two signals at δ 131.6 and 127.1 for the olefinic carbons of the minor *Z*-isomer. The cyclic acetal carbon appeared at δ 108.4 and two signals appeared at δ 79.9 and δ 67.8 for the carbons adjacent to the oxygen atoms. The alkene mixture was then saturated by hydrogenation in ethyl acetate using Pd (10%) on carbon as a catalyst under a hydrogen atmosphere to give the saturated product ester (**52**) (**Scheme 26**).

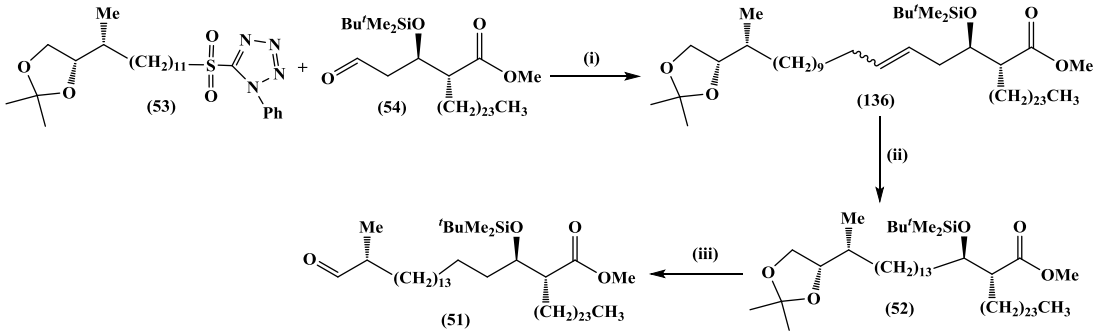

Scheme 26: Reagents and conditions: (i): $LiN(SiMe_3)_2$, dry THF (96%); (ii): -10 °C, H_2, Pd (10%) on C, ethyl acetate (96%); (iii): HIO_4, dry ether (87%)

The ^{1}H and ^{13}C NMR spectra showed that there were no signals in the olefinic region, which proved that the hydrogenation had been successful.

This was followed by the oxidative cleavage of (**52**) with periodic acid in dry ether, and led to the corresponding aldehyde (**51**) in 87% yield. The ^{1}H NMR spectrum showed a doublet at δ 9.77 (*J* 2.0 Hz) for the aldehyde proton, a double double of doublet at δ 2.53 (*J* 3.8, 7.0, 11 Hz) for the α-H next to the ester group, a broad doublet of quartet at δ 2.42 (*J* 1.9, 7.6 Hz) for the proton next to the aldehyde group and a doublet at δ 1.09 (*J* 7.0 Hz) for the methyl protons at the *α*-position to the aldehyde. The ^{13}C NMR spectrum showed signals at δ 202.8 for the carbonyl carbon of the aldehyde, at δ 43.9 for the carbon next to the aldehyde and at δ 18.0 for the carbon of the methyl at the *α*-position with respect to the aldehyde.

On the basis of a consideration of a number of references concerning the synthesis and reaction of closely allied species,[408,409,410] we can be confident that no significant epimerization of the *α*-position occurs under the conditions to which the aldehyde is exposed in the period between its formation and its reaction in the subsequent step. For example, Al Kremawi *et. al.* [411] demonstrated that the oxidative cleavage of the acetal (**137**) with periodic acid in dry ether gave the aldehyde (**138**) with retention of chirality (**Figure 38).**

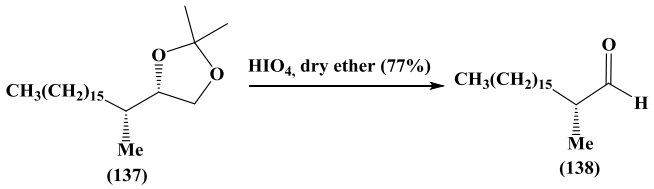

Figure 38: The oxidative cleavage of the acetal (137)

Another example of this occurs in the work of Sarabia *et. al.*[410] Here, the cleavage of the hydrazone moiety by exposure to ozone gave the aldehyde (**139**). This was then treated with a stabilized yield to afford the α,β-unsaturated ester (**141**), **Figure 39.**

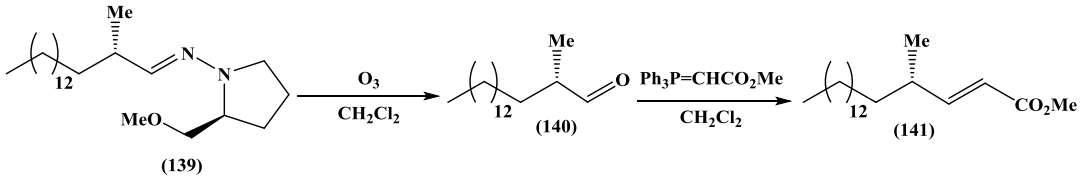

Figure 39: Preparation of α,β-unsaturated ester (141)

2.2.4 Coupling the meromycolate moiety and corynomycolate

A typical modified Julia-Kocienski olefination using lithium *bis*(trimethylsilyl)amide would give the olefin product as a mixture of *cis*- and *trans*- stereoisomers. Therefore, as isolation of the *trans*-olefin would be highly problematic, lithium *bis*(trimethylsilyl)amide was not used as the base. Kocienski *et al*. and Pospíšil *et al*. both discussed the use of different bases, most significantly potassium *bis*(trimethylsilyl)amide, to increase stereoselectivity in favour of the *trans*-isomer. [412 , 413] Koceinski *et al*. discovered that changing the base used increases stereoselectivity in the order Li<Na<K, and Pospíšil *et al*. gives evidence that increases in the size of the alkyl chain of the aldehyde lead to higher stereoselectivity. Therefore, the aldehyde (**51**) was coupled with the sulfone (**50**) in the presence of potassium *bis*(trimethyl-silyl)amide in dry 1,2-dimethoxyethane to give the *trans*-alkene (**49**) (**Scheme 27**).

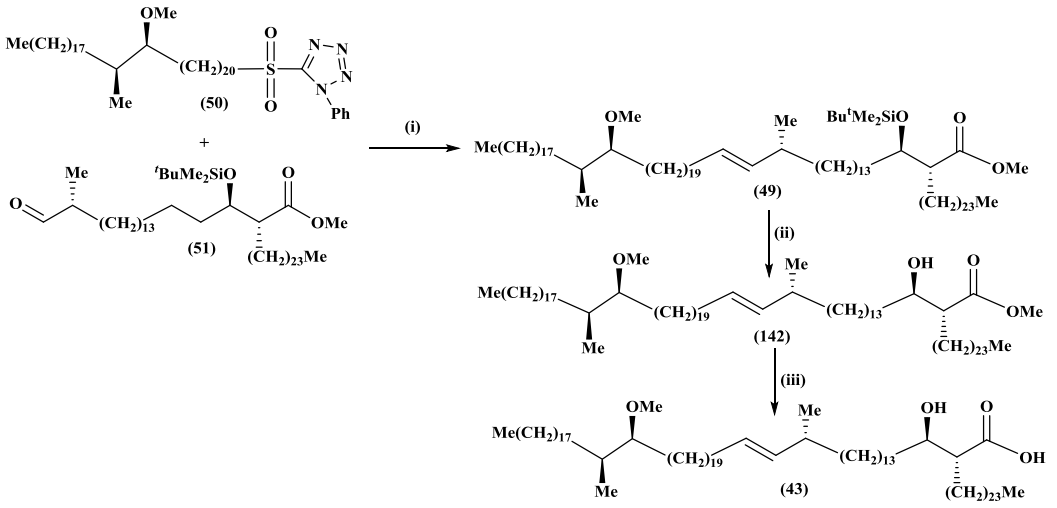

Scheme 27: Reagents and conditions: (i): Potassium *bis*(trimethylsilyl)amide, 1,2-dimethoxyethane (37%); (iii): HF-pyridine complex, pyridine, THF (96%); (iv): LiOH, MeOH, H_2O, THF (82%)

The stereoselective formation of the *trans*-isomer was confirmed by ^{1}H NMR spectroscopy, which showed two olefinic protons at δ 5.33 and δ 5.24, each with a coupling constant of 15 Hz, and corresponding to the two *trans*-protons of the double bond. The ^{13}C NMR spectrum of (**49**) showed signals at δ 136.5 and δ 128.4, corresponding to just two olefinic carbons.

2.2.4.1 The deprotection of the silyl group

The ester (**49**) was dissolved in dry THF in a dry polyethylene vial under nitrogen atmosphere, followed by addition of pyridine and HF.pyridine. Stirring of the mixture at 42 ^{o}C for 17 h gave the alcohol (**142**) as a white solid (**Scheme 27**). The NMR spectra showed that the singlet at δ 0.87 for the nine protons of the *tert*-butyl component and two singlets at δ 0.05 and δ 0.03 for the six protons of the two methyl groups bonded to silicon had disappeared.

2.2.4.2 The hydrolysis of deprotected ester

The hydrolysis of ester (**142**) was achieved using lithium hydroxide monohydrate in a mixture of THF, methanol and water at 43 °C and gave the free mycolic acid (**43**) in 82% yield, (**Scheme 27**). This was confirmed by the loss of the singlet signal at δ 3.72 for the methyl ester in the spectrum of (**43**) corresponding to (COO$\underline{CH_3}$). The IR spectrum also confirmed the formation of free mycolic acid, which showed a broad peak at 3470 cm^{-1} for the O–H stretch. Furthermore, the MALDI MS showed the correct mass ion.

2.2.4.3 The NMR analysis of *S,S-trans*-alkene-methoxy mycolic acid

Detailed analysis of the ^{1}H NMR spectrum of synthetic *S,S-trans*-alkene-methoxy mycolic acid (**Figure 40**) was undertaken in order to characterize all chiral centres and the double bond

present in the structure of the free mycolic acid. Expansions of the various regions of the ^{1}H NMR spectrum of (**43**) are shown in **Figure 41**.

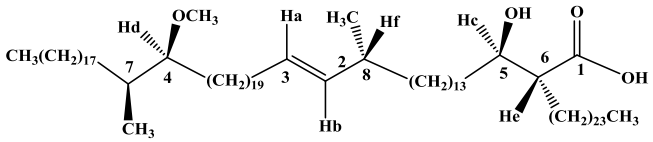

Figure 40: Full ^{1}H NMR analysis of *S,S-trans*-alkene-methoxy mycolic acid (43)

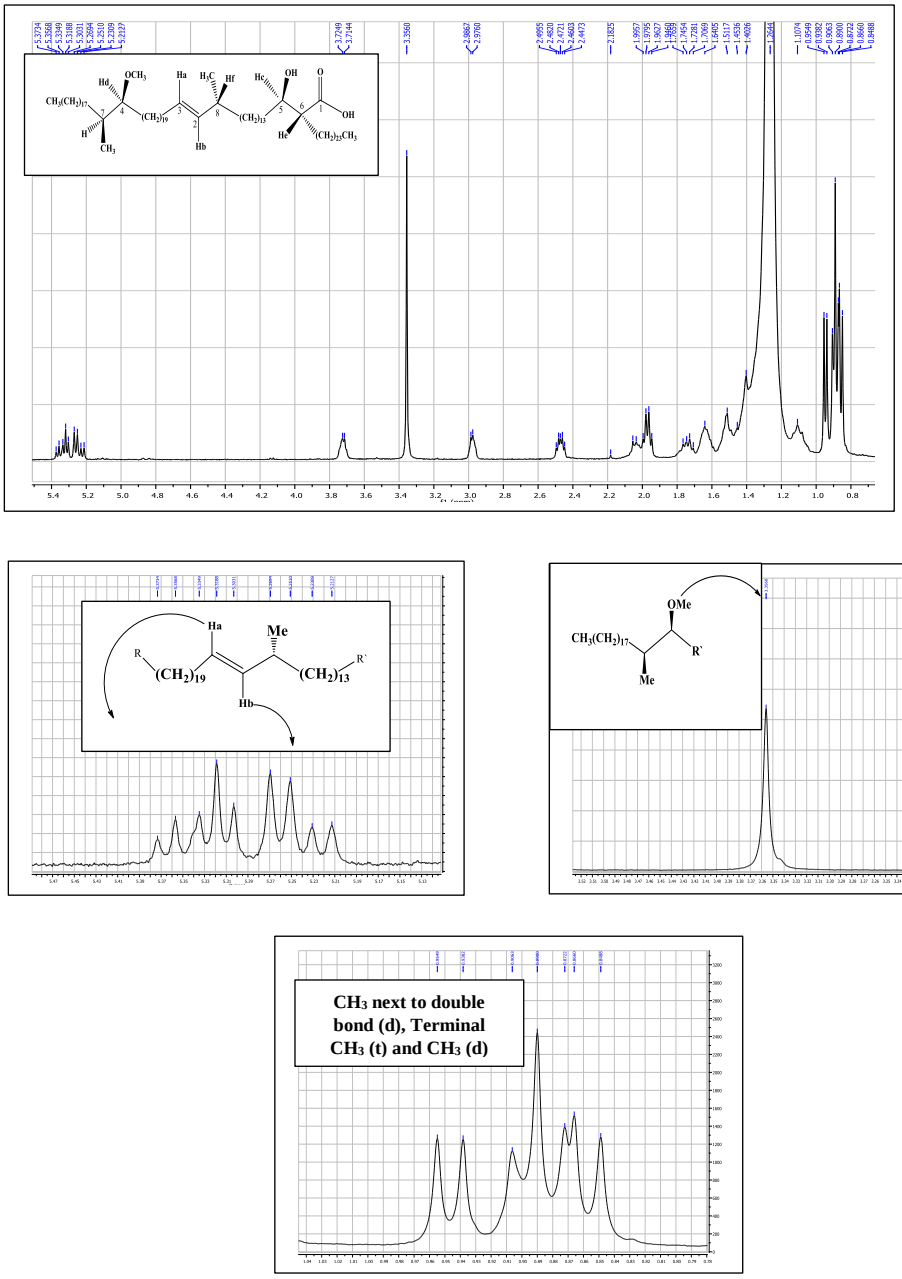

Figure 41: ^{1}H NMR spectrum of *S,S-trans*-alkene-methoxy mycolic acid (43)

The ^{1}H NMR spectrum of acid (**43**) showed a doublet of triplets at δ 5.33 (*J* 6.4, 15.2 Hz) and a double doublet at δ 5.24 (*J* 7.4, 15.2 Hz) corresponding to the alkene protons. The signal corresponding to H_c and H_d is a multiplet at δ 3.73-3.70 and δ 2.98-2.96 respectively, but the protons of the methoxy group appeared as a singlet at δ 3.35. The Figure also shows a multiplet at δ 2.0-1.97 and a broad quartet at δ 1.96 corresponding to H_f and $C\underline{H_2}$ next to the double bond. Also, a signal occurs at δ 1.55-1.15 as a multiplet corresponding to the long-chain protons. Finally, signals occur as a doublet at δ 0.94 (*J* 6.7 Hz), a triplet at δ 0.89 (*J* 6.5 Hz) and a doublet at δ 0.85 (*J* 6.9 Hz), corresponding to the CH_3 next to the double bond, the terminal CH_3 and the CH_3 next to the methoxy group respectively, as seen in **Table 1**.

Table 1: ^{1}H NMR analysis of *S,S-trans*-alkene-methoxy mycolic acid (43)

H_X	H's	Class	δ	*J*/Hz
H_a	1	dt	5.33	6.4, 15.2
H_b	1	dd	5.24	7.4, 15.2
H_c	1	m	3.73-3.70	-
OCH_3	3	s	3.35	-
H_d	1	m	2.98-2.96	-
H_e	1	m	2.49-2.44	-
H_f	1	m	2.0-1.97	-
CH_2 next to double bound	2	br. q	1.96	6.7
CH_3	3	d	0.94	6.7
Terminal CH_3	6	t	0.89	6.5
CH_3	3	d	0.85	6.9

The ^{13}C NMR spectrum showed all expected signals for the carbons present in *S,S-trans*-alkene-methoxy mycolic acid, (**Figure 42 and Table 2**).

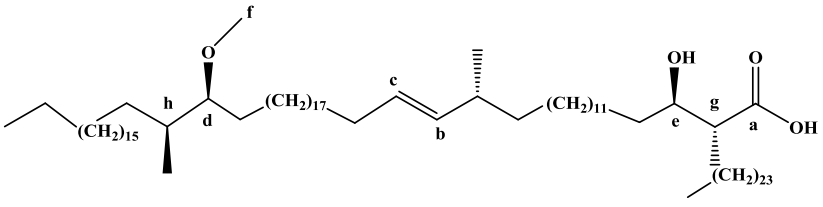

Figure 42: ^{13}C NMR analysis of *S,S*-trans-alkene-methoxy mycolic acid (43)

Table 2: The ^{13}C NMR analysis of *S,S-trans*-alkene-methoxy mycolic acid (43)

C_x	δ	C_x	δ
C_a	179.5	C_e	72.1
C_b	136.5	C_f	57.7
C_c	128.4	C_g	50.7
C_d	85.6	C_h	37.3

The IR spectrum data of full *S,S-trans*-alkene-methoxy mycolic acid indicated the formation of acid **(Table 3**).

Table 3: IR analysis of *S,S-trans*-alkene-methoxy mycolic acid (43)

Stretching	Wave number (cm^{-1})
O-H	3470
C-H	2917
C-H	2854
C=O	1726
$O\text{-}CH_3$	1471

The MALDI-TOF MS spectrum of mycolic acid (**43**) gave 1276.2861 $[M + Na]^+$, the calculated value $C_{85}H_{168}NaO_4$ requires: 1276.2835. The molecular rotation is defined as one-hundredth of the product of the specific rotation and the relative molecular mass of an optically-active compound:

$$[\mathbf{M}]_{\mathbf{D}} = [\boldsymbol{\alpha}]_{\boldsymbol{D}}^{\boldsymbol{x}} \left(\frac{\textbf{Molecular weight}}{\mathbf{100}}\right)$$

In general, the $[M]_D$ in systems where group of chiral centres are separated by long carbon chains are approximately additive. Therefore, the molecular rotations of individual functional groups in natural mixtures of mycolic acids and in model compound have been identified by Quémard *et. al.*[414] The individual values of the *R,R*-centres of the 2-hydroxy acid (ester) fragment in mycolates is estimated as + 40, the $RCH{=}CHCH_3$- fragment as – 25 (for 30% content). The figure for the (*S,S*) α-methyl-methoxy fragment such as (**50**) may be estimated from the present result as - 50 using the relationship above. Therefore, the $[M]_D$ value of the methyl mycolate (**142**) can be estimated as -35 (-50-25+40) based on the sum of methoxy methyl, hydroxy acid and α-methyl trans alkene contributions; the methyl ester gave

experimental value of $[M]_D$= -42. Moreover, the specific rotation of acid (**43**) was determined to be -1.6 (c = 0.99, $CHCl_3$), which corresponds to $[M]_D$ = -20, which is in agreement with the calculated value. By comparison, the specific rotation of the keto mycolic acid (**below**) was determined to be +7.3 (c = 0.79, $CHCl_3$)[4], which corresponds to $[M]_D$ = +92, which is in agreement with the sum of the contributions of an *S*-α-methylketone unit ($[M]_D$ = +44) and an *R, R*-hydroxy acid unit ($[M]_D$ = +40), assuming a very small contribution from the *cis*-cyclopropane component.

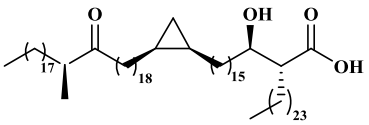

2.3 The synthesis of glycolipids from the *S,S-trans*-alkene-methoxy MA

2.3.1 The synthesis of Cord Factors

The *trans*-alkene mycolic acid **(43)** was protected at the β-hydroxyl group through the addition of *tert*-butyldimethylsilylchloride, imidazole and DMAP in a mixture of dry DMF and dry toluene, and by heating the mixture at 70 ^oC for 24 h, protecting the secondary alcohol and acid group as TBDMS-ether and TBDMS-ester groups, and then selective hydrolysis of the latter using tetrabutyl ammonium hydroxide to give the silyl-protected acid (**143**) in excellent yield (**Scheme 28)**. The ^1H NMR spectrum showed a singlet at δ 0.94 for the nine protons of the *tert*-butyl component and two singlets at δ 0.16 and 0.14 for the six protons of the two methyl groups bonded to silicon. The ^{13}C NMR spectrum also confirmed the protection, which showed that the signals that related to the methyl carbons on the *tert*-butyl group appeared at δ 25.9, the signal for the quaternary carbon at 17.9 and the two signals for the methyl groups bonded to silicon at -4.3 and -4.9.

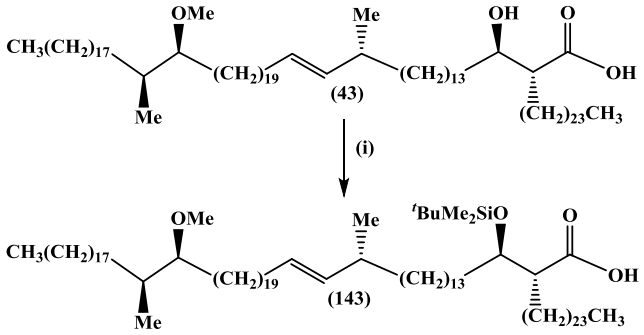

Scheme 28: Reagents and conditions: (i): imidazole, DMF, toluene, *tert*-butyldimethylsilyl chloride, 4-dimethylaminopyridine then tetrabutyl ammonium hydroxide (96%)

Then esterification was achieved between the silyl-protected acid (**143**) and protected trehalose (**144**) after 6 days at r.t. using 1-(3-dimethylaminopropyl)-3-ethylcarbodiimide hydrochloride and DMAP in CH_2Cl_2. This gave two products, protected TDM **(145)** and protected TMM **(146)**, which were separated by column chromatography (**Scheme 29)**.

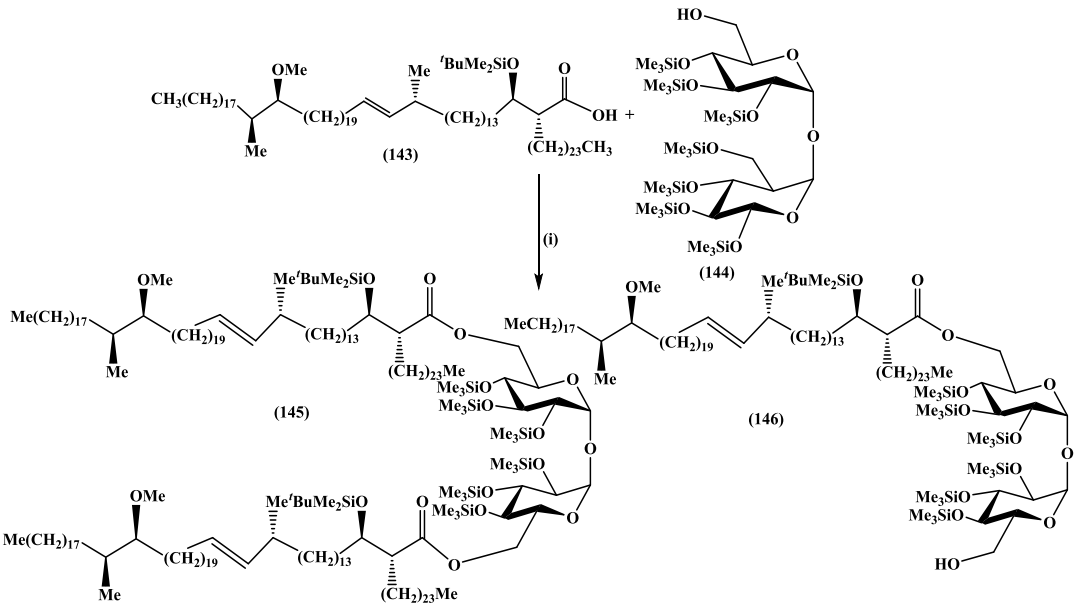

Scheme 29: Reagents and conditions: (i): DMAP/EDCI/CH_2Cl_2; TDM: 25%; TMM: 50%

The ^{1}H NMR spectrum of the TDM **(145)** showed a doublet of triplets at δ 5.35 (*J* 6.4, 15.3 Hz) and a broad double doublet at δ 5.25 (*J* 7.4, 15.3 Hz) for the protons of the double bond, and a broad doublet at δ 4.85 (*J* 3.0 Hz) for the hemiacetal protons. The remaining signals for the sugar protons and the β-hydroxyl protons resonated at δ 4.36, δ 4.01, δ 3.94, δ 3.90, δ 3.52 and δ 3.38. The protons of the methoxy groups showed a singlet at δ 3.34 and the protons adjacent to the methoxy groups showed a broad pentet at δ 2.96 (*J* 4.2 Hz). The α-protons of the mycolic acid appeared as a multiplet at δ 2.57-2.53. The terminal methyl groups gave a triplet at δ 0.89 (*J* 6.6 Hz) and the *tert*-butyl groups showed as a singlet at δ 0.88 with an integration of eighteen protons. The trimethylsilyl protecting groups on the sugar appeared as singlets at δ 0.16, δ 0.15 and δ 0.14 with an integration of eighteen protons for each. The twelve protons of the two methyl groups bonded to silicon in the TBDMS protecting group appeared as a singlet at δ 0.06 in total. The ^{13}C NMR spectrum showed a signal at δ 173.8 for the carbonyl carbon. The double bond carbon signals appeared at δ 136.5 and δ 128.4. Also, the remainder of the sugar carbons gave signals between δ 73.5-70.7. The methyl carbon signals of the protecting silyl groups of the sugar appeared at δ 1.1, δ 0.9 and δ 0.2. Additionally, the carbons of the two methyl groups bonded to silicon in the silyl groups of the mycolate component appeared at δ -4.5 and δ -4.7.

The ^{1}H NMR spectrum of protected TMM **(146)** was more complicated than that of the TDM because of the loss of symmetry. The protons of the double bond appeared in the ^{1}H NMR spectrum as a doublet of triplets at δ 5.34 (*J* 6.4, 15.3 Hz) and a double doublet at 5.24 (*J* 7.4, 15.3 Hz). The hemiacetal protons appeared as two doublets at δ 4.91 (*J* 3.0 Hz) and 4.84 (*J* 3.0 Hz) with an integration of one proton for each. The remaining sugar protons resonated between δ 4.35-3.40. The methoxy protons of the mycolate appeared as a singlet at δ 3.35.

Deprotection of both TDM **(145)** and TMM **(146)** was carried out in two steps; first, the deprotection of the trimethylsilyl groups on the trehalose was achieved with *tetra-n*-butyl ammonium fluoride (TBAF) to give the silyl-protected TDM **(147)** and silyl-protected TMM **(148)** (**Scheme 30)**. The ^{1}H NMR spectrum of TDM **(147)** showed a doublet of triplets at δ 5.27 (*J* 6.5, 15.3 Hz) and a double doublet at δ 5.18 (*J* 7.4, 15.3 Hz) for the protons of the double bond and the doublet for the hemiacetal protons was shifted to δ 5.04 (*J* 3.4 Hz). The remaining signals for the sugar protons and the β-hydroxyl protons resonated at δ 4.3, δ 4.2, δ 3.91, δ 3.85, δ 3.76, δ 3.44 and δ 3.32, and were also shifted. The protons of the methoxy groups showed as a singlet at δ 3.3 and the protons adjacent to the methoxy groups showed as a multiplet at δ 2.94-2.91. The terminal methyl groups gave a triplet at δ 0.84 (*J* 6.3 Hz) and the *tert*-butyl groups showed as a singlet at δ 0.81 with an integration of eighteen protons. The signals corresponding to the trimethylsilyl protecting groups on the sugar were not present in the spectrum, which confirmed that the reaction had been successful.

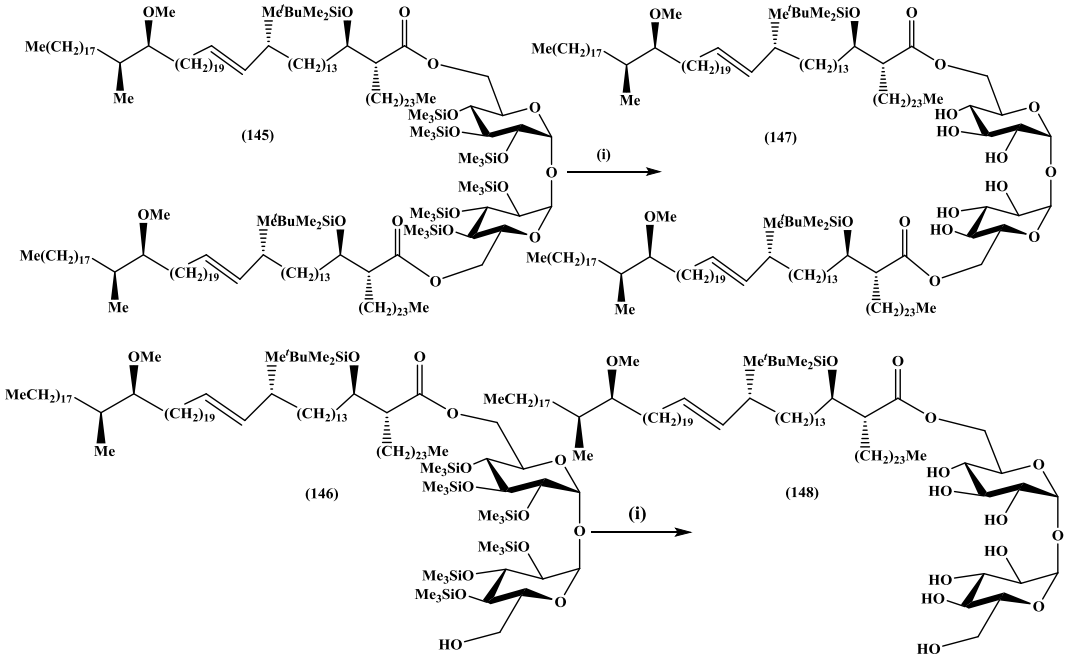

Scheme 30: Reagents and conditions: (i): Tetrabutylammonium fluoride/THF, TDM: (67%); TMM: (65%)

The ^{1}H NMR spectrum of the silyl-protected TMM **(148)** showed a doublet of triplet at δ 5.28 (*J* 6.5, 15.5 Hz) and a double doublet at δ 5.19 (*J* 7.6, 15.5 Hz) for the protons of the double bond, while the hemiacetal protons appeared as a broad triplet at δ 5.05 (*J* 3.5 Hz) and a double doublet at δ 4.3 (*J* 4.6, 12.3 Hz) with an integration of one proton for each. The remaining sugar protons resonated between δ 4.23-3.46. The signal for the methoxy group of the mycolate appeared as a singlet at δ 3.3. The signals belonging to the trimethylsilyl protecting groups of the sugar at δ 0.17, 0.16 and 0.15 were not present in the ^{1}H NMR spectrum, and the signals at δ 1.1, δ 1.0 and δ 0.9, corresponding to the carbons of the trimethylsilyl groups, were also absent from the ^{13}C NMR spectrum.

Subsequently, the deprotection of the silyl group present in the mycolate components of TDM (**147**) and TMM (**148**) was achieved using HF-pyridine and pyridine in dry THF, which gave free TDM (**44**) and TMM (**45**) in 75% and 65% yield respectively as seen in **Scheme 31.**

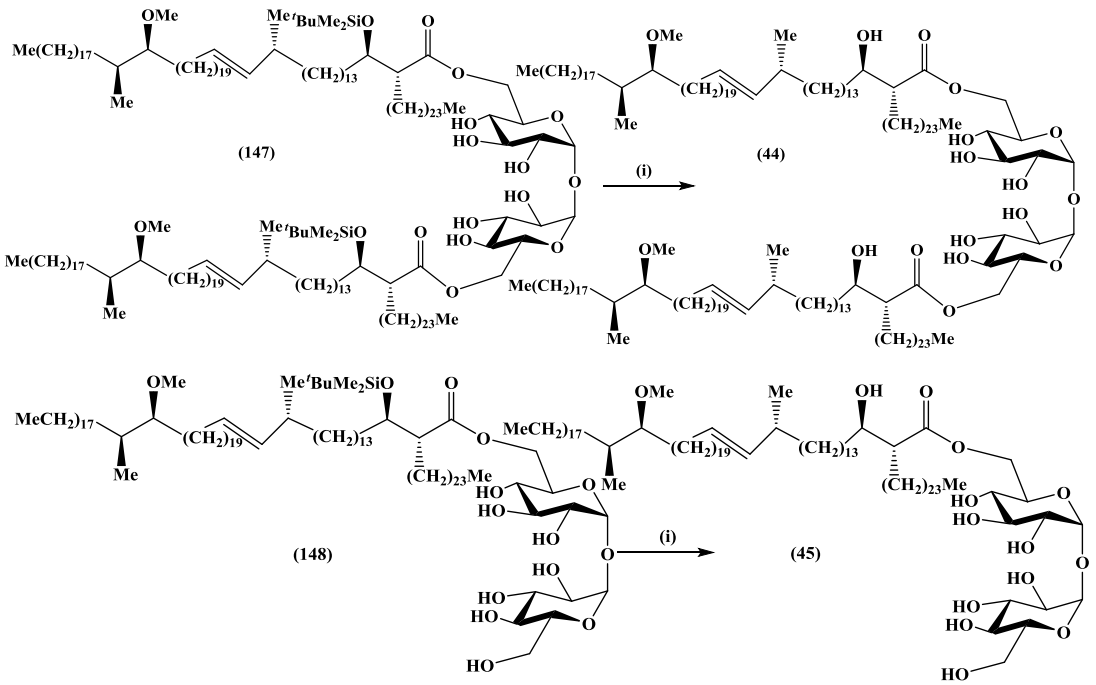

Scheme 31: Reagents and conditions: (i): HF-pyridine complex, pyridine, THF, TDM: (75%); TMM: (65%)

The structure of free TDM **(44)** was confirmed by the ^{1}H NMR spectrum. The hemiacetal protons showed a broad doublet at δ 5.0 (*J* 3.4 Hz). The rest of the sugar protons resonated at δ 4.68, δ 4.23, δ 4.0-3.94, δ 3.67-3.62 and δ 3.5, with an integration of two protons for each. The protons adjacent to the β-hydroxyl of the mycolate components showed a broad triplet at δ 3.74 (*J* 9.3 Hz), while the methoxy groups gave a singlet at δ 3.32. A multiplet signal appeared at δ 2.96-2.93 for the protons adjacent to the methoxy group, and a multiplet occurred between δ 2.40-2.20 for the protons in the α-position next to the alkyl chain of the mycolate. The terminal

methyl groups gave a triplet at δ 0.86 (*J* 6.7 Hz) with an integration of twelve protons, while the methyl adjacent to the methoxy group gave a doublet at δ 0.82 (*J* 6.7 Hz) with an integration of six protons; the signal at δ 0.81 and those at δ -0.003 and -0.023 corresponding to the TBDMS group, were absent from the spectrum. The ^{13}C NMR spectrum showed no signals belonging to the TBDMS group at δ -4.6 and -5.0. The MALDI-TOF MS spectrum also indicated the formation of free TDM **(44)**, which showed the correct mass ion at 2835.6751 ([M + Na]$^{+}$ for $C_{182}H_{354}NaO_{17}$ requires: 2835.6728).

The ^{1}H NMR spectrum of free TMM **(45)** showed that the hemiacetal protons as doublets at δ 5.03 (*J* 3.2 Hz) and δ 4.98 (*J* 3.3 Hz). The rest of the sugar protons resonated between δ 4.61 and δ 3.44. The signals belonging to the methoxymycolate component were similar to those of the free TDM, albeit integrating to half the number of protons. No singlet signal for the nine protons of the *tert*-butyl group was present at δ 0.81, and neither were those signals at δ -0.003 and -0.024 corresponding to the two methyl groups bonded to silicon (**Figure 43**).

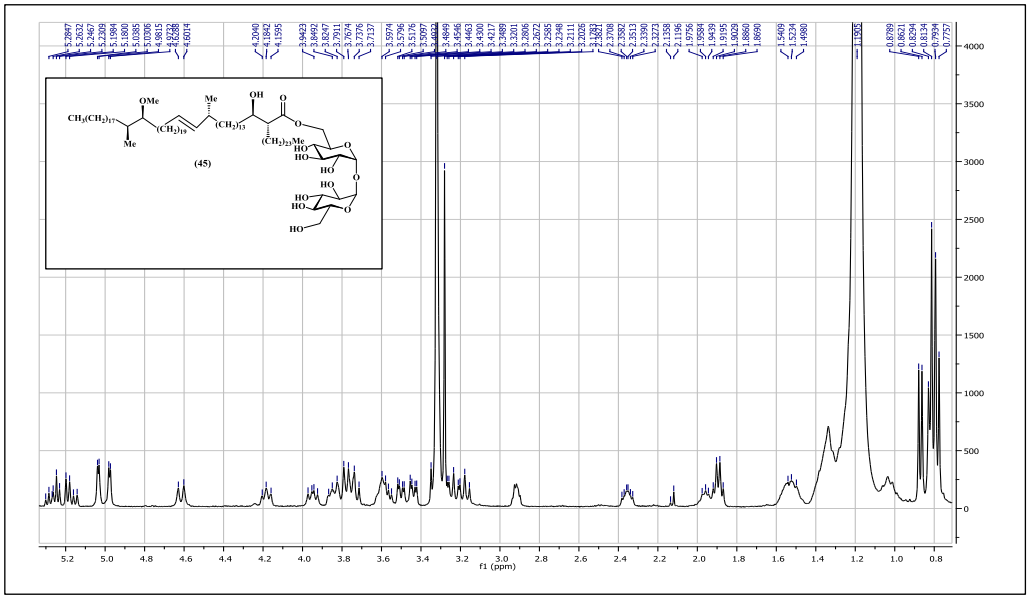

Figure 43: ^{1}H NMR spectrum of TMM (45)

The ^{13}C NMR spectrum confirmed the formation of free TMM with the loss of the signals of the methyl carbons of the *tert*-butyl group at δ 25.7, the signal for the quaternary carbon at δ 17.8 and at δ -4.6 and -5.0 for the carbons of the two methyl groups bonded to silicon.

2.3.2 The synthesis of GroMM

The esterification was undertaken between the free mycolic acid **(43)** and protected glycerol **(149)** using cesium hydrogen carbonate to generate the carboxylate nucleophile, and gave

protected GroMM (**150**) in 89% yield (**Scheme 32**). The ^{1}H NMR spectrum of this showed a multiplet at δ 7.4-7.28 for the ten aromatic protons. The signal for the proton at the α-position in the mycolate component appeared as a broad triplet of doublets at δ 2.44 (*J* 5.4, 9.8 Hz). Protons corresponding to the double bond were revealed as a doublet of triplets at δ 5.34 (*J* 6.4, 15.3 Hz) and a double doublet at δ 5.25 (*J* 7.4, 15.3 Hz) (**Scheme 32**). Two doublets occurred at δ 4.7 (*J* 12.0 Hz) and δ 4.65 (*J* 12.0 Hz) for (PhC$\underline{H}_2$), and one broad singlet at δ 4.6 for the second (PhC$\underline{H}_2$). Two double doublets occurred at δ 4.44 (*J* 4, 11.6 Hz) and δ 4.23 (*J* 5.4, 11.6 Hz) for the protons next to the ester group, and a singlet was present at δ 3.36 corresponding to the methoxy group. The ^{13}C NMR spectrum showed signals for the carbonyl ester at δ 175.4 and for the benzylic carbons at δ 73.5 and 72.3. The signals for C**8**, C**6** and C**7** in the glycerol unit appeared at δ 69.6, 75.8 and 63.5 respectively.

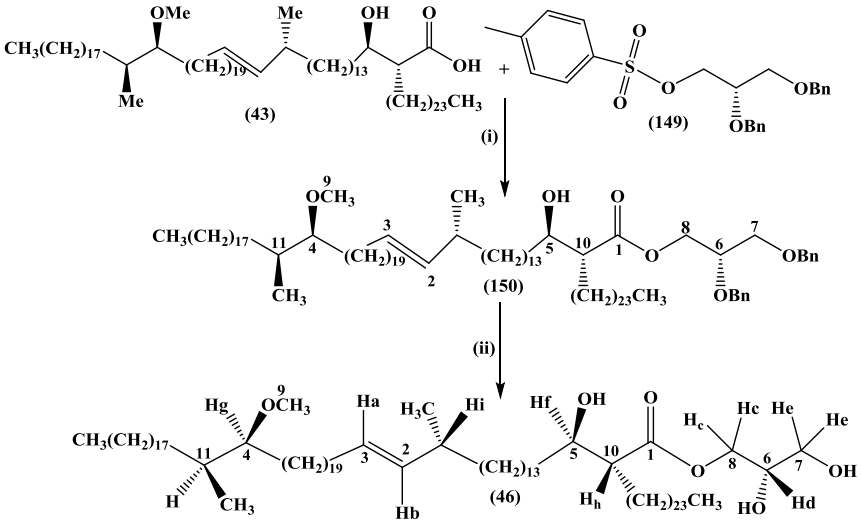

Scheme 32: Reagents and conditions: (i): cesium hydrogencarbonate, (*S*)-2,3-*bis*(benzyloxy)-propyl 4-methylbenzenesulfonate, DMF:THF (1:5), 70 ºC (89%); (ii) Na, NH_3, 1,4-dioxane (40%)

The selective deprotection of the benzyl groups in the presence of both the double bond and methoxy group proved to be difficult, and standard hydrogenation using palladium 10% on carbon failed because it also attacked the double bond in the mycolate component of the GroMM **(150)**. The ^{1}H NMR spectrum showed no signals related to the olefin in the mycolate. Another procedure was therefore used to remove the benzyl group, treating compound **(150)** with BCl_3 in CH_2Cl_2 at - 78 ºC.[415] This removed the benzyl group, however, but also the methoxy group from the mycolate, as confirmed by the ^{1}H NMR spectrum. Selective removal of the benzyl groups in (**150**) was finally achieved using sodium in liquid ammonia, and gave GroMM (**46**) in 40% yield. The ^{1}H NMR spectrum of the glycolipid GroMM (**46**) showed no aromatic signalss, while the two signals presenting as double doublets for the two protons next to the ester group had shifted to δ 4.27 (*J* 4.2, 11.5 Hz) and 4.21 (*J* 6.4, 11.5 Hz). Two multiplets

at δ 3.96-3.91 and 3.71-3.65 corresponded to the three protons next to the hydroxyl groups, and a singlet occurred at δ 3.3 for the methoxy group. A broad multiplet at δ 2.4 corresponded to the proton in the **α** position of the mycolate, as shown in **Figure 44** below.

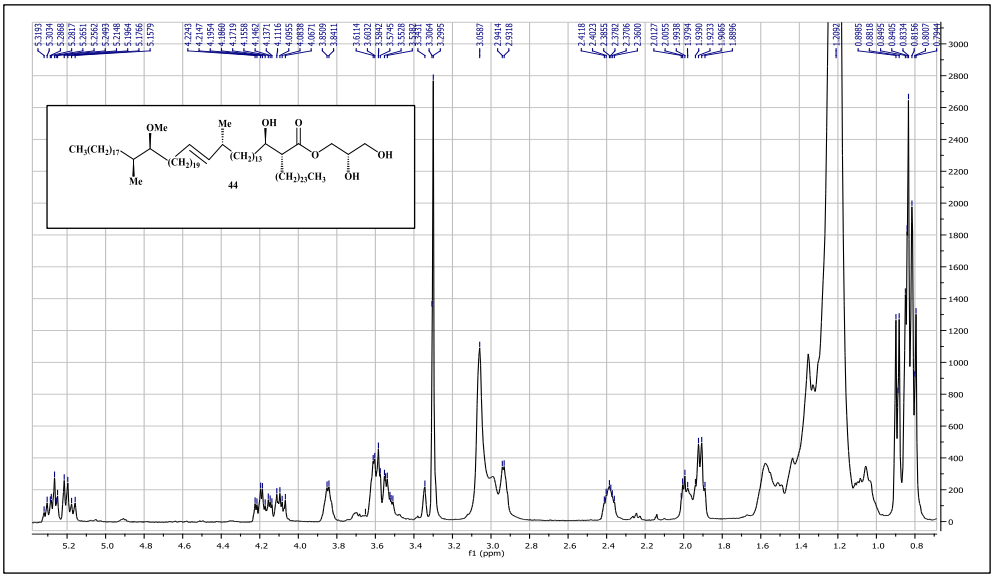

Figure 44: ^{1}H NMR spectrum of free GroMM (46)

Selected ^{1}H NMR data analysis of free GroMM (**46**) can be seen in **Table 4**.

Table 4: The ^{1}H NMR analysis of GroMM (46)

H_X	H's	Class	δ	*J*/Hz
H_a	1	Dt	5.33	6.4, 15.3
H_b	1	Dd	5.23	7.4, 15.3
H_c	1	Dd	4.27	4.2,11.5
H_c	1	Dd	4.21	6.4, 11.5
H_d	1	M	3.96-3.91	-
H_e, H_f	2	M	3.71-3.65	-
H_e	1	br. dd	3.61	5.5, 11.5
OCH_3	3	S	3.3	-
H_g	1	br. m	2.97-2.94	-
H_h	1	M	2.48-2.42	-
H_i	1	M	2.06-2.01	-
CH_2 next to the double bound	2	br. q	1.96	6.6
Long chain	146	M	1.71-1.05	-
CH_3 α-to the double bond	3	D	0.93	6.7
Terminal CH_3	6	T	0.88	6.6
CH_3	3	D	0.84	6.9

The ^{13}C NMR spectrum showed no signals for the benzylic carbons at δ 73.5 and 72.3, but all signals expected for the carbons present in GroMM (**46**) were seen (**Table 5**).

Table 5: The ^{13}C NMR data analysis of free GroMM (46)

C_x	δ	C_x	δ	C_x	δ	C_x	δ
C_1	**175.5**	C_4	**85.5**	C_7	**65.1**	C_{10}	**52.5**
C_2	**136.4**	C_5	**72.6**	C_8	**63.0**	C_{11}	**37.1**
C_3	**128.3**	C_6	**69.8**	C_9	**57.6**		

2.3.3 The synthesis of GMM

The esterification was undertaken between the free mycolic acid (**43**) and the tosylate (**151**) using cesium hydrogen carbonate in THF and DMF (5:1) at 70 ^oC for 18 h, giving protected GMM (**152**) in 70% yield (**Scheme 33**). The ^1H NMR spectrum of this showed a multiplet at δ 7.4-7.26 for twenty aromatic protons, a doublet of triplets at δ 5.34 (*J* 6.4, 15.4 Hz) and a double doublet at δ 5.24 (*J* 7.4, 15.4 Hz), for the alkene protons in the mycolate. The signals for of each benzylic CH_2 group appeared as doublets in the range δ 4.97 - 4.61. A broad doublet occurred at δ 4.56 (*J* 11 Hz), for the proton attached to C-6. A doublet at δ 4.52 (*J* 7.6 Hz) corresponded to the β-anomeric proton attached, and a double doublet at δ 4.22 (*J* 4.6, 11 Hz) to the second proton attached to C-6. The spectrum also showed a broad triplet at δ 3.67 (*J* 8.7 Hz) for the proton on C-2 and C<u>H</u>-OH of the mycolate. A multiplet at δ 3.54-3.47 corresponds to protons attached to C-3, C-4 and C-5. Further, the methoxy group appeared as a singlet at δ 3.35. The ^{13}C NMR spectrum showed signals for the carbonyl at δ 175.2 and for the alkene carbons at δ 136.5 and 128.5. The signals for the aromatic carbons appeared at δ 137.7 - 127.7, while those of the sugar appeared at δ 102.3, 84.5, 82.3, 77.8 and 72.8 from C1 to C5, and C6 at δ 62.9. Positions C10 and C11 (β-hydroxy position) appeared at δ 85.4 and 72.3 respectively; the MA methoxy group at δ 57.7.

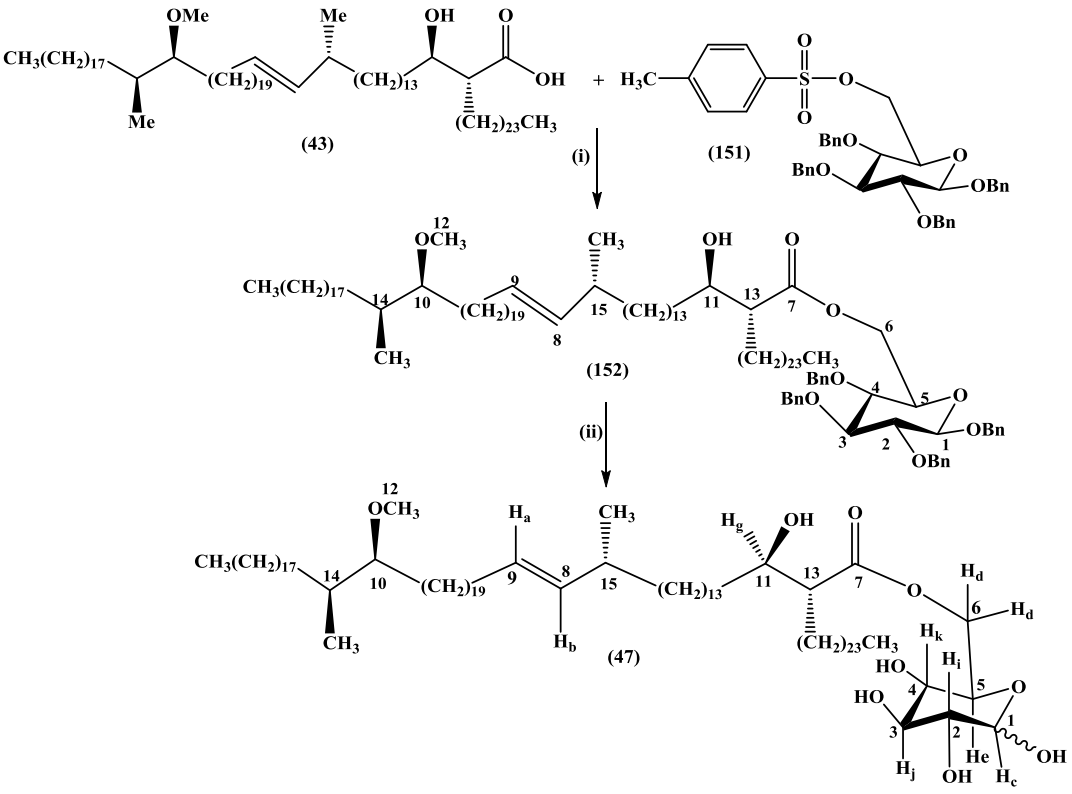

Scheme 33: Reagents and conditions: (i): Cesium hydrogen carbonate, DMF:THF (1:5), 70 ºC (70%); (ii) Na, NH_3, 1,4-dioxane (47%)

Careful removal of the benzyl groups from GMM (**152**) using sodium in liquid ammonia gave deprotected GMM (**47**) as a mixture of α and β anomers in ratio 6:4 in 47% yield. The ^{1}H NMR spectrum confirmed that the deprotection had been successful; the signals for the aromatic protons and for the benzylic CH_2 were not present (**Figure 45**).

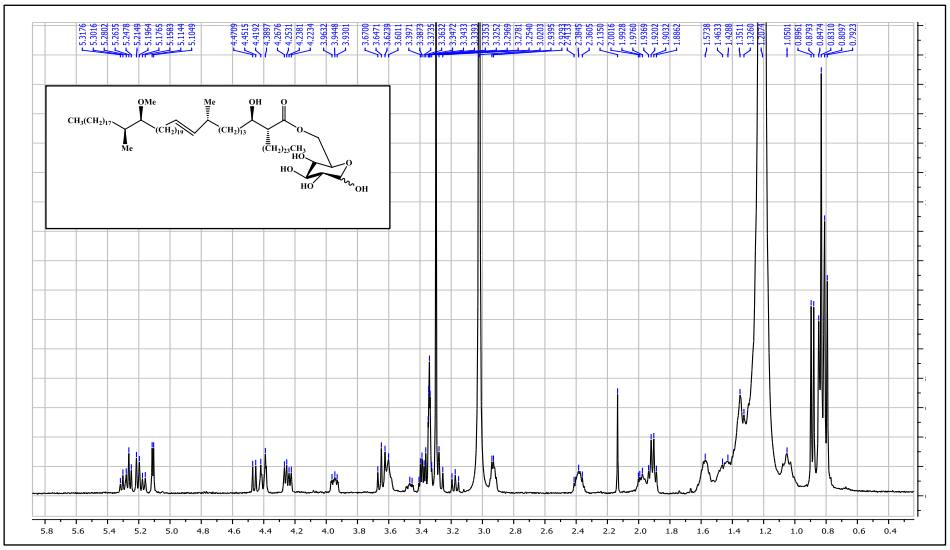

Figure 45: The ^{1}H NMR spectrum of free GMM (47)

The spectrum **(Table 6)** included a doublet of triplets at δ 5.28 and a broad double doublet at δ 5.18 for the alkene protons. A doublet at δ 5.1 corresponds to Hc-α, and another at δ 4.46 to Hc-β. The spectrum also showed a broad doublet at δ 4.4 associated with Hd-α,β, a broad double doublet at δ 4.24 corresponding to Hd-α,β, a double double doublet at δ 3.95 for He-α, and another multiplet at δ 3.67-3.58 for Hk-α and CH-OH of the mycolate component.

Table 6: ^{1}H NMR analysis of GMM (47)

H_X	H's	Class	δ	*J*/Hz
Ha	**1**	**Dt**	**5.28**	**6.4, 15.2**
Hb	**1**	**br.dd**	**5.18**	**7.4, 15.2**
Hc-α	**1**	**D**	**5.1**	**3.8**
Hc-β	**1**	**D**	**4.46**	**7.8**
Hd-α,β	**1**	**br. D**	**4.4**	**11.8**
Hd-α,β	**1**	**br. Dd**	**4.24**	**5.8, 11.8**
He-α	**1**	**Ddd**	**3.95**	**2.2, 5.8, 9.8**
Hk-α and Hg	**2**	**M**	**3.67-3.58**	**-**
He-β	**1**	**Ddd**	**3.46**	**2.2, 5.8, 9.8**
Hi,j-α, Hj,k-β		**M**	**3.43-3.26**	**-**
OCH_3	**3**	**S**	**3.3**	**-**
Hi-β	**1**	**br. T**	**3.17**	**8.4**
CH_3 α-to the double bond	**3**	**D**	**0.88**	**6.7**
Terminal CH_3	**6**	**T**	**0.83**	**6.6**
CH_3	**3**	**D**	**0.80**	**7**

The ^{13}C NMR spectrum showed all the signals expected for GMM (**47**) (**Table 7**).

Table 7: The ^{13}C NMR data analysis of GMM (47)

C_x	δ	C_x	δ	C_x	δ	C_x	δ
C_7	**175.1**	**C-3β**	**76.1**	**C-2α**	**72.1**	**C-6α/β**	**63.4**
C_8	**136.4**	**C-2β**	**74.4**	**C-3α**	**70.4**	**C-12 α/β**	**57.5**
C_9	**128.2**	**C-5β**	**73.6**	**C-4 β**	**70.2**	**C-13α/β**	**52.7**
C-1β	**96.6**	**C-4α**	**73.5**	**C-5α**	**69.1**	**C-13α/β**	**52.5**
C-1α	**92.2**	**C_{11}**	**72.4**	**C-6α/β**	**63.5**	**C_{14}**	**36.6**
C_{10}	**85.5**						

The specific rotation of free GMM **(47)** was $[\alpha]_D^{22}$= +28 (c 0.50, $CHCl_3$). Therefore the $[M]_D$ for the GMM (**47**) is +396, this is high compared to the mycolic acid ester (**142**) which had an $[M]_D$ of -20. This is due to the contribution of the sugar unit.

2.3.4 The synthesis of Arabino-MA fragment from AG

The esterification between the free MA **(43)** and arabinose tosylate (**153**) using cesium hydrogen carbonate gave the protected ester **(154)** in 71% yield (**Scheme 34**). The ^{1}H NMR spectrum showed a multiplet at δ 7.4-7.28 for the aromatic protons, a double triplet at 5.34 (*J* 6.3, 15.4 Hz) and a double doublet at 5.25 (*J* 7.4, 15.4 Hz) for Ha and Hb respectively. A broad singlet at δ 4.92 corresponded to Hc, and the signals for CH_2 of the benzyl group appeared as doublets at δ 4.57-4.48, together with a multiplet at 4.24-4.2 for Hg. A doublet at δ 3.99 (*J* 2.1 Hz) corresponded to Hd and a double doublet at 3.84 (*J* 2.6, 6.5 Hz) to He. A multiplet appeared at δ 4.33-4.26 for Hf. Singlets at δ 3.37 and δ 3.35 corresponded to the two methoxy groups (**Scheme 34**). The ^{13}C NMR spectrum showed signals for the carbonyl at δ 175.0, and at 136.4 and 128.5 for the alkene. The signals for benzyl CH_2 groups appeared at δ 72.4 and 72.1 together with one at δ 72.2 for C11, while C-4, C-5, C-6, C-7 and C-9 were seen at δ 107.2, 87.8, 83.7, 79.4 and 63.4 respectively.

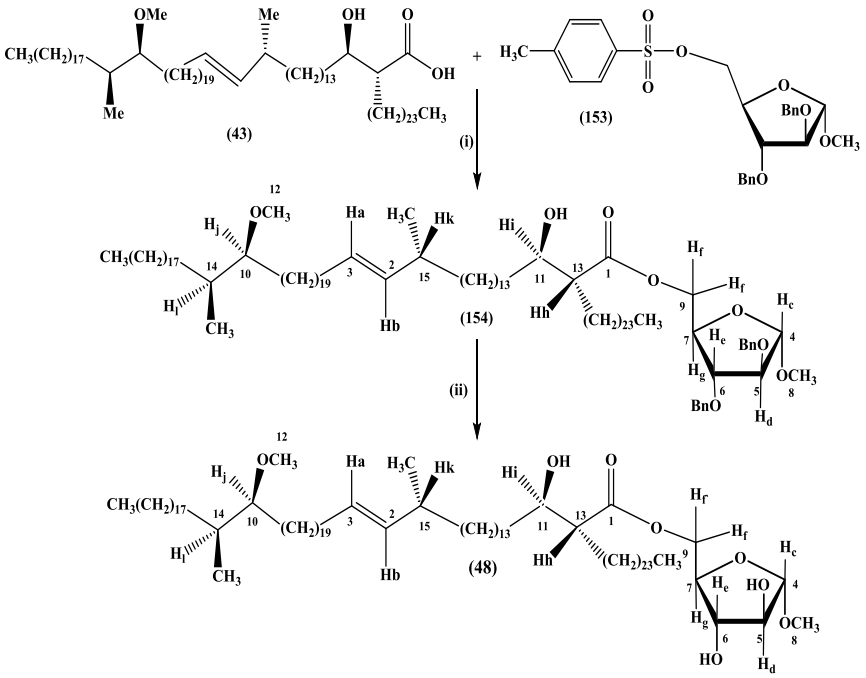

Scheme 34. Reagents and conditions: (i): Cesium hydrogen carbonate, DMF:THF (1:5), 70 °C (71%); (ii) Na, NH_3, 1,4-dioxane (57%)

The removal of the benzyl groups in (**154**) was achieved using sodium in liquid ammonia to give compound (**48**), in 57% yield. In the ^{1}H NMR spectrum (**Figure 46**) the signals for Hc had shifted to δ 4.78 from 4.92 after losing the deshielding effect of the aromatic ring**.**

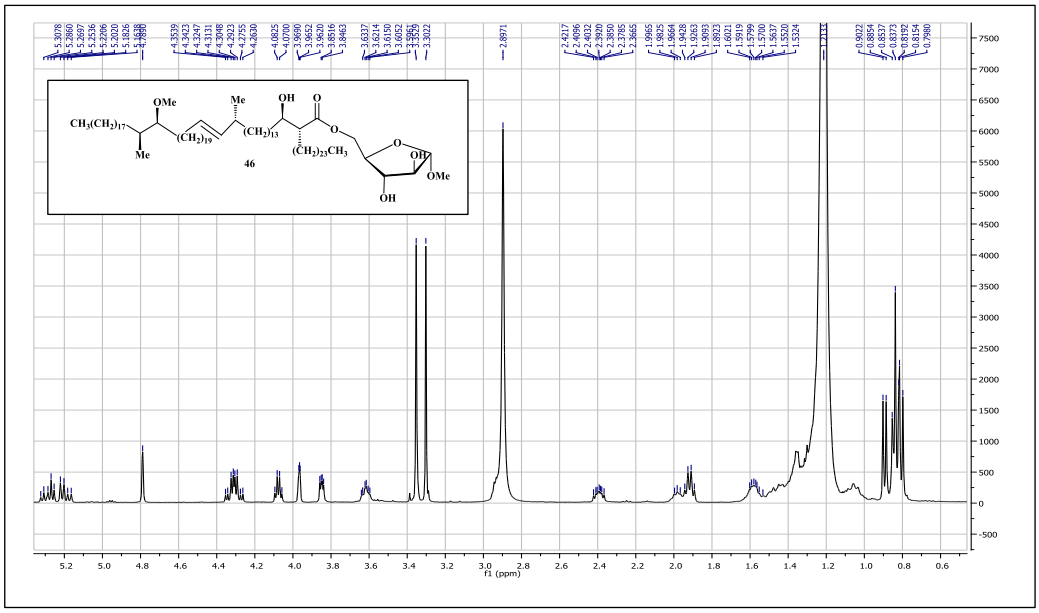

Figure 46. The ^{1}H NMR spectrum of Arabino-MA fragment from AG (48)

Selected ^{1}H NMR data for the Arabino-MA fragment from AG (**48**) can be seen in **Table 8.**

Table 8. ^{1}H NMR analysis of fragment from AG (48)

H_X	H's	Class	δ	*J*/Hz
H_a	1	Dt	5.28	6.4, 15.2
H_b	1	Dd	5.20	7.4, 15.2
H_c	1	br. S	4.78	-
H_f	1	Dd	4.33	4.6, 11.7
H_f	1	Dd	4.28	5, 11.7
H_g	1	br. q	4.08	4.9
H_d	1	Dd	3.96	1.3, 2.8
H_e	1	Dd	3.85	2.8, 5.0
H_i	1	M	3.65-3.60	-
OCH_3	3	S	3.35	-
OCH_3	3	S	3.30	-
H_j	1	M	2.95-2.93	-
H_h	1	Ddd	2.39	4.8, 7.4, 10.2
H_k	1	M	2.01-1.96	-
CH_2 next to the double bond	2	br. Q	1.91	6.6

CH_3 α to the double bond	**3**	**D**	**0.89**	**6.7**
Terminal CH_3	**6**	**T**	**0.84**	**6.6**
CH_3	**3**	**D**	**0.80**	**7**

The ^{13}C NMR spectrum showed all the signals expected for arabinose ester (**48**) (**Table 9**).

Table 9. The ^{13}C NMR data analysis of Arabino-MA (48)

C_x	δ	C_x	δ	C_x	δ	C_x	δ
C_1	175	C_{10}	85.5	C_7	78.0	C_{12}	57.6
C_2	136.4	C_5	81.9	C_{11}	72.4	C_8	55.0
C_3	128.3	C_6	81.2	C_9	63.4	C_{13}	52.6
C_4	108.8						

2.4 Conclusions

The *S,S-trans*-alkene-methoxy mycolic acid (**43**) was prepared using L-ascorbic acid and D-mannitol as starting materials, as they are commercial, cheap and available. The modified Julia-Kocienski olefination, followed by a hydrogenation is an excellent method for chain extension. The modified Julia-Kocienski olefination was also used in the preparation of *trans*-alkene mycolic acid, with retention of the stereochemistry of the adjacent methyl group and optimisation of the *trans*-alkene olefination.

The synthesis of the new cord factors as derivatives of this MA (**43**), started by protection of the secondary hydroxyl group in the MA, followed by esterification between protected mycolic acid (**143**) and protected trehalose (**144**) to give protected TDM (**145**) and TMM (**146**). These were separated and the protecting groups were cleaved in two steps. Firstly, the deprotection of the trehalose sugar with TBAF to give silyl-protected TDM (**147**) and silyl-protected TMM (**148**); secondly the deprotection of the mycolic acids with HF. pyridine complex to get the free TDM (**44**) and TMM **(45**).

The esterification of the free MA (**43**) and protected glycerol (**149**) gave GroMM (**150**). The harder step was the debenzylation in the presence of both the alkene and methoxy group. After attempting different methods, this was achieved using sodium in liquid ammonia. Finally, the free MA (**43**) was esterified with protected glucose tosylate (**151**) and arabinose tosylate (**153**) to give protected GMM (**152**) and the protected Arabino-MA (**154**) respectively. Again, debenzylation in the presence of both the double bond and methoxy was achieved using sodium in liquid ammonia.to give GMM (**47**) and AG (**48**) respectively.

Chapter 3

3. Diagnosis of TB in humans

Immunodiagnostic assays detecting pathogen related Abs in serum of patients with active TB are an attractive alternative for rapid diagnosis.[304] MAs have been the subject of numerous studies for their immunological properties.[375] Antigenic activity of MAs and their glycolipid derivatives such as the extractable lipids, TMM or TDM (cord factors, CFs) has been reviewed recently.[370] CF appears to be one of the most potent immunomodulators in the mycobacterial cell wall.[416] The detection of Abs against CF produced in the serum of patients with pulmonary TB is clinically useful in the rapid seriodiagnosis of the disease;[372] similar approaches have been reported for the diagnosis of Hansen's disease/ leprosy and for *Rhodococcus* ruber.[420]

MAs and their sugar esters, such as TDM, TMM, GMM and GroMM, comprise a large number of structures. In *M. tb*, they consist mainly of α-, keto- and methoxy MA subclasses, each containing mixtures of homologues and, in some cases different stereochemistry around the functional groups in the mero-chain.[188] Synthetic MAs and their derivatives of different functional classes show varying antigenicity against human TB patient serum samples, depending on the functional groups present and on their stereochemistry.[304] Individual synthetic MA significantly can distinguish the TB+ patients from the TB- patients better than the natural mixture of MA.[304] This argues for the potential to improve the specificity of diagnosis of TB with defined single synthetic Ags.

3.1 The aim of the study

The aim of this chapter was to use an ELISA assay with a range of novel synthetic MA and sugar ester antigens to detect Abs as surrogate markers for active human and bovine TB in order to develop a new analytical method for the measurement of disease.

3.2 The contents of this work

In this chapter, the evaluation of a number of sugar esters derived from synthetic mycolic acids as antigens in the diagnosis of active Tb in humans is reported. The mycolic acid structure corresponding to each sugar ester is given in **Table 10**.

Table 10: The structures of different MA and wax ester tested with human sera

Structure	No.	*species*	*TDM*	*TMM*	*GMM*	*GroMM*	*ArM*
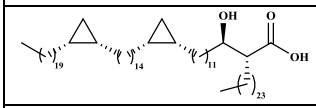	(155)	*M. tb*	(156)	(157)			(158)
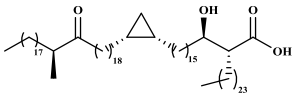	(159)	*M. tb*	(160)	(161)			
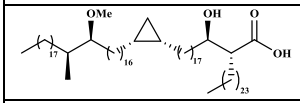	(162)	*M. tb*	(163)	(164)	(165)		
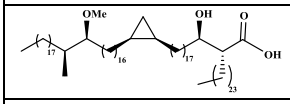		*M. tb*	(166)	(167)			(168)
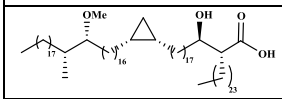		*M. tb*	(169)	(170)			
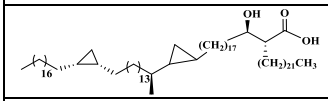		*M. tb*	(171)	(172)			
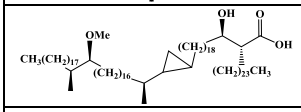		*M. tb*	(173)	(174)			
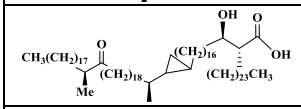		*M. tb*	(175)				
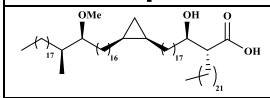		*M. kansasii*			(176)		(177)
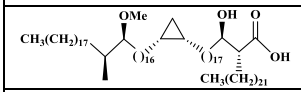		*M. kansasii*			(178)		(179)
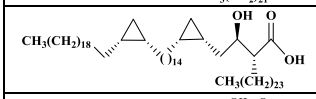		*M. tb*			(180)		
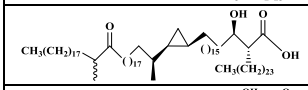		*M. tb*			(181)		
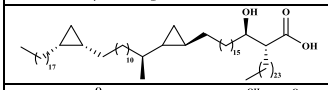		*M. tb*			(182)		
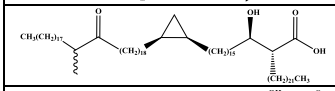		*M. kansasii*					(183)
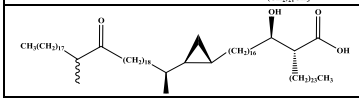		*M. tb*					(184)
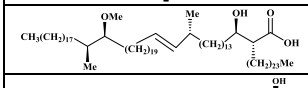		*M. tb*	(44)	(45)	(47)	(46)	(48)
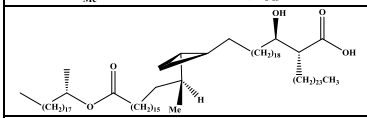	(185)	*M. avium*	(186)				
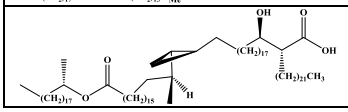	(187)	*M. avium*	(188)	(189)			

In addition, two synthetic TDMs containing different mycolic acids, (**190**) and (**191)** as shown in **Figure 47** were used.

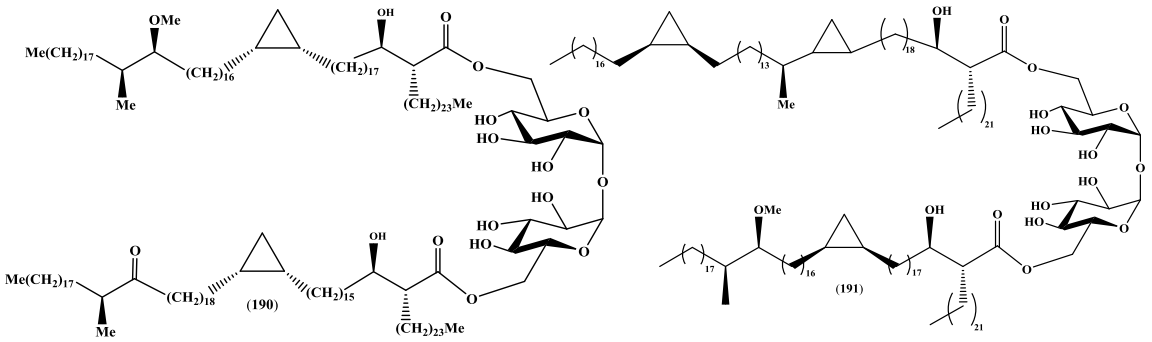

Figure 47: The synthetic TDMs containing different mycolic acids

The first part (**3.5.1**) focused synthetic TDMs (**160**), (**163**), (**188**), and (**190**), TMMs (**164)**, and (**189**), Arabino-MA (177), (**168**), (**183**),(**184**), (**179**) and (**158**) and GMMs (**178**), (**165**), (**176**), (**180**), (**181**) and (**182**) as Ags in the assessment of 9 TB+ and 55 TB- human serum samples obtained from Gambia, and diluted with phosphate-buffered saline containing 0.5% casein/PBS to obtain 1:20 or 1:80 dilution with keto TDM, and a 1:80 dilution with each other Ag. The tests were done by using IgG Fc specific secondary Ab.

The second part (**3.7**) concentrated on the effect of using synthetic keto-MA TDM (**160**), methoxy-MA TDM (**173**), methoxy-MA TDM (**163**) and methoxy-MA TMM (**164**) Ags with 11 TB+ and 51 TB- serum samples from the WHO at a 1:20 dilution, and IgG Fc as secondary antibody. These tests were replicated twice using firstly using 0.5% casein/PBS, secondly with 0.05% PBS-T, to evaluate the effect of the blocking agent.

The third part (**3.8**) used synthetic wax ester (**185**), TDM of this wax ester (**186**), mixed TDM (**191**), keto TMM (**161**), keto MA (**159**) and methoxy TDM (**173**) Ags, with IgG Fc and IgG, and 15 TB+ and 35 TB- serum samples at a 1:20 dilution using casein, again to study the effect of the secondary antibody.

The fourth part (**3.9**) used keto-MA TDM (**160**) from *M. tb* and wax ester (**185**) and its TDM (**186**) from *M. avium* Ags with 14 TB+ and 30 TB- serum samples at a 1:20 dilution, from the WHO, using IgA, IgG, and IgG Fc respectively as a secondary Ab and 0.5% casein/PBS buffer.

The fifth part (**3.10**) used α-TDM (**156**), α-TMM (**157**) and keto-TDM (**175**) and 47 TB- human serum samples from Wales at 1:20 dilution in 0.5% casein/PBS and IgG Fc secondary Ab.

The final part of this study (**3.11**), done by Dr Carys Roberts in the School of Chemistry at Bangor University, focused on the serodiagnostic application of novel glycolipid Ags, TDM (**44**), TMM (**45**), GroMM (**46**), GMM (**47**) and Arabino-MA (**48**) prepared in **Chapter 2**, using 9 TB+ and 11 TB- WHO human serum samples in 1:40 dilution in 0.5% casein/PBS.

3.3 The ELISA method

ELISA assays are direct binding assays for Ab or Ag, and both work on the same principle, but the means of detecting specific binding is different. ELISA has been used in diagnoses of many common infectious diseases such as HIV/AIDS.[366] In this work, synthetic mycolic acid and its glycolipid Ags were used to detect Abs in human (this chapter) and bovine (Chapter 4) serum samples in an ELISA assay using two different procedures.

In the first procedure, the ELISA assay was carried out on 96-well microplates and the purified Ags, either MA or their glycolipids, were dissolved in *n*-hexane at a concentration of 62.5 µg/mL. The Ag solution was diluted and 50 µL was placed in each well. The plates were left to dry at room temperature overnight. Blocking was done with 0.5% casein/PBS (400 µL/ well) and the plates are left to incubate at 25 ^{o}C for 1 h. The casein was aspirated using the LT-3500 plate washer and the plates flicked dry. Then the serum (1:20 dilution in 0.5% casein/PBS, pH 7.4) was added to the plate (50 µL/ well) and left to incubate at 25^{o}C for 1 h. The serum was aspirated and washed three times with (casein/ PBS, 400 µL/ well) using the same plate washer and the plates were flicked dry again. After that, the secondary Ab, i.e. IgG whole molecule (1:1000 dilution in 0.5% casein/PBS) was added to the plate (50 µL/ well) and the plates were left to incubate at 25^{o}C for 30 min. The plates were washed three times again with (casein/ PBS, 400 µL/ well) and dried. Then, the OPD substrate was added to the plates, which were left to incubate at 25^{o}C for 30 min. Finally, 2.5 M H_2SO_4 (50 µL/ well) was added and the absorbances of each well were read at 492, 450 and 630 nm using an LT-4000 plate reader.

In the second procedure, A 50 µl suspension of each mycolic acid or their glycolipids in *n*-hexane at the concentration 62.5 µg/µL was applied to the flat-bottomed wells of 96 well microplates. Plates were dried overnight and washed with tris buffered saline Tween-20 (TSST) buffer, pH 8.5, prepared one day before starting using the method described in the experimental section. This was followed by blocking for 1 h with 0.05% Tween-20 in phosphate-buffered saline (PBS-T). Then the PBS-T was aspirated using the LT-3500 plate washer and the plates flicked dry. Serum (1:20 dilution in 0.5% PBS-T) was added to each well, and plates were

incubated for 1 h at room temperature. Serum was aspirated, and plates were washed 3 times with PBS-T (400 µL/ well). Then, IgG secondary antibody in PBS-T (50 µL, diluted 10 µL in 10,000 µL) was added to each well, followed by incubation for 1 h. Three additional washes with (PBS-T, 400 µL/ well) were carried out, and 50 µL from of OPD substrate was added to the plates. After 10 mins incubation at room temperature, the reaction was stopped by the addition of 50 µl of 2.5 M H_2SO_4 (50 µL/ well) and the absorbances of each well were read at 492, 450 and 630 nm using an LT-4000 plate reader. The sensitivity and specificity of the Ag used were calculated by equation (1) and (2) as in the Introduction (Page 38).

3.4 The synthetic Ags under test

ELISA assays were carried out to test a natural human TDM and bovine TDM from *M. tb* and *M. bovis* and wax ester from *M. avium* and *M. gordonae* and a range of different new synthetic Ags. These Ags, except those described in Chapter 2, were synthesised by Prof. Mark Baird's group in the School of Chemistry at Bangor University.

3.5 The TB+ and TB- serum samples from Gambia

3.5.1 The use a range of new synthetic antigens

An ELISA assay was applied to study the antigenicity of synthetic glycolipid Ags presented in different parts of the cell wall of *M. tb* and other *Mycobacteria*. The tests used 9 TB+ and 55 TB- serum samples obtained from Gambia; these were assigned as TB+ or TB- based on standard WHO protocols using a range of clinical observations, and were either smear+/culture+ or smear-/culture-. The details of the assignment are presented elcetonically in attached Supplementary Information. The serum samples were diluted with phosphate-buffered saline containing 0.5% casein/PBS to obtain 1:20 and 1:80 dilution with keto TDM, and 1:80 dilution with each other Ag. Unless otherwise stated, the assays used IgG Fc specific secondary Ab. **Table 11** shows the absorbances at λ 492 nm in the ELISA assay for each synthetic Ag.

No.	160		188	189	163	164	190	177	168	183	184	179	158	178	165	176	180	181	182
	1 in 20	1 in 80	1 in 80	1 in 80	1 in 80	1 in 80	1 in 80	1 in 80	1 in 80	1 in 80	1 in 80	1 in 80	1 in 80	1 in 80	1 in 80	1 in 80	1 in 80	1 in 80	1 in 80
1	2.95	0.68	0.78	0.38	0.71	0.57	0.51	0.28	0.48	0.33	0.41	0.42	0.74	0.40	0.34	0.44	2.52	0.58	0.69
2	4.41	3.67	3.68	3.75	4.17	4.36	4.00	0.29	0.54	0.26	0.30	0.36	0.76	0.32	2.38	0.47	0.72	1.45	0.50
3	3.66	3.25	3.34	3.58	3.52	3.13	3.77	0.30	1.10	0.44	0.36	0.77	0.99	0.79	2.16	0.59	1.27	3.40	1.08
4	3.92	3.24	3.42	4.00	3.85	3.67	4.40	0.50	1.00	0.48	0.44	0.90	0.97	0.67	3.09	0.81	1.13	3.14	0.87
5	3.31	4.09	3.48	4.36	1.27	2.81	2.52	0.28	0.45	0.40	0.29	0.38	0.99		0.23	0.50	0.82	2.45	0.68
6	4.22	3.37	3.54	4.42	1.09	3.88	2.56	0.28	0.97	0.39	0.41	0.54	1.39		0.31	0.36	1.37	1.29	0.49
7	3.55	2.74	2.81	1.91	1.51	1.16	2.25	0.93	0.87	1.37	1.03	1.15	1.97		0.59	1.01	3.22	1.46	1.47
8	3.88	0.26	0.33	0.21	0.25	0.36	0.28	0.47	0.97	0.46	0.64	0.69	1.67	0.33	0.25	0.40	0.69	0.44	0.41
9	1.31	0.63	0.98	0.74	0.47	0.52	0.60	0.29	0.62	0.35	0.42	0.56	1.09	0.26	0.21	0.33	0.87	0.35	0.39
10	0.39	0.41	0.46	0.31	0.28	0.33	0.31	0.21	0.56	0.22	0.26	0.35	0.59	0.37	0.21	0.56	0.87	0.53	0.72
11	0.71	0.45	0.38	0.28	0.38	0.46	0.53	0.20	0.64	0.20	0.27	0.45	0.92	0.29	0.26	0.40	0.45	0.48	0.67
12	4.06	3.08	2.83	1.77	2.91	2.90	3.12	0.18	0.44	0.18	0.18	0.29	0.84	2.61	1.45	1.09	2.74	0.97	1.76
13	0.64	0.46	0.39	0.36	0.36	0.54	0.51	0.22	0.56	0.24	0.20	0.34	0.60	0.44	0.35	0.47	0.86	0.53	0.91
14	1.25	0.88	0.89	0.33	0.70	0.57	0.74	0.49	0.91	0.56	0.60	0.58	1.30	0.70	0.33	0.79	1.51	1.33	1.98
15	0.60	0.30	0.31	0.21	0.27	0.37	0.35	0.23	0.53	0.22	0.25	0.37	0.64	0.25	0.23	0.25	0.59	0.39	0.43
16	0.21	0.67	0.47	0.50	0.32	0.73	0.55	0.31	0.52	0.30	0.32	0.42	0.56	0.32	0.31	0.45	0.97	0.77	0.69
17	1.54	2.00	1.77	0.86	1.06	1.17	1.41	0.52	0.87	0.57	0.39	0.47	0.81	0.72	0.62	0.85	2.33	1.08	0.81
18	0.36	0.51	0.39	0.25	0.29	0.47	0.40	0.28	0.44	0.32	0.28	0.25	0.68		0.22	0.39	0.55	0.45	0.45
19	1.17	0.93	1.80	1.21	0.62	1.00	0.83	0.20	0.53	0.20	0.14	0.31	0.71	0.29	0.28	0.50	1.22	1.14	1.28
20	0.51	0.48	0.38	0.32	0.53	0.83	0.57	0.34	0.63	0.41	0.23	0.38	1.03	0.50	0.33	0.52	1.26	0.40	0.57
21	0.55	0.49	0.46	0.86	0.44	1.02	0.47	0.47	0.42	0.41	0.41	0.35	0.61	0.22	0.19	0.41	0.74	0.35	0.46
22	2.53	0.40	0.43	1.35	0.34	0.80	0.35	0.23	0.33	0.31	0.28	0.24	0.66	0.24	0.24	0.43	1.06	0.40	0.65
23	0.33	0.34	0.41	0.55	0.37	0.61	0.37	0.25	0.48	0.27	0.42	0.35	0.81	0.23	0.19	0.33	0.77	0.40	0.56
24	1.66	1.79	2.23	1.32	1.41	0.89	1.55	0.29	0.81	0.53	0.39	0.26	0.62	0.44	0.59	0.38	0.88	0.61	0.35
25	0.19	0.33	0.26	1.21	0.28	0.59	0.27	0.18	0.23	0.24	0.25	0.18	0.21	0.34	0.30	0.41	0.37	0.49	0.31
26	0.62	0.79	1.01	0.80	1.19	1.65	1.17	0.52	0.64	0.90	0.66	0.24	0.72	0.85	0.68	1.14	1.23	0.79	0.65
27	0.55	0.61	0.39	1.66	0.44	1.17	0.55	0.31	0.60	0.46	0.43	0.33	0.61	0.51	0.55	0.53	0.78	0.73	0.52
28	0.30	0.53	0.33	0.26	0.50	1.87	0.46	0.28	0.42	0.42	0.38	0.23	0.38	0.95	0.52	0.95	0.96	0.80	0.55
29	0.31	0.58	0.66	0.37	0.52	0.44	0.56	0.28	0.39	0.38	0.34	0.29	0.41	0.43	0.36	0.50	0.75	0.79	0.27
30	0.36	0.54	0.52	0.24	0.49	0.49	0.46	0.32	0.41	0.39	0.31	0.24	0.39	0.41	0.32	0.51	0.59	0.63	0.42
31	0.45	0.35	0.44	0.40	0.46	0.64	0.43	0.31	0.37	0.51	0.42	0.30	0.51	0.38	0.41	0.45	0.61	0.84	
32	1.29	0.96	1.27	0.56	1.14	1.12	1.16	0.34	0.68	1.01	1.09	0.57	0.91	0.39	0.38	0.65	0.89	1.09	
33	0.52	0.32	0.61	0.37	0.47	0.58	0.58	0.18	0.36	0.33	0.28	0.46	0.42	0.41	0.37	0.31	0.56	1.23	
34	0.46	0.38	0.44	2.13	0.46	1.68	0.39	0.39	0.47	0.52	0.46	0.51	0.49	0.30	0.35	0.36	0.35	0.57	
35	0.39	0.48	0.66	0.58	0.42	0.61	0.51	0.23	0.38	0.55	0.38	0.26	0.38	0.31	0.38	0.38	0.64	0.85	
36	0.25	0.20	0.29	0.25	0.28	0.34	0.29	0.11	0.28	0.25	0.17	0.23	0.28	0.22	0.30	0.23	0.46	0.37	
37	1.32	0.61	0.39	0.46	0.61		0.80	0.28	0.40	0.43	0.22	0.41	0.55	0.50	0.40	0.65	0.74	0.67	
38	0.81	0.46	0.51	0.41	0.54	0.77	0.53	0.29	0.44	0.43	0.36	0.40	0.52	0.35	0.49	0.55	0.66	0.84	
39	0.27	0.24	0.33	0.23	0.30	0.33	0.30	0.21	0.31	0.34	0.38	0.31	0.35	0.28	0.27	0.28	0.49	0.54	
40	0.41	0.37	0.33	0.26	0.29	0.48	0.31	0.18	0.28	0.26	0.25	0.25	0.35	0.23	0.25	0.27	0.44	0.46	
41	0.23	0.43	0.31	0.26	0.31	0.38	0.36	0.18	0.51	0.44	0.40	0.33	0.66	0.28	0.34	0.46	0.53	0.57	
42	2.97	0.89	1.37	0.72	0.92	0.85	0.92	0.30	0.49	0.42	0.42	0.42	0.55	0.32	0.38	0.34	0.39	0.43	
43	0.50	0.29	0.71	0.46	0.30	1.04	0.40	0.25	0.28	0.32	0.26	0.29	0.30	0.34	0.32	0.38	0.47	0.75	
44	2.34	1.80	1.74	1.37	1.06	2.81	1.91	0.41	0.60	1.32	1.19	0.67	0.98	0.62	0.63	1.19	1.71	2.08	
45	0.74	0.39	0.43	0.36	0.38	0.62	0.50	0.33	0.34	0.49	0.44	0.35	0.43	0.27	0.30	0.49	0.53	0.55	
46	0.32	0.30	0.29	0.41	0.30	0.58	0.21	0.13	0.27	0.28	0.13	0.26	0.31	0.32	0.33	0.41	0.35	0.45	
47	0.55	0.52	0.34	0.24	0.30	0.55	0.39	0.34	0.35	0.56	0.59	0.41	0.56	0.29	0.28	0.34	0.43	0.66	
48	0.92	0.32	0.61	0.31	0.66	0.44	0.50	0.32	0.29	0.55	0.31	0.17	0.32	0.27	0.35	0.29	0.37	0.78	
49	0.49	0.27	0.28	0.25	0.26	0.45	0.31	0.38	0.47	0.79	0.49	0.25	0.51	0.27	0.27	0.36	0.39	0.39	
50	2.37	0.31	0.41	0.32	0.33	0.42	0.34	0.35	0.31	0.38	0.32	0.30	0.37	0.28	0.31	0.37	0.35	0.50	
51	1.66	0.26	0.31	0.30	0.40	0.64	0.72	0.11	0.22	0.18	0.24	0.18	0.21	0.72	0.37	0.68	0.49	1.95	
52	0.54	0.25	0.39	0.63	0.29	0.39	0.32	0.21	0.28	0.32	0.30	0.26	0.36	0.21	0.28	0.29	0.32	0.39	
53	0.87	0.27	0.29	0.25	0.41	0.49	0.55	0.16	0.24	0.21	0.24	0.25	0.26	0.34	0.36	0.49	0.40	0.61	
54	2.11	0.46	0.74	0.42	0.50	0.77	0.60	0.17	0.25	0.26	0.26	0.20	0.27	0.25	0.27	0.31	0.37	0.32	
55	0.39	0.23	0.26	0.35	0.31	0.55	0.34	0.24	0.27	0.31	0.26	0.22	0.27	0.25	0.27	0.29	0.32	0.33	
56	0.65	0.60	0.63	0.34	0.82	0.85	0.88	0.68	0.42	0.90	0.60	0.31	0.73	0.57	0.40	0.61	0.56	0.57	
57	1.39	0.61	0.67	0.76	0.68	1.00	0.73	0.25	0.40	0.55	0.46	0.29	0.37	0.43	0.38	0.46	0.44	0.47	
58	0.41	0.34	0.36	0.37	0.42	2.19	0.58	0.25	0.32	0.44	0.46	0.28	0.41	0.28	0.34	0.42	0.43	0.54	
59	1.11	0.48	0.97	0.38	1.01	1.15	1.04	0.33	0.30	0.65	0.49	0.25	0.45	0.28	0.29	0.42	0.42	0.39	
60	1.16	0.51	0.59	0.24	0.82	0.62	0.71	0.37	0.36	0.62	0.53	0.29	0.44	0.42	0.39	0.39		0.37	
61	0.63	0.51	0.57	0.37	1.30	1.06	1.30	0.52	0.36	0.76	0.69	0.34	0.41	0.65	0.64	1.07	1.28	1.01	
62	1.64	1.02	1.63	0.87	1.28	1.38	1.10	0.19	0.26	0.19	0.27	0.35	0.30	0.61	0.81	0.98	1.63	1.13	
63	0.48	0.26	0.30	0.47	0.32	1.37	0.31	0.16	0.21	0.26	0.27	0.22	0.25	0.30	0.28	0.33	0.49	0.43	
64	4.32	3.31	3.48	0.24	3.20	0.78	3.60	2.50	2.33	0.37	4.00	3.98	0.29	3.86	3.91	3.46	0.96	4.13	
Cut-off.	>1.30	>0.625	>0.75	>0.742	>0.705	>1.155	>2.20	>0.276	>0.454	>0.25	>0.285	>0.356	>0.742	>0.319	>0.592	>0.467	>0.67	>1.255	>0.355
Cut-off ROC	>1.30	>0.620	>0.760	>0.730	>0.705	>1.155	>2.080	>0.265	>0.445	>0.255	>0.285	>0.355	>0.735	>0.385	>0.335	>0.460	>0.64	>1.390	>0.370
Tru.+	9	8	8	7	7	6	6	9	9	9	9	9	9	5	4	5	9	6	9
Fal. +	13	12	12	13	13	10	2	29	20	44	33	15	8	30	7	22	22	4	18
Sens. %	100	89	89	78	78	67	67	100	100	100	100	100	100	56	44	56	100	67	100
Spec.%	76	78	78	76	76	82	96	47	64	20	40	73	85	45	87	60	60	93	67
Sens. by ROC	100	89	89	78	78	67	67	100	100	100	100	100	100	50	67	50	100	50	100
Spec.by ROC	78	78	78	76	76	82	96	47	64	20	40	73	86	45	60	40	20	100	15

Table (11): ELISA responses for synthetic CF Ags with serum samples from Gambia using IgG Fc secondary antibody. The red and blue colours in column 1 show TB+ and TB- serum samples, numbers 1-9 and 10-64 respectively

The average of absorbances of TB+/TB- sera for each Ag from **Tables 11** are presented in **Figure 48**.

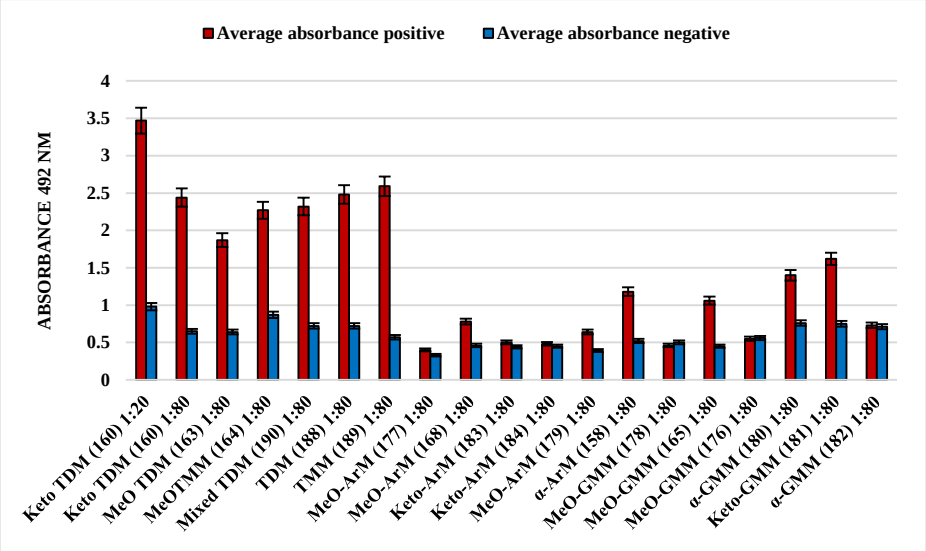

Figure 48: Average absorbances for a range of synthetic Ags with TB+ and TB- Gambia serum

Figure 48 shows that the average absorbances were variable among this set of Ags and that the keto-MA TDM (**160**) gave higher responses with 1:20 dilution than 1:80 dilution of serum samples. Moreover, all the TDMs and TMMs gave considerably higher average absorbances with TB+ serum samples rather than TB- serum samples. This is probably because *M. tb* and MAC share subclasses of MAs and therefore, cross-reactivity is inevitable.[417] The results with glycolipid fragments from arabinogalactans, (**177**), (**168**), (**183**), (**184**), (**179**) and (**158**) and GMMs (**178**), (**165**), and (**176**), (**180**), (**181**) and (**182**) show variable responses but still some discrimination.

In order to calculate the best cut-off values for each Ag, conditional formatting was applied column by column in Excel to the results in **Table 11; t**he pink boxes correspond to the results that were above the chosen cut-off. In addition, the optimal combinations of sensitivity and specificity of each Ag were calculated by using ROC curves. These are used in medicine to determine a cut off value and display the full picture of the trade-off between the sensitivity (true positive rate) and (1-specificity) (false positive rate) across a series of cut-off points. The ROC curve is a graph of sensitivity (y-axis) against 1 – specificity (x-axis). The cut off values that can minimize the number of false+ and false-, maximizing the sensitivity and specificity are calculated from the ROC curve. The area under the ROC curve is considered as an effective measure of the inherent validity of a diagnostic test. If is equal to 1.0 then the ROC curve consists of two straight lines, one vertical from 0,0 to 0,1 and the next horizontal from 0,1 to 1,1. In this case, the test is 100% accurate because both the sensitivity and specificity are 100% and no false+ or false- can be observed. The ROC analysis will find a cut off value that will

minimize the number of false+ and false-, maximizing the sensitivity and specificity. The area under the ROC curve was calculated for each synthetic Ag.

In the first experiments, keto-MA TDM (**160**), methoxy-MA TDM (**163**), methoxy-MA TMM (**164)**, mixed TDM (**190**) from *M. tb* and TDM (**188**) and TMM (**189**) from *M. avium* were examined (**Table 11**). The optimal cut-off values for sensitivity and specificity were calculated for each Ag in Excel (**Table 12** below).The keto-MA TDM (**160**) gave higher Ab binding signals at 1:20 dilution of serum than with 1:80 dilution. However, a 1:80 dilution was used for assays of other Ags because limited serum was available.

Id		Sens. (%)	Spec. (%)	Spec. for 100% sens.
Keto TDM (160)	1 in 20	89	95	76
TDM (188)	1 in 80	89	78	16
Keto TDM (160)	1 in 80	89	78	7
TMM (189)	1 in 80	78	76	0
Mixed TDM (190)	1 in 80	67	96	0
MeO TDM (163)	1 in 80	78	76	0
MeO TMM (164)	1 in 80	67	82	2

Table 12: Optimal pairs of sensitivity and specificity to distinguish TB+/TB- with synthetic CFs

The ROC analysis for this set of antigens is shown in **Figure 49**.

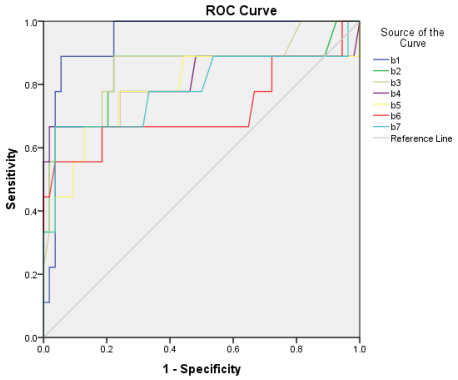

No.	Id.			Area Under the Curve	Sens. (%)	Spec. (%)	Spec. for 100% sens.
1	Keto TDM (160)	1 in 20	b1	0.947	89	94	78
2	TDM (188)	1 in 80	b3	0.858	89	78	18
3	Keto TDM (160)	1 in 80	b2	0.844	89	78	7
3	TMM (189)	1 in 80	b4	0.809	78	76	0
4	Mixed TDM (190)	1 in 80	b7	0.787	67	96	4
5	MeO TDM (163)	1 in 80	b5	0.785	78	76	0
6	MeO TMM (164)	1 in 80	b6	0.718	67	82	6

Figure 49: The ROC analysis using data from Table 11

The figure demonstrates that the best area under the curve (0.947) was obtained using keto-MA TDM (**160**) with serum samples at a 1:20 dilution, which shows that the test is 95% accurate. The values with other antigens were lower but still significant.

Thus, these results show that the Abs in TB+ serum samples can recognize the epitope made by the keto-MA TDM (**160**), methoxy-MA TDM (**163**), methoxy-MA TMM (**164)**, mixed

TDM (**190**) from *M. tb* and also that made by the TDM (**188**) and TMM (**189**) from *M. avium*, and this cross-reactivity to infection by other mycobacteria may explain some false positive results. These might be removed if Ags can be developed. That are specific for other infections.

The synthetic arabino-MA (**177**), (**168**), (**183**), (**184**), (**179**) and (**158**) Ags were then examined, using the same serum samples at 1 in 80 dilution (**Table 11**). The results showed lower Ab binding signals but the best signals were observed with the α-MA derivatve. However, some of the molecules were actually good at distinguishing TB+ from TB-. The best cut-off values for determining sensitivity and specificity are as shown in **Table 13**.

Id.		Sens. (%)	Spec. (%)	Spec. for 100% sens.
α-ArM (158)	1 in 80	100	85	85
MeO-ArM (179)	1 in 80	89	75	73
MeO-ArM (168)	1 in 80	89	67	64
MeO-ArM (177)	1 in 80	67	56	47
Keto-ArM (184)	1 in 80	67	62	40
Keto-ArM (183)	1 in 80	89	40	20

Table 13: Optimal pairs of sensitivity and specificity to distinguish TB+/TB- with synthetic ArMs

The ROC curves for each Ag are shown in **Figure 50** below.

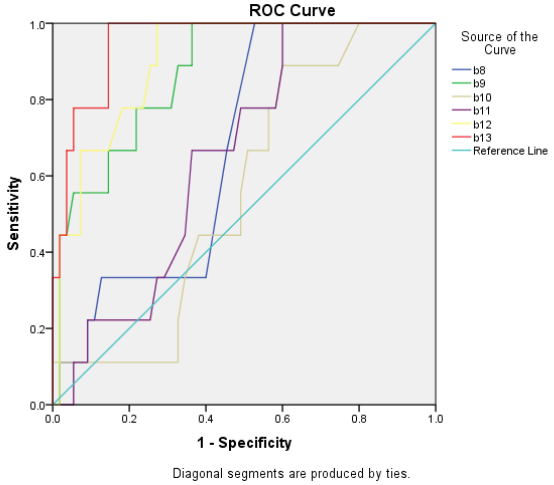

No	Id			Area Under the Curve	Sens. (%)	Spec. (%)	Spec. for 100% sens.
1	α-ArM (158)	1 in 80	b13	0.952	100	86	86
2	MeO-ArM (179)	1 in 80	b12	0.900	89	75	73
3	MeO-ArM (168)	1 in 80	b9	0.871	89	69	64
4	MeO-ArM (177)	1 in 80	b8	0.669	67	55	47
5	Keto-ArM (184)	1 in 80	b11	0.655	67	64	40
6	Keto-ArM (183)	1 in 80	b10	0.562	89	40	20

Figure 50: The ROC analysis using data from Table 11

The values for the area under the curve of α-MA (**158**) and methoxy-MA (**179**) arabinose, 0.952 and 0.900 respectively, do indicate good discrimination.

The third set of antigens studied were the synthetic GMMs (**178**), (**165**), (**176**), (**180**), (**181**) and (**182**) from *M. tb* and *M. kansasii* (**Table 11**). Only 21 TB- serum samples for GMM6 (**182**),

because only a limited amount of this serum was available. The best pairs of sensitivity and specificity using the data from **Table 11** are shown in**Table 14**.

Id.		Sens. (%)	Spec. (%)	Spec. for 100% sens.
α-MA GMM (182)	1 in 80	89	67	67
α-MA GMM (180)	1 in 80	89	60	60
Keto-MA GMM (181)	1 in 80	67	93	0
MeO-MA GMM(165)	1 in 80	44	87	4
MeO-MA GMM (176)	1 in 80	56	60	13
MeO-MA GMM (178)	1 in 80	56	45	4

Table 14: Optimal pairs of sensitivity and specificity to distinguish TB+/TB- with synthetic GMMs

The best sensitivity and specificity were observed with α-GMM (**182**). The ROC analysis of the sensitivity and specificity of each Ag were also studied **(Figure 51**).

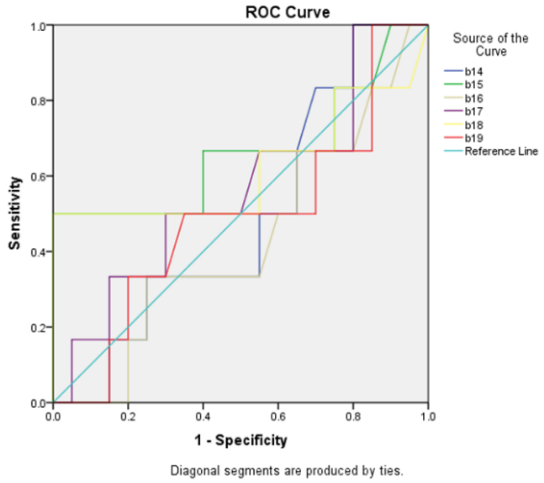

No.	Id			Area Under the Curve	Sens. (%)	Spec. (%)	Spec. for 100% sens.
1	MeO-MA GMM (165)	1 in 80	b15	0.663	67	60	0
2	Keto-MA GMM (181)	1 in 80	b18	0.621	50	95	0
3	α-MA GMM (180)	1 in 80	b17	0.563	50	70	20
4	MeO-MA GMM (178)	1 in 80	b14	0.488	50	45	20
5	α-MA GMM (182)	1 in 80	b19	0.488	50	65	15
6	MeO-MA GMM (176)	1 in 80	b16	0.429	50	40	15

Figure 51: The ROC analysis using data from Table 11

The figure shows low values of area under the curve for this set of Ags and the best value was observed for GMM2 (**165**).

A plot of the specificity for each antigen when the sensitivity was set to 100 is shown in **Figure 52**. The best specificity was observed with keto-MA TDM (**160**) at 1:20, α-MA ArM (**158**) and methoxy-MA ArM (**179**), at 1:80 dilution.

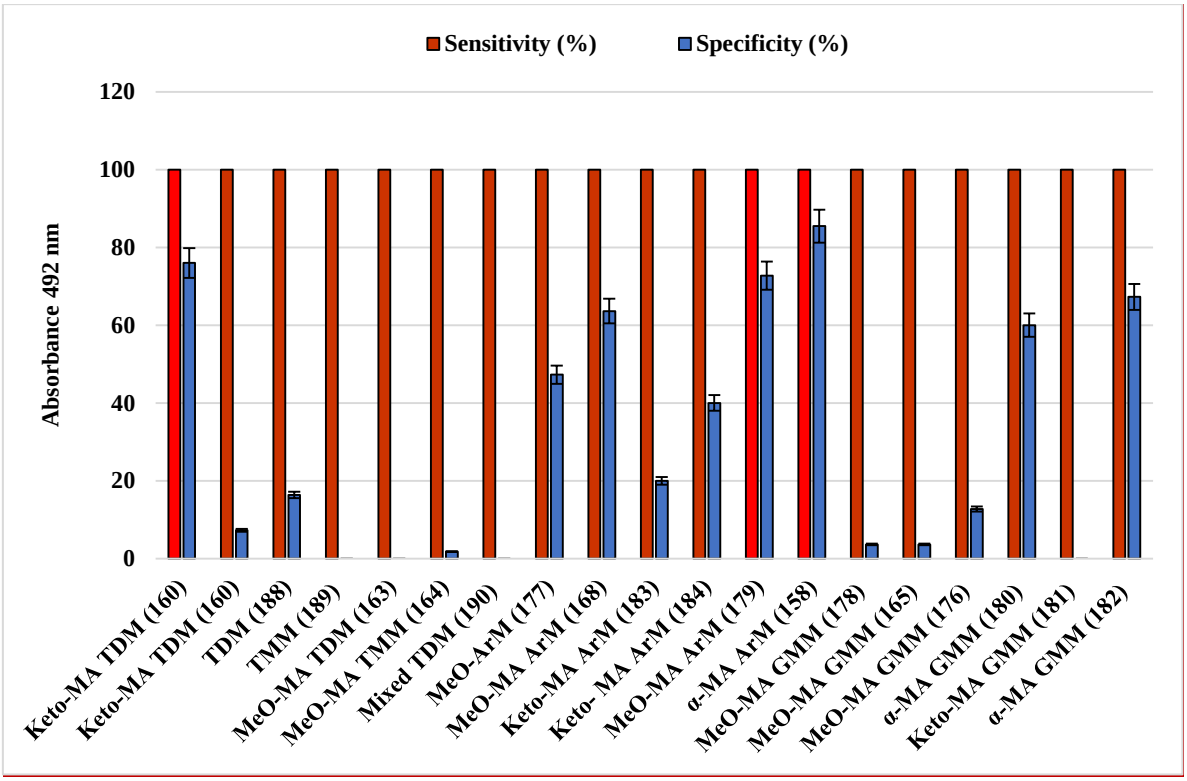

Figure 52: The specificity of each Ag when cut-off is set for 100% sensitivity

The figure shows the specificity for each synthetic Ag corresponding to 100% sensitivity. The best combinations of sensitivity and specificity were observed with a keto-MA based TDM (**160**) (100 and 78%) Ag at 1:20 dilution of serum samples and MeO-MA based ArM (**179**) (100 and 73%) and α-MA based ArM (**158**) (100 and 86%) Ags at 1:80 dilution.

3.5.2 The effect of the structure of the of MA and the sugar (Gambia samples)

The results of the ELISA assays using the samples from Gambia are summarised in **Table 15** below, with the key structural features of the MA identified.

Id	Length of chain				Stereochemistry		organism	No. of MA	Sens. (%)	Spec. (%)	AVG ABS+	AVG ABS-
	a	B	c	d	Proximal	Distal						
(160)	17	18	15	23	Cis, RS	Keto, R	*M. tb*	2	100	76	3.47	0.98
									67	96	2.44	0.65
(163)	17	16	17	23	Cis, RS	MeO, SS	*M. tb*	2	78	75	1.87	0.64
(164)	17	16	17	23	Cis, RS	MeO, SS	*M. tb*	1	56	96	2.27	0.87
(190)	17	16	17	23	Cis, RS	MeO, SS	*M. tb*	2	67	95	2.32	0.72
	17	18	15	23	Cis, RS	Keto, R	*M. tb*					
(188)	17	15	17	21	S, Trans, RS	Keto, S	*M. avium*	2	89	75	2.48	0.72
(189)	17	15	17	21	S, Trans, RS	Keto, S	*M. avium*	1	78	75	2.59	0.57
(177)	17	16	17	21	Cis, SR	MeO, SS	*M. kansasii*	1	100	47	0.4	0.33
(168)	17	16	17	23	Cis, SR	MeO, SS	*M. tb*	1	100	64	0.78	0.46
(183)	17	18	15	21	Cis, SR	Keto, mix	*M. kansasii*	1	100	20	0.5	0.44
(184)	17	18	16	23	S, Trans, RS	Keto, mix	*M. tb*	1	100	38	0.48	0.45
(179)	17	16	17	21	Cis, RS	MeO, SS	*M. kansasii*	1	100	84	0.64	0.39
(158)	19	14	11	23	Cis, RS	Cis, RS	*M. tb*	1	100	85	1.18	0.52
(178)	17	16	17	21	Cis, RS	MeO, SS	*M. kansasii*	1	56	42	0.46	0.5
(165)	17	16	17	23	Cis, RS	MeO, SS	*M. tb*	1	100	4	1.06	0.45
(176)	17	16	17	21	Cis, SR	MeO, SS	*M. kansasii*	1	100	13	0.55	0.56
(180)	18	14		23	Cis, RS	Cis, RS	*M. b*	1	100	60	1.4	0.76
(181)	17	17	15	23	S, Trans, RS	Keto, mix	*M. b*	1	78	87	1.62	0.75
(182)	17	10	15	23	S, Trans, SR	Cis, RS	*M. b*	1	100	67	0.73	0.71

Table (15): Effect of structure and the sugar on the antigenicity of synthetic Ags with Gambia samples

- In general, all the TDMs gave strong absorbances with TB+ serum, and rather weaker average absorbances with TB- serum.
- The mixed TDM (**190**) with one methoxy and one keto MA gave higher responses than methoxy-MA TDM (**163**) and TMM (**164)** but lower than keto-MA TDM (**160**).
- The TDM (**188**) from *M. avium* with two wax esters gave higher responses than keto-MA TDM (**160**) from *M. tb*, but lower than TMM (**189**) with one wax ester.
- The TDMs from both *M. tb* and *M. avium* gave a good distinction between TB+ and TB- serum samples.
- The arabino-MA (**177**), (**168**), (**183**), (**184**), (**179**) and (**158**) Ags and GMMs (**178**), (**165**), (**176**), (**180**), (**181**) and (**182**) from *M. tb* and *M. kansasii* with different chain length in meromycolate and in corynomycolate parts gave variable responses with TB+ serum.

- The Abs in TB+ serum samples cannot recognize glycolipid fragments from arabinogalactan from *M. tb* MeO MA present in (**177**), (**168**) and (**179**) and keto MA presented in (**183**) and (**184**), but the Abs can recognize α-MA without oxygen functionality present in (**158**) more than keto and methoxy MA subclasses.
- The Abs in TB+ serum recognize the MeO MA in GMM (**165**) from *M. tb* more than GMM (**178**) and GMM (**176**) from *M. kansasii*, but recognize α-MA without oxygen functionality in GMM (**180**) and GMM (**182**) from *M. tb* to different levels.
- The Abs can recognize keto MA in GMM (**181**) from *M. tb* more than methoxy and α-MA. The antigenic epitope in CF molecules is thus the MAs and Abs against TDM from TB patients can distinguish between MAs subclasses.[2]
- The results indicate that the Abs in serum samples can recognise both the hydrophobic MA part and the carbohydrate moieties in the synthetic glycolipid Ags.

In *M. tb* and related organisms,[418] methoxy and ketomycolates are generally less abundant than α-mycolates, although the exact ratios are dependent upon growth conditions. Ketomycolates occur in a variety of mycobacterial species,[61] while methoxymycolates have only been isolated from *M. tb*, *M. bovis* BCG strain Moreau (but not strains Glaxo, Prague, or Pasteur), *M. microti*, *M. marinum*, *M. ulcerans*, *M. asiaticum*, *M. gastri*, *M. gordonae*, *M. kansasii*, *M. szulgai*, and *M. africanum*.[61] The reactivity of human antisera to various MA subclasses is different, anti-CF Ab recognising methoxy more than keto- or α-MAs.[372,381]

3.5.3 What if we use a combination of results from different antigens?

The best results above used (**160**), (**180**) and (**158**). These each individually gave sensitivities of 100 % and specificities of around 75 – 85 %. These results are good, but can be improved by using a combination of assays. Thus **Table 16** shows the results for just these antigens.

No.	Keto TDM (160)	α-Ar M (158)	α-GMM (180)	All three above cut-off
	1 in 20	1 in 80	1 in 80	
1	2.95	0.74	2.52	
2	4.41	0.76	0.72	
3	3.66	0.99	1.27	
4	3.92	0.97	1.13	
5	3.31	0.99	0.82	
6	4.22	1.39	1.37	
7	3.55	1.97	3.22	
8	3.88	1.67	0.69	
9	1.31	1.09	0.87	
10	0.39	0.59	0.87	
11	0.71	0.92	0.45	
12	4.06	0.84	2.74	
13	0.64	0.60	0.86	
14	1.25	1.30	1.51	
15	0.60	0.64	0.59	
16	0.21	0.56	0.97	
17	1.54	0.81	2.33	
18	0.36	0.68	0.55	
19	1.17	0.71	1.22	
20	0.51	1.03	1.26	
21	0.55	0.61	0.74	
22	2.53	0.66	1.06	
23	0.33	0.81	0.77	
24	1.66	0.62	0.88	
25	0.19	0.21	0.37	
26	0.62	0.72	1.23	
27	0.55	0.61	0.78	
28	0.30	0.38	0.96	
29	0.31	0.41	0.75	
30	0.36	0.39	0.59	
31	0.45	0.51	0.61	
32	1.29	0.91	0.89	
33	0.52	0.42	0.56	
34	0.46	0.49	0.35	
35	0.39	0.38	0.64	
36	0.25	0.28	0.46	
37	1.32	0.55	0.74	
38	0.81	0.52	0.66	
39	0.27	0.35	0.49	
40	0.41	0.35	0.44	
41	0.23	0.66	0.53	
42	2.97	0.55	0.39	
43	0.50	0.30	0.47	
44	2.34	0.98	1.71	
45	0.74	0.43	0.53	
46	0.32	0.31	0.35	
47	0.55	0.56	0.43	
48	0.92	0.32	0.37	
49	0.49	0.51	0.39	
50	2.37	0.37	0.35	
51	1.66	0.21	0.49	
52	0.54	0.36	0.32	
53	0.87	0.26	0.40	
54	2.11	0.27	0.37	
55	0.39	0.27	0.32	
56	0.65	0.73	0.56	
57	1.39	0.37	0.44	
58	0.41	0.41	0.43	
59	1.11	0.45	0.42	
60	1.16	0.44		
61	0.63	0.41	1.28	
62	1.64	0.30	1.63	
63	0.48	0.25	0.49	
64	4.32	0.29	0.96	
			Sensitivity	100
			Specificity	94

Table (16): The combination of the results from three different Ags with Gambia samples and IgG Fc

By setting the same cut off vlues as before for each individual antigen to provide 100% sensitivity, it can be seen that the number of TB- serum samples that are also false positive to all three assays is reduced to three, corresponding to a specificity of 94 %.

3.6 The nature of antibody recognition with keto TDM

Patients with active TB usually exhibit strong IgG responses but poor IgM and IgA responses. Anti-*M. tb* IgG Abs increase in patients with active disease.[419] Anti-MA and anti-CF Abs are present in TB+ patients[371,373] and the reactivity of sera to various MA subclasses is different, anti-CF IgG Ab recognising methoxy MAs more strongly than keto- or α-MAs[373,381] An epitope and it is binding site must become closely related, for most of the forces responsible for binding are short-range (less than 4 A^{o}).[420] These include hydrophobic and van der Waals forces, which are spherically symmetrical, and hydrogen bonds, which are directional. Electrostatic forces might also contribute; however, at longer distance. The formation of stable immune complexes normally occurs only when the epitope and the paratope fit together. Grant *et al.*[237] suggested that keto and methoxy-MA fold so that the three polar functions of the lipid chain are in proximity and form an epitope, acting as a site for recognition within the immune system as stated in the Introduction, (Page 28). In order to compare the epitope for the keto MA suggested by Grant, **Figure 53** represents a possible epitope of the TDM (**160**) with the MA folded in a similar fashion.

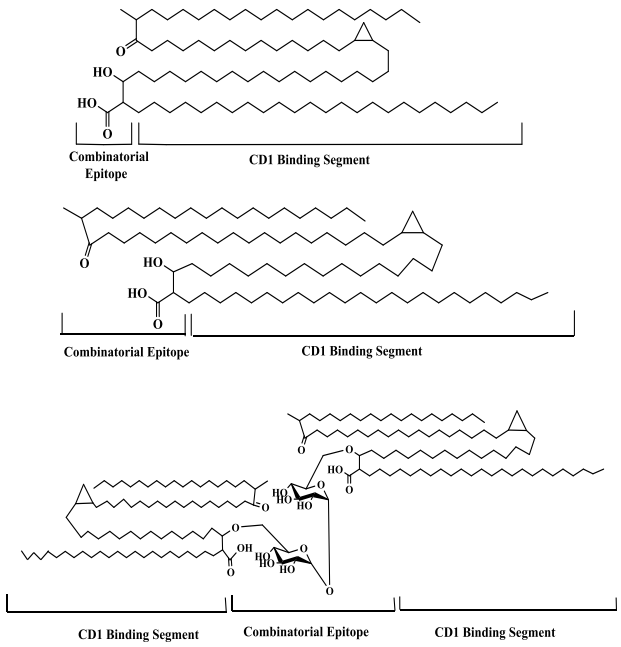

Figure 53: Model keto MA and keto TDM under test; modified from Grant *et al*

Structural evidence has suggested that Abs with high affinity manifest a ‘‘lock and key’’ type of binding, involving greater polar and charged interactions that contribute to the rigidity of the antigen-binding site and to a higher binding energy for the antibody-antigen interaction.[421]

3.7 The effect of changing the diluent from casein-PBS to PBS-Tween

In order to try to improve the performance of the assay, the effect of blocking and washing with a different buffer was examined. ELISA assays were carried out (at a 1:20 serum dilution) to detect the Abs present in 11 TB+ and 51 TB- serum samples from the WHO using a range of synthetic glycolipid Ags from *M. tb*., a keto-MA TDM (**160**), methoxy-MA TDM (**173**), methoxy-MA TDM (**163**) with different stereochemistry and methoxy-MA TMM (**164**) (**Table 20**), and human IgG Fc specific molecule secondary Ab. They were replicated twice using 0.5% casein/PBS and 0.05% PBS-T as shown in **Table 17** below. The average absorbances of positives and negative for each Ag were calculated (**Figure 54**).

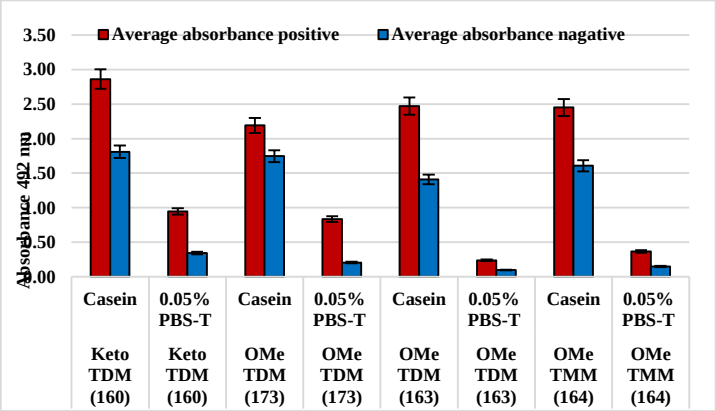

Figure 54: The average absorbances using TB+ and TB- WHO serum samples

The results show higher Abs binding signals using casein than 0.05% PBS-T buffer solution. The best pairs of sensitivity and specificity in keto-MA TDM (**160**) (100, 61) are as shown in **Table 18**.

No.	Id		Sens. (%)	Spec. (%)	Spec. for 100% sens.
1	Keto TDM (160)	Casein	82	82	61
2		0.05% PBS-T	55	67	16
3	MeO TDM (173)	Casein	64	75	6
4		0.05% PBS-T	55	88	20
5	MeO TDM (163)	Casein	73	84	14
6		0.05% PBS-T	55	61	0
7	MeO TMM (164)	Casein	73	71	0
8		0.05% PBS-T	64	55	12

Table 18: The pairs of sensitivity and specificity of synthetic with different buffers

No.	TDM (160)		TDM (173)		TDM (163)		TMM (164)	
	Casein	0.05% PBS-T	Casein	0.05% PBS-T	Casein	0.05% PBS-T	Casein	0.05% PBS-T
1	3.46	3.43	3.52	1.28	3.68	0.10	3.71	0.10
2	2.98	0.07	1.58	0.05	2.13	0.07	0.89	0.21
3	3.36	0.21	3.22	1.66	3.41	0.13	3.20	0.10
4	2.80	0.07	1.04	0.07	1.33	0.11	3.43	0.19
5	2.95	2.84	2.94	2.82	3.05	1.33	3.02	2.71
6	2.12	0.09	0.65	0.06	0.68	0.13	0.35	0.11
7	3.07	0.16	2.36	0.20	3.05	0.06	1.90	0.06
8	2.72	0.73	2.63	0.33	2.74	0.05	3.12	0.08
9	3.13	0.11	2.25	0.09	2.98	0.06	2.82	0.06
10	2.02	0.21	0.96	0.11	1.14	0.08	1.52	0.09
11	2.87	2.44	2.97	2.49	2.98	0.51	3.01	0.34
12	0.91	0.07	0.84	0.08	0.82	0.16	1.24	0.09
13	1.21	0.11	1.14	0.08	1.13	0.16	1.73	0.13
14	1.06	0.30	1.02	0.14	0.84	0.07	0.97	0.08
15	1.58	0.06	2.31	0.05	1.27	0.06	1.11	0.07
16	1.47	0.19	1.08	0.05	0.54	0.12	0.62	0.25
17	1.95	0.05	1.07	0.06	0.97	0.06	0.99	0.10
18	3.09	2.73	3.12	2.08	3.16	0.08	3.22	0.22
19	1.58	0.13	1.73	0.06	1.38	0.07	1.32	0.09
20	2.30	0.09	2.16	0.07	1.75	0.15	1.39	0.08
21	1.34	0.13	1.78	0.08	0.95	0.22	0.71	0.17
22	0.99	0.08	0.83	0.04	0.45	0.08	0.99	0.18
23	1.31	0.08	1.36	0.05	0.93	0.09	0.95	0.05
24	2.21	0.11	3.22	0.04	0.95	0.09	1.01	0.06
25	2.35	0.05	1.72	0.05	1.11	0.11	2.61	0.16
26	2.45	0.05	2.06	0.04	1.13	0.07	1.26	0.07
27	3.24	0.07	2.17	0.06	3.01	0.07	2.71	0.05
28	1.13	0.38	1.36	0.17	0.83	0.11	1.59	0.06
29	3.49	0.76	4.00	0.18	4.00	0.18	2.23	0.10
30	1.44	0.05	0.53	0.04	0.85	0.09	2.07	0.13
31	2.18	0.27	2.93	0.07	1.69	0.07	2.42	0.17
32	2.62	0.08	1.02	0.08	1.40	0.08	3.02	0.13
33	1.35	0.05	1.11	0.05	0.68	0.09	0.67	0.09
34	0.98	0.05	0.92	0.05	0.71	0.10	0.72	0.13
35	1.11	0.07	1.21	0.05	0.84	0.11	0.94	0.15
36	0.96	0.06	1.29	0.06	0.98	0.13	1.05	0.09
37	2.95	3.29	3.19	2.95	3.05	0.12	3.20	2.24
38	2.45	0.74	2.58	0.48	2.81	0.10	2.48	0.12
39	1.74	0.27	1.04	0.18	1.08	0.14	1.15	0.15
40	2.99	0.10	1.28	0.07	1.87	0.05	3.27	0.05
41	1.53	0.13	1.07	0.09	0.95	0.10	1.26	0.09
42	1.02	0.15	0.57	0.11	0.55	0.07	0.61	0.06
43	1.89	0.15	3.04	0.09	0.93	0.08	0.83	0.07
44	2.19	0.32	3.09	0.18	1.78	0.06	2.90	0.06
45	2.79	0.20	2.05	0.11	2.01	0.05	2.86	0.08
46	0.81	0.19	0.53	0.10	0.37	0.12	0.42	0.15
47	1.02	0.21	1.35	0.16	0.75	0.12	1.71	0.09
48	0.73	0.09	1.01	0.05	0.42	0.05	0.54	0.05
49	2.86	1.35	3.10	0.46	3.00	0.09	2.23	0.08
50	1.65	0.65	1.94	0.14	1.01	0.06	1.89	0.06
51	3.12	0.15	3.43	0.10	3.68	0.09	3.57	0.10
52	1.85	0.20	1.65	0.13	1.44	0.08	1.44	0.08
53	0.61	0.14	0.85	0.06	0.49	0.09	0.69	0.11
54	1.01	0.15	0.67	0.08	0.63	0.09	0.82	0.09
55	2.10	0.66	2.78	0.32	1.75	0.18	1.63	0.16
56	1.20	0.53	1.34	0.18	1.03	0.09	0.83	0.07
57	1.21	0.11	1.81	0.07	1.03	0.09	1.54	0.09
58	2.07	0.61	3.13	0.15	2.04	0.08	1.87	0.09
59	2.71	0.14	1.20	0.08	1.78	0.10	2.39	0.28
60	1.56	0.22	1.36	0.22	1.41	0.09	1.67	0.08
61	2.34	0.48	1.86	0.15	2.39	0.09	1.87	0.10
62	1.58	0.28	1.12	0.12	1.23	0.14	0.74	0.14
Cut-off	>1.95	>0.21	>2.24	>0.20	>2.1	>0.095	>1.90	>0.095
Cut-off ROC	>1.985	>0.205	>2.21	>0.21	>2.085	>0.095	>1.895	>0.095
Tru.+	11	6	7	6	8	6	8	7
Fal. +	20	17	13	6	8	20	15	23
Sens. %	100	55	64	55	73	55	73	64
Spec.%	61	67	75	88	84	61	71	55
Sens.% ROC	100	55	64	55	73	55	73	64
Spec.% ROC	61	65	75	88	84	61	71	55

Table (17): Effect of using casein or PBS-Tween dilution and washing on a range of synthetic Ags. The red and blue colours in column 1 show infected and uninfected serum samples in rows 1-11 and 12-62 respectively. Pink boxes reflect values above the cut-off selected for each antigen

The ROC analysis of the results is seen in **Figure 55**.

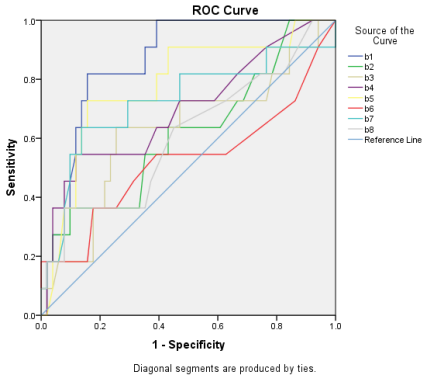

No.	Id			Area Under the Curve	Sens. (%)	Spec. (%)	Spec. for 100% sens.
1	Keto TDM (160)	Casein	b1	0.862	82	84	61
2		0.05% PBS-T	b2	0.614	55	65	16
3	MeO TDM (173)	Casein	b3	0.622	64	75	6
4		0.05% PBS-T	b4	0.698	55	88	8
5	MeO TDM (163)	Casein	b5	0.781	73	84	14
6		0.05% PBS-T	b6	0.524	55	61	0
7	MeO TMM (164)	Casein	b7	0.725	73	71	0
8		0.05% PBS-T	b8	0.606	64	55	8

Figure 55: The ROC analysis using data from Table 17

Figure 55 shows none of these antigens distinguished well TB+ and TB- in this set of sera. The values of the area under the curve were significantly higher in casein in contrast with the 0.05% PBS-T buffer solution. The best area under the curve were obtained in keto-MA TDM (**160**) Ag in casein (0.862). This gave a higher average response than methoxy-MA TDMs (**173**) or (**163**) and methoxy-MA TMM (**164**). The methoxy-MA TDM (**163**) and TMM (**164**) and methoxy-MA TDM (**173**), gave high responses in casein, and good distinction between TB+ and TB- serum samples. The responses with all these antigens and this set of serum samples were very much lower when PBS-T was used as buffer (**Table 19**), though TDM (**160**) did show a much higher average response for TB+ than TB- sera.

Id		Length of the chain				No. of MA	Sens. (%)	Spec. (%)	AVG ABS+	AVG ABS-
		a	b	c	d					
Keto TDM (160)	Casein	17	18	15	23	2	100	61	2.86	1.81
	0.05% PBS-T						55	67	0.95	0.35
MeO TDM (173)	Casein	17	16	18	23	2	64	75	2.19	1.75
	0.05% PBS-T						55	88	0.83	0.21
MeO TDM (163)	Casein	17	16	17	23	2	73	84	2.47	1.41
	0.05% PBS-T						55	61	0.24	0.1
MeO TMM (164)	Casein					1	73	71	2.45	1.61
	0.05% PBS-T						64	55	0.37	0.15

Table (19): The effect of structure on the antigenicity of synthetic Ags from *M. tb*

3.8 The use of a range of new synthetic Ags present in *M. tb* with WHO samples

No.	Wax ester (185)	TDM of wax ester (186)	MA (159)	TMM (161)	TDM (191)	TDM (173)
	IgG	IgG Fc	IgG Fc	IgG Fc	IgG Fc	IgG Fc
1	3.43	3.18	0.38	3.15	2.12	2.81
2	3.23	0.44	0.18	0.16	2.10	0.23
3	2.74	2.93	0.35	2.92	3.16	2.92
4	2.36	1.46	0.39	1.76	1.38	1.35
5	2.89	3.58	0.47	3.26	3.88	3.56
6	1.97	0.40	0.33	2.37	1.61	0.72
7	2.67	3.06	0.41	3.15	3.47	3.07
8	2.73	0.64	0.27	0.59	0.82	0.50
9	4.39	0.34	0.33	0.72	4.29	0.71
10	1.16	3.54	0.30	3.47	2.06	3.45
11	3.04	3.38	0.38	3.41	3.52	3.32
12	3.12	3.49	0.33	3.18	3.49	3.41
13	2.76	3.07	0.35	3.28	3.33	3.00
14	2.35	2.15	0.27	0.34	1.82	0.13
15	3.97	3.67	0.24	2.39	3.64	1.75
16	2.06	0.91	0.33	2.41	1.02	0.93
17	3.69	1.04	0.40	2.14	1.17	1.05
18	1.77	1.54	0.46	1.15	0.57	2.23
19	2.58	2.00	0.19	0.14	1.08	0.14
20	3.02	0.52	0.41	1.37	0.42	1.29
21	1.86	1.73	0.40	2.59	1.13	1.69
22	2.65	0.83	0.38	1.20	0.64	0.86
23	2.56	2.48	0.39	2.72	3.68	2.86
24	2.36	1.49	0.42	3.76	0.97	0.98
25	2.32	1.51	0.39	2.27	1.52	1.21
26	3.64	0.21	0.35	0.39	0.48	0.29
27	2.10	0.48	0.34	0.56	0.35	0.56
28	2.65	1.31	0.40	2.14	0.95	1.29
29	1.85	0.36	0.48	0.35	0.30	0.27
30	1.85	2.96	0.25	0.41	3.71	0.32
31	2.80	2.85	0.33	4.00	2.42	3.60
32	1.23	1.15	0.37	3.92	1.03	1.84
33	2.54	3.41	0.32	1.89	3.64	0.78
34	2.72	1.00	0.33	4.09	0.86	3.80
35	3.63	1.53	0.33	1.85	2.86	0.74
36	3.94	3.30	0.54	1.80	2.86	1.99
37	3.26	1.30	0.53	4.11	1.63	3.03
38	3.50	0.94	0.72	3.70	0.95	2.91
39	2.91	1.31	0.88	3.47	0.71	1.48
40	3.69	3.95	0.36	2.54	2.73	1.12
41	3.90	3.33	0.46	4.00	2.74	1.88
42	3.62	0.87	0.41	3.94	1.15	2.75
43	3.22	1.00	0.54	3.77	1.08	1.18
44	4.39	1.23	0.39	1.73	1.16	1.21
45	1.75	0.29	0.45	1.19	0.30	0.96
46	2.12	0.55	0.24	0.42	0.52	0.23
47	3.24	4.08	0.33	1.32	4.23	0.72
48	3.82	0.97	0.39	4.00	0.86	3.91
49	2.35	1.11	0.29	2.91	0.52	1.03
50	2.70	0.42	0.35	1.63	0.40	0.97
Cut-off	>2.74	>1.46	>0.35	>2.92	>1.61	>1.75
Cut-off ROC	>2.725	>2.890	>0.345	>2.320	>0.765	>1.320
Tru.+	9	11	6	8	13	9
Fal. +	16	14	22	11	10	11
Sens.%	60	73	40	53	87	60
Spec.%	54	60	37	69	71	69
Sens.% ROC	67	60	47	67	93	67
Spec.% ROC	54	83	31	54	69	63

Table (20): Effect of a range of synthetic Ags on TB+ and TB- WHO serum samples. Red boxes in column 1 are TB+, blue TB-. Pink boxes are values above cut-offs set for each antigen

An ELISA assay were applied using 15 TB+ and 35 TB- serum samples, at a 1: 20 dilution, from the WHO using a range of new synthetic glycolipid Ags These included wax ester (**185**)

and its TDM (**186**) from *M. avium*, mixed TDM (**191**) from *M. kansasii* and the free keto MA (**159**) and its TMM (**161**) and methoxy TDM (**173**) from *M. tb*. The tests were done using IgG whole molecule or IgG Fc, and 0.5% casein/PBS buffer (**Table 20**).

The average of absorbances for positive and negative serum of each Ag were calculated using the data from **Table 20**, (**Figure 56**).

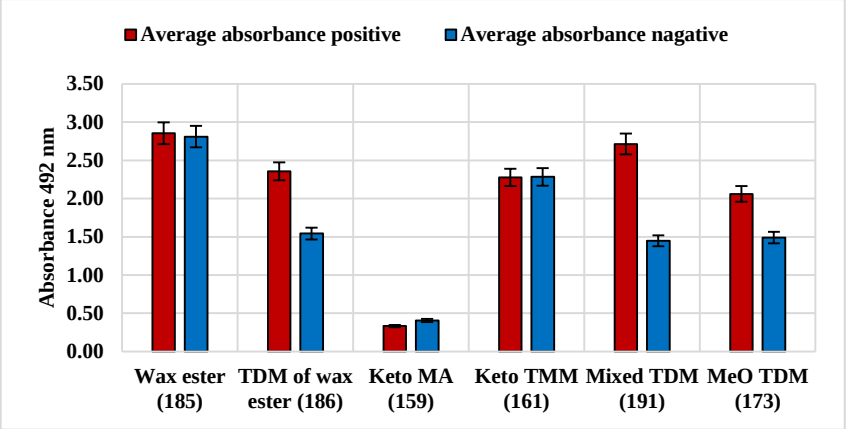

Figure 56: The average of absorbances of synthetic antigens using TB+ and TB- WHO serum samples

The figure shows high antibody binding signal were observed with this set of Ags, except for free keto MA (**159**), which showed no significant response. However, the average values for TB+ and TB- were rather close. The TDM of *M. avium* wax ester (**186**) using IgG gave a higher distinction than its wax ester (**185**); the keto TMM (**161**) from *M. tb* gave a higher antibody binding signal higher than than keto MA (**159**). Furthermore, the mixed TDM (**191**) gave high responses and moderate distinction between TB+ and TB- serum using IgG Fc.

The results from **Table 20** show that the glycolipid Ags gave many false+ using this set of serum samples. The best pairs of sensitivity and specificity are shown in **Table 21**.

No.	Id		Sens. (%)	Spec. (%)	Spec. for 100% sens.
1	Mixed TDM (191)	IgG Fc	87	71	31
2	TDM of wax ester (186)	IgG Fc	73	60	6
3	MeO TDM (173)	IgG Fc	60	69	0
4	Keto TMM (161)	IgG Fc	53	69	3
5	Wax ester (185)	IgG	60	54	0
6	Keto MA (159)	IgG Fc	40	37	0

Table (21): The sensitivity and specificity of synthetic Ags tested in this section

The ROC analysis of the results with each antigen is given in **Figure 57**.

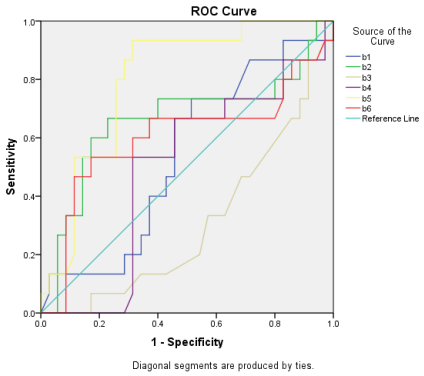

Id			Area Under the Curve	Sens. (%)	Spec. (%)	Spec. for 100% sens.
Mixed TDM (191)	IgG Fc	b5	0.799	93	69	33
TDM of wax ester (186)	IgG Fc	b2	0.661	60	83	6
MeO TDM (173)	IgG Fc	b6	0.602	67	63	0
Wax ester (185)	IgG	b1	0.538	67	54	0
Keto TMM (161)	IgG Fc	b4	0.490	67	54	3
Keto MA (159)	IgG Fc	b3	0.305	47	31	0

Figure 57: The ROC analysis using data from Table 20

The best area under the curve was observed with mixed TDM (**191**) using IgG Fc as secondary antibody, but even this was rather low. The different structural features of each of these antigens are presented in **Table 22**, together with their sensitivity and specificity.

Id	Length of chain				Stereochemistry		organism	No. of MA	Sens. (%)	Spec. (%)	AVG ABS+	AVG ABS-
	a	b	c	d	Proximal	Distal						
Wax ester (185)	17	15	18	23	Trans,RS	Wax,S	*M. avium*	1	73	49	2.85	2.81
TDM (186)								2	73	60	2.36	1.54
Keto MA (159)	17	18	15	23	Cis, RS	Keto, R	*M. kansasii*	1	40	37	0.33	0.40
Keto TMM (161)									87	14	2.28	2.28
Mixed TDM (191)	16	13	18	21	Trans,SR	Cis, SR	*M. tb*	2	100	31	2.71	1.45
	17	16	17		Cis, SR	MeO, SS						
MeO TDM (173)	17	16	18	23	Trans,SR	MeO, SS	*M. tb*	2	67	63	2.06	1.49

Table (22): Effect of the chain length and number of chain in the antigenicity of synthetic Ags

The table shows that the Abs can recognize the epitope made by wax ester (**185**) and its TDM (**186**) from *M. avium* using IgG and IgG Fc specific secondary antibody respectively to a high level, but the latter showed better distenction between TB+ and TB- serum. The Abs recognize the epitope made by the mixed TDM (**191**) from *M. kansasii* with good distenction using IgG Fc.They do not recognize the epitope made by the free keto MA (**159**), but can recognize its TMM (**161**) albeit with no distinction. Furthermore, the methoxy TDM (**173**) from *M. tb* gave a high response with good distinction using IgG Fc as a secondary antibody.

3.9 The effect of use a different range of synthetic glycolipid Ags

An ELISA assay was carried out to detect the Abs presented in a 14 TB+ and 30 TB- serum samples, at a 1:20 dilution, from the WHO using two Ags, wax ester (**185**) and its TDM (**186**)

from *M. avium* Ags, using IgG (whole, because other assays on free mycolic acids had been run with this antibody) and IgG Fc respectively as a secondary Ab and 0.5% casein/ PBS buffer (**Table 23**). In addition, keto-MA TDM (**160**) from *M. tb* was used as antigen with IgA secondary antibody, to determine the effect of using the latter.

No.	Wax ester (185)	TDM of wax (186)	Keto TDM (160)
	IgG	IgG Fc	IgA
1	0.66	3.40	0.61
2	2.23	0.53	1.03
3	1.43	3.21	0.46
4	0.67	3.20	0.63
5	1.95	3.81	0.46
6	1.42	3.25	0.89
7	1.12	1.92	0.62
8	2.62	0.31	1.36
9	0.82	1.09	0.34
10	1.56	4.09	3.64
11	2.92	3.66	0.45
12	4.27	3.75	1.97
13	1.01	2.41	0.49
14	2.28	2.34	3.61
15	0.83	0.41	0.39
16	0.75	0.66	0.53
17	0.81	0.66	0.34
18	1.15	0.52	0.40
19	1.39	1.10	0.26
20	0.67	1.97	0.42
21	1.82	0.68	0.46
22	1.34	1.27	0.45
23	0.68	0.29	0.70
24	1.15	2.47	0.51
25	0.66	0.40	0.55
26	2.04	0.47	0.47
27	1.09	1.28	0.50
28	1.58	0.54	0.38
29	1.77	0.94	0.47
30	0.58	0.71	0.26
31	1.69	2.93	1.40
32	1.21	1.30	0.63
33	1.90	2.12	0.26
34	0.82	3.10	2.03
35	1.32	3.25	0.61
36	0.71	0.25	0.24
37	0.64	0.25	0.98
38	1.22	1.21	0.56
39	3.20	1.00	0.36
40	0.66	0.26	0.23
41	3.81	2.80	0.72
42	0.79	0.47	0.62
43	0.76	0.41	0.47
44	1.27	0.45	0.53
Cut-off	>1.41	>1.73	>0.315
Cut-off ROC	>1.405	>1.610	>0.30
Tru.+	9	11	14
Fal. +	8	7	25
Sens.%	64	79	100
Spec.%	73	77	17
Sens.% ROC	64	79	100
Spec.(% ROC	73	77	17

Table (23): Effect of keto TDM, wax ester and its TDM as Ags. The red and blue colours in column 1 in table 23 show infected and uninfected serum samples in rows 1-14 and 15-44 respectively.

The average absorbances of positive and negative sera were calculated using the data from **Table 23**, (**Figure 58**). The TDM (**186**) from *M. avium* using IgG Fc as a secondary Ab gave a higher antibody binding signal than wax ester (**185**) Ag using IgG respectively. The keto-MA TDM (**160**) gave some very high responses, though most were moderate.

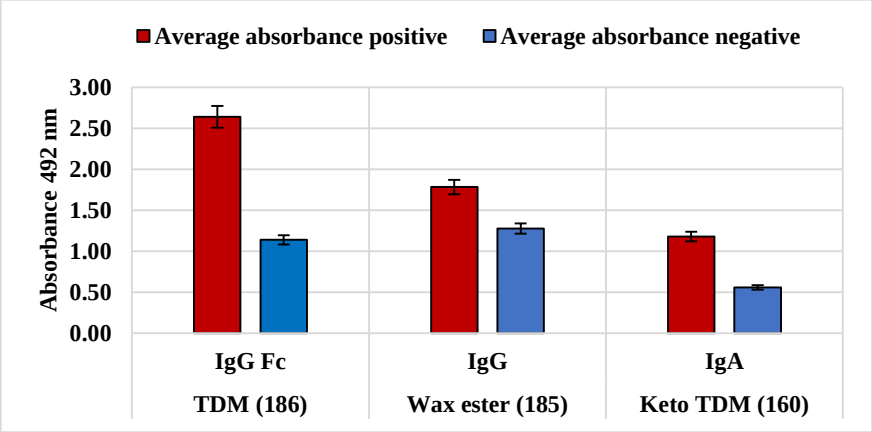

Figure 58: The average of absorbances of three new antigens using TB+ and TB- WHO serum samples

The figure shows that the TDM of wax ester (**186**) gave higher Ab binding signal than other Ags with good distinction between TB+ and TB- serum samples. The sensitivity and specificity of each Ag tested are presented in **Table 24** below.

No.	Id		Sens. (%)	Spec. (%)	Spec. for 100% sens.
1	Wax ester (185)	IgG	64	73	7
2	TDM of wax ester (186)	IgG Fc	79	77	13
3	Keto MA (160)	IgA	100	17	17

Table (24): The sensitivity, specificity for synthetic Ags from Table 23

Table 24 shows the best pair of sensitivity and specificity was observed with the TDM of wax ester (**186**) (86, 60) using IgG Fc. The ROC analysis was also studied **(Figure 59)**.

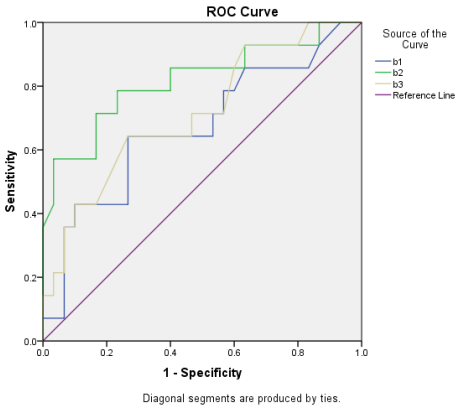

No.	Id			Area Under the Curve	Sens. (%)	Spec. (%)	Spec. for 100% sens.
1	TDM of wax ester (186)	IgG Fc	b2	0.818	64	73	7
2	Keto TDM (160)	IgA	b3	0.715	79	77	13
3	Wax ester (185)	IgG	b1	0.669	100	17	17

Figure 59: The ROC analysis using data from Table 23

The best area under the curve was observed with wax ester TDM (**186**) using IgG Fc as a secondary antibody.

3.10 The effect of use a range of CF Ags using human TB- serum samples from Wales

In order to examine possible reasons for false positive results, ELISA assays were carried out using α-TMM (**157**) and Keto TDM (**175**) and α-TDM (**156**) using 47 human serum samples from Wales, using IgG Fc specific secondary Ab and 0.5% casein/PBS in 1: 20 dilution (**Table 25**). The serum samples were from people living in Wales and with no known mycobacterial infections and were taken from three population groups, 1-20 farmers, 21-39 urban residents, and 40- 47 rural residents. The results for these serum samples then compared with the averages for 27 TB+ and 34 TB- WHO serum samples.

These samples were all expected to correspond to TB- serum. Indeed, the average response for each antigen was low. However, it is important to note that some of the samples did lead to absorbances above 1. This suggests that even in a healthy population, there are individuals with antibodies to MA derivatives in their immune systems, but these values still very low in contrast with the absorbances of TB+WHO serum samples, (**Figure 60**).

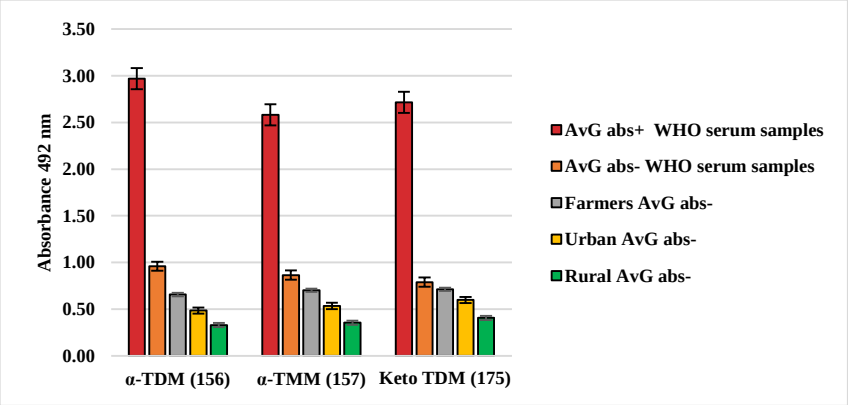

Figure 60: The average response of CFs Ags using TB- serum samples from Wales, farmers, urban residents, and rural residents, compared with TB+ and TB- WHO serum samples

The average response of each CF Ag were below the average of the WHO-; however, in all cases the avarages for serum from farmers were somewhat above those for urban and rural residents. **Table 25** also shows that a considerable numberof farmer's samples were above the average of WHO-. Perhaps reflecting the greater exposure of this group to mycobacteria.

No	Id	α-TDM (156) 1 in 20 IgG (Fc specific)	α-TMM (157) 1 in 20 IgG (Fc specific)	Keto TDM (175) 1 in 20 IgG (Fc specific)
1	Farmers	0.66	0.39	0.52
2		0.69	0.51	0.53
3		0.97	1.75	1.30
4		0.93	0.70	0.94
5		0.55	0.51	0.57
6		0.52	0.36	0.66
7		0.70	0.39	0.63
8		1.33	1.29	1.50
9		0.41	0.96	0.37
10		0.56	0.37	0.63
11		0.60	0.40	0.48
12		0.36	0.32	0.44
13		1.09	0.93	1.35
14		0.53	0.48	0.63
15		0.36	0.50	0.35
16		0.31	1.37	0.51
17		0.45	0.42	0.38
18		0.96	1.63	1.84
19		0.46	0.29	0.33
20		0.68	0.51	0.28
21	Urban	0.33	0.39	0.58
22		0.21	0.24	0.38
23		0.56	0.42	0.62
24		0.55	0.50	0.66
25		0.25	0.28	0.45
26		0.47	0.96	0.91
27		0.21	0.24	0.30
28		0.25	0.58	0.40
29		1.20	1.03	1.47
30		0.30	0.36	0.42
31		0.42	1.06	1.02
32		1.51	1.04	1.16
33		0.84	0.78	0.79
34		0.33	0.78	0.43
35		0.29	0.32	0.33
36		0.28	0.29	0.25
37		0.29	0.25	0.29
38		0.50	0.32	0.52
39		0.44	0.32	0.40
40	Rural	0.29	0.29	0.34
41		0.29	0.60	0.52
42		0.25	0.21	0.29
43		0.21	0.18	0.28
44		0.31	0.32	0.44
45		0.27	0.20	0.26
46		0.55	0.56	0.59
47		0.47	0.50	0.53
Cut-off		>1	>.9	>1.6

Table (25): The effect of use CFs Ags using TB- serum samples from Wales, 1-20 farmers, 21-39 urban residents, and 40- 47 rural residents. The cut-off for 'postive' is average of the WHO- TB- samples. In this set there were no responses above the average of the WHO+ set with any antigen

3.11 *S,S-trans*-Alkene-methoxy MA glycolipids synthesised in this work as antigens

The set Ags prepared in this work, TDM (**44**), TMM (**45**), GroMM (**46**), GMM (**47**) and Arabino-MA (**48**), all based on a common *S,S-trans*-alkene-methoxy MA, were tested by Dr Carys Roberts in the School of Chemistry using an ELISA assay. The test was done using 9 TB+ and 11 TB- WHO human serum samples at 1:40 dilution in casein and the IgG Fc specific secondary Ab (**Table 26**).

No.	TDM (44)	TMM (45)	GroMM (46)	GMM (47)	ArM (48)
1	1.39	0.87	0.08	0.21	0.07
2	0.64	0.38	0.27	0.34	0.17
3	0.83	0.51	0.07	0.11	0.06
4	2.92	2.35	0.10	0.15	0.06
5	1.57	0.60	0.46	0.81	0.42
6	0.92	0.54	0.20	0.28	0.12
7	1.98	1.16	0.29	1.24	0.16
8	1.11	0.55	0.10	0.14	0.11
9	0.44	0.52	0.12	0.30	0.20
10	0.76	0.42	0.18	0.24	0.15
11	0.67	0.41	0.13	0.23	0.10
12	0.31	0.13	0.16	0.15	0.14
13	0.33	0.16	0.16	0.30	0.14
14	0.26	0.24	0.12	0.16	0.11
15	0.24	0.28	0.08	0.18	0.10
16	0.19	0.18	0.07	0.11	0.08
17	0.32	0.15	0.09	0.17	0.08
18	0.86	0.56	0.19	0.71	0.13
19	0.12	0.12	0.07	0.09	0.06
20	0.18	0.09	0.11	0.67	0.09
Cut-off	>0.40	>0.50	>0.42	>0.80	>0.42
Cut-off ROC	>0.385	>0.465	>0.375	>0.760	>0.31
Tru.+	9	8	1	2	1
Fal. +	3	1	0	0	0
Sens.%	100	89	11	22	11
Spec.%	73	91	100	100	100
Sens.% ROC	100	89	11	22	11
Spec.% ROC	73	91	100	100	100

Table (26): Alkene glycolipid Ags and TB+ and TB- WHO human serum samples using casein. The red and blue colours in column 1 show TB+ and TB- serum samples in rows 1-9 and 10-20 respectively.

The average absorbances in all cases were rather low (**Table 27**).

No.	Id	AVG ABS+	AVG ABS-
1	TDM (44)	1.31	0.39
2	TMM (45)	0.83	0.25
3	GroMM (46)	0.19	0.12
4	GMM (47)	0.40	0.27
5	ArM (48)	0.15	0.11

Table (27): The average of absorbances from Table 26

The Abs in the TB+ serum samples can best recognize the epitope made by CFs Ags either TDM (**44**) or TMM (**45**). The results are plotted in **Figure 61**.

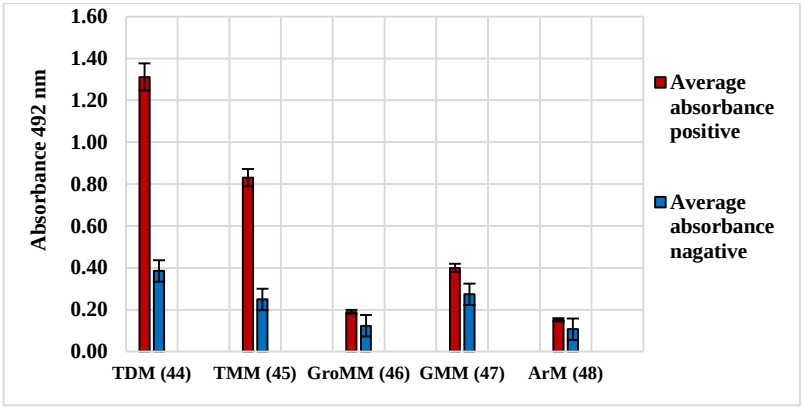

Figure 61: The average of absorbances using the data from Table 26

The results showed that the synthetic methoxy MA TDM (**44**) and methoxy MA TMM (**45**) gave significant values for sensitivity and specificity (100, 73 %) and (89, 91) using cut-off values of >0.40, >0.50 respectively. However, the GroMM (**46**), GMM (**47**) and Arabino-MA (**48**) Ags showed very small responses, in most cases very close to the values obtained for controls with no antigen.

The ROC analysis is shown in **Figure 62**.

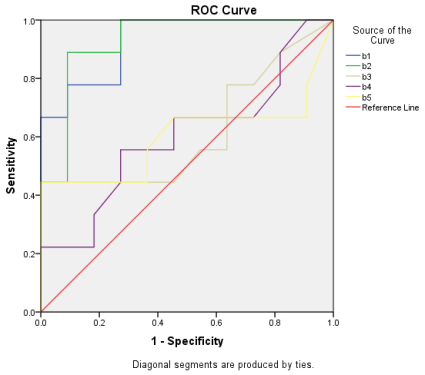

No.	Id		Area under the curve	Sensitivity (%)	Specificity (%)
1	TDM (44)	b1	0.929	100	73
2	TMM (45)	b2	0.929	89	91
3	GMM (47)	b4	0.616	22	100
4	GroMM (46)	b3	0.601	11	100
5	ArM (48)	b5	0.601	11	100

Figure 62: The ROC analysis using data from Table 26

The best areas under the curve were observed with TDM (**44**) and TMM (**45**), 0.929 in each case. These both gave very good values of specificity and sensitivity.

The values for the three other antigens were very close to 0.5, i.e. they showed no distinction between TB+ and TB- samples – there was very little signal with any of the samples. The *S,S-trans*-alkene-methoxy MA acid present in each glycolipid Ag was the same indicating that the

Abs can identify the hydrophobic and the carbohydrate moieties in the structure of the glycolipid Ags.

3.12 Explaining some false results

Cell wall MA from *M. tb* are CD1b presented Ags that can be used to detect Abs as surrogate markers of active TB, even in HIV co-infected patients. The use of the complex mixtures of natural MA is complicated by an apparent Ab cross-reactivity with cholesterol. The ability of MA to attract cholesterol to the macrophage may be critical for these phenomena. Cholesterol has been shown to play a role in the entry and survival of *M. tb* in the host macrophage.[422,423] The cholesteroid nature of at least some MAs may imply their active participation in this manifestation of virulence. The presence of cholesterol in the serum samples that can cross-react with same antibodies to the MA Ags, may therefore give false negatives. Pan *et. al.* reported that even small changes in the structure of MAs present in TDM are important for their antigenicity. Yolandy *et al*,[371,421] investigated the possibility that the low accuracy for a serodiagnostic ELISA assay based on the use of MA as Ag could be the result of the folding of free MAs to resemble a "cholesteroid" shape as stated before. They used an approach similar to that employed by Prendergast *et al*.[372] to suggest molecular mimicry between microbial and self-structures in autoimmune diseases. The basic assumption of this approach is that the specific molecular recognition of two substances by an established binding agent indicates resemblance in the three-dimensional structure of the two compounds and this may explain the false+ and false- results.

It was also suggested that some false- results were from patients who were co-infected with HIV or who had compromised immune systems. However, the potential for detection of Abs to MA as biomarker for diagnosis of active TB was emphasized when Schleicher *et al*.[370] demonstrated in 2002 that the Ab binding signal to MA was not affected by the degree to which the patient was affected by HIV-co-infection.[370] MAs are lipid Ags and unlike protein Ags they are displayed by CD1 molecules and not on MHC molecules. The CD1-Ag complex is in turn recognised by T-cells without CD4 and CD8 surface markers. The ability of MAs to elicit CD4-, CD8- double negative T cells by means of their presentation on CD1b proteins of DCs [429] may well be the reason that Ab binding to MAs in AIDS patients with even very low CD4 T cell counts, [370,428] relative to other patients that are not infected with HIV, or have normal CD4 T cell counts.[370]

Also, MAC prevalence increased dramatically with the emergence of HIV-1-induced immunodeficiency.[39,424] disseminated infection with *M. avium* is rare in immune competent individuals and is highly suggestive of compromised cellular immune functions.[425]

3.13 Conclusion

The aim of project was achieved using an ELISA assay to investigate the potential of the synthesized molecules for the diagnosis of TB. First, in order to determine the most sensitive and specific diagnostic test Ag, ELISA assays were carried out using a range of novel synthetic Ags from different parts of the cell wall and different *mycobacteria*, different secondary Abs and a range of TB+ and TB- human serum samples from sources which included tropical regions of Asia, Africa and the America. The best combinations of sensitivity and specificity with a sub-set of Gambia samples were observed with keto-MA based TDM (**160**) (100 and 78%), methoxy arabino-MA (**179**) (100 and 73%) and α-arabino-MA (**158**) (100 and 86%). Combining the results from synthetic keto-MA TDM (**160**), α-MA ArM (**158**) and α-MA GMM (**180**) gave 100 and 94% sensitivity and specificity. These represent very much better values than those reported with many recognised assays. The second part attempted to clarify the exact antigenic epitope in a synthetic MA or its glycolipids Ags recognized by a specific Ab. It was concluded that the Abs to MAs or its derivatives can recognize both the hydrophobic and the carbohydrate moieties in the structure of the glycolipid Ags at different levels.

The results also showed higher Abs binding signals using WHO serum samples with dilution and washing by casein than 0.05% PBS-T buffer solution, and the best pairs of sensitivity and specificity were observed with keto-MA TDM (**160**) (100, 61) using casein.

The results from a further set of serum samples from WHO with a new range of synthetic Ags showed that the best pairs of sensitivity and specificity (87, 71) was with mixed TDM (**191**), containing one α- and one methoxy using IgG Fc secondary antibody and casein/PBS dilution. The results from all these experiments showed that the ELISA assay can distinguish between TB+ and TB- serum samples with accurate results, but that the results with different antigens are also very different.

ELISA assays also carried using a range of synthetic CFs Ags using serum samples from people in Wales with no known mycobacterial infection; these were collected from farmers, urban residents, and rural residents and the results then compared with those for TB+ and TB- WHO serum samples from patients with suspected TB, generally in high burden TB populations. The results show low average absorbances and average of absorbances. Indeed, the average response

for each Ag was somewhat lower that that for the WHO- negative group. The average response for the farmers group was somewhat higher than the other two Welsh group. There were no responses above the average of the WHO+ serum samples, but quite a lot above the average of the WHO-group. More of these occurred among the farmers. It is possible that this is because this group is genrally more exposed to high mycobacterial loads.

The serodiagnostic behaviour of a set of TDM, TMM, GroMM, GMM and ArM Ags from *M. tb* from the same *trans*-alkene MA was studied using WHO human serum samples. The results indicated that the Abs to MAs or its derivatives can recognize the hydrophobic and the carbohydrate moieties in the structure of the glycolipid Ags at different levels. The best combinations of sensitivity and specificity were observed in TDM (**44**) (100, 73%) and TMM (**45**) (89,91%). The best areas under the ROC curve was also observed with these Ags, 0.952 in each case, with excellent distinction between TB+ and TB- serum samples.

Chapter 4

4.1 Diagnosis of BTB and TB in Bovine serum samples

In this part of the work, a number of ELISA studies were carried out to determine the best antigens for detecting mycobacterial infection in cattle.

The first part (**4.2**) of this work used the natural bovine TDM from *M. bovis* as Ag and IgG whole molecule as a secondary Ab, using bovine serum samples obtained from Veterinary Laboratory Agency (VLA). The samples were from different categories, `naturally infected` and `vaccinated` serum samples [either `pre-challenge BCG` or `pre-challenge BCG+ AdenoAg85A]; the vaccinated samples from cattle after exposure to infected cattle for a significant period. Extensive experimental observations were provided by VLA for these cattle; the details are provided in the Supplementary Information

The second part (**4.3**) focused on optimization of the ELISA assay with bovine serum samples. This was achieved in two parts. First (**4.3.1**), different concentrations of natural bovine TDM Ag in each well were used with different categories of bovine serum samples from VLA, `naturally infected` and vaccinated [`pre-challenge BCG` and `pre-challenge BCG+ AdenoAg85A] and again using `naturally infected`, non-vaccinated `pre-challenge` and vaccinated `pre-challenge BCG` serum samples.

The second part (**4.3.2**) of this study centred on the optimization of serum sample concentration, this done using *M-bovis* serum samples, which were diluted to 1:20 and 1:80 in casein and assayed with natural bovine TDM Ag from *M. bovis* and a range of new synthetic Ags represented, methoxy TDM (**166**), methoxy TMM (**167**), α-TDM (**156**), α-TMM (**157**) and unsaturated TDM (**197**) with IgG as secondary Ab (**Table 28**).

The third part (**4.4**) used natural *M.bovis* TDM and synthetic methoxy TDM (**166**) and α-TDM (**156**) Ags from *M. tb* with `naturally infected', `pre-challenge non-vaccinated` and vaccinated [`pre-challenge BCG` and `pre-challenge BCG+ AdenoAg85A] serum samples.

The fourth part (**4.5.1**) used natural human TDM from *M. tb* and *M. bovis* TDM and a range of synthetic Ags, methoxy-TDM (**166**), methoxy-TMM (**174**), α-TDM (**156**), α-TMM (**157**) from *M. tb* and unsaturated MA (**192**) from *M. fortuitum* and epoxy-MA (**193**) from *M. smegmatis* with 20 BTB+ serum samples from cattle infected naturally and 18 BTB- serum samples from young uninfected cattle.

Table 28: The structures of different MA and wax ester tested with bovine sera

Structure	No.	*Species*	*tdm*	*Tmm*
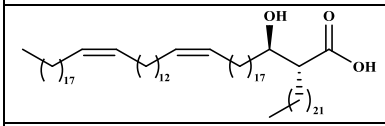	**(192)**	***M. fortuitum***		
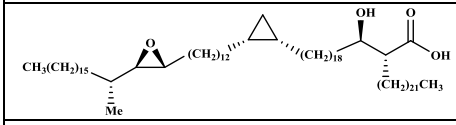	**(193)**	***M. smegmatis***		
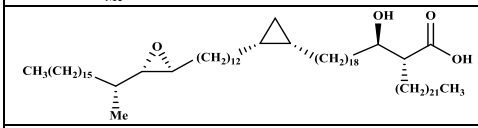	**(194)**	***M. smegmatis***		
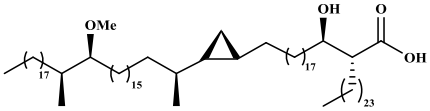	**(195)**	***M. tb***		
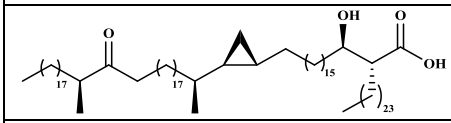	**(196)**	***M. tb***		
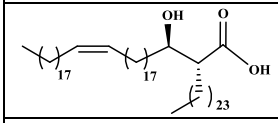		***M. tb***	**(197)**	
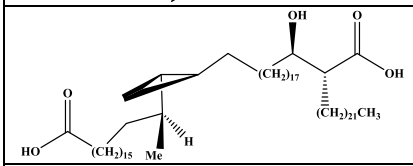	**(198)**	***M. avium***		
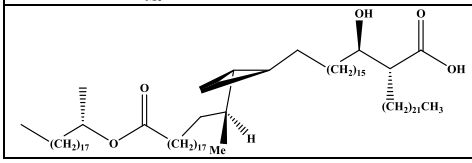	**(199)**	***M. gordonae***	**(200)**	**(201)**

The fifth part (**4.6**) compared natural human and bovine TDM Ags from *M. tb* and *M. bovis* with methoxy TMM (**167**), methoxy TDM (**169**), methoxy TMM (**170**), keto TDM (**160**), α-TDM (**156**) and α-TMM (**157**) again using `naturally infected`, `pre-challenge non-vaccinate` and `pre-challenge BCG vaccinated` serum samples.

The sixth part (**4.7**) focused on the effect of MA with different functional groups [methoxy (**195**), keto (**196**), unsaturated (**192**) and epoxy- (**193**)] MA from *M. tb*, *M. fortuitum* and *M. smegmatis* respectively.

The seventh part (**4.8**) examined the effect of using synthetic keto TDM (**160**) and α-TDM (**156**) Ags using either IgG whole molecule or IgG Fc as secondary Ab.

The eighth part (**4.9**) involved three elements: firstly (**4.9.1**), the effect of using synthetic α-TDM (**171**) and α-TMM (**172**) Ags from *M. kansasii*. The test used IgG whole molecule as

secondary Ab and 0.5% casein/PBS buffer. Secondly (**4.9.2**), two synthetic epoxy-MA (**194**) and epoxy-MA (**193**) from *M. smegmatis* were used with IgG whole molecule. Lastly (**4.9.3**), the effect of natural wax ester from *M. Avium* and synthetic wax-ester (**185**) was studied.

The ninth part (**4.9.4**) used natural TDM isolated from *M. bovis* and natural wax ester from *M. avium* and synthetic wax ester (**187**), diacid (**198**), TDM (**188**) and TMM (**189**) from *M. avium* and synthetic wax ester (**199**), TDM (**200**), TMM (**201**) from *M. gordonae* and α-TDM (**156**), α-TMM (**157**), keto TDM (**160**), keto TMM (**161**), methoxy TDM (**163**), methoxy TMM (**164**), α-MA (**155**), keto MA (**159**) and methoxy MA (**162**) from *M. tb*. The tests were done using 1:20 dilution in serum samples in 0.05% PBS-T and IgG Fc specific molecule as a secondary Ab.

Finally (**4.10**), In order to understand whether the stage of infection would interfere with the assay, the time profile in sets of serum samples from thirteen different cattle were studied with natural bovine TDM and a set of synthetic antigens represented on methoxy TDM (**166**), methoxy TMM (**167**), α-TDM (**156**), α-TMM (**157**) and unsaturated TDM (**197**). The sets of serum sample were obtained from Agri-Food and Biosciences Institute (AFBI) in North Ireland and had tried to infect with disease through an aerosol system.

4.2 Initial tests of natural Ags with VLA bovine serum samples

Bovine serum samples were obtained from Veterinary Laboratory Agency (VLA). The samples obtained were in different categories, labelled `naturally infected` and `vaccinated` serum samples [either `pre-challenge BCG` or `pre-challenge BCG+ AdenoAg85A]; the vaccinated samples were from cattle after exposure to infected cattle for a significant period. Extensive experimental observations were provided by VLA for these cattle (data are provided in the Supplementary Information).

An initial test was done on these samples using the basic ELISA method described in the experimental section to see if it could distinguish among these classes of serum samples. The test was done using natural bovine TDM from *M. bovis* as Ag and IgG whole molecule as a secondary Ab (**Figure 63**).

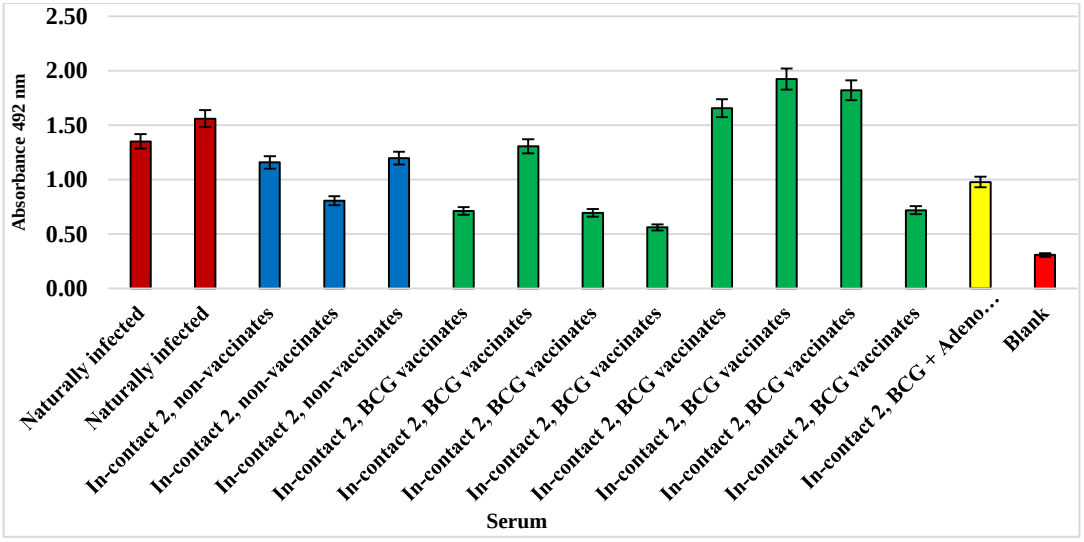

Figure (63): Initial Test using natural *M. bovis* TDM Ag using `naturally infected` and vaccinated samples

Each bar in **Figure 63** shows the average of three replicates on the same serum sample against natural bovine TDM Ag. In general all the serum samples gave higher responses than the blank. The natural Ag gave a high Ab binding signal with naturally infected serum samples but the vaccinated [BCG and BCG+ AdenoAg85A] serum samples also showed rather large signals in some cases. This is a limited set of results; there are a number of possible explanations for the relatively high results from the vaccinated cattle - one being that vaccination leads to long-lasting lipid Ab responses.

4.3 Optimization of the ELISA assay

4.3.1 The natural Ag concentrations

Different concentrations of natural bovine TDM Ag from 6.25, 3.13, 1.56, 0.78, 0.39 to 0.2 µg/ well were assayed with two different categories of bovine serum samples from VLA labelled `naturally infected` and vaccinated [`pre-challenge BCG` and `pre-challenge BCG+ AdenoAg85A] serum samples to determine the best concentration of Ag (**Figure 64**).

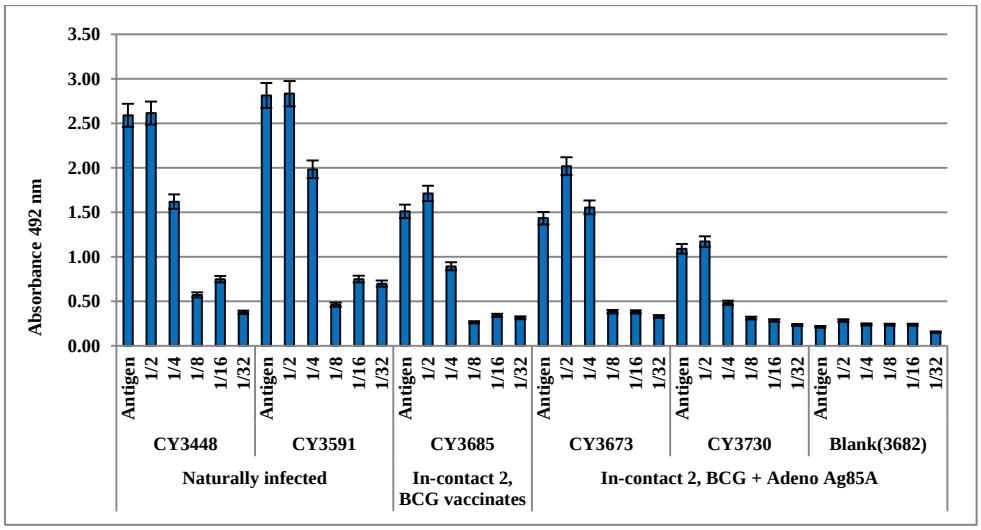

Figure (64): Natural TDM Ag using 6.25, 3.13, 1.56, 0.78, and 0.39 to 0.2 µg / well concentrations

Figure 64 shows that the best concentration of Ag was 3.13 µg/ well (1/2 amount of Ag). The ELISA assay was repeated using `naturally infected`, non-vaccinated `Pre-challenge 2` and vaccinated `pre-challenge BCG` serum samples; again the best concentration was 3.13 µg/ well, (**Figure 65**).

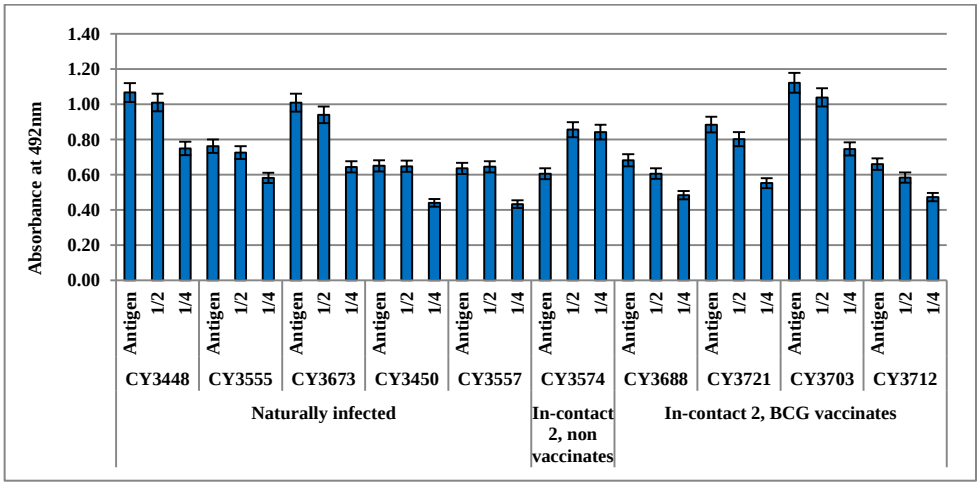

Figure (65): Natural TDM Ag using 6.25, 3.13 and 1.56 µg/ well concentration

The dilution of serum samples used in the initial tests and in optimizing the Ag concentration was 1:20.

4.3.2 The serum sample concentration

Serum samples concentration may influence the results of ELISA. Therefore, *M-bovis* serum samples were diluted with 0.5% casein/PBS buffer to get concentrations of 1:20 and 1:80. The samples were assayed with natural *M. bovis* TDM Ag and a range of synthetic Ags, methoxy

TDM (**166**), methoxy TMM (**167**), α-TDM (**156**), α-TMM (**157**) and unsaturated TDM (**197**). The results showed that 1:20 gave a higher absorbance than 1:80 (**Figure 66**).

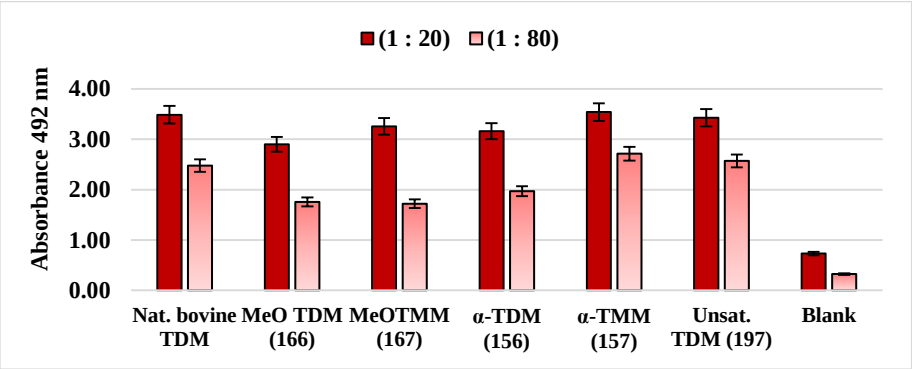

Figure (66): Effect of change the serum concentration

The α-MA TMM (**157**) and unsaturated-MA TDM (**197**) gave Ab binding signals similar to the natural bovine TDM Ag at the two dilutions.

4.4 Use of different synthetic Ags

Natural bovine TDM from *M. bovis* and synthetic methoxy TDM (**166**) and α-TDM (**156**) Ags from *M. tb* were examined using IgG whole molecule as a secondary Ab and using `naturally infected`, `pre-challenge non-vaccinated` and vaccinated [`pre-challenge BCG` and `pre-challenge BCG+ AdenoAg85A`] serum samples at a 1:20 dilution in 0.5% casein/PBS buffer (**Table 29**). Naturally infected samples are from animals diagnosed as BTb+ by skin test and other standard assays. Pre-challenge vaccinated cattle had been kept for an extended period with infected cattle; it was expected that they would have bTB. The vaccinated cattle had also been kept with infected cattle for an extended period; it was expected that most would be protected from infection.

Categories of Sera	No.	Nat. bovine TDM	α-TDM (156)	MeO TDM (166)
`naturally infected` (Class1)	1	1.86	0.84	1.53
	2	1.8	1	1.62
	3	0.6	0.36	0.44
	4	0.47	0.48	0.36
	5	1.01	1.11	1
	6	1.6	2.11	1.71
	7	0.57	0.47	0.4
`pre-challenge non-vaccinated` (Class 2)	8	0.48	0.51	0.39
	9	0.61	0.6	0.71
	10	0.5	0.52	0.8
	11	0.87	0.36	0.64
	12	2.47	1.55	2.63
	13	0.21	0.22	0.22
	14	0.99	0.66	0.67
	15	1.05	0.78	0.88
`pre-challenge BCG` (Class 3)	16	0.21	0.28	0.26
	17	0.68	0.48	0.51
	18	1	0.71	0.72
	19	0.59	0.44	0.38
`pre-challenge BCG+ AdenoAg85A` (Class 4)	20	0.23	0.28	0.27
	21	0.77	0.52	0.67
	22	1.29	0.99	0.73
	23	0.4	0.41	0.39
Cut-off		>0.56	>0.46	>0.39
Tru.+		6	6	6
Fal. +clas 1		5	6	6
Fal. +clas 2		3	2	2
Fal. +clas 3		2	2	2
Fal. + over all		10	10	10
Sens.%		86	86	86
Spec. %clas 1		38	25	25
Spec. %clas 2		25	50	50
Spec. %clas 3		50	50	50
spec.% overall 4		38	38	38

Table (29): Effect of natural bovine and two synthetic TDMs using different categories of serum. The red, blue, yellow and green colours in column 1 show `naturally infected', `pre-challenge non-vaccinated` and vaccinated [`pre-challenge BCG` and `pre-challenge BCG+AdenoAg85A] serum samples in rows 1-7, 8-15, 16-19 and 20-23 respectively. The specificity for class 1, 2, 3 and 4 was calculated relative to the cut-off set for TB+; overall 4 was calculated for a combination of 1, 2 and 3 relative to that cut-off

The average absorbances for each Ag for different serum categories are shown in **Figure 67**.

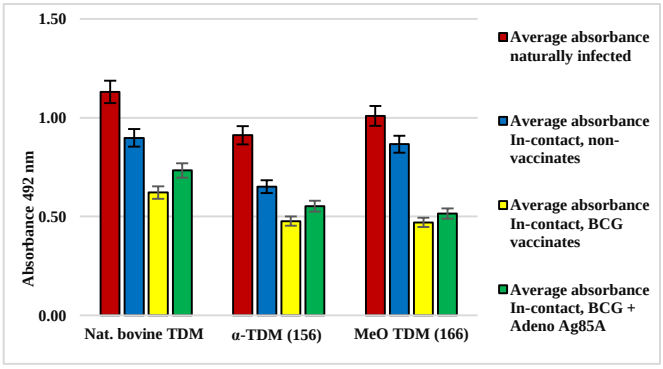

Figure (67): Effect of use different categories of serum samples

This shows that the three Ags gave a higher binding signal with `naturally infected' serum samples than `pre-challenge non-vaccinated` and vaccinated [`pre-challenge BCG` and `pre-challenge BCG+ AdenoAg85A] samples.

The pairs of sensitivity and specificity derived from **Table 29** are displayed in **Table 30**.

Id	Sens.%	Spec. %clas 1	Spec. %clas 2	Spec. %clas 3	spec.% overall
Nat. bovine TDM	**86**	**38**	**25**	**50**	**38**
α-TDM (156)	**86**	**25**	**50**	**50**	**38**
MeO TDM (166)	**86**	**25**	**50**	**50**	**38**

Table (30): The pairs of sensitivity and specificity of natural TDM and synthetic TDMs Ags calculated using the data from Table 29. The sensitivity was calculated using the data from naturally infected, but the specificity calculated as : class (1) using the data from pre-challenge non-vaccinated; (2) pre-challenge BCG vaccinated; (3) pre-challenge BCG+ AdenoAg85A vaccinated and (4) is a combination of 1, 2 and 3.

ROC analysis was carried out using the four classes (**Figure 68).**

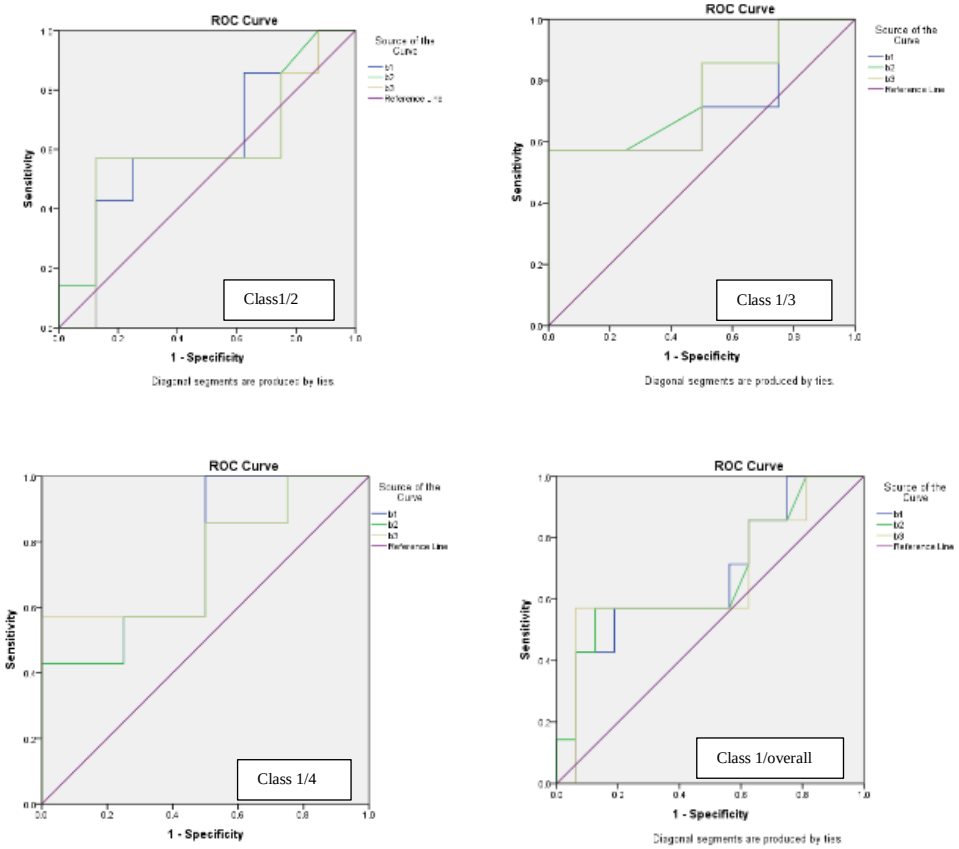

Figure 68: ROC analysis using data from Table 29: (a) ROC for TB+ versus pre-challenge non-vaccinated; (b) pre-challenge BCG vaccinated; (c) pre-challenge BCG+ AdenoAg85A and (d) combination of a, b and c

The ROC curve in each case show very little distinction between TB+ and any of the sub-classes.

4.5 Use of a larger set of Ags with a larger serum set

4.5.1 The use a range of new synthetic antigens with bTB+ and bTB- serum samples

The natural TDM from *M. tb* and natural TDM from *M. bovis* and a range of synthetic Ags, methoxy-TDM (**166**), methoxy-TMM (**174**), α-TDM (**156**), α-TMM (**157**) from *M. tb* and unsaturated MA (**192**) from *M. fortuitum* and epoxy-MA (**193**) from *M. smegmatis*, were assayed with 20 bTB+ serum samples from cattle infected naturally on the farms in South Wales and 18 bTB- serum samples from young uninfected cattle (non-vaccinated), run at 1:20 dilution in casein using IgG whole molecule as a secondary Ab (**Table 31**).

No.	Human TDM	Bovine TDM	MeO TDM (166)	α-TDM (156)	α-TMM (157)	Unsat. MA (192)	Epoxy MA (193)	MeO TMM (174)
	b1	b2	b3	b4	b5	b6	b7	b8
1	2.36	2.80	0.88	2.17	2.33	0.31	0.27	
2	2.55	0.57	0.48	1.73	3.03	0.35	0.36	0.66
3	1.28	1.57	0.83	0.83	1.51	0.34	0.29	0.89
4	1.50	0.85	0.92	1.49	2.58	0.23	0.25	1.31
5	1.64	0.83	0.57	0.95	2.53	0.30	0.30	1.83
6	0.68	0.59	0.35	0.61	3.08	0.23	0.23	1.36
7	2.07	0.61	0.36	0.64	3.51	0.33	0.24	1.91
8	1.79	1.37	0.85	1.31	1.88	0.35	0.30	1.52
9	1.26	1.05	0.48	1.62	2.65	0.30	0.34	1.27
10	1.32	0.68	0.53	1.05	2.64	0.37	0.38	1.22
11	0.42	0.26	0.30	0.34	0.75	0.22	0.28	0.37
12	0.83	0.54	0.30	0.51	0.85	0.26	0.23	0.61
13	0.83	0.80	0.56	0.57	1.90	0.37	0.33	1.15
14	0.90	0.85	0.56	0.69	1.10	0.32	0.31	1.18
15	2.37	1.92	0.51	1.29	2.40	0.30	0.39	0.62
16	0.95	0.42	0.27	0.86	1.46	0.18	0.24	0.68
17	0.91	0.98	0.52	0.82	0.79	0.29	0.30	0.62
18	1.80	2.83	0.88	1.45	1.93	0.41	0.46	
19	3.23	1.37	0.80	2.26	3.17	0.22	0.30	2.93
20	1.38	0.90	0.43	1.43	0.76	0.32	0.37	
21	0.85	0.59	0.28	0.81	0.75	0.19	0.27	0.43
22	1.30	0.64	0.42	0.83	3.43	0.21	0.29	1.00
23	3.18	1.52	0.32	3.11	1.45	0.20	0.23	0.31
24	0.75	0.47	0.36	0.55	0.76	0.27	0.23	0.74
25	0.53	0.33	0.23	0.36	0.33	0.23	0.23	
26	0.82	1.25	0.62	0.64	0.79	0.31	0.31	0.37
27	0.42	0.45	0.17	0.42	0.36	0.20	0.29	0.15
28	0.57	0.55	0.23	0.45	1.21	0.24	0.30	0.35
29	1.42	1.41	0.69	0.82	1.21	0.23	0.28	0.19
30	0.51	0.38	0.28	0.43	0.67	0.31	0.25	0.43
31	2.24	1.36	0.44	2.08	1.29	0.22	0.20	0.36
32	0.37	0.32	0.30	0.39	0.39	0.20	0.24	0.51
33	0.47	0.37	0.32	0.53	0.39	0.20	0.22	0.30
34	0.51	0.74	0.43	0.46	0.46	0.21	0.25	0.39
35	0.60	0.52	0.41	0.53	1.28	0.30	0.25	0.78
36	1.00	0.55	0.45	0.70	1.04	0.20	0.22	0.50
37	0.76	0.54	0.45	0.66	0.69	0.21	0.20	0.83
38	3.35	2.46	1.95	3.13	2.28	0.26	0.30	1.64
Cut-off	>0.77	>0.65	>0.47	>0.571	>0.7	>0.28	>0.25	>0.55
Cut-off ROC	>0.715	>0.545	>0.465	>0.675	>0.720	>0.215	>0.225	>0.560
Tru.+	18	14	14	18	20	14	16	16
Fal. +	8	6	3	9	11	3	9	5
Sens.%	90	70	70	90	100	70	80	80
Spec.%	56	67	83	50	39	83	50	72
Sens.% ROC	89	82	71	71	100	94	100	100
Spec.% ROC	59	59	82	59	35	53	23	35

Table (31): ELISA assay data using natural and synthetic Ags with bTB+ and bTB- serum samples

The average absorbances calculated using the data from Table 31 are presented in **Figure 69**.

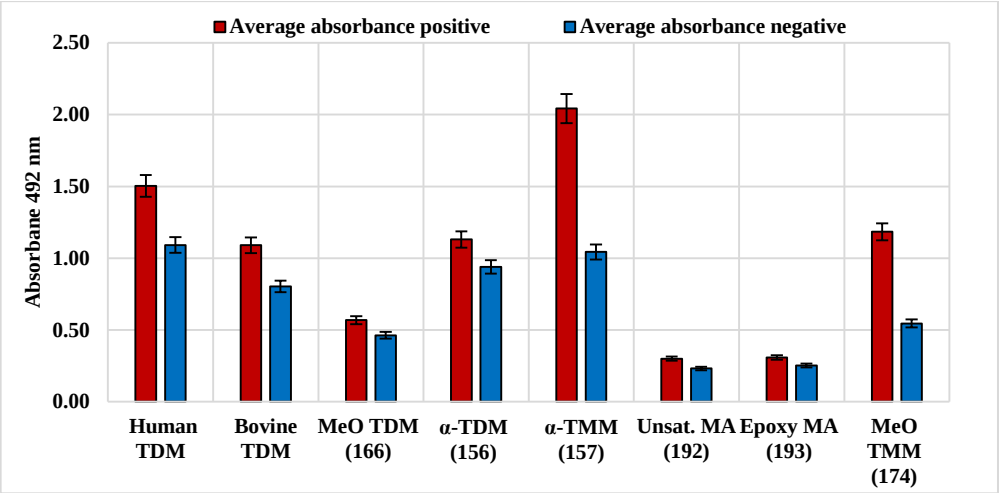

Figure 69: The average absorbances of natural and synthetic Ags using bTB+ and bTB- serum samples

The figure shows that the α-TMM (**157**) from *M. tb* gave higher Ab binding signals than the natural Ags and other synthetic Ags. Also, the Abs can recognize α-TDM (**156**) and methoxy TMM (**174**) from *M. tb* to the same level as natural bovine TDM. The Abs do not recognize the unsaturated MA (**192**) from *M. fortuitum* and epoxy-MA (**193**) from *M. smegmatis*. Further, the ELISA assay showed a clear distinction between bTB+ and bTB- serum samples using natural and synthetic Ags from different *Mycobacteria;* the best distinction was observed in α-TDM (**156**) and methoxy TMM (**174**) from *M. tb* with this set of samples.

Table 32 shows the pairs of sensitivity and specificity of the natural and synthetic Ags.

Id	Sens. (%)	Spec. (%)
Human TDM	90	56
Bovine TDM	70	67
MeO TDM (166)	70	83
α-TDM (156)	90	50
α-TMM (157)	70	89
Unsat. MA (192)	70	83
Epoxy MA (193)	80	50
MeO TMM (174)	80	72

Table (32): The sensitivity and specificity of natural bovine TDM and synthetic Ag

The table demonstrates that the best pairs of sensitivity and specificity observed in α-TMM (**157**) (70, 89). The ROC analysis of this set of Ags gave very similar figures (**Figure 70**).

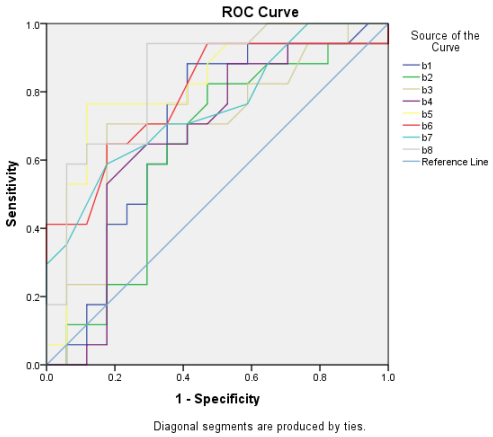

No.	Id		Area Under Curve	Sens. (%)	Spec. (%)
1	Methoxy TMM (174)	b8	0.846	80	72
2	α-TMM (157)	b5	0.827	77	88
3	Unsat. MA (192)	b6	0.792	70	83
4	Epoxy MA (193)	b7	0.753	80	50
5	Methoxy TDM (166)	b3	0.697	70	83
6	Human TDM	b1	0.694	90	56
7	α-TDM (156)	b4	0.666	90	50
8	Bovine TDM	b2	0.626	70	67

Figure 70: The ROC analysis using data from Table 31

4.5.2 Combining the results with several Ags

Statistical analysis using multidimensional scaling (MDS) and a Random Forest Classifier utilizing the results from antigens b1-b8 in **Tables 31** was carried out by Dr James Gibbons (**Figure 71**). The Random Forest analysis shows the rank order of each antigen in distinguishing between the defined bTB+ and bTB- samples.

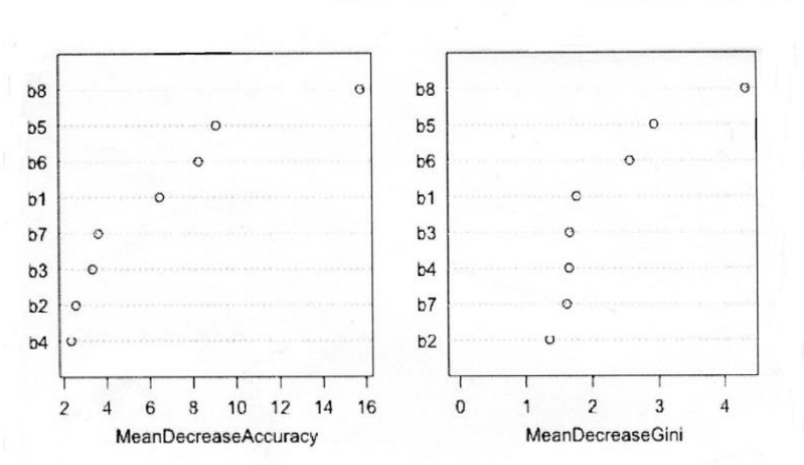

Figure (71): Random Forest variables importance plot

Figures 71 shows, in two different plots using mean decrease accuracy and mean decrease Gini, that methoxy TMM (**174, b8**), α-TMM (**157, b5**) and unsaturated MA (**192**, **b6**) all give a better

distinction than natural human TDM (**b1**) between bTB+ and bTB- serum samples. A principal coordinate analysis using all these Ags generates a probability distribution in two principal axis as shown in **Figures 72**. This gives a good split between bTB+ and bTB- samples, the positive samples represented in 1-20 data largely appearing on the left of the plot as a quite tight group, and the negative serum samples 21-38 as a more spread group on the right hand side; clearly there are some positives and negatives that do not fit this patterns.

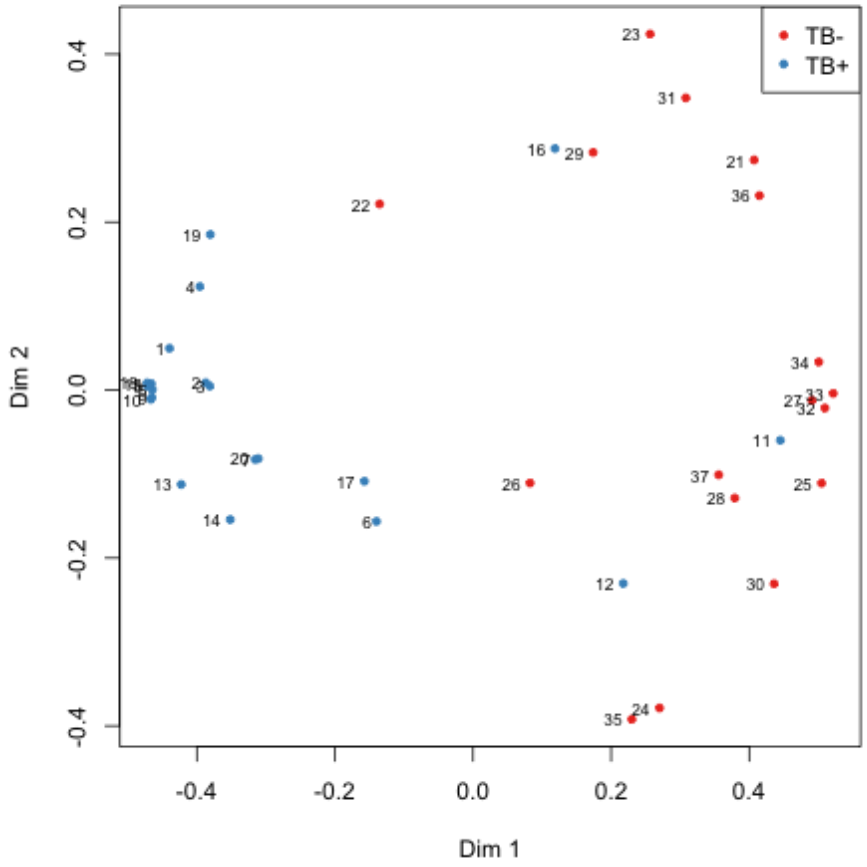

Figure (72): MDS plot for Random Forest Classifier with variables b1-b8 (1-20, bTB+, 21-38 bTB-)

The results demonstrated that the combining the results from different Ags gives a good distinction between different class of serum samples.

4.5.3 The effect of structure of MAs on the immune response

The effect of the structure of the meromycolate and corynomycolate parts of free MAs and MA in synthetic CFs from different *Mycobacteria* and the number of MA attached to the trehalose

in the immune response were analysed. The different structural features of each of these antigens are presented in **Table 33**, together with their sensitivity and specificity. The Abs in bTB+ serum samples can recognize the epitope made by α-TMM (**157, b5**) from *M. tb* to a high level, higher than the natural and other synthetic Ags, and higher than α-TDM (**156, b4**) with same MA sub-class.

No.	Id		Length of chain				Stereochemistry		Organism	AVG ABS+	AVG ABS-
			a	b	c	d	Proximal	Distal			
1	Human TDM	b1							*M. tb*	1.5	1.09
2	Bovine TDM	b2							*M. tb*	1.09	0.8
3	MeO TDM (166)	b3	17	16	17	23	Cis,SR	MeO,SS	*M. tb*	0.57	0.46
4	α-TDM (156)	b4	19	14	11	23	Cis,RS	Cis,RS	*M. tb*	1.13	0.94
5	α-TMM (157)	b5	19	14	11	23			*M. tb*	2.04	1.04
6	Unsat. MA (192)	b6	17	12	17	21	Cis,=	Cis,=	*M. smegmatis*	0.3	0.23
7	Epoxy MA (193)	b7	15	12	18	21	R,Cis,RS	Cis,RS	*M. fortuitum*	0.31	0.25
8	MeO TMM (174)	b8	17	16	18	23	Trans,RS	MeO,SS	*M. tb*	1.18	0.55

Table (33): Effect of the chain length and number of chain in the antigenicity of synthetic Ags

The Abs also recognize the epitope made by methoxy MA in TMM (**174, b8**) better than the methoxy TDM (**166, b3**). Further, the unsaturated MA (**192, b6**) from *M. fortuitum* and the epoxy-MA (**193, b7**) from *M. smegmatis* show low responses using this set of serum samples.

4.6 A comparison of IgG (whole) and IgG (Fc specific) as secondary Ab

Natural human (b1) and bovine TDM (b2) and several synthetic CFs, (**167**, b3), (**169**, b4 and b5), (**170**, b6**)**, (**160**, b7 and b8), (**156**, b9) and (**157**, b10) were studied as Ags using two secondary antibodies, IgG (whole) and IgG (Fc) and three different categories of serum samples, `naturally infected`, `pre-challenge non-vaccinated` (with the same sample set for these as above) and, in addition, `pre-challenge BCG vaccinated`, at a 1:20 serum dilution in 0.5% casein/PBS (**Table 34**). The average absorbances are shown in **Figure 73**.

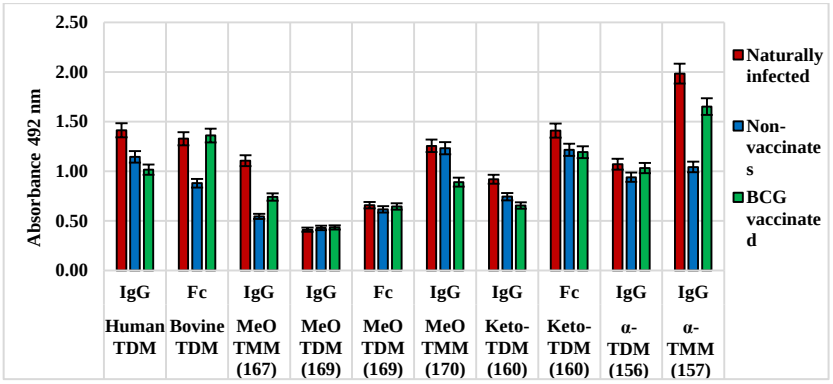

Figure 73: The average of absorbance of synthetic antigens using `naturally infected`, `pre-challenge non-vaccinate` and `pre-challenge BCG vaccinated` serum samples and IgG and IgG Fc secondary Ab

The figure shows that, with some antigens, the `pre-challenge BCG vaccinated` serum samples showed relatively high signals in contrast with `naturally infected` and the non-vaccinated samples. A possible explanation is that vaccination leaves a residual lipid Ab response; later results suggest this does not interfere with diagnosis. The figure also shows that the α- TMM (**157, b10**) gave higher average values of absorbances than natural and other synthetic Ags using IgG whole molecule secondary Ab. Also, the response of keto TDM (**160**) using Fc specific secondary Ab (b8) was higher than using IgG whole molecule (b7), but the latter shows good distinction between the `naturally infected`, `pre-challenge non-vaccinate` and `pre-challenge BCG vaccinated` serum samples. Also, the response of α-TDM (**156, b9**) with IgG was higher than methoxy TMM (**167, b3)**, but the later shows high distinction between the three classes of serum samples. However, the response of methoxy TDM (**169**) using IgG and Fc (b4 and b5 respectively) were low.

No.	Human TDM	Bovine TDM	MeO TMM (167)	MeO TDM (169)		MeO TMM (170)	Keto-TDM (160)		α- TDM (156)	α- TMM (157)
	IgG	Fc	IgG	IgG	Fc	IgG	IgG	Fc	IgG	IgG
	b1	b2	b3	b4	b5	b6	b7	b8	b9	b10
1	2.36	2.48		0.42	0.67	1.89	1.51	1.77	2.17	2.33
2	2.55	2.23	0.66	0.78	1.02	1.33	2.24	2.65	1.73	3.03
3	1.28	1.01	0.89	0.53	0.61	1.38	0.83	1.38	0.83	1.51
4	1.50	3.12	1.31	0.48	2.04	1.50	1.19	2.90	1.49	2.58
5	1.64	1.11	1.83	0.50	0.65	1.13	1.29	1.15	0.95	2.53
6	0.68	0.62	1.36	0.38	0.46	1.67	0.75	0.69	0.61	3.08
7	2.07	0.85	1.91	0.29	0.37	2.88	0.51	0.55	0.64	3.51
8	1.79	1.14	1.52	0.34	0.49	1.37	0.93	1.11	1.31	1.88
9	1.26	1.82	1.27	0.32	0.57	0.65	0.89	1.25	1.62	2.65
10	1.32	1.59	1.22	0.62	0.99	1.14	1.22	2.21	1.05	2.64
11	0.42	0.43	0.37	0.32	0.36	0.38	0.37	0.42	0.34	0.75
12	0.83	0.79	0.61	0.37	0.43	0.64	0.46	0.65	0.51	0.85
13	0.83	0.61	1.15	0.33	0.34	1.32	0.67	0.58	0.57	1.90
14	0.90	0.92	1.18	0.34	0.40	0.94	0.73	1.07	0.69	1.10
15	2.37	2.79		0.44	0.83	1.56	1.20	2.52	1.29	2.40
16	0.95	1.61	0.68	0.31	0.57	1.14	0.57	1.51	0.86	1.46
17	0.91	0.78	0.62	0.29	0.50	0.56	0.74	0.88	0.82	0.79
18	1.80	0.62		0.43	0.79	1.95	0.87	1.54	1.45	1.93
19	1.38	0.70		0.32	0.40	0.42	0.53	1.94	1.43	0.76
20	1.81	1.44	0.43	0.36	0.65	0.72	0.63	2.49	0.81	0.75
21	1.30	1.03	1.00	0.67	0.56	3.29	1.40	1.18	0.83	3.43
22	3.18		0.31						3.11	1.45
23	0.75	0.83	0.74	0.38	0.40	1.66	0.64	0.73	0.55	0.76
24	0.53	0.54		0.34	0.33	0.50	0.46	0.62	0.36	0.33
25	0.82	0.84	0.37	0.33	0.35	1.06	0.57	0.66	0.64	0.79
26	0.42	0.52	0.15		0.30			0.42	0.42	0.36
27	0.57	0.81	0.35	0.27	0.35	1.10	0.55	0.66	0.45	1.21
28	1.42	0.62	0.19	0.74	0.79	1.86	1.04	1.86	0.82	1.21
29	0.51		0.43						0.43	0.67
30	2.24	0.81	0.36	0.50	0.79	1.64	1.36	2.06	2.08	1.29
31	0.37	0.43	0.51	0.31	0.31	0.60	0.42	0.50	0.39	0.39
32	0.47	0.83	0.3	0.30	0.27	0.37	0.40	0.77	0.53	0.39
33	0.51		0.39						0.46	0.46
34	0.60	1.02	0.78	0.38	0.30	1.19	0.69	0.97	0.53	1.28
35	1.00	0.93	0.50		0.65			0.77	0.70	1.04
36	0.76	1.12	0.83	0.58	0.54	0.79	0.75	0.96	0.66	0.69
37	3.35	3.47	1.64		2.66			3.60	3.13	2.28
38	0.56	0.53	2.50	0.25	0.37	2.56	0.45	0.67	0.54	2.57
39	0.55	0.79	0.92	0.27	0.48	0.68	0.51	0.66	0.67	1.89
40	0.69	0.43	1.05	0.34	0.51	1.38	0.49	0.39	0.73	2.77
41	1.09	1.49	0.22	0.41	0.63	1.35	0.78	1.53	1.18	2.66
42	0.52	0.46	0.57	0.30	0.30	0.32	0.41	0.45	0.51	0.70
43	1.24	2.80	1.35	0.40	0.72	1.20	0.65	1.85	1.61	3.44
44	0.60	1.20	0.95	0.37	0.46	0.32	0.67	1.47	0.70	0.66
45	2.61	3.13	0.23	1.17	2.49	1.85	2.19	3.07	2.80	3.11
46	0.77	0.84	0.91	0.37	0.48	0.56	0.56	0.82	0.69	2.17
47	0.99	2.41	0.72	0.42	0.74	0.47	0.57	1.81	1.23	1.16
48	0.43	0.66	0.63	0.36	0.32	0.45	0.42	0.55	0.55	0.90
49	1.26	3.21	0.58	0.84	1.48	1.26	1.23	3.07	1.55	2.41
50	0.68	1.14	0.40	0.35	0.33	0.35	0.43	0.57	0.69	0.57
51	0.60	0.81	0.56	0.39	0.39	0.54	0.45	0.52	0.57	0.92
52	0.37	0.47	0.43	0.30	0.34	0.45	0.36	0.45	0.40	1.07
53	0.86	0.80	0.48	0.46	0.41	1.46	0.54	0.81	0.78	2.25
54	1.84	3.26	0.97	0.55	1.26	0.89	1.05	3.09	2.01	2.23
55	0.66	0.80	0.59	0.36	0.37	0.34	0.40	0.83	0.60	0.73
56	0.68	1.43	0.50	0.39	0.52	0.39	0.43	0.95	0.58	0.58
57	0.61	0.54	0.28	0.40	0.32	0.98	0.50	0.29	0.16	0.24
Cut-off	**>0.770**	**>0.85**	**>0.59**	**>0.373**	**>0.40**	**>0.38**	**>0.65**	**>0.88**	**>0.815**	**>0.725**
Tru.+	**17**	**12**	**14**	**10**	**16**	**19**	**14**	**14**	**13**	**19**
Fal.+ clas1	**8**	**6**	**5**	**6**	**7**	**11**	**5**	**7**	**5**	**11**
Fal.+ clas2	**7**	**9**	**10**	**11**	**12**	**16**	**5**	**8**	**6**	**15**
Fal.+ overall	**15**	**15**	**15**	**17**	**19**	**27**	**10**	**15**	**11**	**26**
Sens. %	**89**	**63**	**74**	**53**	**84**	**100**	**74**	**74**	**68**	**100**
Spec.% clas1	**56**	**67**	**72**	**67**	**61**	**39**	**72**	**61**	**72**	**39**
Spec.% clas2	**65**	**55**	**50**	**45**	**40**	**20**	**75**	**60**	**70**	**25**
Spec.% overall 3	**61**	**61**	**61**	**55**	**50**	**29**	**74**	**61**	**71**	**32**

Table (34): Effect of secondary antibody. The red, blue and green colours in column 1 show `naturally infected`, `pre-challenge non-vaccinated` and `pre-challenge BCG vaccinated` serum samples, in rows 1-19, 20-37 and 38-57 respectively. The specificity for class 1 and 2 were calculated relative to the cut-off set for TB+; the overall figure for a combination of 1 and 2 relative to that cut-off.

The pairs of sensitivity and specificity were calculated from **Table 34** and are shown in **Table 35** below. The sensitivity for TB+ was calculated using the data from `naturally infected' (TB+)

sera, but the specificity was calculated using different individual classes. The overall 2 was calculated by combining the data from class 1 and 2 relative to the cut-off set for TB+.

Id			Sens. %	Spec.% class1	Spec.% class2	Spec.% overall
Human TDM	IgG	b1	89	56	65	61
Bovine TDM	Fc	b2	63	67	55	61
MeO TMM (167)	IgG	b3	74	72	50	61
MeO TDM (169)	IgG	b4	53	67	45	55
	Fc	b5	84	61	40	50
MeO TMM (170)	IgG	b6	100	39	20	29
Keto-TDM (160)	IgG	b7	74	72	75	74
	Fc	b8	74	61	60	61
α- TDM (156)	IgG	b9	68	72	70	71
α- TMM (157)	IgG	b10	100	39	25	32

Table (35): The pairs of sensitivity and specificity of natural TDM and synthetic Ags, using data from Table 35. The sensitivity for TB+ was calculated using the data from `naturally infected' (TB+) sera, but the specificity was calculated using different classes: Class 1 using the data from pre-challenge non-vaccinated; class 2 using the data from pre-challenge BCG vaccinated and the overall is a combination of 1 and 2 relative to that cut-off set for TB+

The table demonstrates that the best values of sensitivity and the three classes of specificity were observed in b7 keto TDM (**160**), which equal to (74, 72, 75 and 74%) respectively using IgG whole molecule as a secondary Ab.

The ROC analysis of this set of Ags was also studied using three different combination of the results, class1 the data from `naturally infected` and `pre-challenge non-vaccinate` serum samples and class2 using the data from `naturally infected` (TB+) and `pre-challenge BCG vaccinated` and overall using the data from`naturally infected` compared to the total of `pre-challenge non-vaccinate` and `pre-challenge BCG vaccinated` serum samples (**Figure 74**).

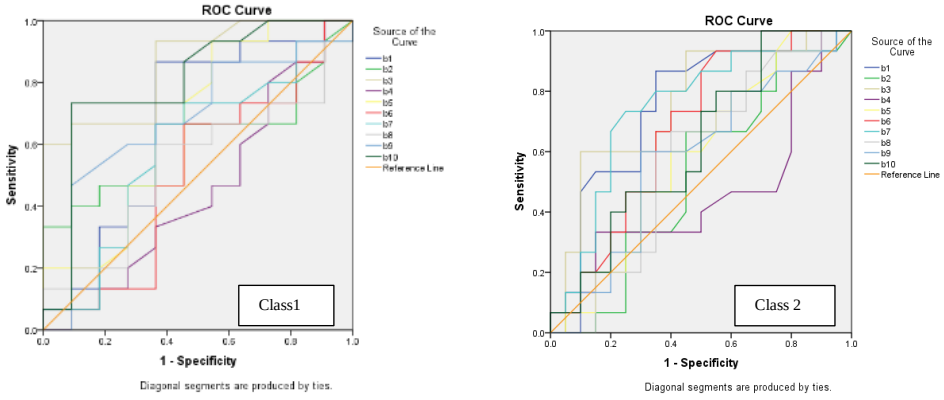

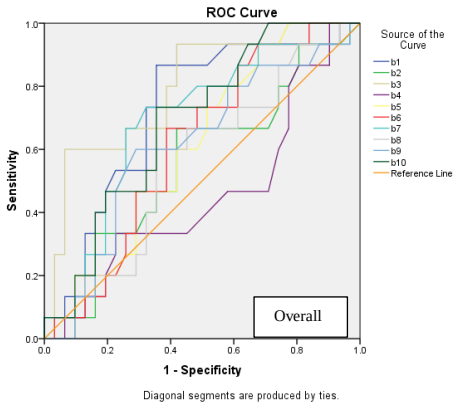

Id			Aerea Under the Curve			Sensitivity (%)			Specificity (%)		
			Class								
			1	2	3	1	2	3	1	2	3
Human TDM	**IgG**	**b1**	**0.667**	**0.761**	**0.719**	**87**	**88**	**87**	**64**	**65**	**65**
Bovine TDM	**Fc**	**b2**	**0.618**	**0.536**	**0.554**	**60**	**69**	**67**	**64**	**55**	**58**
MeO TMM (167)	**IgG**	**b3**	**0.858**	**0.713**	**0.795**	**60**	**75**	**60**	**100**	**60**	**97**
MeO TDM (169)	**IgG**	**b4**	**0.458**	**0.470**	**0.453**	**60**	**50**	**40**	**36**	**40**	**48**
	Fc	**b5**	**0.655**	**0.597**	**0.611**	**73**	**63**	**80**	**55**	**60**	**42**
MeO TMM (170)	**IgG**	**b6**	**0.497**	**0.694**	**0.613**	**60**	**75**	**67**	**55**	**60**	**61**
Keto-TDM (160)	**IgG**	**b7**	**0.588**	**0.755**	**0.687**	**60**	**75**	**73**	**64**	**75**	**68**
	Fc	**b8**	**0.533**	**0.586**	**0.560**	**60**	**69**	**60**	**64**	**60**	**65**
α- TDM (156)	**IgG**	**b9**	**0.682**	**0.600**	**0.614**	**60**	**63**	**60**	**73**	**70**	**71**
α- TMM (157)	**IgG**	**b10**	**0.800**	**0.628**	**0.686**	**73**	**75**	**73**	**91**	**50**	**65**

Figure (74). ROC analysis using data from Table 34: (a) ROC for TB+ versus pre-challenge non-vaccinated; (b) pre-challenge BCG vaccinated; and (c) is a combination of (a) and (b)

The figure shows that the natural and synthetic Ags all showed rather low values of area under the curve, sensitivity and specificity for the three different combinations of the results. However, the best area under the curve and the pairs of sensitivity and specifisity were observed in methoxy TMM (**167,** b3) and α- TMM (**157,** b10), this equal to 0.858 and 0.800, (60 and 100%) and (73, 91%) respictivily, using IgG secondary Ab and class 1.

4.6.1 Combining the results with several Ags using multidimensional scaling

Multidimensional scaling MDS using a Random Forest Classifier utilizing the results from **Table 34** is shown in **Figure 75**. The results illustrate that the synthetic b3 methoxy TMM (**167**) and b10 α-TMM (**157**) Ags gave high antigenicity to naturally infected serum samples using IgG whole molecule as secondary Ab. On the other hand, the b5 methoxy TDM (**169**) and b8

keto TDM (**160**) gave lower antigenicity than natural bovine Ag using IgG Fc as a secondary Ab.

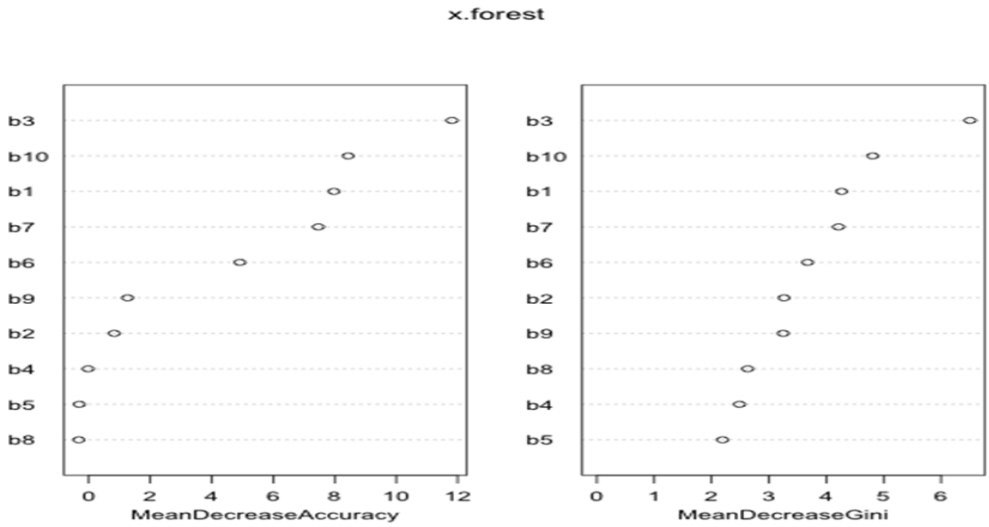

Figure (75). Data from Table 34 analysed using Mean Decrease Accuracy and Mean Decrease Gini

Forest Classifier principal coordinates analysis combining the results from the whole set of Ags using 57 bovine serum samples consisting of 19 bTB+, 18 bTB- and 20 BCG vaccinated serum samples is shown in **Figure 76** below.

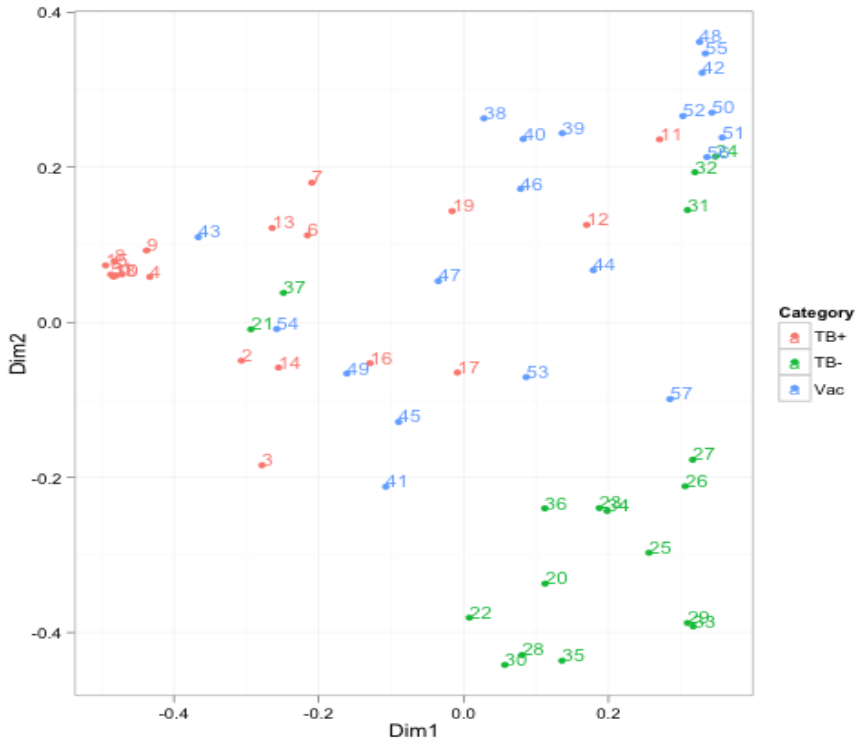

Figure (76): Principal co-ordinate analysis combining the results from Table 34

Figure 76 demonstrates the probability of distribution of three different groups on two axes. Each axis corresponds to a different linear combination of the results with all the antigens optimized to separate the three groups. The figure shows a good split among bTB+, bTB- and BCG vaccinated serum samples, the positive serum samples represented in 1-19 data largely appearing on the middle left of the plot as a quite tight group, the negative serum samples 20-37 appearing as a more spread group on the down right hand side of the plot and the BCG vaccinated serum samples 38-57 as quite tight group on the up right hand side. Clearly there are some positives and negatives data that do not fit this pattern. On the other hand, the results of BCG vaccinated serum samples show that the vaccine may cause a long term change in the immune system of an animal. Adverse events linked to BCG vaccination range from mild,[426] localized complications to more serious, systemic or disseminated BCG disease in which *M. bovis* BCG is confirmed in one or more anatomical sites far from both the site of injection and regional lymph nodes. Disseminated BCG disease is associated with a case-fatality rate of >70% in infants. TDMs show a number of immunomodifying effects, by their ability to induce a range of *chemokines* and *cytokines*. Although *Mycobacteria* contain several classes of immunostimulants, TDM has been demonstrated to be the most potent stimulator of IL-1, TNF and granuloma formation among the BCG cell wall glycolipids.[427] After early studies showed that natural TDMs enhanced Ab production by B cells, synthetic TDMs with simplified structures are being developed as therapeutic adjuvants.[427] The other aspect of this, however, is that it appears that with some improvement, this assay can distinguish active TB in animals that have been vaccinated.

4.6.2 The effect of the structure of the MA on the antigenic response

The different structural features of each of these antigens are presented in **Table 36**, together with their sensitivity and specificity.

Id		Length of the chain				No of MA	Stereochem.		Sens %	Spec % class 1	Spec .% class 2	Spec .% over all	BTB +	Non-vacn	BCG vacn
		a	b	c	d		Proximal	Distal							
Human TDM	**IgG**								**89**	**56**	**65**	**61**	**1.41**	**1.15**	**1.02**
Bovine TDM	**Fc**								**63**	**67**	**55**	**61**	**1.33**	**0.88**	**1.36**
MeO TMM (167)	**IgG**	**17**	**16**	**17**	**23**	**1**	**Cis, SR**	**S,MeO,SS**	**74**	**72**	**50**	**61**	**1.11**	**0.55**	**0.74**
MeO TDM (169)	**IgG**	**17**	**16**	**17**	**23**	**2**	**Cis, RS**	**R,MeO,SS**	**53**	**67**	**45**	**55**	**0.41**	**0.43**	**0.43**
	Fc	**17**	**16**	**17**	**23**	**2**	**Cis, RS**	**R,MeO,SS**	**84**	**61**	**40**	**50**	**0.66**	**0.62**	**0.65**
MeO TMM (170)	**IgG**	**17**	**16**	**17**	**23**	**1**	**Cis, RS**	**R,MeO,SS**	**100**	**39**	**20**	**29**	**1.25**	**1.23**	**0.89**
Keto-TDM (160)	**IgG**	**17**	**18**	**15**	**23**	**2**	**Cis, RS**	**Keto, R**	**74**	**72**	**75**	**74**	**0.92**	**0.74**	**0.66**
	Fc	**17**	**18**	**15**	**23**	**2**	**Cis, RS**	**Keto, R**	**74**	**61**	**60**	**61**	**1.41**	**1.22**	**1.19**
α- TDM (156)	**IgG**	**19**	**14**	**11**	**23**	**2**	**Cis, RS**	**Cis, RS**	**68**	**72**	**70**	**71**	**1.07**	**0.94**	**1.03**
α- TMM (157)	**IgG**	**19**	**14**	**11**	**23**	**1**	**Cis, RS**	**Cis, RS**	**100**	**39**	**25**	**32**	**1.98**	**1.04**	**1.65**

Table (36): Effect of the structure of MA attached to trehalose on the antigenicity. The sensitivity calculated using the data from `naturally infected` sera. The specificity, class 1, was calculated using the data for `pre-challenge non-vaccinate`, class 2 using `pre-challenge BCG vaccinated` and the overall calculated by combining the these data

The strongest Ab binding signal with `naturally infected' serum samples was observed with α-MA TMM (**157**), with good distinction between these and `pre-challenge non-vaccinate` serum samples using IgG ; this Ag also gave high Ab binding signal in `pre-challenge BCG vaccinated` serum samples. However, the best combination of sensitivity and specificity for pre-challenge non-vaccinated serum (class 1) was observed with keto-MA TDM (**160**) using IgG whole molecule (74, 72). The keto-MA TDM (**160**) also gave the best distinction between `naturally infected` and `pre-challenge BCG vaccinated` (class 2) (74, 75) and overall (74, 74).

4.7 MA with different functional group

The effect of different MA with different functional group [methoxy (**195**), keto (**196**), unsaturated (**192**) and epoxy- (**193**)] MA from *M. tb*, *M. fortuitum* and *M. smegmatis* respectively with different functional groups were studied using IgG whole molecule as a secondary Ab and a 1:20 serum dilution in 0.5% casein/PBS buffer, (**Table 37**).

No.	MeO MA (195)	Keto MA(196)	Unsat. MA(192)	Epoxy MA (193)
1	0.36	0.25	0.40	0.30
2	0.32	0.25	0.46	0.32
3	0.33	0.24	0.42	0.35
4	0.28	0.25	0.32	0.31
5	0.37	0.29	0.42	0.45
6	0.29	0.21	0.28	2.05
7	0.35	0.24	0.28	1.97
8	0.35	0.20	0.26	2.28
9	0.24	0.17	0.25	2.30
10	0.22	0.27	0.28	0.35
11	0.31	0.30	0.43	0.47
12	0.31	0.26	0.39	0.38
13	0.22	0.25	0.33	0.35
14	0.15	0.22	0.27	0.30
15	0.20	0.25	0.39	0.36
16	0.22	0.20	0.23	0.38
17	0.24	0.23	0.22	0.25
18	0.26	0.20	0.24	0.30
19	0.24	0.22	0.27	0.32
20	1.96	0.22	0.21	0.27
21	2.25	0.24	0.18	0.27
22	2.00	0.21	0.19	0.30
Cut-off	>0.241	>0.242	>0.246	>0.300
Cut-off ROC	>0.230	>0.225	>0.245	>0.335
Tru.+	9	6	9	9
Fal. +	6	5	7	8
Sens.%	100	67	100	100
Spec.%	54	62	46	38
Sens. % ROC	100	67	100	67
Spec.% ROC	39	54	47	54

Table (37): The effect of use different MAs Ags in bTB+ and bTB- serum samples. The red and blue colours in column 1 and 2 show naturally infected and non-vaccinated pre-challenge serum samples in rows 1-9 and 10-22 respectively

The average of absorbances were calculated, (**Figure 77**).

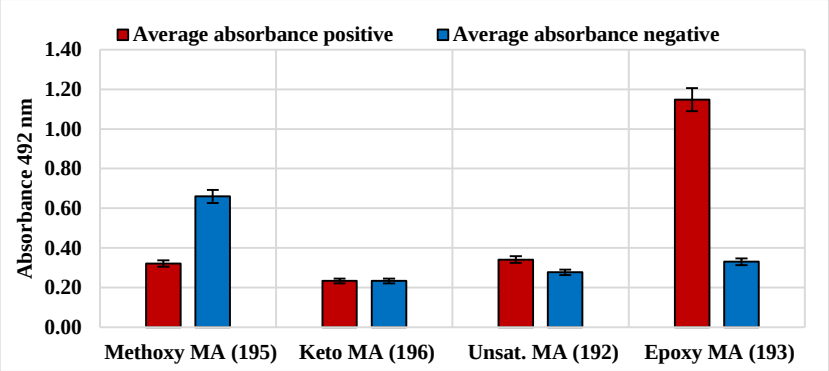

Figure 77: The average of absorbances of synthetic MAs Ags using bTB+ and bTB- serum samples

Each of these Ags gave low absorbance values and many false+ and false- were observed. The figure shows that the average absorbances of free methoxy MA (**195**) Ag from *M. tb* with the negatives was higher than the positives. However, surprisingly, the epoxy MA (**193**) from *M. smegmatis* showed high responses with good distinction between bTB+ and bTB- serum samples. The keto MA (**196**) and unsaturated MA (**192**) from *M. tb* and *M. fortuitum* showed no responses in this set of serum samples. The calculated values of the pairs of sensitivity and specificity of each Ag are shown in **Table 38**.

Antigens	Sens. (%)	Spec. (%)	Spec. for 100% sens.
Methoxy MA (195)	89	62	54
Keto MA (196)	67	62	0
Unsat. MA (192)	78	62	46
Epoxy MA (193)	56	96	38

Table (38): The sensitivity and specificity of synthetic MAs Ags using data from Table 37

The table shows that the best pairs of sensitivity and specificity was observed in methoxy MA (**195**) (100,54). The results for (**195**) are most unexpected – the average absorbance being skewed very considerably by very strong responses for the final three serum samples; this needs to be checked with a larger serum set.

The area under the ROC curve and sensitivity and specificity were also calculated, (**Figure 78**).

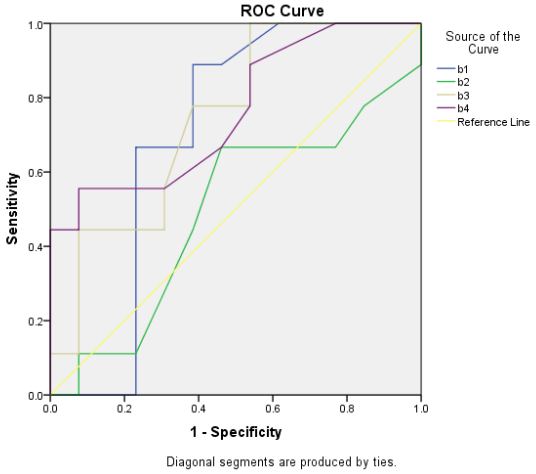

No.	Antigens		Area Under Curve	Sens. (%)	Spec. (%)
1	Epoxy MA (193)	b4	0.761	67	54
2	Unsat. MA (192)	b3	0.744	100	47
3	MeO MA (195)	b1	0.701	100	39
4	Keto MA (196)	b2	0.491	67	54

Figure 78: SPSS ROC analysis using data from Table 37

The synthetic MA Ags gave modest values of the area under the curve and that the best was epoxy MA (**193**) at 0.761. This showed that the accuracy of the test is 76%, higher than the literature value using mixtures of natural free MAs, which was not adequate for serodiagnosis of TB (accuracy = 57%) (Page 44).

4.8 Using synthetic keto- and α-TDM Ags with IgG (whole) and IgG Fc

Synthetic keto TDM (**160**) and α-TDM (**156**) Ags from *M. tb* were studied with `naturally infected` and non-vaccinated pre-challenge serum samples, at a 1:20 serum dilution, using 0.5% casein/PBS buffer and using IgG whole molecule or IgG Fc as secondary Ab (**Table 39**).

No.	keto-TDM (160)		α-TDM (156)	
	Fc	IgG	Fc	IgG
1	2.57	0.95	3.63	1.67
2	2.25	0.76	2.96	0.97
3	3.22	1.36	3.41	1.47
4	1.64	0.87	1.48	0.51
5	1.02	0.43	1.50	0.55
6	3.03	1.29	3.22	2.61
7	2.13	0.93	2.48	1.03
8	0.57	0.36	0.72	0.42
9	0.66	0.37	1.14	0.53
10	0.54	0.33	0.72	0.34
11	1.00	0.42	1.02	0.26
12	1.52	0.52	2.40	1.03
13	0.67	0.48	0.77	0.42
14	1.03	0.43	1.27	0.48
Cut-off	>1.00	>0.432	>1.302	>0.492
Cut-off ROC	>1.010	>0.425	>1.375	>0.495
Tru.+	7	7	7	7
Fal. +	2	2	1	2
Sens. %	100	100	100	100
Spec. %	71	71	86	71
Sens. % ROC	100	100	100	100
Spec. % ROC	71	57	86	71

Table (39): Effect of a range of synthetic antigens on bTB+ and bTB- serum samples

The average absorbances are as shown in **Figure 79** below.

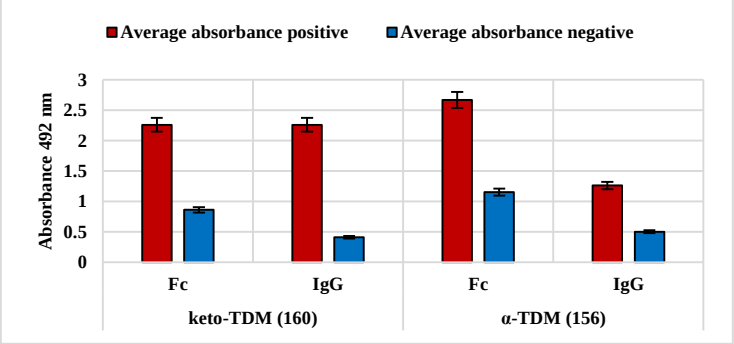

Figure 79: The average of absorbances of synthetic TDMs Ags using bTB+ and bTB- serum samples

The values of sensitivity and specificity were as seen in **Table 40**.

Id		Sens. (%)	Spec. (%)
keto TDM (158)	Fc	100	71
	IgG	100	71
α TDM (154)	Fc	100	86
	IgG	100	71

Table (40): The sensitivity and specificity using data from Table 39

The table indicates that the best pairs of sensitivity and specificity were observed in α TDM (**154**) with IgG Fc (100, 86).

The ROC analysis is shown in **Figure 80**.

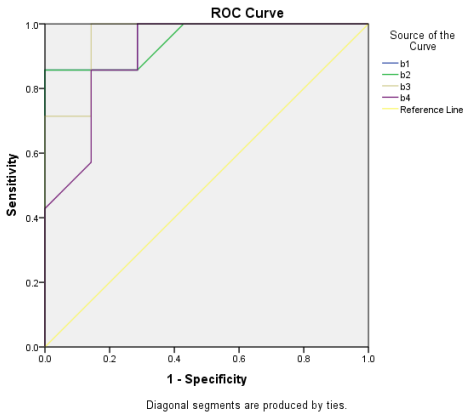

No.	Antigens			Area Under Curve	Sens. (%)	Spec. (%)
1	α TDM (156)	b3	Fc	0.959	100	86
2	keto TDM (160)	b1	Fc	0.959	100	71
3	keto TDM (160)	b2	IgG	0.949	100	57
4	α TDM (156)	b4	IgG	0.908	100	71

Figure (80): The ROC analysis using data from Table 39

The figure shows high area under the curve in this set of Ags using IgG and IgG Fc specific and this set of serum samples. The best values of area under the curve, sensitivity and specificity were observed in α TDM (**156**), which equal to 0.959, 100 and 86 respectively.

4.9 Attempted diagnosis of non-tuberculous mycobacterial infections

The possibility that prior infection with atypical *Mycobacteria* might in some way interfere with and possibly risk BCG vaccination processes is an area of considerable practical importance. Youmans *et. al.* were among the first to examine the possibility that prior infection with various atypical *Mycobacteria* might in some way cross-protect against subsequent *M. tb* infection;[428] prior infection with certain strains of *Mycobacteria* (*M. avium*, *M. kansasii*, and *M. intracellulare*) resulted in a significant reduction in mortality when mice were subsequently challenged with virulent *M. tb*. An extensive study by Collins[429] confirmed these results and provided evidence that anti-tuberculous resistance in prior-infected mice may depend upon the ability of the atypical *Mycobacteria* to survive *in vivo*.[428] Infection with NTM may also interfere with the serodiagnosis of bTB.

In the following experiments, mycolic acids and sugar esters characteristic of non-tuberculous mycobacteria were examined using serum samples from animals not known to have active bTB, but which tested positive for other mycobacteria at slaughter (**Table 41**).

Serum sample	Infection at slaughter	Serum sample	Infection at slaughter
CY3675	*M. fortuitum 2*	CY3709	AFB
CY3702	*M. fortuitum 1*	CY3725	*M. fortuitum 1*
CY3732	AFB	CY3681	*M. fortuitum 2*
CY3671	*M. fortuitum 1*	CY3698	*M. fortuitum 1*
CY3691	AFB	CY3720	*M. fortuitum 2*
CY3696	*M. fortuitum 1*		

Table 41: The bTB- samples from animals with other mycobacterial infections at slaughter

4.9.1 Effect of using synthetic α-TDM and α-TMM Ags from *M. Kansasii*

M. kansasii and *M. tb* have been found, on the basis of the 16S–23S rRNA gene internal transcribed spacer (ITS) regions, to be phylogenetically related.[430] *M. kansasii* pneumonia is clinically and radiographically indistinguishable from classical pulmonary TB, which could reflect similarities in pathogenesis.[431] The effect of use two synthetic CFs from *M. kansasii*, α-TDM (**171**) and α-TMM (**172**) with same α-MA sub-class were studied using non-vaccinated [`pre-challenge`] and vaccinated [`pre-challenge BCG` and `pre-challenge BCG+ Adeno Ag85A] serum samples known to have other mycobacterial infections at slaughter. The test was done using IgG whole molecule as a secondary Ab and a 1:20 serum dilution in 0.5% casein/PBS buffer. (**Figure 81**).

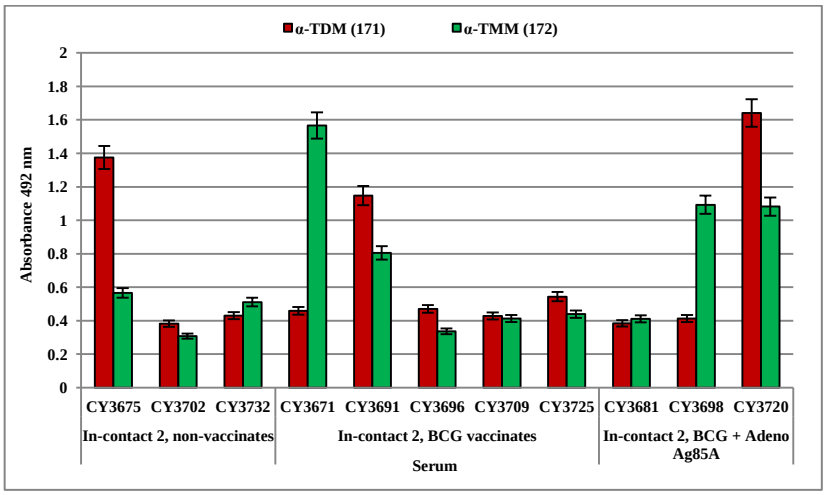

Figure 81: ELISA responses with synthetic α-TDM and α-TMM antigens from *M. Kansasii*

Figure 81 shows that the two Ags gave modest responses with most serum samples, but rather high responses with CY3675, CY3671 and CY3720.

4.9.2 The effect of using synthetic epoxy-MA Ags from *M. smegmatis*

M. smegmatis has a number of properties that may make it an effective vaccine vector. Some *M. smegmatis* strains are non-pathogenic and commensal in humans.[432] Therefore, two synthetic MAs with different stereochemistries, (*S*,*R*)-cis-cyclopropane (*R*,*R*)-epoxy-mycolic acid (**194**) and (*S*,*R*)-cis-cyclopropane (*S*,*S*)-epoxy-mycolic acid (**193**) present in natural *M. smegmatis* were assayed in the same way as above.

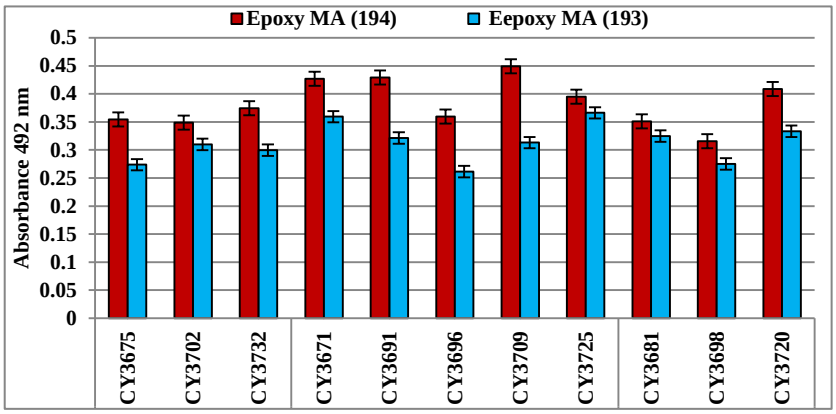

Figure 82: Epoxy-MA from *M. smegmatis*

Figure 82 illustrates that the two epoxy-MA showed low responses with all of this set of serum samples, but the responses with (*S*,*R*)-*cis*-cyclopropane (*R*,*R*)-epoxy-mycolic acid (**194**) are slightly higher than with its stereoisomer (**193**).

4.9.3 Effect of using natural and synthetic wax ester from *M. Avium* as antigens

The effect of natural wax ester was separated from natural mixture of *M. Avium* cells and synthetic wax-ester (**185**) were then studied using the same method (**Figure 83**).

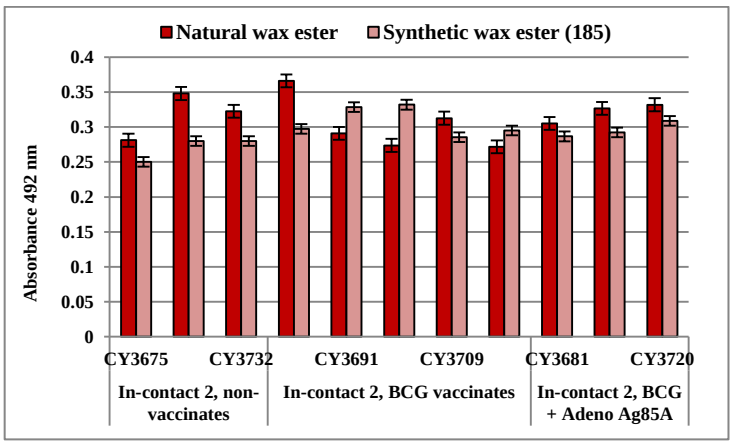

Figure 83: The natural wax ester and synthetic wax ester Ags from *M. Avium*

Figure 83 demonstrates that the natural and synthetic wax esters Ags from *M. avium* showed essentially no responses with this set of serum samples.

4.9.4 Diagnosis of *M. avium* subsp. *paratuberculosis* (MAP) using bovine serum samples

In the next set of experiments, samples from two cattle one naturally and one experimentally infected with MAP, 16 samples from non-vaccinated in-contant cattle (expected bTB-) and 20 tuberculin skin test positive bTB samples (naturally infected) were examined. A range of Ags were used including TDM from *M. bovis*, natural wax ester from *M. avium* and synthetic wax ester (**187**), diacid (**198**), TDM (**188**) and TMM (**189**) from *M. avium* and wax ester (**199**), TDM (**200**), TMM (**201**) from *M. gordonae* and α-TDM (**156**), α-TMM (**157**), keto TDM (**160**), keto TMM (**161**),methoxy TDM (**163**), methoxy TMM (**164**), α-MA (**155**), keto MA (**159**) and methoxy MA (**162**) from *M. tb*. The tests were done using a 1:20 serum dilution in 0.05% PBS-T and IgG Fc specific molecule as a secondary Ab, (**Table 42**).

No.	Id	Nat. TDM	Nat. Wax ester	187	198	188	189	199	200	201	156	157	160	161	163	164	155	159	162
1	MAP Exp.	3.72	0.41	3.70	0.76	3.07	3.29	2.97	1.44	4.38	4.21	3.7	3.45	3.16	0.7	2.93	0.42	0.62	0.34
2	MAP Nat.	4.00	0.5	4.38	0.72	4.06	4.00	3.88	4.00	4.38	4.01	3.68	4.06	3.99	1.83	3.67	0.56	0.73	0.36
3	Nat. Inf	3.27	0.12	1.49	0.17	2.74	3.12	0.38	1.07	3.68	3.87	2.14	1.85	1.51	0.27	1.93	0.1	0.1	0.08
4		2.7	0.13	2.59	0.15	1.81	3.2	0.54	0.67	2.78	3.03	1.5	1.09	1.78	0.17	1.89	0.13	0.13	0.08
5		3.91	0.12	1.85	0.13	2.94	3.08	1.24	2.47	4.06	3.57	1.58	3.96	1.86	0.52	0.69	0.14	0.13	0.08
6		1.77	0.08	2.51	0.16	2.15	1.69	1.82	0.67	0.63	2.24	0.49	1.21	0.58	0.16	0.4	0.19	0.15	0.09
7		0.39	0.06	0.68	0.2	0.61	3.05	1.56	0.29	1.04	0.77	1.42	0.39	0.48	0.15	1.07	0.11	0.12	0.12
8		0.3	0.11	1.7	0.21	0.26	1.43	2.03	0.18	0.88	1.04	0.52	0.42	0.3	0.16	1.2	0.12	0.11	0.1
9		1.01	0.06	1.2	0.16	0.61	3.07	2.77	0.51	2.34	2.91	1.31	0.83	0.86	0.2	0.78	0.12	0.13	0.09
10		2.13	0.07	3.02	0.21	1.86	1.51	3.29	2.23	1.39	2.8	0.89	1.25	0.63	0.35	1.51	0.18	0.2	0.15
11		0.23	0.07	0.91	0.14	0.2	0.73	2.62	0.18	0.4	0.4	0.25	0.29	0.27	0.16	1.09	0.15	0.19	0.12
12		0.35	0.07	0.57	0.19	0.22	0.82	1.02	0.24	0.52	0.66	0.28	0.31	0.31	0.15	1.04	0.18	0.18	0.19
13		0.47	0.08	0.52	0.19	0.36	1.64	0.98	0.31	1.63	0.7	0.48	0.4	0.35	0.25	1.06	0.2	0.22	0.18
14		0.62	0.13	3.94	0.27	0.64	0.95	4.05	1.08	1.54	1.28	0.35	0.94	0.31	0.35	0.7	0.21	0.29	0.17
15		0.41	0.05	0.14	0.05	0.37	0.28	0.17	0.66	0.26	0.41	0.18	0.41	0.12	0.14	0.08	0.07	0.12	0.07
16			0.05	0.19	0.05	0.99	0.4	0.13	0.23	0.22									
17		0.19	0.06	1.85	0.06	0.29	0.31	0.98	0.12	0.15	0.28	0.18	0.25	0.12	0.14	0.15	0.08	0.13	0.08
18		0.21	0.08	1.3	0.07	0.12	0.18	1.25	0.62	0.15	0.2	0.1	0.22	0.13	0.15	0.17	0.11	0.13	0.12
19		1.56	0.1	3.05	0.1	1.8	0.78	1.2	0.47	0.11	1.35	0.38	1.81	0.16	0.74	0.17	0.08	0.11	0.11
20		0.55	0.08	0.87	0.08	0.7	0.19	0.39	0.52	0.27	0.66	0.14	0.65	0.15	0.3	0.19	0.06	0.12	0.09
21		0.86	0.09	0.69	0.07	0.68	0.28	1.45	0.69	0.11	0.77	0.15	0.89	0.17	0.25	0.16	0.13	0.11	0.11
22		0.49	0.17	0.59	0.1	0.36	0.18	0.73	1.08	1.54	0.35	0.15	0.24	0.18	0.19	0.23	0.1	0.17	0.17
23	Non Vac	0.42	0.13	1.34	0.12	0.24	0.47	0.33	0.25	0.37	0.51	0.21	0.23	0.29	0.14	0.55	0.18	0.12	0.07
24		0.76	0.07	0.47	0.1	0.51	0.27	0.21	0.25	0.14	0.55	0.14	0.41	0.18	0.09	0.17	0.17	0.16	0.1
25		0.12	0.06	0.65	0.11	0.14	0.45	0.47	0.17	0.24	0.2	0.18	0.12	0.25	0.07	0.42	0.18	0.12	0.08
26		0.46	0.07	0.47	0.1	0.34	1.17	0.32	0.21	0.51	0.56	0.25	0.25	0.3	0.09	0.44	0.21	0.14	0.08
27		0.27	0.05	0.6	0.12	0.18	0.5	0.87	0.15	0.27	0.64	0.28	0.74	0.2	0.12	0.52	0.12	0.11	0.11
28		3.61	0.06	0.43	0.12	4.03	1.13	1.03	3.66	0.82	3.64	0.62	3.36	0.49	1.09	1.04	0.15	0.13	0.12
29		4.21	0.07	0.5	0.15	3.79	1.18	0.62	1.96	0.55	3.64	1.21	2.63	0.27	0.25	0.93	0.14	0.14	0.13
30		0.84	0.07	0.79	0.17	0.71	0.91	0.96	0.36	0.46	0.84	0.57	0.53	0.26	0.21	0.9	0.14	0.18	0.11
31		0.7	0.06	0.33	0.16	0.64	2.86	0.45	0.29	1.58	0.61	0.65	0.51	0.35	0.18	1.02	0.14	0.15	0.12
32		0.44	0.06	0.76	0.19	0.26	0.3	0.74	0.26	0.16	0.48	0.21	0.44	0.23	0.21	0.97	0.14	0.19	0.13
33		1.49	0.06	0.35	0.22	0.7	1.58	0.67	0.45	1.99	3.22	1.13	1.04	0.62	0.27	1.13	0.18	0.21	0.13
34		0.16	0.06	0.14	0.06	0.21	0.11	0.16	0.06	0.06	0.22	0.24	0.32	0.11	0.08	0.1	0.11	0.09	0.09
35		0.11	0.05	0.14	0.05	0.07	0.08	0.14	0.08	0.1	0.14	0.07	0.11	0.1	0.12	0.09	0.12	0.1	0.07
36		0.11	0.05	0.14	0.05	0.08	0.08	0.15	0.11	0.07	0.2	0.08	0.15	0.1	0.11	0.11	0.11	0.11	0.09
37		0.24	0.07	0.14	0.06	0.22	0.11	0.2	0.31	0.07	0.31	0.12	0.23	0.13	0.14	0.14	0.1	0.13	0.11
38		0.22	0.05	0.13	0.06	0.5	0.1	0.16	0.12	0.07	1.31	0.12	0.49	0.11	0.12	0.1	0.1	0.09	0.09
Cut-off		>0.46	>0.40	>0.51	>0.41	>0.609	>0.7	>0.975	>0.46	>0.5	>0.65	>0.316	>0.61	>0.30	>0.23	>0.555	>0.30	>0.30	>0.30
Sens.%		60	0	90	0	60	65	70	65	60	70	55	50	50	40	55	0	0	0
Spec.%		63	100	69	100	69	63	94	88	69	69	69	75	81	81	63	100	100	100

Table (42): Effect of a range of synthetic Ags from *M. tb, M. avium* and *M. gordonae* in ELISA. Samples 1 and 2 were infected with high doses of MAP; 3-22 were VLA (Naturally infected) and 23-38 (Non-vaccinated) serum respectively. The sensitivity was calculated using Naturally infected samples; the specificity was calculated relative to this cut-off ; the MAP samples infected with MAP were excluded

The average absorbances of the synthetic Ags are given in **Figure 84**.

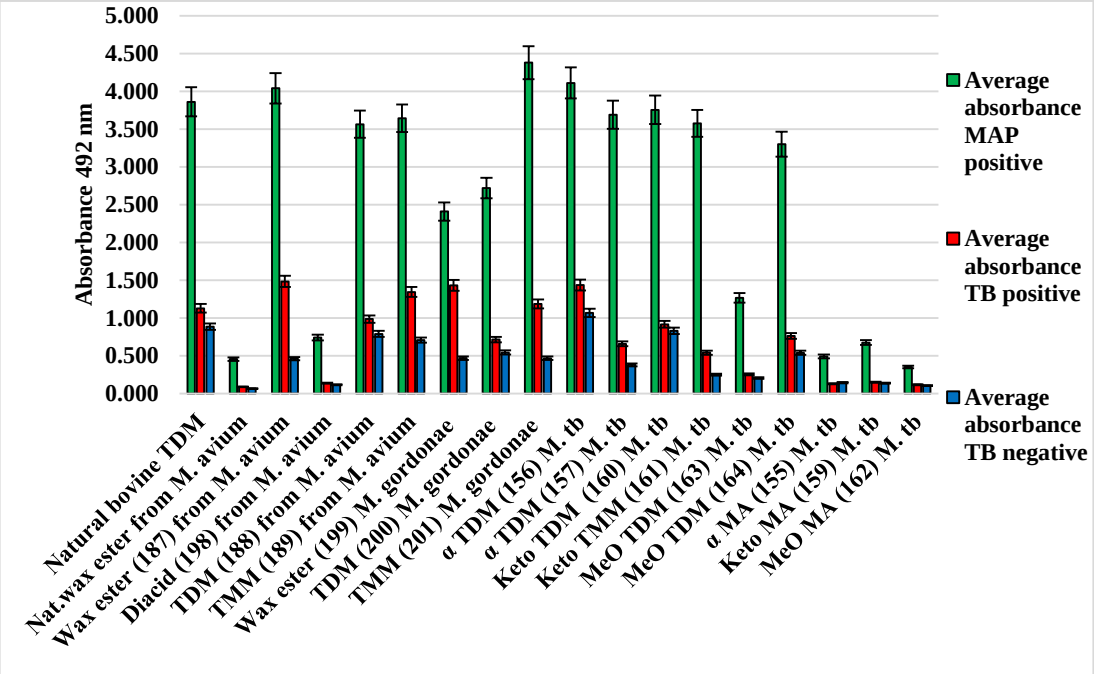

Figure 84: The average absorbances of a range of synthetic Ags from *M. tb*, *M. avium* and *M. gordonae* on a serum infected with high doses of MAP; VLA (Naturally infected) and VLA (Non-vaccinated) serum samples

The sensitivity and specificity of natural and synthetic Ags were calculated in **Table 42** and are displayed in **Table 43**. The sensitivity was calculated using the data from Naturally infected bTB+ serum samples, the specificity using the data from Non-vaccinated TB- serum samples.

Id	Sens.%	Spec.%	Id	Sens.%	Spec.%
Nat. TDM	60	63	156	70	69
Nat. wax ester	0	100	157	55	69
187	90	69	160	50	75
198	0	100	161	50	81
188	60	69	163	40	81
189	65	63	164	55	63
199	70	94	155	0	100
200	65	88	159	0	100
201	60	69	162	0	100

Table (43): The sensitivity and the specificity using data from Table 42. The sensitivity 1 calculated using the data from TB+ serum samples, specificity using the data from Non-vaccinated TB- serum samples and the cutoff of this combination set for TB+

Table 43 indicates that the natural and synthetic Ags from different *Myobacteria* gave resonable values of sensitivity and specificity in the first combination between TB+ and TB- serum samples.

Figure 84 shows each natural and synthetic Ag showed high responses with serum infected with high doses of MAP, this response being above the average of the VLA (Naturally infected) serum samples. In some cases, essentially no signal was seen except with the MAP samples. This shows that the ELISA assay can be a diagnostic tool for detection of MAP in present of bovine TB+, but this is a very limited set of serum samples. **Table 44** below shows the sensitivity and specificity for the MAP samples relative to the the pre-challenge non-vaccinated samples.

Id	Nat. TDM	Nat. Wax ester	187	198	188	189	199	200	201	156	157	160	161	163	164	155	159	162
Cut off MAP	>2	>2	>2	>2	>2	>2	>2	>2	>2	>2	>2	>2	>2	>2	>2	>2	>2	>2
Tru.+ MAP	2	2	2	2	2	2	2	2	2	2	2	2	2	2	2	2	2	2
Fal. + MAP	2	0	0	0	2	1	0	1	0	3	0	2	0	0	0	0	0	0
Sens.%	100	100	100	100	100	100	100	100	100	100	100	100	100	100	100	100	100	100
Spec.%	88	100	100	100	88	94	100	94	100	81	100	88	100	100	100	100	100	100

Table (44): Effect of a range of synthetic Ags from *M. tb, M. avium* and *M. gordonae* in ELISA. The cut-off was set to give 100 % sensitivity using MAP serum samples and the specificity was calculated relative this

Thus the MAP samples can be clearly distinguished from the naturally infected bTB samples and the non-infected samples, albeit with a very small sample set.

4.10 The time profile of bTB

To understand whether the stage of infection would interfere with the assay, the time profile in sets of serum samples from thirteen different cattle were studied with natural bovine TDM and a set of synthetic antigens, methoxy TDM (**166**), methoxy TMM (**167**), α-TDM (**156**), α-TMM (**157**) and unsaturated TDM (**197**). The serum sample were obtained from AFBI in North Ireland and were infected with disease through an aerosol system. The assay was run using a 1:20 serum dilution in 0.5% casein/PBS buffer and IgG whole molecule was used as secondary Ab. **Figure 85** shows the responses of serum over a six week period in assays with seven different antigens.

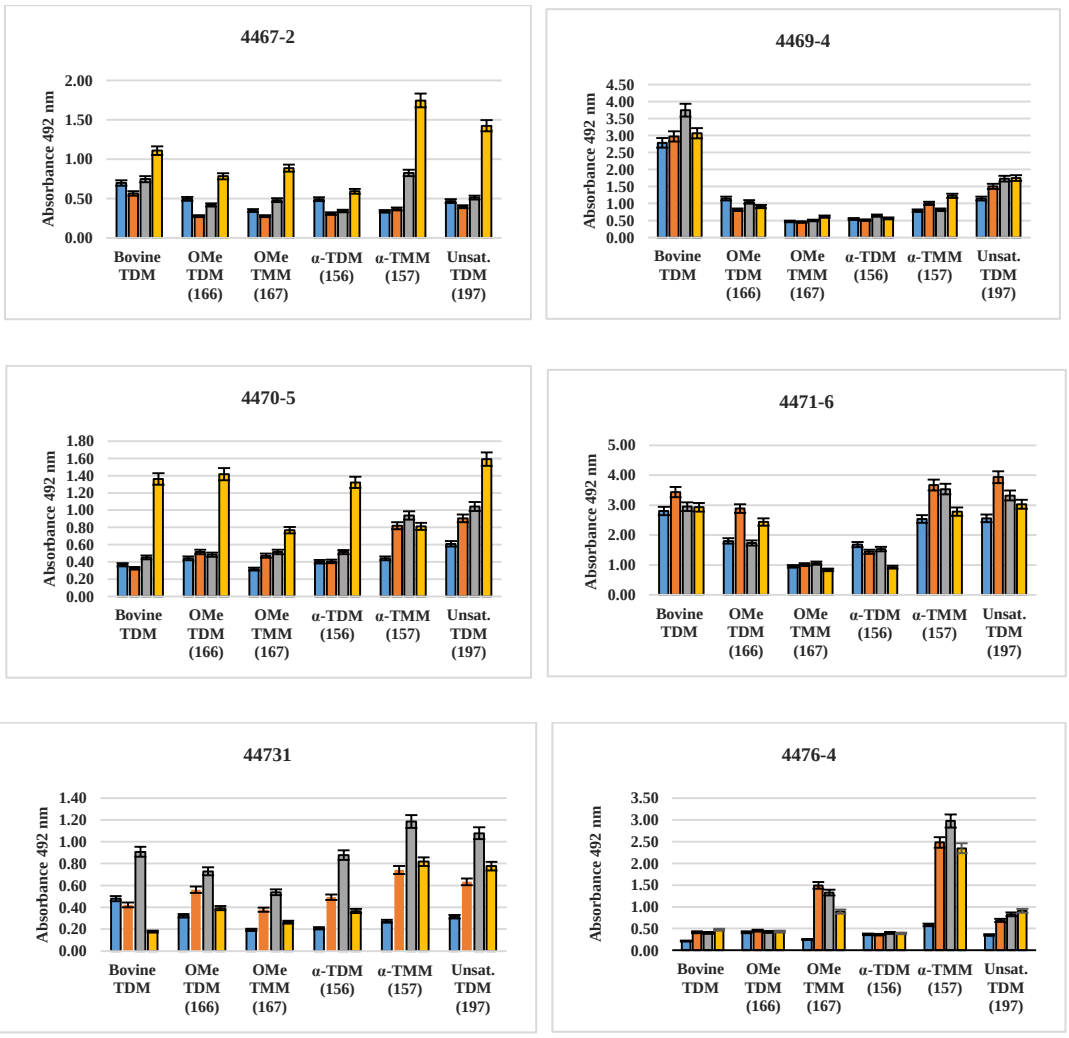

Figure 85: Time profile of ELISA responses for six cattle infected by aerosol route over a six week period using six antigens; dates are (left to right) 11/3/2010, 24/3/2010, 8/4/2010 and 26/4

In general, the responses did not grow significantly with time, as might be expected for an increasing infection. However, there is some evidence of an initial response that then deceases in the middle time points, increasing again towards the end of the time period. If the test was repeated over a six month period with serum from different animals, the results were as in **Figure 86**.

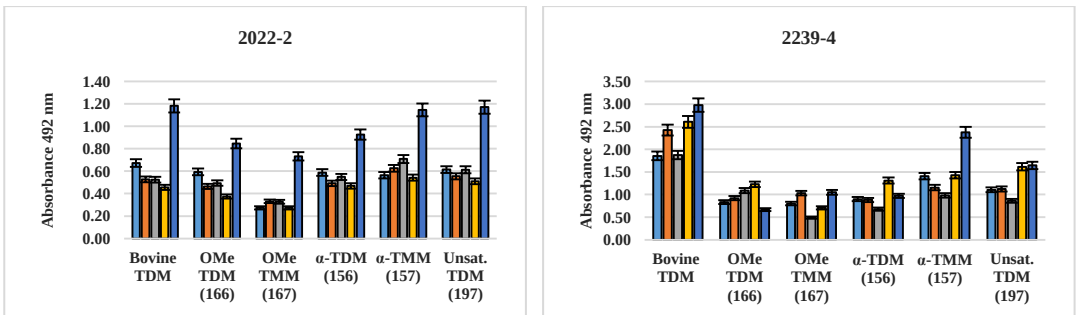

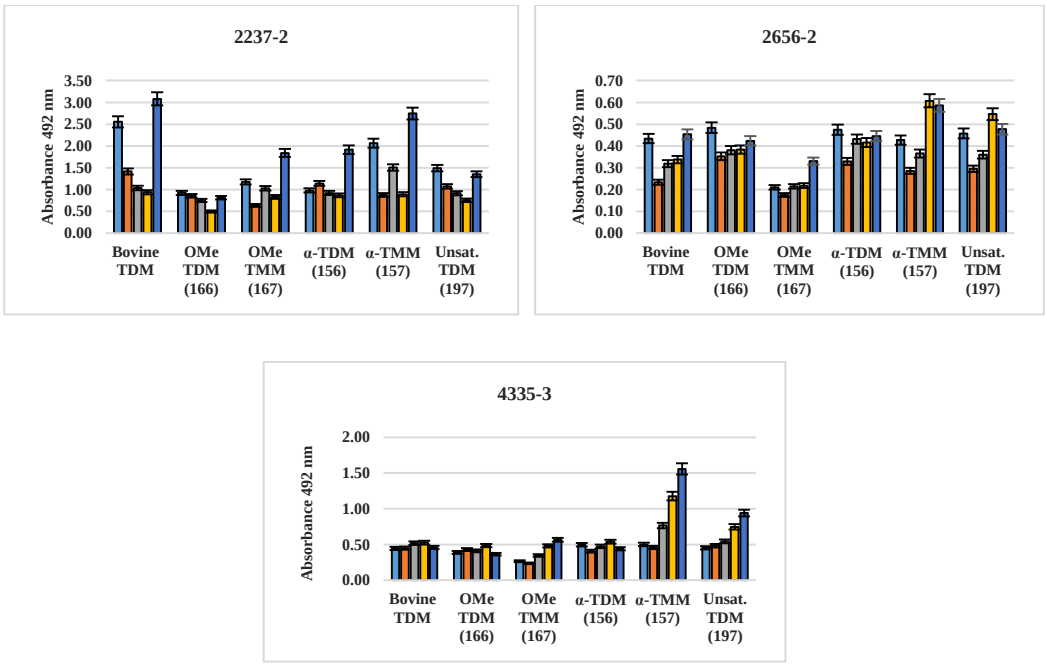

Figure 86: Time profile of ELISA responses for six cattle infected by aerosol route over a six month period using six antigens

Again, there is no real evidence of a strong increase in response with time, but some evidence of a dip in response in the middle of the period. Finally, the test was repeated over a one year period with serum from different animals; the results were as in **Figure 87**.

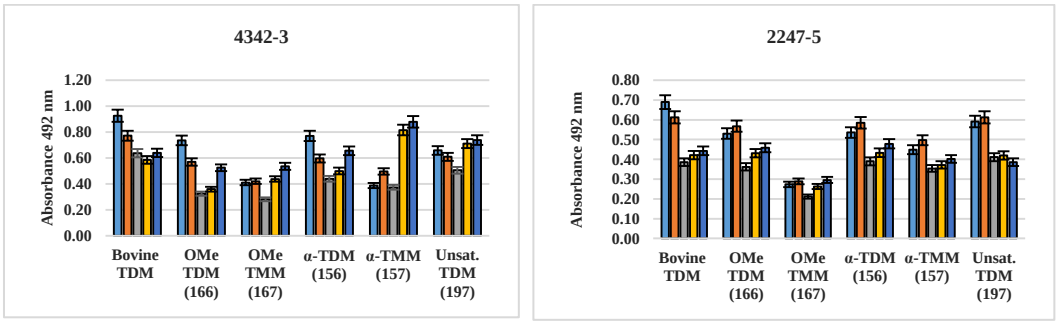

Figure 87: Time profile of ELISA responses for six cattle infected by aerosol route over a one year period using six antigens

4.11 Conclusion

The goal of project was to use an ELISA assay to investigate the potential of synthetic MA and sugar esters molecules for the diagnosis of bovine TB, using different secondary Abs with several classes of bovine serum samples from the Veterinary Laboratory Agency (VLA) in

United Kingdom. Higher Ab binding signals were observed with CFs than with MA subclasses or natural Ags. Also, with some antigens, relatively high Ab binding signals were observed even with BCG vaccinated serum samples (see Figure 73, p131), suggesting that vaccination does not stop infection.

The TB- samples were in groups `pre-challenge non-vaccinate` and `pre-challenge BCG vaccinated` to see the effect of each group on the diagnosis. The best sensitivity and specificity were observed in keto TDM (**160, b7**), which was 74, 72, 75 and 74% using `naturally infected`, `pre-challenge non-vaccinate`, `pre-challenge BCG vaccinated ` and overall TB- serum samples. ROC curves also gave areas under the curves for the synthetic Ags that were higher than the natural Ags. Furthermore, the best pairs of sensitivity and specificity were observed with α- TDM (**156**) (100 and 86 %), good values in comparison with natural and other synthetic Ags.

The use of a range of free MAs showed that the accuracy of the test is 76%, higher than the literature value using of mixtures of natural free MAs which was not adequate for serodiagnosis of TB (accuracy = 57%) (page 43).

Combining the results from a set of Ags using mean decrease accuracy and mean decrease Gini illustrated that the synthetic Ags gave responses higher than the natural Ags. Statistical analysis using multidimensional scaling (MDS) and Random Forest (RF) analysis showed that the ELISA assay can distinguish between different categories of serum sample with reasonably accurate results. Thus it appears that, with some improvement, the ELISA assay can distinguish active TB in animals that have been vaccinated.

The results from the use of synthetic MAs, CFs and wax esters Ags from different *Mycobacteria* showed rather a large number of false positives. This happened even with antigens from other mycobacteria; one possible reason for the false positives is that the samples are infected with atypical *Mycobacteria;* however, it may simply be that the non-bTB antigens cross react with bTB antibodies.

Finally, *M. avium subsp.* paratuberculosis (MAP) was studied using a range of natural and synthetic wax esters and serum samples obtained from serum infected with high doses of MAP, Naturally infected TB+ and Non-vaccinated TB- serum samples. The best combination of sensitivity and specificity (90, 69%) between naturally infected and non-vaccinated) TB- serum samples were observed using synthetic wax ester (**187**) from *M. avium*. The comparison of MAP versus VLA Naturally infected or Non-vaccinated TB- serum samples gave a complete

distinction between these sample sets with some antigens. These are very limited results but give good evidence that the cattle infected with MAP can identified in the presence or absence of bTB.

In a final set of experiments, sets of serum from cattle experimentally infected with bTB by an aerosol method were studied over extended time periods after infection. There was little change in the responses with time, though in a number of cases there was evidence of a cycling of the response, also seen in responses to protein antigens.

Chapter 5

5. Overall Conclusions and future work

The aim of project was achieved successfully in three main parts. First of all, The *S,S-trans*-alkene-methoxy MA (**43**) was prepared using L-ascorbic acid and D-mannitol as starting materials, as they are commercial, cheap and available. The modified Julia-Kocienski olefination, followed by a hydrogenation is an excellent method for chain extension. The modified Julia-Kocienski olefination was also used in the preparation of *trans*-alkene MA, with retention of the stereochemistry of the adjacent methyl group and optimisation of the *trans*-alkene olefination.

The synthesis of the new CFs as derivatives of this MA (**43**), started by protection of the secondary hydroxyl group in the MA, followed by esterification between protected MA (**143**) and protected trehalose (**144**) to give protected TDM (**145**) and TMM (**146**). These were separated and the protecting groups were cleaved in two steps. Firstly, the deprotection of the trehalose sugar with TBAF to give silyl-protected TDM (**147**) and silyl-protected TMM (**148**); secondly the deprotection of the MAs with HF. pyridine complex to get the free TDM (**44**) and TMM **(45**).

The esterification of the free MA (**43**) and each protected glycerol (**149**), glucose tosylate (**151**) and arabinose tosylate (**153**) gave protected GroMM (**150**), GMM (**152**) and ArM (**154**). The harder step was the debenzylation in the presence of both the alkene and methoxy group. After attempting different methods, this was achieved using sodium in liquid ammonia to give free GroMM (**46**), GMM (**47**) and ArM (**48**) respectively.

This synthetic work provides a series of sugar esters of a single mycolic acid that are evaluated below as antigens in the serodiagnosis of TB. The series may also provide a useful means by which the importance of each sugar to the wider biological effects of these compounds, such as their effects on cytokines and chemokines, can be understood. This work is part of an on-going collaboration. [433]

The second part of this study was also achieved successfully using an ELISA assay to investigate the potential of the synthesized molecules for the diagnosis of TB. In order to determine the most sensitive and specific diagnostic test Ag, ELISA assays were carried out using a range of novel synthetic Ags from different parts of the cell wall and different *mycobacteria*, different secondary Abs and a range of TB+ and TB- human serum samples from sources which included tropical regions of Asia, Africa and the America. The best combinations

of sensitivity and specificity with a sub-set of Gambia samples were observed with keto-TDM (**160**) (100 and 78%), MeO-ArM (**179**) (100 and 73%) and α- ArM (**158**) (100 and 86%). Combining the results from synthetic keto- TDM (**160**), α- ArM (**158**) and α- GMM (**180**) gave 100 and 94% sensitivity and specificity. These represent very much better values than those reported with many recognised assays. If these results can be shown to be repeated with a much larger set of samples, they will provide the basis of a rapid means of detecting TB with excellent sensitivity and very high specificity.

ELISA assays also carried using a range of synthetic CFs Ags using serum samples from people in Wales with no known mycobacterial infection; these were collected from farmers, urban residents, and rural residents and the results then compared with those for TB+ and TB- WHO serum samples. Indeed, the average response for set for each Ag was lower than the WHO- set, and no responses were above the average of the WHO+ serum set. However, in some cases, the results were above the average for the WHO- set. This confirms that the synthetic Ags gave good distinction between the three population groups using ELISA assay, and suggest its use it as a regular test for TB- and healthy control.

The serodiagnostic behaviour of a set of TDM, TMM, GroMM, GMM and ArM Ags from *M. tb* from the same *trans*-alkene MA was studied using WHO human serum samples. The results indicated that the Abs to MAs or its derivatives can recognize the hydrophobic and the carbohydrate moieties in the structure of the glycolipid Ags at different levels. The best combinations of sensitivity and specificity were observed in TDM (**44**) (100, 73%) and TMM (**45**) (89, 91%). The best areas under the ROC curve was also observed with these Ags, 0.952 in each case, with excellent distinction between TB+ and TB- serum samples.

The third part was to use an ELISA assay to investigate the potential of the synthetic MA and sugar esters molecules for the diagnosis of bovine TB, using of a range of natural and new synthetic MAs and CFs Ags, and different secondary Abs with several classes of bovine serum samples from the Veterinary Laboratory Agency (VLA) in United Kingdom.

The first main experiment used a set of natural and synthetic antigens in ELISA assays for antibodies in the serum of naturally infected and young un-infected cattle. In general, the infected samples gave higher signals than the un-infected ones but no single antigen gave a very good combination of sensitivity and specificity. The methoxy TMM (**174**, b8), α-TMM (**157**, b5) and unsaturated MA (**192**, b6) all give a better distinction than natural human TDM (b1) between bTB+ and bTB- serum samples. However, if the results for several antigens were combined, a good separation was achieved. Thus, statistical analysis using multidimensional

scaling (MDS) and Random Forest (RF) analysis showed that the ELISA assay can distinguish between different categories of serum sample with accurate results. A principal coordinate analysis using natural and whole set of synthetic Ags generates a probability distribution in two principal axis (Figure 72, Page 130). This gives a good split between bTB+ and bTB- samples; clearly there are some positives and negatives that do not fit this patterns. The results demonstrated that the combining the results from different Ags gives a good distinction between different class of serum sample

Higher Ab binding signals were observed with CFs than with MA subclasses or natural Ags. Higher singals were observed infected serum than with BCG vaccinated, and these were slightly higher than for pre-challenge non-vaccinated serum. The strongest Ab binding signal with `naturally infected' serum samples was observed with α-MA TMM (**157**), with good distinction between these and `pre-challenge non-vaccinate` serum samples using IgG. However, the best combination of sensitivity and specificity was observed with keto-MA TDM (**160**) (74, 72) using IgG whole molecule. The `pre-challenge BCG vaccinated` serum samples showed somewhat higher signals in contrast with non-vaccinated pre-challenge samples; there are a number of possible explanations, one being that vaccination leads to a residual lipid Ab response,

The next major part of this work compared the responses with the serum of 19 naturally infected, 18 `pre-challenge non-vaccinated`, and 20 `pre-challenge BCG vaccinated` groups of animals to understand the effect of each group in the diagnosis of TB. Again the experiment was carried out with two natural TDMs and eight sythetic sugar esters of mycolic acids. The best combinations of sensitivity and specificity compared to the infected samples were observed with a keto TDM (**160**), at 74, 72 % for `pre-challenge non-vaccinated`, and 75 and 74 % for `pre-challenge BCG vaccinated` serum. In order to improve this distinction, the results from the set of antigens were combined. Forest Classifier principal coordinates analysis combining the results from the set of Ags showed a good split among the three sets of serum samples (Figure 76, Page 136). Thus, using this method it appears possible to distinguish infected animals, from un-vaccinated animals, but also from animals have have been given a BCG vaccination. This would provide a unique advantage over current methods for rapid diagnosis. The method needs to be validated with a much larger sample set in future work.

Almost all the previous experiments with cattle serum had used sugar esters of mycolic acids. An experiment was carried out to study the use of free mycolic acids [methoxy (**195**), keto (**196**), alkene (**192**) and epoxy (**193**)] from *M. tb*, *M. fortuitum* and *M. smegmatis* respectively were studied using `naturally infected` and non-vaccinated pre-challenge serum samples and IgG whole molecule as a secondary Ab. The accuracy of the test was 76%, higher than the literature value using of mixtures of natural free MAs (57%), which was not adequate for serodiagnosis of bTB. This suggests that the use of a wider range of free synthetic MAs Ags with a different categories of serum samples needs to be examined in more detail.

In a set of experiments using serum from cattle that were diagnosed with non-tuberculous mycobacterial infections at slaughter, using synthetic MAs, CFs and wax esters Ags from different *Mycobacteria*, no significant signals were seen. However, *M. avium subsp.* paratuberculosis (MAP) was studied using two strongly infected serum samples; one naturally infected the other artificially infected. In this set of experiments, a range of natural and synthetic wax esters and serum from the MAP animals, and from VLA naturally infected TB+ and non-vaccinated TB- animals were studied. Each natural and synthetic Ag showed high responses with serum infected with high doses of MAP, this response being above the average of the VLA (Naturally infected) serum samples. In some cases, essentially no signal was seen except with the MAP samples. This shows that the ELISA assay can be a diagnostic tool for detection of MAP in present of bovine TB+, but this is a very limited set of serum samples, (Table 44, Page 147). This needs to be validated using a wider range of Ags and serum samples.

In a final set of experiments, sets of serum from cattle experimentally infected with bTB by an aerosol method were studied over extended time periods after infection. There was little change in the responses with time, though in a number of cases there was evidence of a cycling of the response, also seen in responses to protein antigens.

Chapter 6

6. The experimental section

6.1 General considerations

Chemicals used were obtained from commercial suppliers or prepared from them by methods described. Solvents, which had to be dry, e.g., ether and tetrahydrofuran were dried over sodium wire. Petrol was of boiling point 40–60 ^{o}C. Reactions carried under inert conditions were carried out under a slow stream of nitrogen. Those carried out at low temperatures were cooled using a bath of methylated spirit with liquid nitrogen. Silica gel (Merck 7736) and silica plates used for column and thin layer chromatographies were obtained from Aldrich. Organic solutions were dried over anhydrous magnesium sulfate. GLC was carried out on a Perkin–Elmer Model 8410 on a capillary column (15 m × 0.53 mm). IR spectra were carried out on a Perkin–Elmer 1600 FTIR spectrometer as liquid films. NMR spectra were recorded on a Bruker Avance 400 or 500 spectrometer. $[\alpha]_D$ values were recorded in $CHCl_3$ on a POLAAR 2001 Optical Activity polarimeter. Mass spectra were recorded on a Bruker MALDI-TOF MS to an accuracy of 1 d.p.; accurate mass values obtained in Bangor were run on a Bruker Microtof LC-MS and also MALDI-TOF MS in Bristol University (thanks to Dr Paul Gates).

6.2 Experiments

Experiment 1: 1,2:5,6-Di-*O*-isopropylidene–D-mannitol (120)

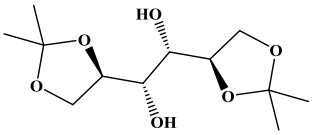

Anhydrous zinc chloride (98.75 g, 725.0 mmol) was dissolved in HPLC grade acetone (600 mL) and the mixture was stirred until the $ZnCl_2$ was dissolved. D-mannitol (**59**) (60 g, 33 mmol) was added to the solution and the mixture was stirred for 18 h. at r. t. K_2CO_3 (118.4 g, 856.0 mmol) in water (100 mL) was added to the mixture. The solid inorganics were filtered under suction and washed with CH_2Cl_2 (3 × 100 mL) and then the solvent was evaporated to give a crude oil. This was dissolved in CH_2Cl_2 (300 mL), washed with water (100 mL) and brine (150 mL), dried and the solvent was evaporated to give a white solid. Recrystallisation from petroleum/ethyl acetate (7:1) was gave a glassy white solid of the title compound (74.0 g, 86%), $[\alpha]_D^{24}$= + 8.3 (c 0.63, $CHCl_3$). (lit.[434]. $[\alpha]_D^{25}$= + 2.4 (c 1.0, EtOH), m.p. 118 – 119 ^{o}C (lit.[435], 119.5-121 ^{o}C). This showed that δ_H, δ_C and IR data match those in the literature.

Experiment 2: Methyl (*E*)-3-((*S*)-(2,2-dimethyl-1,3-dioxolan-4-yl)acrylate (121)

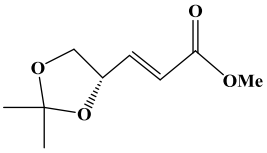

A solution of $NaIO_4$ (19.6 g, 91.6 mmol) in water (100 mL) was added dropwise to a stirred solution of 1,2:5,6-di-*O*-isopropylidene–D-mannitol (**120**) (20.0 g,76.3 mmol) in 5% $NaHCO_3$ (200 mL) at 0 ^oC and stirring was continued for 1 h. at r. t. then the mixture was cooled to 0 ^oC and methyl (diisopropoxy phosphoryl)-acetate (40.0 g, 168 mmol) was added with stirring followed by add 6 M solution of aq. K_2CO_3 (260 mL) at 0-4 ^oC. The mixture was allowed to reach r. t. and the stirring was continued for 20 h. then the product was extracted with CH_2Cl_2 (3 × 300 mL), the combined organic extracts were dried and the solvent was evaporated. The crude product was purified and separated by column chromatography eluting with petroleum/ethyl acetate (5:1) to give the title compound as a colourless oil (20.0 g, 70%), $[\alpha]_D^{24}$= + 45.2 (c 1.25, $CHCl_3$) (lit.[379,435] $[\alpha]_D^{24}$= + 40.4 (c 1.09, $CHCl_3$)). The δ_H, δ_C and IR data match those in the literature.

Experiment 3: Methyl (*R*)- 3-((*S*)-2,2-dimethyl-[1,3]-dioxolan-4-yl)butanoate (122)

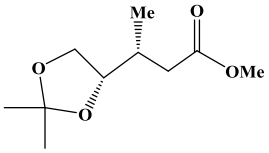

Methyl (*E*)-3-((*S*)-(2,2-dimethyl-1,3-dioxolan-4-yl)acrylate (**121**) (10.0 g, 53.8 mmol) was dissolved in dry ether (300 mL) and stirred under nitrogen atomspher. It was cooled to -78 ^oC and MeLi (77 mL, 107.5 mmol, 1.4 M) was added at -78 ^oC. The mixture was maintained at -78 ^oC for 2.5 h. and then allowed to gradually warm up to -60 ^oC then water (10 mL) was added. After 5 min, sat. aq. NH_4Cl (60 mL) was added, whereupon the temperature rose to -40 ^oC. The cooling bath was removed and the temperature of the mixture brought to 0 ^oC by addition of water (100 mL). The organic layer was seprated and the aqueous layer was re-extracted with ether (100 mL). The combined organic layers were washed with brine (2 × 100 mL), dried and the solvent was evaporated. The product was purified by column chromatography eluting with petroleum/ethyl acetate (5:1) to give a colourless oil, the title compound (8.4 g, 77%), $[\alpha]_D^{23}$ = + 7.4 (c 1.2, $CHCl_3$) (lit.[379] $[\alpha]_D^{22}$= = + 8.34 (*c* 1.12, $CHCl_3$)). The NMR and IR data match those in the literature.

Experiment 4: (*R*)-3-((*S*)-2,2-Dimethyl-[1,3]-dioxolan-4-yl)butan-1-ol (123)

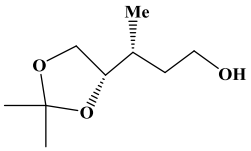

A solution of methyl (*R*)-3-((*S*)-2,2-dimethyl-[1,3]-dioxolan-4-yl)butanoate (**122**) (14.7 g, 72.8 mmol) in dry THF (100 mL) was added dropwise over 15 min. to a suspension of to a stirred suspension of $LiAlH_4$ (4.150 g, 109.2 mmol) in dry THF (250 mL) at -20 ^oC under nitrogen atomosphere. The mixture was heated at reflux for 1 h then quenched with sat. aq. sodium sulphate decahydrate at 0 ^oC until a white precipitate had formed. The solution was dried with $MgSO_4$ and THF (60 mL) was added. The mixture was filtered through a bed of silica and the solvent was evaporated. The product was purified by column chromatography eluting with petroleum/ethyl acetate (5:2) to give a colourless oil, the title compound (11.0 g, 90%), $[\alpha]_D^{25}$= + 19.9 (c 1.24, $CHCl_3$). (lit.[379] $[\alpha]_D^{24}$= +18.1 (*c* 1.35, $CHCl_3$)). The NMR and IR data matched those in the literature.

Experiment 5: (*R*)-3-((*S*)-2,2-Dimethyl-[1,3]-dioxolan-4-yl)butanal (58)

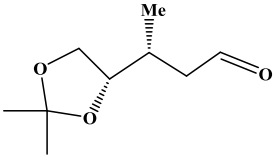

A solution of (*R*)-3-((*S*)-2,2-dimethyl-1,3-dioxolan-4-yl)butan-1-ol (**123**) (11.4 g, 65.6 mmol) in CH_2Cl_2 (50 mL) was added dropwise to a stirred solution of PCC (28.20 g, 131.3 mmol) in CH_2Cl_2 (140 mL) and during the addition a black colour appeared. The mixture was stirred at r. t. for 2 h. Petrol /ethyl acetate (5:1) (200 mL) was added to the mixture, forming a thick black precipitate. The precipitate was removed by filtration through a bed of silica, dried and the solvent was evaporated. The product was purified by column chromatography on silica, eluting with petroleum/ethyl acetate (5:1) to give a colourless oil, the title compound (8.7 g, 77%), $[\alpha]_D^{23}$= + 8.24 (c 1.06, $CHCl_3$). (lit.[379]. $[\alpha]_D^{23}$ = + 8.27 (*c* 1.44, $CHCl_3$). The NMR and IR data matched those in the literature.

Experiment 6: 9-Bromo-nonan-1-ol (124)

$Br(CH_2)_9OH$

1,9-Nonanediol (**63**) (26.0 g, 0.16 mol) was dissolved in toluene (300 mL) and aq. HBr (30 mL, 48 % w.w.) was added and the mixture refluxed for 18 h. The organic layer was washed with

water (200 mL) and then with sat. aq. $NaHCO_3$ (150 mL), dried and the toluene was removed by simple distillation at atm. pressure. The product was purified by column chromatography eluting with petroleum/ether (4:1 then 1:1) to give a white solid, the title compound (29.0 g, 81%), which showed NMR and IR data matching those in the literature.[186]

Experiment 7: 2,2-Dimethylpropionic acid 9-bromo-nonyl ester (62)

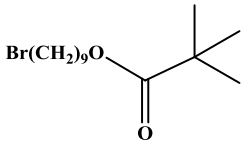

A solution of trimethylacetyl chloride (18.50 g, 153.4 mmol, 1.2 mol eq.) in CH_2Cl_2 (65 mL) was added to a stirred solution of 9-bromo-nonan-1-ol (**124**) (28.50 g, 127.8 mmol), CH_2Cl_2 (200 mL), triethylamine (38.70 mL, 383.4 mmol) and 4-dimethylaminopyridine (0.5 g, 4.0 mmol), over a period of 15 min. at 5 ^oC and stirred at r. t. for 18 h. Then dilute HCl (200 mL, 5%) was added and the organic phase was separated. This was then washed with dilute HCl (150 mL) and brine (2 × 200 mL), dried and evaporated. The product was purified by column chromatography eluting with petroleum/ether (4:1) to give a colourless oil, the title compound (38.1 g, 96%), which showed that NMR and IR data matching those in the literature.[186]

Experiment 8: 2,2-Dimethylpropionic acid 9-(2-phenyl-2*H*-pentazol-1-ylsulfanyl)nonyl ester (61)

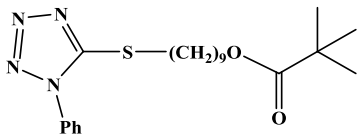

Anhydrous potassium carbonate (18.90 g, 136.8 mmol) was added to a stirred solution of 1-phenyl-1*H*-tetrazole-5-thiol (11.03 g, 61.90 mmol) and 2,2-dimethyl-propionic acid 9-bromononyl ester (**62**) (20.0 g, 65.1 mmol) in acetone (320 mL) at r. t. The mixture was vigorously stirred for 18 h at r. t. Water (1L) was added and the organic layer was separated. The aqueous layer was re-extracted with CH_2Cl_2 (4 × 150 mL, 2 × 25 mL). The combined organic layers were washed with brine (2 × 200 mL), dried and evaporated. The product was purified by column chromatography eluting with petroleum/ether (7.0:2.5 and then 1:1) to give a colourless oil, the title compound (24.0 g, 91%).[382]

Experiment 9: 2,2-Dimethylpropionic acid 9-(2-phenyl-2*H*-pentazol-1-sulfonyl)nonyl ester (60)

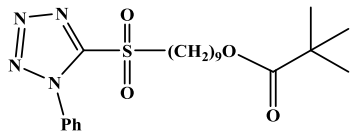

A solution of ammonium molybdate (VI) tetrahydrate (35.6 g, 28.8 mmol) in 35% H_2O_2 (80 mL) was prepared and cooled in an ice bath, then added to a stirred solution of 2,2-dimethyl-propionic acid 9-(2-phenyl-2*H*-pentazol-1-ylsulfanyl)-nonyl ester (**61**) (20.8 g, 51.5 mmol) in THF (200 mL) and IMS (400 mL) at 10 ^oC and stirred at r. t. for 2 h. A further solution of ammonium molybdate (VI) tetrahydrate (15.9 g, 12.9 mmol) in 35% H_2O_2 (40 mL) was added and the mixture was stirred at r. t. for 18 h. The mixture was poured into water (2 L) and the organic layer was separated. The aqueous layer was re-extracted with CH_2Cl_2 (3 × 200 mL). The combined organic layers were washed with water (2 × 300 mL), dried and the solvent was evaporated. The product was purified by column chromatography eluting with petroleum/ether (7:2 and then 1:1) to give a colourless oil, the title compound (22.0 g, 97%).The NMR and IR data matched those in the literature. [186,382]

Experiment 10: (*R*)-12-((*S*)-2,2-Dimethyl-[1,3]-dioxolan-4-yl)tridecyl pivalate (57)

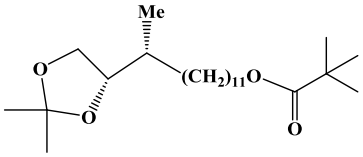

Lithium bis (trimethylsilyl) amide (87.70 mL, 92.97 mmol, 1.06 M) was added to stirred solution of 2,2-dimethyl-propionic acid 9-(2-phenyl-2*H*-pentazol-1-sulfonyl)-nonyl ester (**60**) (22.45 g, 61.98 mmol) and (*R*)-3-((*S*)-2,2-dimethyl-[1,3]-dioxolan-4-yl)butanal (**58**) (8.20 g, 47.6 mmol) in dry THF (200 mL) at - 10 ^oC under nitrogen atmosphere. The solution was allowed to reach r. t. and stirred for 2 h. Petroleum/ether (1:1) (100 mL) and sat. aq. NH_4Cl (100 mL) were added. The organic layer was separated and the aqueous layer was re-extracted with petroleum/ether (1:1, 2 × 100 mL). The combined organic layers were dried and the solvent was evaporated. The product was purified by column chromatography eluting with petroleum/ether (50:1) to give a colourless oil of (*E*/*Z*)-(*R*)-12-((*S*)-2,2-dimethyl-[1,3]-dioxolan-4-yl)tridec-9-en-1-yl pivalate (**125**) (14.0 g, 76%) as a mixture of two isomers in ratio (2.3:1). Palladium (10% on carbon, 1 g) was added to a stirred solution of the above alkene (14 g, 36 mmol) in IMS (200 mL) under hydrogen atmosphere. Hydrogenation was carried out for 2 h. The solution was filtered on a bed of celite and the solvent was evaporated to give a

colourless oil, the title compound (13.0 g, 92%), $[\alpha]_D^{26}$= + 16.1 (c 1.14, $CHCl_3$) {Found [M – CH_3]$^+$: 369.2989, $C_{22}H_{41}O_4$ requires: 369.2989}. This showed δ_H (400 MHz, $CDCl_3$): 4.05 (2H, t, *J* 6.6 Hz), 4.0 (1H, dd, *J* 6.3, 7.9 Hz), 3.87 (1H, br. q, *J* 6.9 Hz), 3.60 (1H, br. t, *J* 7.9 Hz), 1.62 (2H, quintet, *J* 6.6 Hz,), 1.40 (3H, s), 1.35 (3H, s), 1.32-1.26 (18H, m), 1.2 (9H, s), 1.1-1.05 (1H, m), 0.96 (3H, d, *J* 6.6 Hz); δ_C (126 MHz, $CDCl_3$) : 178.6, 108.5, 80.4, 67.8, 64.5, 38.7, 36.5, 32.7, 29.9, 29.7, 29.6, 29.59, 29.54, 29.50, 29.2, 28.6, 27.2, 27.0, 26.6, 25.9, 25.5, 15.6; ν_{max}: 2926, 2855, 1731, 1463, 1368, 1284, 1158 cm^{-1}.

Experiment 11: (*R*)-12-((*S*)-2,2-Dimethyl-[1,3]-dioxolan-4-yl)tridecan-1-ol (56)

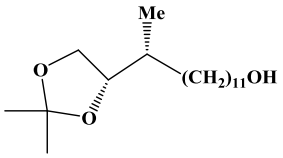

A solution of (*R*)-12-((*S*)-2,2-dimethyl-[1,3]-dioxolan-4-yl)tridecyl pivalate (**57**) (12.70 g, 33.07 mmol) was dissolved in dry THF (100 mL) and added slowly to a stirred suspension of $LiAlH_4$ (1.88 g, 49.6 mmol) at -20 ^oC under nitrogen atomosphere, the reaction mixture was heated and refluxed for 1 h. then quenched with sat. aq. sodium sulfate decahydrate (20 ml) at 0 ^oC until a white precipitate had formed. The mixture was dried with $MgSO_4$ and THF (60 mL) was added. The mixture was filtered through a bed of silica and the solvent was evaporated. The product was purified and separated by column chromatography eluting with petroleum/ether (5:1) to give a colourless oil of the title compound (8.0 g, 81%), $[\alpha]_D^{23}$= + 19.3 (c 1.12, $CHCl_3$) {Found [M–CH_3]$^+$: 285.2443, $C_{17}H_{33}O_3$ requires: 285.2425}. This showed δ_H (400 MHz, $CDCl_3$)*:* 3.84 (1H, dd, *J* 6.2, 7.7 Hz), 3.77 (1H, br. q, *J* 7.0 Hz), 3.50 (1H, br. t, *J* 7.7 Hz), 3.41 (2H, t, *J* 6.6 Hz,), 1.52-1.47 (1H, m), 1.45 (3H, s), 1.43-1.40 (1H, m), 1.36 (3H, s), 1.34-1.15 (20H, m), 1.01 (3H, d, *J* 6.9 Hz); δ_C (126 MHz, $CDCl_3$): 108.7, 80.6, 68.2, 62.7, 37.0, 33.3, 33.2, 30.4, 30.2, 30.18, 30.15, 30.14, 30.12, 30.0, 27.4, 27.0, 26.3, 25.9, 15.9; ν_{max}: 3395, 2926, 2853, 1466, 1377, 1266, 1205, 1155, 1058 cm^{-1}.

Experiment 12: 5-(((*R*)-12-((*S*)-2,2-Dimethyl-[1,3]-dioxolan-4-yl)tridecyl)thio)-1-phenyl-1*H*-tetrazole (55)

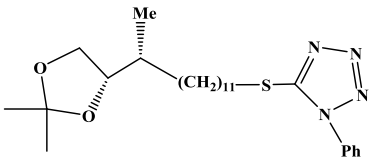

Diethyl azodicarboxylate (6.1 g, 35 mmol) in dry THF (2 mL) was added to a stirred solution of 1-phenyl-1*H*-tetrazole-5-thiol (6.2 g, 35 mmol), triphenylphosphine (9.12 g, 35.0 mmol) and (*R*)-12-((*S*)-2,2-dimethyl-[1,3]-dioxolan-4-yl)tridecan-1-ol (**56**) (8.0 g, 27 mmol) in dry THF (50 mL) at 0 ^{o}C, The mixture was vigorously stirred and refluxed for 2.5 h. Petroleum/ethyl acetate 5:1 (150 mL) was added and the mixture was filtered through a bed of celite and the solvent was evaporated. The product was purified by column chromatography eluting with petroleum/ether (5:1) to give a white solid, the title compound (10.0 g, 84%), $[\alpha]_D^{22}$= + 13.6 (c 0.88, $CHCl_3$) {Found $[M - CH_3]^+$: 445.2635, $C_{24}H_{37}N_4O_2S$ requires: 445.2637}. This showed δ_H (500 MHz, $CDCl_3$): 7.60-7.52 (5H, m), 4.0 (1H, dd, *J* 6.3, 7.9 Hz), 3.87 (1H, br. q, *J* 7.1 Hz), 3.60 (1H, br. t, *J* 7.6 Hz), 3.39 (2H, t, *J* 7.4 Hz,), 1.82 (2H, quintet, *J* 7.3 Hz), 1.58-1.53 (1H, m), 1.46-1.41 (2H, m), 1.40 (3H, s), 1.35 (3H, s), 1.33-1.25 (15H, m), 1.11-1.04 (1H, m), 0.96 (3H, d, *J* 6.6 Hz); δ_C (126 MHz, $CDCl_3$) : 154.5, 133.8, 130.0, 129.7, 123.8, 108.4, 80.4, 67.8, 36.5, 33.3, 32.7, 29.8, 29.6, 29.59, 29.5, 29.1, 29.0, 28.6, 27.0, 26.6, 25.5, 15.6; ν_{max}: 2925, 2854, 1598, 1501, 1464, 1380, 1245, 1161, 1065 cm^{-1}.

Experiment 13: 5-(((*R*)-12-((*S*)-2,2-Dimethyl-[1,3]-dioxolan-4-yl)tridecyl)sulfonyl)-1-phenyl-1*H*-tetrazole (53)

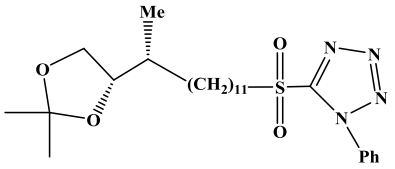

A solution of ammonium molybdate (VI) tetrahydrate (13 g, 10 mmol) in 35% H_2O_2 (40 mL) was prepared and cooled in an ice bath and added to a stirred solution of the 5-(((*R*)-12-((*S*)-2,2-dimethyl-[1,3]-dioxolan-4-yl)tridecyl)thio)-1-phenyl-1*H*-tetrazole (**55**) (10.3 g, 22.2 mmol) in THF (100 mL) and IMS (250 mL) at 10 ^{o}C and stirred at r. t. for 2 h. A further solution of ammonium molybdate tetrahydrate (6.94 g, 5.60 mmol) in 35% H_2O_2 (20 mL) was added and the mixture was stirred at r. t. for 18 h. The mixture was poured into water (1.2 L) and the organic layer was separated. The aqueous layer was re-extracted with CH_2Cl_2 (3 × 30 mL). The combined organic layers were washed with water (500 mL), dried and the sovent was evaporated. The product was purified by column chromatography eluting with petroleum/ether (5:1) to give a white solid, the title compound (9.20 g, 84%), $[\alpha]_D^{25}$= + 12.6 (c 1.01, $CHCl_3$). {Found $[M - CH_3]^+$: 477.2523, $C_{24}H_{37}N_4O_4S$ requires: 477.2531}. This showed δ_H (500 MHz, $CDCl_3$): 7.71-7.69 (2H, m), 7.65-7.59 (3H, m), 4.00 (1H, dd, *J* 6.3, 7.9 Hz), 3.87 (1H, br. q, *J* 7.0 Hz), 3.75-3.72 (2H, m), 3.60 (1H, br. t, *J* 7.9 Hz), 1.99-1.92 (2H, m), 1.53-1.47 (2H, m), 1.41 (3H, s), 1.35 (3H, s), 1.32-1.26 (16H, m), 1.11-1.04 (1H, m), 0.96 (3H, d, *J* 6.6 Hz); δ_C

(126 MHz, $CDCl_3$): 153.5, 133.0, 131.4, 129.7, 125.0, 108.5, 80.4, 67.8, 56.0, 36.5, 33.7, 29.8, 29.6, 29.58, 29.5, 29.4, 29.2, 28.9, 28.1, 27.0, 26.6, 25.5, 21.9, 15.6; ν_{max}: 3069, 2917, 2854, 1594, 1498, 1473, 1356, 1259, 1209, 1150, 1064 cm^{-1}.

Experiment 14: (*S*)-1-Benzyloxy-hex-5-en-3-ol (70)

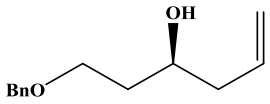

Copper iodide (4.60 g, 24.2 mmol) was dissolved in dry THF (300 mL) at r. t. under argon and cooled to –75 ºC. Vinylmagnesium bromide (155 ml, 155 mmol, 1M in THF) was added between –75 ºC to –50 ºC and the mixture was stirred at –50 ºC to –40 ºC for 30 min. it was re-cooled to –75 ºC and a solution of (*R*)-(2-benzyloxyethyl)oxirane (**126**) (14.3 g, 80.3 mmol) in dry THF (100 mL) was added between –75 ºC to –40 ºC and the reaction was stirred at –40 to –30 ºC for 1 h, then at –20 ºC for 15 min. Sat. aq. NH_4Cl (400 mL) was added and the product was extracted with ethyl acetate (3 × 300 mL). The combined organic layers were washed with water, dried and the solvent was evaporated. The product was purified by column chromatography eluting with petroleum/ethyl acetate (2:1) to give a colourless oil, the title compound (15.7 g, 95%), $[\alpha]_D^{24}$ = – 4.77 (*c* 1.2, $CHCl_3$) (lit.[186]. $[\alpha]_D^{24}$ = – 5.3 (*c* 1.2, $CHCl_3$). The NMR and IR data matched those in the literature.[186]

Experiment 15: Acetic acid (*S*)-1-(2-benzyloxy-ethyl)-but-3-enyl ester (127)

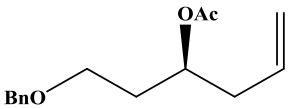

A mixture of acetic anhydride (80 mL) and anhydrous pyridine (80 mL) were added to a stirred solution of (*S*)-1-benzyloxyhex-5-en-3-ol (**70**) (23.5 g, 114 mmol) in dry toluene (180 mL) at r. t. The mixture was stirred for 18 h. Then diluted with toluene (100 mL) and the solvent was evaporated under reduced pressure to give a residue. This was purified by column chromatography eluting with petroleum/ether (6:1) to give a colourless oil, the title compound (28 g, 99%), $[\alpha]_D^{23}$ = + 37.0 (*c* 1.1, $CHCl_3$) (lit. [186]. $[\alpha]_D^{23}$ = + 49.0 (*c* 1.13, $CHCl_3$)).This showed that the NMR and IR data match those in the literature.[186]

Experiment 16: (*R*)-3-Acetoxy-5-benzyloxy-pentanoic acid (128)

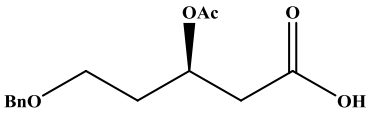

Acetic acid (*S*)-1-(2-benzyloxyethyl)-but-3-enyl ester (**127**) (17.8 g, 71.8 mmol) was dissolved in dry DMF (450 mL). Then the oxone (176.5 g, 287.1 mmol) and OsO_4 2.5% in 2-methyl-2-propanol (9.0 mL, 0.72 mmol) were added to the mixture at 10 °C. The mixture was allowed to reach 32 °C and stirred for 3 h, then diluted with water (3 L). The organic layer was separated and the aqueous layer was re-extracted with ethyl acetate (2 × 250 mL). The combined organic layers were washed with water (700 mL), dried and the solvent was evaporated. The product was purified by column chromatography eluting with petroleum/ethyl acetate (1:1 then 1:2) to give a colourless oil, the title compound (14.9 g, 78%), $[\alpha]_D^{22}$ = + 10.2 (*c* 0.86, $CHCl_3$) (lit.[381] $[\alpha]_D^{22}$ = + 15.2 (*c* 0.89, $CHCl_3$)). This showed NMR and IR data matching those in the literature.[186]

Experiment 17: Methyl (*R*)-5-benzyloxy-3-hydroxy-pentanoate (129)

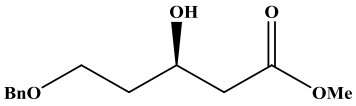

Conc. H_2SO_4 (70 drops) was added to a stirred solution of (*R*)-3-acetoxy-5-benzyloxy-pentanoic acid (**128**) (14.75 g, 55.45 mmol) in methanol (300 mL) and refluxed for 3.5 h, then the methanol was evaporated. The residue was diluted with ethyl acetate (250 mL) and sat. aq. $NaHCO_3$ (200 mL). The organic layer was separated and the aq. layer was re-extracted with ethyl acetate (2 × 150 mL). The combined organic layers were dried and the solvent was evaporated. The product was purified by column chromatography eluting with petroleum/ethyl acetate (3:2) to give a colourless oil, the title compound (10.0 g, 78%), $[\alpha]_D^{26}$ = – 12.5 (*c* 0.920, $CHCl_3$). (lit.[186] $[\alpha]_D^{26}$ = – 12.2 (*c* 1.23, $CHCl_3$)). This showed NMR and IR data matching those in the literature.[186]

Experiment 18: Methyl (*R*)-2-((*R*)-3-benzyloxy-1-hydroxy-propyl)-pent-4-enoate (69)

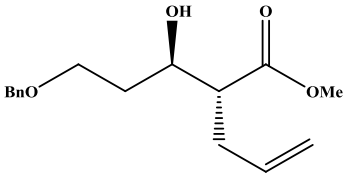

Diisopropylamine (7.86 g, 77.7 mmol) in dry THF (100 mL) was cooled to – 78 °C. MeLi (54.4 mL, 81.6 mmol, 1.5 M) was added and stirred at - 16 °C for 30 min. Then re-cooled to – 61 °C and methyl-(*R*)-5-benzyloxy-3-hydroxy-pentanoate (**129**) (8.60 g, 36.1 mmol) in dry THF (50 mL) was added and the mixture was stirred at – 45 °C for 1 h. and at - 20 °C for 40 min. then at - 20 °C to – 10 °C for 20 min. It was re-cooled to – 62 °C and allyl iodide (5.0 mL, 54.2 mmol) in dry THF (20 mL) and hexamethyl phosphorotriamide (HMPA) (12.6 mL, 72.3 mmol) were added and the mixture was stirred at – 45 °C for 1 h. and at - 45 °C to – 20 °C for 30 min. and then at – 20 °C for 30 min. Further allyl iodide (0.9 mL) was added and stirred at – 20 °C to – 10 °C for 30 min. and at – 10 °C for 30 min. Then sat. aq. NH_4Cl (70 mL) was added and extracted with petroleum/ethyl acetate (1:1, 3 × 100 mL), dried and the solvent was evaporated. The product was purified by column chromatography eluting with petroleum/ethyl acetate (2:1) to give a colourless oil, the title compound (7.6 g, 76%), $[\alpha]_D^{21} = -5.53$ (*c* 1.61, $CHCl_3$). (lit.[186] $[\alpha]_D^{21} = -6.9$ (*c* 1.09, $CHCl_3$)).

Experiment 19: Methyl (*R*)-2-[(*R*)-3-benzyloxy-1-(*tert*-butyl-dimethyl-silanyloxy)-propyl]-pent-4-enoate (134)

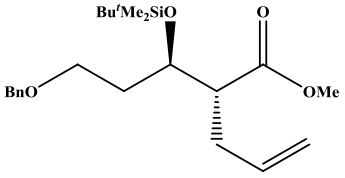

Imidazole (3.67 g, 54.0 mmol) was added to a stirred solution of methyl (*R*)-2-((*R*)-3-benzyloxy-1-hydroxy-propyl)-pent-4-enoate (**69**) (6.00 g, 21.8 mmol) in dry DMF (100 mL) at r. t. followed by addition of *tert*-butyldimethylchlorosilane (4.23 g, 28.1 mmol) and stirred at 45 °C for 18 h. The mixture was quenched with water (350 mL) and extracted with CH_2Cl_2 (3 × 200 mL). The combined organic layers were washed with water (200 mL), dried and the solvent was evaporated. The product was purified by column chromatography eluting with petroleum/ether (4:1) gave a colourless oil, the title compound (7.4 g, 87%), $[\alpha]_D^{26} = -16.1$ (*c*

2.51, $CHCl_3$) (lit.[186] $[\alpha]_D^{26} = -17.2$ (*c* 0.93, $CHCl_3$)). The NMR and IR data matched those in the literature.

Experiment 20: Methyl (2*R*,3*R*)-5-benzyloxy-3-(*tert*-butyl-dimethyl-silanyloxy)-2-(2-oxo-ethyl)-pentanoate (68)

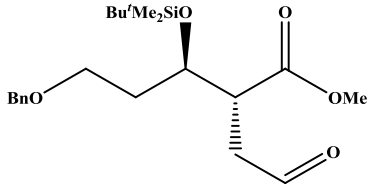

2,6-Lutidine (2.36 g, 22.0 mmol), OsO4 2.5% in 2-methyl-2-propanol (2.0 mL, 0.2 mmol), and then NaIO4 (9.4 g, 44 mmol) were added with stirring to methyl (*R*)-2-[(*R*)-3-benzyloxy-1-(*tert*-butyl-dimethyl-silanyloxy)-propyl]-pent-4-enoate (**134**) (4.0 g, 11.0 mmol) in 1,4-dioxane–water (160 mL, 3:1) at r. t. then the reaction was stirred at 25 ^oC for 2 h. Water (300 mL) and CH_2Cl_2 (300 mL) were added and the organic layer was separated. The aqueous layer was re-extracted with CH_2Cl_2 (2 × 100 mL) and the combined organic layers were washed with brine (200 mL), dried and evaporated. The crude product was purified by column chromatography eluting with petroleum/ether (2:1) to give a colourless oil, the title compound (3.5 g, 88%), $[\alpha]_D^{24} = -20.3$ (*c* 0.58, $CHCl_3$) (lit.[186] $[\alpha]_D^{26} = -18.4$ (*c* 0.97, $CHCl_3$)). This showed NMR and IR data matching those in the literature.

Experiment 21: 5-Docosylsulfanyl-1-phenyl-1*H*-tetrazole (133)

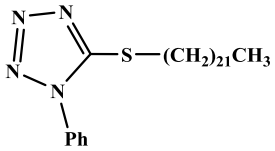

1-Phenyl-1*H*-tetrazole-5-thiol (6.00 g, 33.7 mmol), 1-bromodocosane (**67**) (12.5 g, 32.1 mmol), anhydrous potassium carbonate (9.30 g, 67.4 mmol) and acetone (500 mL) were mixed at room temperature and vigorously stirred for 30 min. then refluxed at 60 ^oC for 3 h. The inorganic salts were filtered off and washed with acetone. The filtrate was evaporated to a small bulk and dissolved in CH_2Cl_2 (200 mL). The solution was washed with water (300 mL) and the aqueous layer was re-extracted with CH_2Cl_2 (2 × 50 mL). The combined organic phases were washed with water (300 mL), dried and evaporated to give a solid residue. The product was re-

crystallised from acetone (90 mL) and methanol (180 mL) to give a white solid of the title compound (14.5 g, 73%). This showed NMR and IR data matching those in the literature.[186]

Experiment 22: 5-(Docosane-1-sulfonyl)-1-phenyl-1*H*-tetrazole (66)

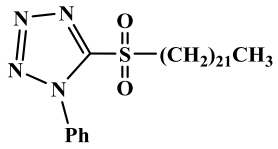

A solution of ammonium molybdate (VI) tetrahydrate (16.5 g, 13.4 mmol) in 35% H_2O_2 (37 mL) was prepared and cooled in an ice bath and added to a stirred solution of 5-docosylsulfanyl-1-phenyl-1*H*-tetrazole (**133**) (14.3 g, 29.4 mmol) in THF (200 mL) and IMS (400 mL) at 12 °C and stirred at 15-20 °C for 2 h. A further solution of ammonium molybdate (VI) tetrahydrate (6.27 g, 5.07 mmol) in 35% H_2O_2 (16 mL) was added and the mixture was stirred at r. t. for 18 h. The mixture was poured into 3 L of water and extracted with CH_2Cl_2 (3 × 200 mL). The combined organic layers were washed with water (2 × 300 mL), dried and the solvent was evaporated. The product was re-crystallised from methanol/acetone to give the title compound (13.0 g, 85%), m.p.: 56–58 °C (lit.[186] m.p.: 56–59 °C). This showed NMR and IR data matching those in the literature.

Experiment 23: Methyl (*R*)-2-((*R*)-3-(benzyloxy)-1-((*tert*-butyldimethylsilyl)oxy)propyl)-hexacosanoate (65)

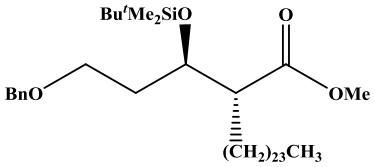

Lithium bis(trimethylsilyl) amide (23.2 mL, 24.5 mmol, 1.06 M) was added to stirred solution of 5-(docosane-1-sulfonyl)-1-phenyl-1*H*-tetrazole (**66**) (8.48 g, 16.4 mmol) and methyl (2*R*,3*R*)-5-benzyloxy-3-(*tert*-butyl-dimethyl-silanyloxy)-2-(2-oxoethyl)pentanoate (**68**) (4.4 g, 11 mmol) in dry THF (150 mL) at -10 °C under nitrogen atmosphere. The mixture was allowed to reach r. t. and stirred for 3 h. Ether (200 mL) and sat. aq. NH_4Cl (200 mL) were added. The organic phase was separated and the aqueous layer was extracted with ether (2 × 50 mL). The combined organic layers were dried, evaporated and the product was purified by column chromatography eluting with petroleum/ether (25:1) to give a colourless oil, methyl (*E/Z*)-(*R*)-2-((*R*)-3-(benzyloxy)-1-((*tert*-butyldimethylsilyl)- oxy)propyl)hexacos-4-enoate (**135**) (6.43 g, 83%) as a mixture of two isomers in ratio 3.7:1. Palladium (10% on carbon, 0.3 g) was added to a stirred solution of the alkene (6.43 g, 9.36 mmol) in ethyl acetate (100 mL) under hydrogen

atmosphere. Hydrogenation was carried out for 1 h., then the mixture was filtered over a bed of celite and the filtrate was evaporated. The product was purified by column chromatography eluting with petroleum/ether (20:1) to give a colourless oil, the title compound (6.3 g, 98%), $[\alpha]_D^{23} = -6.2$ (*c* 0.79, $CHCl_3$) (lit.[186] $[\alpha]_D^{23} = -5.4$ (*c* 1.13, $CHCl_3$)). This showed NMR and IR data matching those in the literature.

Experiment 24: Methyl (*R*)-2-((*R*)-1-((*tert*-butyldimethylsilyl)oxy)-3-hydroxy propyl) hexa- cosanoate (64)

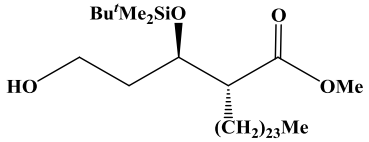

Palladium (10% on carbon, 1.5 g) was added to a stirred solution of methyl ester (**65**) (13.55 g, 19.72 mmol) in ethyl acetate (100 mL) under hydrogen atmosphere. Hydrogenation was carried out for 3 days. The mixture was filtered over a bed of celite and the filtrate was evaporated. The product was purified by column chromatography eluting with petroleum/ether (2:1) to give a white solid, the title compound (11 g, 95%), $[\alpha]_D^{22} = -4.88$ (*c* 1.23, $CHCl_3$) (lit.[387] $[\alpha]_D^{22} = -0.97$ (*c* 0.86, $CHCl_3$). This showed NMR and IR data matching those in the literature.

Experiment 25: Methyl (*R*)-2-((*R*)-1-((*tert*-butyldimethylsilyl)oxy)-3-oxopropyl)-hexa cosanoate (54)

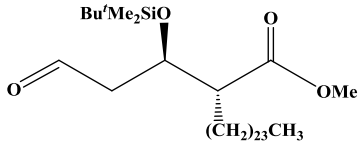

A solution of ester (**64**) (7.20 g, 12.1 mmol) in CH_2Cl_2 (100 mL) was added dropwise to a stirred solution of PCC (6.50 g, 30.2 mmol) in CH_2Cl_2 (300 mL) at r. t. and during the addition a black colour precipitate was appeared. The reaction was stirred for 2 h. at r. t. The reaction was diluted with ether (250 mL), filtered through a bed of silica and the solvent was evaporated. The crude product was purified by column chromatography eluting with petroleum/ether (4:1) to give a colourless oil of the title compound (6.5 g, 90%), $[\alpha]_D^{28} = -5.0$ (*c* 1.2, $CHCl_3$) (lit.[387] $[\alpha]_D^{26} = -4.42$ (*c* 1.29, $CHCl_3$) This showed NMR and IR data matching those in the literature.

Experiment 26: Methyl (*R*)-2-((1*R*,15*R*)-1-((*tert*-butyldimethylsilyl)oxy)-15-((*S*)-2,2-dimethyl-[1,3]-dioxolan-4-yl)hexadecyl)hexacosanoate (52)

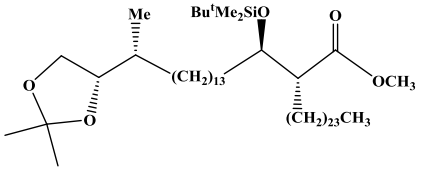

Lithium bis(trimethylsilyl)amide (9.32 mL, 9.88 mmol, 1.06 M) was added to a stirred solution of tetrazole (**53**) (3. 23 g, 6.58 mmol) and ester (**54**) (3.27 g, 5.49 mmol) in dry THF (50 mL) at - 10 ^oC for 2 h. The mixture was quenched with sat. aq. NH_4Cl (100 mL) and the product was extracted with ethyl acetate (3 × 100 mL). The combined organic layers were dried, evaporated and the crude product was purified by column chromatography eluting with petroleum/ether (15:1) to give a colourless oil, methyl (*E*/*Z*)-(*R*)-2-((1*R*,15*R*)-1-((*tert*-butyldimethylsilyl)oxy)-15-((*S*)-2,2-dimethyl-[1,3]-dioxolan-4-yl)hexadec-3-en-1-yl)hexa cosanoate (**136**) (4.5 g, 96%) as a mixture in ratio 2.3:1. Palladium (10% on carbon, 1 g) was added to a stirred solution of the mixture (4.50 g, 5.21 mmol) in ethyl acetate (150 mL) under hydrogen atmosphere. Hydrogenation was carried out for 1.5 h. The mixture was filtered over a bed of celite and the solvent was evaporated. The product was purified by column chromatography eluting with petroleum/ether (15:1) to give a colourless oil, the title compound (4.3 g, 96%), $[\alpha]_D^{22}$ = + 3.6 (*c* 0.94, $CHCl_3$) {Found $[M+Na]^+$: 887.7857, $C_{54}H_{108}NaO_5Si$ requires: 887.7863}. This showed δ_H (400 MHz, $CDCl_3$): 4.0 (1H, dd, *J* 6.3, 7.9 Hz), 3.93-3.90 (1H, m), 3.87 (1H, br. q, *J* 7.0 Hz), 3.66 (3H, s), 3.61 (1H, br. t, *J* 7.9 Hz), 2.53 (1H, ddd, *J* 3.8, 7.3, 11.1 Hz), 1.59-1.52 (4H, m), 1.41 (3H, s), 1.36 (3H, s), 1.35-1.26 (68H, m, v. br.), 1.10-1.07 (1H, m), 0.97 (3H, d, *J* 6.6 Hz), 0.89 (3H, t, *J* 6.9 Hz), 0.87 (9H, s), 0.05 (3H, s), 0.03 (3H, s); δ_C (101 MHz, $CDCl_3$): 175.1, 108.5, 80.4, 73.2, 76.8, 51.6, 51.2, 36.5, 33.7, 32.7, 31.9, 29.9, 29.8, 29.7, 29.66, 29.62, 29.60, 29.58, 29.5, 29.4, 29.3, 27.8, 27.5, 27.0, 26.6, 25.7, 25.5, 23.7, 22.7, 18.0, 15.6, 14.1, -4.4, -4.9; ν_{max}: 2925, 2854, 1741, 1465, 1368, 1253, 1165, 1068 cm^{-1}.

Experiment 27: 5-(2,2-Dimethyl-1,3-dioxolan-4-yl)-3,4-dihydroxydihydrofuran-2(3*H*)-one (74)

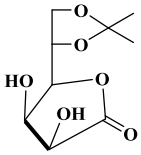

A solution of *L*-gulono-1,4-lactone[436] (**73**) (44.3 g, 0.084 mol) in dimethyl formamide (400 mL) is cooled to 10 ^oC and *p*-toluene sulfonic acid (0.36 g, 2.0 mol) was added portionwise with

stirring. To the resultant solution, isopropenyl methyl ether (23.3 g, 32.2 mol) was added dropwise at 10 ^{o}C. The cooling bath was removed and the mixture was further stirred at r. t. for 24 h. The mixture was then treated with sodium carbonate decahydrate (44 g) and the suspension was vigorously stirred for 2 h. It was then filtered over a celite and the filtrate was evaporated under reduced pressure to give a pink precipitate. The product wash with petroleum/ ethanol (9:1; 100 mL) to yield a white precipitate of the title compound (52 g, 96%), $[\alpha]_D^{20}$ = + 40.2 (c 1.2, CH_3OH, (lit.[381] $[\alpha]_D^{20}$ = + 38.3^{o} (c 0.7, CH_3OH). This showed NMR and IR data matching those in the literature.

Experiment 28: Methyl (*E*)-3-((*R*)-2,2-dimethyl-[1,3]dioxolan-4-yl)acrylate (75)[1]

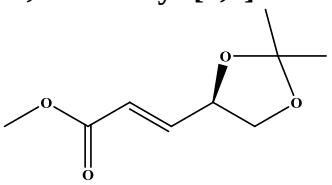

In a three nicked round bottom flask 5-(2,2-dimethyl-[1,3]-dioxolan-4-yl)-3,4-dihydroxyfuran-2-(3*H*)-one (**74**) (10.0 g, 45.8 mmol) was dissolved in water (100 mL), to which a few drops of 2M NaOH solution had been previously added (to ensure pH of mixture was ca. 5.5). The mixture was stirred vigorously at r. t. until the complete dissolution of the lactone had been achieved and then the solution was cooled to ~ + 5 °C. $NaIO_4$ (20.6 g, 96.3 mmol, 2.10 mol. equiv.) was now added in portions over ~30 min, it being ensured throughout this period, that the pH of the reaction mixture was maintained at ca. 5.5 (via the judicious administration of 2M NaOH solution), and that the internal temperature did not exceed + 11 °C. The mixture was stirred vigorously for a period of 2 h. with gradual warming to r. t. whereupon solid NaCl (20 g) was administered in one portion and the resulting mixture stirred for a further period of 10 min. The mixture was filtered through a sinter-funnel into a pre-cooled round-bottomed flask, with careful operation of the vacuum in order to minimise loss of the volatile aldehyde product. The flask and filter-cake were then washed with 50-70 mL of THF. The filtrate was cooled to ~5 °C, and methyl 2-(diisopropoxyphosphoryl)acetate (21.8 g, 91.7 mmol, 2 mole equivalents) was administered in one portion. The pH of the mixture was then adjusted to 12.5-12.7 through the addition of 6 M K_2CO_3 solution (~ 100 mL), and the reaction mixture was then stirred vigorously for a period of 48 h. at r. t. The mixture was extracted with CH_2Cl_2 (6 × 200 mL) and the combined organic extracts were dried over $MgSO_4$ and concentrated *in vacuo* (water-bath temperature maintained at 20 °C) to give a clear pale yellow oil. Material was purified by column chromatography eluting with petroleum/EtOAc (5:1) to afford the title compound as a

clear, colourless oil (5.5 g, 64%), $[\alpha]_D^{22}$ = - 43 (c 1.25, $CHCl_3$), (lit.[381] $[\alpha]_D^{20}$ = - 46 (c 1.00, $CHCl_3$). This showed NMR and IR data matching those in the literature.

Experiment 29: (*S*)-3-((*R*)-2,2-Dimethyl-[1,3]dioxolan-4-yl)butyric acid methyl ester (76)

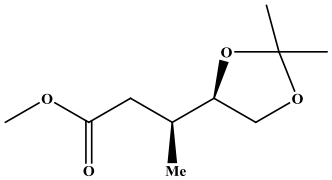

MeLi (46 mL, 65 mmol, 1.4 M in ether) was added to a stirred solution of methyl-(*E*)-3-((*R*)-2,2-dimethyl-[1,3]dioxolan-4-yl)acrylate (**75**) (6.0 g, 32 mmol) in dry ether (180 mL) at -78 ^oC under nitrogen. The mixture was stirred at this temperature for 2.5 h. and then allowed to reach - 60 ^oC followed by the addition of water (10 mL). After 5 min. sat. aq. NH_4Cl (60 mL) was added, whereupon the temperature rose to - 40 ^oC. The cooling bath was removed and the temperature of the mixture brought to 0 ^oC by addition of water (100 mL). The organic layer was saperated and the aqueous layer was extracted with ether (2 × 100 mL). The combined organic phases were washed with brine (2 × 100 mL), dried and evaporated. The crude product was purified by column chromatography eluting with petroleum/ethyl acetate (5:1) to give a colourless oil, the title compound (5.3 g, 81%), $[\alpha]_D^{22}$ = - 7.5 (c 1.2, $CHCl_3$), (lit.[379] $[\alpha]_D^{22}$ = - 8.16 (c 1.47, $CHCl_3$)). This showed NMR and IR data matching those in the literature.

Experiment 30: (*S*)-3-((*R*)-2,2-Dimethyl-[1,3]dioxolan-4-yl)butan-1-ol (77)

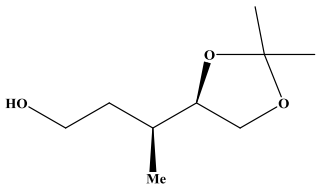

A solution of (*S*)-3-((*R*)-2,2-dimethyl[1,3]dioxolan-4-yl)butyric acid methyl ester (**76**) (3.8 g, 19 mmol) was dissolved in HPLC grade THF (60 mL) and added dropwise over 15 min to a stirred suspension of $LiAlH_4$ (1.1 g, 28 mmol) in THF (200 mL) at r. t. The mixture was refluxed for 1 h, then cooled to 0 ^oC and quenched carefully with freshly prepared sat. aq. sodium sulfate decahydrate until a white precipitate had formed, followed by the addition of $MgSO_4$ (10 g) and then THF (60 mL) was added. The mixture was filtered through a bed of celite and the filtrate was evaporated. The crude product was purified by column chromatography eluting with petroleum/ethyl acetate (5:1) to give a colourless oil of the title

compound (2.7 g, 82%), $[\alpha]_D^{22}$ = - 18.9 (c 1.5, $CHCl_3$) (lit.[379] $[\alpha]_D^{22}$ = - 18.64 (c 1.15, $CHCl_3$)). This showed NMR and IR data matching those in the literature.

Experiment 31: (*S*)-3-((*R*)-2,2-Dimethyl-[1,3]dioxolan-4-yl)butyraldehyde (72)

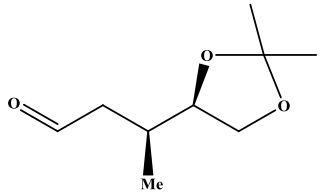

A solution of (*S*)-3-((*R*)-2,2-dimethyl-[1,3]-dioxolan-4-yl)butan-1-ol (**77**) (2.72 g, 15.6 mmol) in CH_2Cl_2 (40 mL) was added dropwise to a stirred suspension of PCC (6.72 g, 31.3 mmol) in CH_2Cl_2 (250 mL) at r. t. then the mixture was stirred vigorously at r. t. for 2 h. Petroleum/ethyl acetate (5:1) (200 mL) was added to the reaction mixture, forming a thick black precipitate. The precipitate was removed by filtration through a bed of silica and evaporated to yield the crude product, which was purified by column chromatography, eluting with petroleum/ethyl acetate (5:1) to give a colourless oil of the title compound (1.60 g, 59.5%), $[\alpha]_D^{22}$ = - 8.4 (c 1.3, $CHCl_3$), (lit.[379] $[\alpha]_D^{22}$ = - 8.6 (c 1.035, $CHCl_3$)). This showed NMR and IR data matching those in the literature.

Experiment 32: 5-Hexadecylsulfanyl-1-phenyl-1*H*-tetrazole (79)

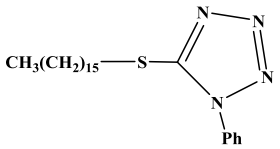

1-Bromohexadecane (**78**) (16.2 g, 53.0 mmol) was added with vigorous stirring to 1-phenyl-1*H*-tetrazole-5-thiol (8.4 g, 47 mmol) and anhydrous potassium carbonate (15.2 g, 110 mmol) in acetone (165 mL). The mixture was refluxed for 2.5 h. The inorganic salts were filtered off and washed with acetone; the filtrate was evaporated to a small bulk and the residue extracted between CH_2Cl_2 (150 mL) and water (300 mL). The aqueous layer was extracted with CH_2Cl_2 (2 × 50 mL). The combined organic phases were washed with water (300 mL), dried and the solvent was evaporated to give a solid. This was dissolved in acetone (50 mL) and diluted with methanol (100 mL) and left at ambient temperature for 1 h and then at 0 ^oC for 1 h The crystals were filtered off and washed with cold acetone/methanol (1:2) to yield a white solid, the title compound (18.0 g, 95%), mp.: 48-50 ^oC. This showed NMR and IR data matching those in the literature.[379]

Experiment 33: 5-(Hexadecane-1-sulfonyl)-1-phenyl-1*H*-tetrazole (80)

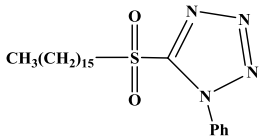

A solution of ammonium molybdate (VI) tetrahydrate (23.7 g, 19.2 mmol) in ice cold H_2O_2 (35% w/w, 35 mL) was added to a stirred solution of 5-hexadecylsulfanyl-1-phenyl-1*H*-tetrazole (**79**) (17.0 g, 42.2 mmol) in THF (180 mL) and IMS (360 mL) at 12 ^oC and stirred at 15- 20 ^oC for 2 h. A further solution of ammonium molybdate (VI) tetrahydrate (9.0 g, 7.3 mmol) in ice cold H_2O_2 (35% w/w, 23 mL) was added and the mixture was stirred at r. t. for 18 h. The mixture was poured into 3L of water and extracted with CH_2Cl_2 (3 × 200 mL). The combined organic phases were washed with water (2 × 300 mL), dried and the solvent was evaporated. The residue was dissolved in methanol (200 mL) and left at ambient temperature for 1 h. and then at 0 ^oC for 1 h to form a white solid; this was filtered and washed with cold methanol to give the title compound (17.0 g, 93%), m.p.: 65-67 ^oC (lit.[379] m.p.: 65-67 ^oC). This showed NMR and IR data matching those in the literature.

Experiment 34: (*R*)-4-((*S*)-Eicosan-2-yl)-2,2-dimethyl-1,3-dioxolane (97)

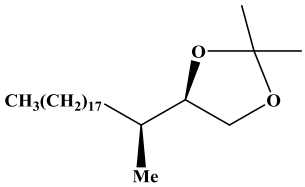

Lithium bis(trimethylsilyl)amide (19.7 mL, 20.9 mmol, 1.06 M) was added to a stirred solution of 5-(xadecane-1-sulfonyl)-1-phenyl-1*H*-tetrazole (**80**) (6.0 g, 14 mmol) and (*S*)-3-((*R*)-2,2-dimethyl-[1,3]-dioxolan-4-yl)butyraldehyde (**72**) (1.6 g, 9.3 mmol) in dry THF (140 mL) at -10 ^oC under nitrogen atmosphere. The solution was allowed to reach r. t. and stirred for 2 h. Petroleum/ether (1:1) (100 mL) and sat. aq. NH_4Cl (100 mL) were added. The organic phase was separated and the aqueous layer was extracted with petroleum/ether (1:1, 2 × 100 mL). The combined organic layers were dried and evaporated. The crude product was purified by column chromatography eluting with petroleum/ethyl acetate (5:1) to give a colourless oil of (*E*/*Z*)-(*S*)-2,2-dimethyl-4-(*R*)-1-methyl-nonadec-3-enyl)-[1,3]dioxolane (**96**) (2.85 g, 81%) as a mixture of two isomers in ratio 2.3:1. Palladium 10% on carbon (0.2 g) was added to a stirred solution of the alkenes (1.72 g, 4.53 mmol) in IMS (25 mL) under hydrogen atmosphere. Hydrogenation was carried out for 2 h. The mixture was filtered on a bed of celite and the filtrate was

evaporated to give a colourless oil of the title compound (1.7 g, 99%).[379] This showed NMR and IR data matching those in the literature.

Experiment 35: 3-Methyl-(2*R*,3*S*)-3-henicosane-1,2-diol (98)

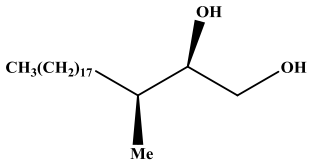

Pyridinium *p*-toluenesulfonate (PTSA) (0.240 g, 9.55 mmol) was added to a stirred solution of (*R*)-4-((*S*)-eicosan-2-yl)-2,2-dimethyl-1,3-dioxolane (**97**) (1.69 g, 4.42 mmol) in THF (10 mL), methanol (10 mL) and water (2 mL) at r. t. The mixture was refluxed for 2 h. Ether (20 mL), petrol (20 mL) and Na_2CO_3 (50 mL) were added. The mixture was separated and the aqueous layer was re-extracted with petroleum/ether (1:1, 50 mL). The combined organic layers were washed with brine (2 × 50 mL) and dried and evaporated. The crude product was purified by column chromatography eluting with petroleum/ethyl acetate (5:1) to give a white solid, the title compound (1.5 g, 99%), m.p.: 68-67 ºC, $[\alpha]_D^{22}$ = -11.5 (c 1.2, $CHCl_3$) (lit.[379] $[\alpha]_D^{22}$ = -12.9 (c 1.34, $CHCl_3$)).This showed NMR and IR data matching those in the literature.

Experiment 36: (*R*)-2-((*S*)-Eicosan-2-yl)oxirane (71)

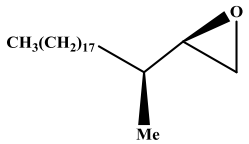

3-Methyl-(2*R*,3*S*)-3-henicosane-1,2-diol (**98**) (1.6 g, 4.7 mmol) was dissolved in CH_2Cl_2 (74 mL) by heating and then cetrimide (0.2 g) was added. NaOH solution (10 mL, 50% in water) and *p*-toluenesulfonylchloride (1.12 g, 5.88 mmol) in CH_2Cl_2 (8 mL) were added to the stirred mixture and the stirring was continued for 45 min. at r. t. Water (80 mL) and CH_2Cl_2 (32 mL) were added. The organic layer was separated and the aqueous layer was re-extracted with CH_2Cl_2 (2 × 50 mL). The combined organic layers were dried and evaporated. The crude product was purified by column chromatography eluting with petroleum/ethyl acetate (10:1) to give a white solid, the title compound (0.9 g, 59%), $[\alpha]_D^{22}$ = - 0.8 (c 1.1, $CHCl_3$), (lit.[379] $[\alpha]_D^{22}$ = - 0.66 (c 1.054, $CHCl_3$). This showed NMR and IR data matching those in the literature.

Experiment 37: 6-Bromohexan-1-ol (100)

$Br(CH_2)_6OH$

1,6-Hexanediol (**99**) (47 g, 0.40 mol) was dissolved in toluene (200 mL) and aqueous HBr (56 mL, 0.5 mol, 48% w.w.) was added. The mixture was refluxed for 18 h, then cooled to r. t. and quenched with water (200 mL), ether (100 mL) and sat. aq. $NaHCO_3$ (150 mL); the organic layer was separated and the aqueous layer was re-extracted with ether (2 × 50 mL). The combined organic layers were dried and the solvent was removed by simple distillation. Column chromatography eluting with petroleum/ether (3:1) and then petroleum/ether (1:1) gave a colourless oil, the title compound (40 g, 55%). This showed NMR and IR data matching those in the literature.[382]

Experiment 38: 2-(6-Bromohexyloxy)tetrahydropyran (101)

$Br(CH_2)_6OTHP$

3,4-Dihydro-2*H*-pyran (31.2 g, 0.370 mol) and pyridinium-*p*-toluene-sulfonate (3 g) were added to a stirred solution of 6-bromo-hexan-1-ol (**100**) (32.0 g, 0.13 mol) in dry CH_2Cl_2 (250 mL) under argon at room temperature. The reaction was stirred at r. t. for 3 h. then quenched with sat. solution of $NaHCO_3$ (100 mL). The organic layer was separated and the aqueous layer was re-extracted with CH_2Cl_2 (2 × 50 mL). The combined organic layers were dried, evaporated and the product was purified by column chromatography eluting with petroleum/ether (9:1) to give a colourless oil, the title compound (40 g, 85%). This showed NMR and IR data matching those in the literature.[186]

Experiment 39: (8*S*)-9-Methyl-1-((tetrahydro-2*H*-pyran-2-yl)oxy)heptacosan-8-ol (103)

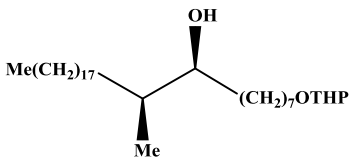

A solution of 2-(6-bromo-hexyloxy)-tetrahydropyran (**101**) (11.3 g, 42.4 mmol) in THF (25 mL) was added drop wise to a suspension of magnesium turnings (2.1 g, 86 mmol) in THF (30 mL) under nitrogen. The mixture was refluxed for 2 h. then cooled to r. t. and added dropwise to a stirred solution of copper iodide (0.75 g, 3.9 mmol) in dry THF (30 mL) at -30 ^oC. After 10 min, a solution of (*R*)-2-((*S*)-icosan-2-yl)oxirane (**71**) (5.5 g, 16.94 mol) in THF (10 mL) was added dropwise. The mixture was stirred for 3 h. at -30 ^oC, allowed to reach -15 ^oC, and then

quenched with sat. aq. NH_4Cl (100 mL) and allowed to reach r. t. The product was extracted with petroleum/ether 1:1 (3 × 100 mL). The combined organic layers were washed with sat. aq. NaCl (250 mL), dried and evaporated. Chromatography on silica eluting with petroleum/ethyl acetate gave the title compound as a colourless oil (6.4 g, 75%). This showed NMR and IR data matching those in the literature.[379]

Experiment 40: 2-((8*S*,9*S*)-8-Methoxy-9-methylheptacosyloxy)-tetrahydropyran (104)

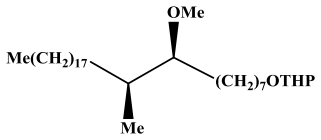

Sodium hydride (5.50 g, 13.7 mmol, 60 % dispersion) was washed with petrol (3 × 30 mL) and then suspended in dry THF (60 mL), cooled to 5 °C and (8*S*)-9-methyl-1-((tetrahydro-2*H*-pyran-2-yl)oxy)heptacosan-8-ol (**103**) (10.0 g, 19.6 mmol) in THF (60 mL) was added over 5 min. After 15 min. methyl iodide (16.19 g, 114.0 mmol) was added. The mixture was stirred for 16 h. at r. t. then quenched with sat. aq. NH_4Cl (50 mL) followed by ether (100 mL), then the organic layer was separated and the aqueous layer was re-extracted with petroleum/ether 1:1 (2 × 50 mL). The combined organic layers were washed with brine (2 × 80 mL), dried and evaporated. Chromatography on silica eluting with petroleum/ether (10:2) gave the title compound as a pale yellow oil (10.3 g, 100%). This showed NMR and IR data matching those in the literature.[379]

Experiment 41: (8*S*,9*S*)-8-Methoxy-9-methylheptacosan-1-ol (105)

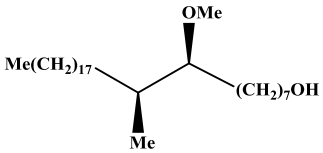

p-Toluenesulfonic acid monohydrate (1.0 g, 5.3 mmol) was added to a stirred solution of 2-((8*S*,9*S*)-8-methoxy-9-methylheptacosyloxy)tetrahydropyran (**104**) (10.0 g, 19.1 mmol) in THF (40 mL), methanol (70 mL) and water (1 mL) at r. t. The mixture was refluxed for 30 min, evaporated to approximately half its volume and diluted with sat. aq. $NaHCO_3$ (50 mL) and petroleum/ether (1:1, 150 mL) was added. The organic layer was separated and the aqueous layer was extracted with petroleum/ether (2 × 250 mL). The combined organic layers were washed with sat. aq. NaCl (100 mL), dried and evaporated to give a residue, which was purified by column chromatography on silica eluting with petroleum/ether (5:2) to give the title

compound (8.0 g, 95%), $[\alpha]_D^{22}$ = - 12.1 (c 1.35, $CHCl_3$), (lit.[379]. $[\alpha]_D^{22}$ = - 10.7 (c 1.20, $CHCl_3$)). This showed NMR and IR data matching those in the literature.

Experiment 42: (8*S*,9*S*)-8-Methoxy-9-methylheptacosanal (106)

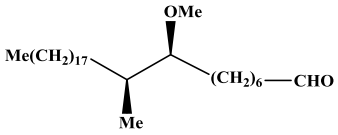

A solution of (8*S*,9*S*)-8-methoxy-9-methylheptacosan-1-ol (**105**) (7.9 g, 17.92 mmol) in CH_2Cl_2 (50 mL) was added dropwise to a stirred solution of PCC (7.2 g, 33.4 mmol) in CH_2Cl_2 (250 mL). The mixture was stirred at r. t. for 45 min. then petroleum/ethyl acetate (5:1) (100 mL) was added, forming a thick black precipitate. This was removed by filtration through a bed of silica and the filtrate was evaporated to yield the crude product, which was purified by column chromatography on silica, eluting with petroleum/ethyl acetate (5:1) to give a colourless oil, the title compound (6.5 g, 83%), $[\alpha]_D^{22}$ = - 10.7 (c 1.5, $CHCl_3$), (lit.[379] $[\alpha]_D^{22}$ = - 11.3 (c 1.5, $CHCl_3$)). This showed NMR and IR data matching those in the literature.

Experiment 43: 7-Bromoheptyl pivalate (109)

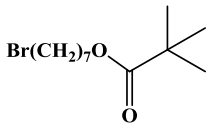

A solution of trimethylacetyl chloride (15.0 g, 12.4 mmol) in CH_2Cl_2 (50 mL) was added to a stirred solution of 7-bromoheptan-1-ol (**108**) (23.1 g, 11.8 mmol), CH_2Cl_2 (200 mL), triethylamine (35.9 g 35.5 mmol) and 4-dimethylaminopyridine (0.41g, 3.3 mmol) over a period of 15 min. at 5 ^oC and stirred at r. t. for 18 h. Dilute HCl (150 mL) was added and the organic layer was separated. The aqueous layer was extracted with CH_2Cl_2 (2 × 200 mL). The combined organic layers were washed with brine (2 × 200 mL), dried and evaporated. The product was purified by column chromatography on silica eluting with petroleum/ether 1:1 to give a colourless oil, the title compound (33.0 g, 98%). This showed NMR and IR data matching those in the literature. [437]

Experiment 44: 7-((1-Phenyl-1*H*-tetrazol-5-yl) thio)heptyl pivalate (110)

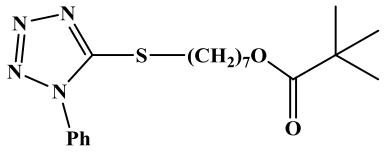

1-Phenyl-1*H*-tetrazole-5-thiol (6.20 g, 34.8 mmol), 7-bromoheptyl pivalate (**109**) (10.0 g, 35.8 mmol), anhydrous K_2CO_3 (2.40 g, 17.2 mmol) and acetone (150 mL) were mixed. The mixture was vigorously stirred for 18 h. at r. t. Water (1 L) was added and the organic layer was separated. The aqueous layer was extracted with CH_2Cl_2 (1 × 150 mL, 2 × 25 mL). The combined organic phases were washed with brine (2 × 200 mL), dried, evaporated and the crude product was purified by column chromatography eluting with petroleum/ether (7:2.5 and then 1:1) to give a colourless oil, the title compound (12.0 g, 90%). This showed NMR and IR data matching those in the literature.[489]

Experiment 45: 7-((1-Phenyl-1*H*-tetrazol-5-yl)sulfonyl)heptyl pivalate (111)

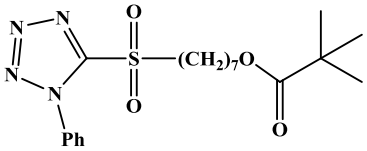

A solution of ammonium molybdate (VI) tetrahydrate (24.89 g, 20.14 mmol) in 35% H_2O_2 (53 mL) was cooled in an ice bath and added to a stirred solution of the 7-((1-phenyl-1*H*-tetrazol-5-yl)thio)heptyl pivalate (**110**) (5.00 g, 13.3 mmol) in THF (200 mL) and IMS (350 mL) at 10 ^oC and stirred at r. t. for 2 h. A further solution of ammonium molybdate (VI) tetrahydrate (17.4 g, 14.1 mmol) in 35% H_2O_2 (20 mL) was added and the mixture was stirred at r. t. for 18 h. The mixture was poured into water (1.2 L) and the organic layer was separated. Then the aqueous layer was extracted with CH_2Cl_2 (1 × 200 mL, 3 × 30 mL). The combined organic layers were washed with water (2 × 500 mL), dried, evaporated and the crude product was purified by column chromatography eluting with petroleum/ether (3:1 and then 1:1) to give the title compound as a yellow oil (4.5 g, 83%). This showed NMR and IR data matching those in the literature.[489]

Experiment 46: 6-Bromohexanal (107)

$Br(CH_2)_5CHO$

A solution of 6-bromohexan-1-ol (**100**) (10.0 g, 55.25 mmol) in CH_2Cl_2 (50 mL) was added dropwise to a stirred suspension of PCC (23.74 g, 110.5 mmol) in CH_2Cl_2 (300 mL). The mixture was stirred vigorously at r. t. for 2 h. Petroleum/ethyl acetate (5:1) (200 mL) was added

to the reaction mixture, forming a thick black precipitate. The precipitate was removed by filtration through a bed of silica and the solvent was evaporated to yield the crude product, which was purified by column chromatography on silica, eluting with petroleum/ethyl acetate (5:1) to give a colourless oil of the title compound (8.7 g, 87%). This showed δ_H (500 MHz, $CDCl_3$): 9.73 (1H, br. t, *J* 1.9 Hz), 3.38 (2H, t, *J* 6.6 Hz), 2.40 (2H, dq, *J* 1.9 Hz), 1.82 (2H, pent, *J* 6.95 Hz), 1.63–1.57 (2H, m), 1.35–1.26 (2H, m); δ_C (126 MHz, $CDCl_3$): 202.8, 43.8, 33.9, 29.1, 24.5, 21.9, 14.1; ν_{max}: 2937, 2858, 2719, 1727, 1463, 1249 cm^{-1}.

Experiment 47: 2,2-Dimethyl-propionic acid 13-bromo-tridecyl ester (113)

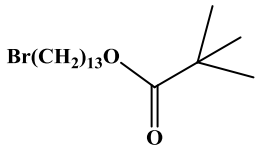

Lithium bis (trimethylsilyl) amide (87.5 mL, 92.7 mmol, 1.06 M) was added to the stirred solution of 6-bromohexanal (**107**) (7.90 g, 44.1 mmol) and 7-((1-phenyl-1*H*-tetrazol-5-yl)sulfonyl)heptyl pivalate (**111**) (25.2 g, 61.8 mmol) in dry THF (200 mL) at - 10 ^oC under nitrogen atmosphere. The reaction mixture was allowed to reach r. t. and stirred for 2 h. then quenched with sat. aq. NH_4Cl (100 mL) and ether (50 mL). The organic layer was separated and the aqueous layer was extracted with petroleum/ether 1:1 (2 × 100 mL). The combined organic layers were dried, evaporated and the crude product was purified by column chromatography eluting with petroleum/ether (50:1) to give a colourless oil of (*E*/Z)-13-bromo-tridec-7-en-1-yl pivalate (**112**) (9.3 g, 58%) as a mixture of two isomers in ratio 2.4:1. Palladium 10% on carbon (0.2 g) was added to a stirred solution of 13-bromotridec-7-en-1-yl pivalate (9.30 g, 25.8 mmol) in THF (150 mL) and IMS (50 mL) under hydrogen atmosphere. Hydrogenation was carried out 1 h. The solution was filtered over a bed of celite, evaporated and the crude product was purified by column chromatography eluting with petroleum/ether (15:1) to give a colourless oil, compound (**113**) (8.2 g, 88%) {Found $[M+Na]^+$: 385.1695, $C_{18}H_{35}BrNaO_2$ requires: 385.1713}. This showed δ_H (500 MHz, $CDCl_3$): 4.05 (2H, t, *J* 6.6 Hz), 3.42 (2H, t, *J* 6.9 Hz), 1.86 (2H, quintet, *J* 6.9 Hz), 1.62 (2H, quintet, *J* 6.6 Hz), 1.46–1.27 (18 H, m), 1.20 (9H, s); δ_C (126 MHz, $CDCl_3$): 178.7, 64.5, 38.7, 34.0, 32.8, 29.6, 29.5, 29.49, 29.4, 29.2, 28.8, 28.6, 28.2, 27.2, 25.9; ν_{max}: 2927, 2855, 1730, 1480, 1462, 1285, 1157 cm^{-1}.

Experiment 48: 2,2-Dimethyl-propionic acid 13-(1-phenyl-1*H*-tetrazol-5-ylsulfanyl)-tridecyl ester (114)

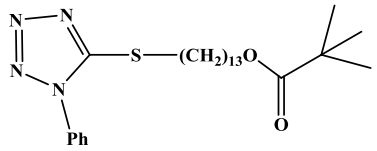

2,2-Dimethylpropionic acid 13-bromo-tridecyl ester (**113**) (9.1 g, 25 mmol), was added to a stirred solution of 1-phenyl-1*H*-tetrazole-5-thiol (5.3 g, 30 mmol) and anhydrous K_2CO_3 (4.2 g, 30 mmol) in acetone (100 mL) at r. t. Then the mixture was vigorously stirred for 18 h. at r. t. Water (250 mL) was added, the organic layer was separated and the aqueous layer was extracted with CH_2Cl_2 (2 × 50 mL). The combined organic phases were washed with brine (2 × 100 mL), dried, evaporated and the crude product was purified by column chromatography eluting with petroleum/ether (3:2) to give a colourless oil, the title compound (7.9 g, 69%) {Found $[M+Na]^+$: 483.2768, $C_{25}H_{40}N_4NaO_2S$ requires: 483.2770}. This showed δ_H (500 MHz, $CDCl_3$): 7.6–7.52 (5H, m), 4.04 (2H, t, *J* 6.6 Hz), 3.39 (2H, t, *J* 7.4 Hz), 1.82 (2H, quintet, *J* 7.4 Hz), 1.62 (2H, quintet, *J* 6.6 Hz), 1.49–1.26 (18H, m), 1.19 (9H, s); δ_C (126 MHz, $CDCl_3$): 178.6, 154.5, 133.7, 130.0, 129.7, 123.8, 64.4, 38.7, 33.3, 29.5, 29.48, 29.4, 29.3, 29.2, 29.1, 29.0, 28.6, 28.5, 27.2, 25.9; ν_{max}: 2927, 2854, 1727, 1598, 1501, 1480, 1462, 1388, 1285, 1159 cm^{-1}.

Experiment 49: 2,2-Dimethyl-propionic acid 13-(1-phenyl-1*H*-tetrazole-5-sulfonyl)-tridecyl ester (115)

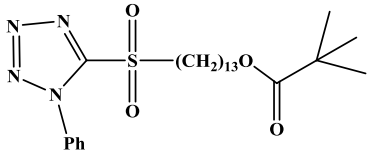

A solution of ammonium molybdate (VI) tetrahydrate (17.5 g, 14.2 mmol) in 35% H_2O_2 (40 mL), prepared and cooled in an ice bath, was added to stirred solution of 2,2-dimethyl-propionic acid 13-(1-phenyl-1*H*-tetrazol-5-ylsulfanyl)-tridecyl ester (**114**) (7.60 g, 16.5 mmol) in THF (190 mL) and IMS (200 mL) at 10 ºC and stirred at r. t. for 2 h. A further solution of ammonium molybdate (VI) tetrahydrate (9.0 g, 7.3 mmol) in 35% H_2O_2 (20 mL) was added and the mixture was stirred at r. t. for 18 h. The mixture was poured into water (500 mL) and the organic layer was separated. The aqueous layer was extracted with CH_2Cl_2 (3 × 50 mL). The combined organic phases were washed with water (150 mL), dried and evaporated. The product was purified by column chromatography eluting with petroleum/ether (1:1) to give a white solid, compound (**115**) (7.8 g, 96%), m.p.: 46–47 ºC {Found $[M+Na]^+$: 515.2668, $C_{25}H_{40}NaN_4O_4S$ requires: 515.2668}. This showed δ_H (500 MHz, $CDCl_3$): 7.71–7.68 (2H, m), 7.64–7.27 (3H,

m), 4.04 (2H, t, *J* 6.6 Hz), 3.74–3.71 (2H, m), 1.98-1.92 (2H, m), 1.62 (2H, quintet, *J* 6.6 Hz), 1.52–1.26 (18H, m), 1.19 (9H, m); δ_C (126 MHz, $CDCl_3$): 178.6, 153.5, 133.0, 131.4, 129.7, 125.0, 64.4, 56.0, 38.7, 29.4, 29.37, 29.2, 29.1, 28.8, 28.6, 28.1, 27.2, 25.8, 21.9; ν_{max}: 3072, 2917, 2853, 1727, 1593, 1476, 1420, 1358, 1285, 1150 cm^{-1}.

Experiment 50: (21*S*,22*S*)-21-Methoxy-22-methyltetracontyl pivalate (117)

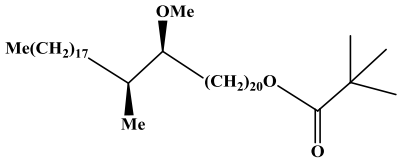

Lithium bis (trimethylsilyl)amide (1.10 mL, 1.20 mmol, 1.06 M) was added dropwise to a stirred solution of (8*S*,9*S*)-8-methoxy-9-methylheptacosanal (**106**) (0.34 g, 0.77 mmol) and 2,2-dimethyl-propionic acid 13-(1-phenyl-1*H*-tetrazole-5-sulfonyl)-tridecyl ester (**115**) (0.46 g, 0.93 mmol) in dry THF (50 mL) under nitrogen atmosphere at - 15 ^oC. The reaction mixture was allowed to reach r. t. and stirred for 2 h. Petroleum/ether (1:1) (50 mL) and sat. aq. NH_4Cl (50 mL) were added. The organic phase was separated and the aqueous layer was extracted with petroleum/ether (1:1, 2 × 50 mL). The combined organic layers were dried and evaporated. The crude product was purified by column chromatography eluting with petroleum/ethyl acetate (20:1) to give a colourless oil of ***(****E/Z)*-(24*S*,25*S*)-4-hydroxy-24-methoxy-2,2,25-trimethyltritetraconta-5,7,9,11,13,16-hexaen-3-one (**116**) (0.46 g, 85%) in ratio (2.6:1, *E/Z*). Palladium 10% on carbon (0.5 g) was added to a stirred solution of the alkene (0.46 g, 0.65 mmol) in ethyl acetate (50 mL) under hydrogen atmosphere. Hydrogenation was carried out for 1 h, then the mixture was quenched with water (0.2 mL), filtered over a bed of celite and the solvent was evaporated. The product was purified by column chromatography eluting with petroleum/ethyl acetate (20:1) to give a colourless oil, the title compound (0.46 g, 100%), $[\alpha]_D^{22}$= - 6.5 (c 1.5, $CHCl_3$) {Found $[M+Na]^+$: 729.7102, $C_{47}H_{94}NaO_3$ requires: 729.7100}.This showed δ_H: (500 MHz, $CDCl_3$): 4.05 (2H, t, *J* 6.7 Hz), 3.34 (3H, s), 2.97–2.94 (1H, m), 1.62 (2H, pent, *J* 6.7 Hz), 1.46–1.22 (70H, m), 1.20 (9H, s), 1.12–1.06 (1H, m), 0.88 (3H, t, *J* 6.7 Hz), 0.85 (3H, d, *J* 7.0 Hz); δ_C (126 MHz, CDCl3): 178.5, 85.4, 64.4, 57.7, 38.7, 35.3, 32.4, 31.9, 30.8, 30.5, 30.0, 29.9, 29.7, 29.69, 29.66, 29.6, 29.5, 29.4, 29.2, 28.6, 27.6, 27.2, 26.2, 25.9, 22.7, 14.8, 14.1; ν_{max}: 2923, 1731,1154 cm^{-1}.

Experiment 51: (21*S*,22*S*)-21-Methoxy-22-methyltetracontan-1-ol (118)

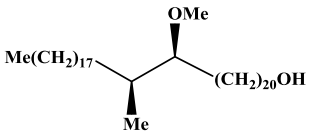

$LiAlH_4$ (0.20 g, 1.6 mmol) was added to a stirred solution of (21*S*,22*S*)-21-methoxy-22-methyltetracontyl pivalate (**117**) (0.75 g, 1.1 mmol) in HPLC grad THF (50 mL) at 0 °C under nitrogen atmosphere. The mixture was allow to reach r. t. and refluxed for 1 h, then cooled to ~ -10 °C, quenched with sat. solution of sodium sulphate decahydrate (10 mL) until a white precipitate had formed, then diluted with THF (20 mL). The mixture was stirred at r. t. for 30 min. filtered through a bed of silica and the solvent was evaporated. The product was purified by column chromatography eluting with petroleum/ethyl acetate (10:1) then (5:1) to give a white solid, the title compound (0.65 g, 98%), mp.: 46-48 °C, $[\alpha]_D^{22}$= –8.5 (c 1.2, $CHCl_3$) {Found $[M–H]^+$: 621.6545, $C_{42}H_{85}O_2$ requires: 621.6549}. This showed δ_H: (500 MHz, $CDCl_3$): 3.66 (2H, t, *J* 6.6 Hz), 3.36 (3H, s), 2.99–2.96 (1H, m), 1.67–1.64 (1H, m), 1.59 (2H, pent, *J* 6.6 Hz), 1.49 (1H, br. s), 1.48–1.22 (69H, m), 1.14–1.07 (1H, m), 0.90 (3H, t, *J* 7.0 Hz), 0.87 (3H, d, *J* 6.7 Hz); δ_C (126 MHz, $CDCl_3$): 85.5, 63.1, 57.7, 35.3, 32.8, 32.4, 31.9, 30.5, 30.0, 29.9, 29.7, 29.68, 29.63, 29.5, 29.4, 27.6, 26.2, 25.7, 22.7, 14.9, 14.1; ν_{max}: 3373, 2921, 1098,1076 cm^{-1}.

Experiment 52: 5-(((21*S*,22*S*)-21-Methoxy-22-methyltetracontyl)thio)-1-phenyl-1*H*-tetrazole (119)

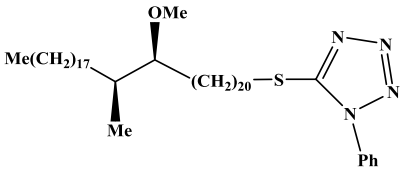

Diethyl azodicarboxylate (0.236 g, 1.356 mmol) in dry THF (2 mL) was added to a stirred solution of 1-phenyl-1*H*-tetrazole-5-thiol (0.242 g, 1.356 mmol), triphenylphosphine (0.356 g, 1.356 mmol) and (21*S*,22*S*)-21-methoxy-22-methyltetracontan-1-ol (**118**) (0.65 g, 1.04 mmol) in dry THF (50 mL) at 0 °C. The mixture was vigorously stirred and refluxed for 2.5 h Then 10:1 petroleum/ethyl acetate (100 mL) was added to the solution mixture. The mixture was filtered through a bed of celite, dried and evaporated. The product was purified by column chromatography eluting with petroleum/ether (10:1) to give compound **(119)** (0.8 g, 98%) as a colourless oil, $[\alpha]_D^{22}$= – 5.9 (c, 1.2, $CHCl_3$). {MALDI, Found $[M+Na]^+$: 805.3; $C_{49}H_{90}NaN_4OS$ requires: 805.6} This showed δ_H: (500 MHz, $CDCl_3$): 7.65–7.61 (5H, m), 3.66 (2H, t, *J* 6.3 Hz), 3.36 (3H, s), 2.98–2.96 (1H, m), 1.97 (2H, br. pent, *J* 7.5 Hz), 1.68–1.61 (2H, m), 1.52 (2H, br.

pent, *J* 7.5 Hz), 1.45–1.22 (66H, m), 1.15–1.07 (1H, m), 0.90 (3H, t, *J* 6.6 Hz), 0.87 (3H, d, *J* 6.9 Hz); δ_C: (126 MHz, $CDCl_3$): 153.5, 133.1, 131.5, 129.7, 125.1, 85.5, 57.7, 56.0, 35.3, 32.4, 31.9, 30.5, 30.0, 29.97, 29.7, 29.65, 29.6, 29.5, 29.4, 29.2, 28.9, 28.2, 27.6, 26.2, 22.7, 21.9, 14.9, 14.1; ν_{max}: 3072, 2917, 2853, 1343, 1096 cm^{-1}.

Experiment 53: 5-(((21*S*,22*S*)-21-Methoxy-22-methyltetracontyl)sulfonyl)-1-phenyl-1*H*-tetrazole (50)

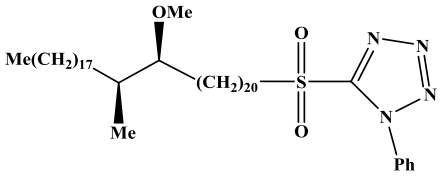

To a stirred solution of 5-(((21*S*,22*S*)-21-methoxy-22-methyltetracontyl)thio)-1-phenyl-1*H*-tetrazole (**119**) (0.80 g, 1.0 mmol) and $NaHCO_3$ (0.34, 4.09 mmol) in CH_2Cl_2 (50 mL) was added m-chloro-perbenzoic acid (0.41 g, 2.35 mmol) at r. t. and stirred for 24 h. The mixture was quenched with 10% NaOH solution (25 ml) and vigorously stirred for 2 h. The organic layer was separated and the aqueous layer was extracted with CH_2Cl_2 (2 × 50 mL). The combined organic layers were washed with water, dried and evaporated. Chromatography on silica eluting with petroleum/ether (10:1) gave a white solid, the title compound (0.81 g, 97%), mp.: 44–46 ^oC , $[\alpha]_D^{22}$ = – 6.2 (c 1.39, $CHCl_3$)} {MALDI Found $(M+Na)^+$: 837.3, $C_{49}H_{90}N_4NaO_3S$ requires: 837.6}. This showed δ_H (500 MHz, CDCl3): 7.73–7.71 (2H, m), 7.65–7.61 (3H, m), 3.75 (2H, distorted t, *J* 7.9 Hz), 3.36 (3H, s), 2.98–2.96 (1H, m), 1.97 (2H, br. pent, *J* 7.5 Hz), 1.68–1.61 (2H, m), 1.52 (2H, br. pent, *J* 7.5 Hz), 1.45–1.22 (66H, m), 1.15–1.07 (1H, m), 0.90 (3H, t, *J* 6.6 Hz), 0.87 (3H, d, *J* 6.9 Hz); δ_C (126 MHz, CDCl3): 153.5, 133.1, 131.5, 129.7, 125.1, 85.5, 57.7, 56.0, 35.3, 32.4, 31.9, 30.5, 30.0, 29.9, 29.7, 29.65, 29.6, 29.5, 29.4, 29.2, 28.9, 28.2, 27.6, 26.2, 22.7, 21.9, 14.9, 14.1; ν_{max}: 2924, 2849, 1343, 1157, 1096 cm^{-1}.

Experiment 54: Methyl (*R*)-2-((1*R*,15*R*)-1-((*tert*-butyldimethylsilyl)oxy)-15-methyl-16-oxohexadecyl)hexacosanoate (51)

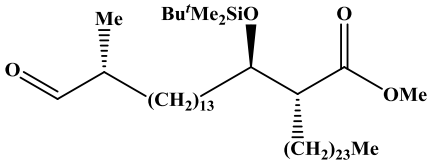

Periodic acid (0.40 g, 1.7 mmol) was added to a stirred solution of methyl-(*R*)-2-((1*R*,15*R*)-1-((*tert*-butyldimethylsilyl)oxy)-15-((*S*)-2,2-dimethyl-1,3-dioxolan-4-yl)hexadecyl) hexa cosanoate (**52**) (0.50 g, 0.58 mmol) in dry ether (140 mL) at r. t. under nitrogen atmosphere and

stirred for 18 h. The mixture was filtered through a bed of celite and washed with ether (20 mL), dried and evaporated. The product was purified by column chromatography eluting with petroleum/ethyl acetate (5:1) to give a white solid, the title compound (0.40 g, 87%) {Found [M-^{t}Bu]: 735.6679; $C_{46}H_{191}O_4Si$ requires: 735.6687}. This showed δ_H (400 MHz, CDCl3): 9.77 (1H, d, *J* 2.0 Hz), 3.93–3.89 (1H, m), 3.66 (3H, s), 2.53 (1H, ddd, *J* 3.8, 7.0, 11.0 Hz), 2.42 (1H, br. dq, *J* 2.0, 7.0 Hz), 1.75-1.68 (1H, m), 1.55–1.22 (71H, m), 1.09 (3H, d, *J* 7.0 Hz), 0.88 (3H, t, *J* 7 Hz), 0.87 (9H, s), 0.05 (3H, s), 0.027 (3H, s); δ_C (126 MHz, CDCl3): 202.8, 175.1, 73.2, 51.6, 51.2, 43.9, 33.7, 31.9, 29.8, 29.7, 29.65, 29.6, 29.5, 29.4, 29.35, 29.3, 29.2, 27.9, 27.5, 25.8, 23.8, 22.7, 22.1, 18.0,14.1, - 4.4, - 4.9; ν_{max}: 3855, 3821, 3648, 3432, 2924, 2853, 1738, 1462 cm^{-1}.

Experiment 55: Methyl (2*R*,3*R*,17*R*,39*S*,40*S*,*E*)-3-((*tert*-butyldimethylsilyl)oxy)-39-methoxy-17,40-dimethyl-2-tetracosyloctapentacont-18-enoate (49)

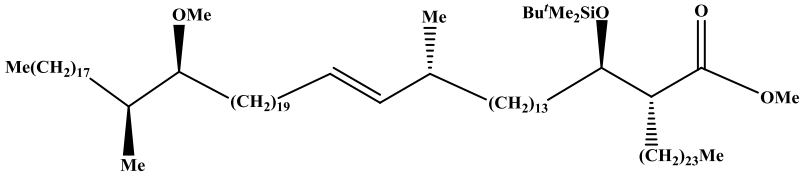

Methyl (*R*)-2-((1*R*,15*R*)-1-((*tert*-butyldimethylsilyl)oxy)-15-methyl-16-oxohexadecyl) hexa cosa-noate (**51**) (0.30 g, 0.38 mmol) in dry 1,2-dimethoxyethane (60 mL) was added to stirred solution of 5-(((21*S*,22*S*)-21-methoxy-22-methyltetracontyl)sulfonyl)-1-phenyl-1*H*-tetrazole (**50**) (0.339 g, 0.416 mmol) in dry 1,2-dimethoxyethane (25 mL) under nitrogen atmosphere at r. t. The mixture was cooled to -20 ^{o}C and potassium bis (trimethylsilyl)amide (1.1 mL, 0.54 mmol, 0.5 M in toluene) was added and the mixture was allowed to reach r. t. and then stirred for 1.5 h. Sat. aq. NH_4Cl (30 mL) and 1:1 petroleum/ether (55 mL) were added. The organic layer was separated and the aqueous layer was re-extracted with 1:1 petroleum/ether (2 × 45 mL). The combined organic layers were dried and evaporated. The compound was purified via column chromatography eluting with petroleum/ether (18:1) to give a semi solid, the title compound (0.18 g, 37%) {MALDI Found [M+Na]$^+$: 1404.3; $C_{92}H_{184}NaO_4Si$ requires: 1404.3}. This showed δ_H (500 MHz, $CDCl_3$): 5.33 (1H, dt, *J* 6.36, 15.0 Hz), 5.24 (1H, dd, *J* 7.4, 15.0 Hz), 3.9 (1H, td, *J* 4.3, 6.8 Hz), 3.65 (3H, s), 3.35 (3H, s), 2.98-2.94 (1H, m), 2.53 (1H, ddd, *J* 3.71, 7.0, 10.8 Hz), 2.05-2.0 (1H, m), 1.97 (2H, q, *J* 6.9 Hz), 1.68–1.26 (142H, m, v.br.), 1.08–1.01 (1H, m), 0.94 (3H, d, *J* 7.0 Hz), 0.90 (6H, t, *J* 6.7 Hz), 0.87 (9H, s), 0.85 (3H, d, *J* 7.0 Hz), 0.05 (3H, s), 0.03 (3H, s); δ_C: (101 MHz, $CDCl_3$): 175.2, 136.5, 128.4, 85.4, 73.2, 57.7, 51.6, 51.2, 37.3, 36.7, 35.3, 33.7, 32.6, 32.4, 31.9, 30.5, 30.0, 29.9, 29.8, 29.81, 29.7, 29.66, 29.6,

29.5, 29.45, 29.4, 29.1, 27.8, 27.6, 27.5, 27.4, 26.2, 25.8, 23.7, 22.7, 20.9, 18.0, 14.9, 14.1, -4.4, -4.9; ν_{max} : 3584, 2924, 2854, 1741, 1465, 1377, 1254, 1099 cm^{-1}.

Experiment 56: Methyl (2*R*,3*R*,17*R*,39*S*,40*S*,*E*)-3-hydroxy-39-methoxy-17,40-dimethyl-2-tetra-cosyloctapentacont-18-enoate (142)

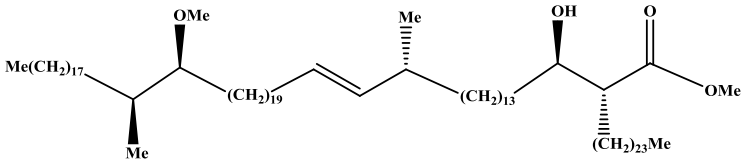

Pyridine (0.07 mL) and hydrogen fluoride-pyridine complex (0.5 mL) were added to the stirred solution of methyl (2*R*,3*R*,17*R*,39*S*,40*S*,*E*)-3-((*ter*t-butyldimethylsilyl)oxy)-39-methoxy-17,40-dimethyl-2-tetracosyloctapentacont-18-enoate (**49**) (0.70 g, 0.05 mmol) in dry THF (10 mL) in a dry polyethylene vial under nitrogen at r. t. The mixture was stirred for 17 h. at 42 °C, then neutralized by poured it in to a sat. aq. $NaHCO_3$ until no more carbon dioxide was liberated. The aqueous layer was extracted with petroleum/ethyl acetate (1:5, 3 × 50 mL). The combined organic layers were washed with brine, dried and evaporated. The product was purified by column chromatography eluting with petroleum/ethyl acetate (20:1) to give a white solid, the title compound (0.62 g, 96%), m.p.: 34-36 ^oC, $[\alpha]_D^{22}$= – 3.3 (c 0.48, $CHCl_3$) {MALDI Found $[M+Na]^+$: 1290.3; $C_{86}H_{170}NaO_4$ requires: 1290.2}. This showed δ_H (500 MHz, CDCl3): 5.33 (1H, dt, *J* 6.4, 15.0 Hz), 5.24 (1H, dd, *J* 7.5, 15.0 Hz), 3.72 (3H, s), 3.68-3.64 (1H, m), 3.35 (3H, s), 2.98-2.93 (1H, m), 2.46-2.41 (1H, td, *J* 5.4, 9.1 Hz), 2.05-2.0 (1H, m), 1.97 (2H, br. q, *J* 7 Hz), 1.76-1.68 (1H, m), 1.65-1.5 (12H, m), 1.48-1.2 (130H, m), 1.15-1.05 (1H, m), 0.95 (3H, d, *J* 6.7 Hz), 0.89 (6H, t, *J* 7.1 Hz), 0.86 (3H, d, *J* 6.8 Hz); δ_C (101 MHz, $CDCl_3$): 176.2, 136.5, 128.4, 85.5, 72.3, 57.7, 51.5, 51.0, 37.2, 36.7, 35.7, 32.6, 32.4, 31.9, 30.5, 30.0, 29.9, 29.8, 29.7, 29.6, 29.57, 29.5, 29.4, 29.36, 29.1, 27.6, 27.4, 27.36, 26.2, 25.7, 22.7, 20.9, 14.9, 14.1; ν_{max} 3431, 2917, 2850, 1739, 1638, 1466, 1099 cm^{-1}.

Experiment 57: (2*R*,3*R*,17*R*,39*S*,40*S*,*E*)-3-Hydroxy-39-methoxy-17,40-dimethyl-2-tetracosyl- octapentacont-18-enoic acid (43)

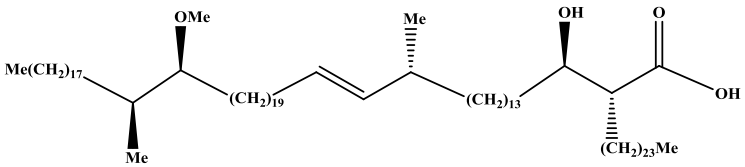

Lithium hydroxide monohydrate (0.31 g, 7.3 mmol) was added to a stirred solution of methyl (2*R*,3*R*,17*R*,39*S*,40*S*,*E*)-3-hydroxy-39-methoxy-17,40-dimethyl-2-tetracosyloctapentacont-18-enoate (**142**) (0.62 g, 0.49 mmol) in THF (15 mL), methanol (1.3 mL) and water (1.5 mL) at r.

t. The mixture was stirred at 43 °C for 18 h. The mixture was cooled to r. t. and acidified with HCl (5%, 2 mL) and the aqueous layer was extracted with warm petroleum/ether (1:1, 3 × 50 mL). The combined organic extracted were dried and evaporated and then purified via column chromatography eluting with warm petroleum/ethyl acetate (7:2) to give a white solid, the title compound (0.50, 82%), m.p.: 43-45 °C, $[\alpha]_D^{22} = -1.6$ (c 0.99, $CHCl_3$) {Found $[M+Na]^+$: 1276.2861; $C_{85}H_{168}NaO_4$ requires: 1276.2835}. This showed δ_H (500 MHz, CDCl3): 5.33 (1H, dt, *J* 6.4, 15.2 Hz), 5.24 (1H, dd, *J* 7.4, 15.2 Hz), 3.73-3.70 (1H, m), 3.35 (3H, s), 2.98-2.96 (1H, m), 2.49-2.44 (1H, m), 2.0-1.97 (1H, m), 1.96 (2H, br. q, *J* 6.7 Hz), 1.77-1.70 (1H, m), 1.67-1.57 (2H, m), 1.55-1.15 (141 H, m), 1.14-1.05 (1H, m), 0.94 (3H, d, *J* 6.7 Hz), 0.89 (6H, t, *J* 6.5 Hz), 0.85 (3H, d, *J* 6.9 Hz); δ_C (101 MHz, $CDCl_3$): 179.5, 136.5, 128.4, 85.6, 72.1, 57.7, 50.7, 37.3, 36.7, 35.6, 35.3, 32.6, 32.4, 31.9, 30.5, 29.9, 29.7, 29.5, 29.4, 29.36, 29.1, 27.6, 27.4, 22.4, 21.0, 14.9, 14.1; ν_{max} 3470, 2917, 2854, 1726, 1689, 1471, 1392, 1202, 1099, 968, 887.30, 839, 718 cm^{-1}.

Experiment 58: (2*R*,3*R*,19*R*,41*S*,42*S*,*E*)-3-((*tert*-butyldimethylsilyl)oxy)-41-methoxy-19,42-dimethyl-2-tetracosylhexacont-20-enoic acid (143)

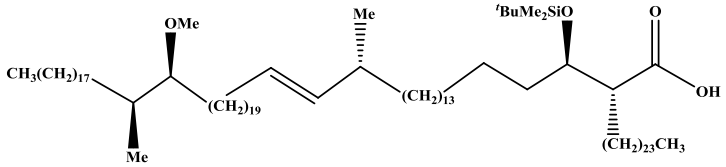

Imidazole (0.125 g, 1.80 mmol) was added to a stirred solution of (2*R*,3*R*,17*R*,39*S*,40*S*,*E*)-3-hydroxy-39-methoxy-17,40-dimethyl-2-tetracosyloctapentacont-18-enoic acid (**43**) (0.23 g, 0.18 mmol) in dry DMF (1.5 mL) and dry toluene (2.5 mL) at r. t. followed by the addition of *tert*-butyldimethylsilyl-chloride (0.27 g, 1.80 mmol) and 4-dimethylaminopyridine (10 mg). The mixture was stirred at 70 °C for 24 h. The solvent was evaporated under reduced pressure and the residue was diluted with ethyl acetate (50 mL) and with (20 mL). The organic layer was separated and the aqueous layer was extracted with ethyl acetate (2 × 30 mL). The combined organic layers were washed with water, dried and evaporated to give a colourless oil of residue. The residue was dissolved in THF (8 mL) and tetrabutylammonium hydroxide (0.9 mL, 4%) at r. t. the reaction mixture was stirred 10 min. at r. t. The mixture was diluted with water (10 mL) and extracted with ethyl acetate (2 × 20 mL), dried and evaporated to give a residue, which was purified by column chromatography on silica eluting with petroleum/ethyl acetate (20:1) to give a colourless oil, the title compound (0.25 g, 96%) {MALDI Found $[M+Na]^+$: 1390.3; $C_{91}H_{182}NaO_4Si$ requires: 1390.3}. This showed δ_H (500 MHz, CDCl3): 5.33 (1H, dt, *J* 6.4, 15.0

Hz), 5.25 (1H, dd, *J* 7.5, 15.0 Hz), 3.86-3.80 (1H, m), 3.35 (3H, s), 2.99-2.94 (1H, m), 2.57-2.51 (1H, m), 2.07-2.01 (1H, m), 1.96 (2H, br. q, *J* 6.8 Hz), 1.73-1.68 (1H, m), 1.65-1.54 (4H, m), 1.5-1.2 (138H, m), 1.1-1 (1H, m), 0.95 (3H, s), 0.94 (9H, s), 0.89 (6H, t, *J* 6.7 Hz), 0.85 (3H, d, *J* 6.9 Hz), 0.16 (3H, s), 0.14 (3H, s); δ_C (101 MHz, $CDCl_3$): 174.9, 136.5, 128.4, 85.5, 73.7, 57.7, 50.0, 37.3, 36.7, 35.8, 35.3, 32.6, 32.4, 31.9, 30.5, 30.1, 30.0, 29.9, 29.8, 29.7, 29.63, 29.6, 29.54, 29.5, 29.4, 29.36, 29.1, 27.6, 27.4, 27.36, 26.2, 25.9, 25.7, 25.5, 25.1, 22.7, 20.9, 17.9, 14.9, 14.1, -4.3, -4.9; ν_{max}: 2922, 2852, 1709, 1467, 1362, 1253, 1180, 1101, 836 cm^{-1}.

Experiment 59: ((3*R*,4*S*,5*S*,6*S*)-6-(((2*S*,3*S*,4*S*,5*S*)-6-((((2*R*,3*R*,17*R*,39*S*,40*S*,*E*)-3-((*tert*-butyldi- methylsilyl)oxy)-39-methoxy-17,40-dimethyl-2-tetracosyloctapentacont-18-enoyl)oxy)- methyl)-3,4,5-tris((trimethylsilyl)oxy)tetrahydro-2*H*-pyran-2-yl)oxy)-3,4,5-tris((trimethyl- silyl)oxy)tetrahydro-2*H*-pyran-2-yl)methyl(2*R*,3*R*,17*R*,39*S*,40*S*,*E*)-3-((*tert*-butyldimethyl-silyl)- oxy)-39-methoxy-17,40-dimethyl-2-tetracosyloctapentacont-18-enoate TDM (145) and ((3*S*,4*S*,5*S*,6*S*)-6-(((2*S*,3*S*,4*S*,5*R*)-6-(hydroxymethyl)-3,4,5-tris((trimethylsilyl)oxy)tetra-hydro-2*H*-pyran-2-yl)oxy)-3,4,5-tris((trimethyl silyl)oxy) tetra hydro-2*H*-pyran-2-yl)methyl (2*R*,3*R*,17*R*,39*S*,40*S*,*E*)-3-((*tert*-butyldimethylsilyl)oxy)-39-methoxy-17,40-dimethyl-2-tetracosylocta-pentacont-18-enoate TMM (146)

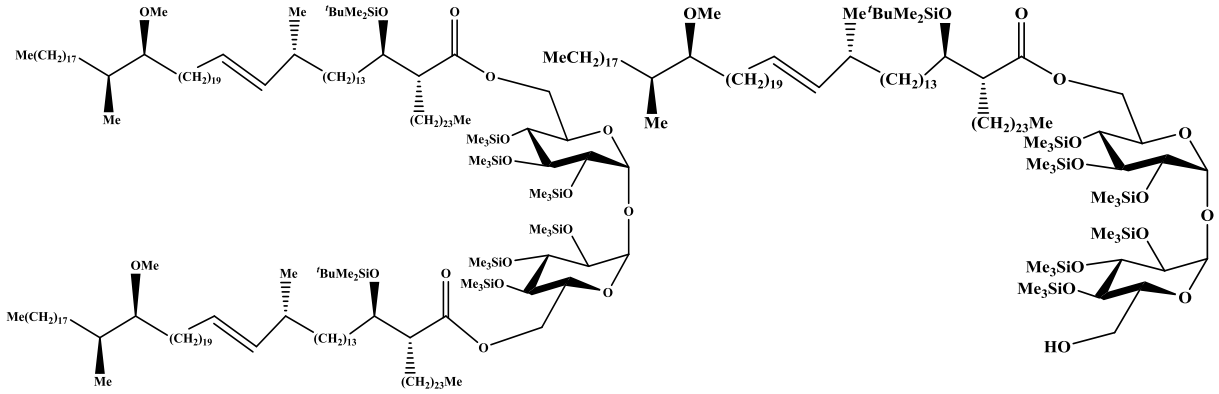

1-(3-Dimethylaminopropyl)-3-ethylcarbodiimidehydrochloride (EDCI) (0.044 g, 0.230 mmol) and DMAP (0.028 g, 0.23 mmol) were added to a stirred solution of *(2R,3R,17R,39S,40S,E)-3-*((*tert*-butyldimethylsilyl)oxy)-39-methoxy-17,40-dimethyl-2-tetracosyloctapentacont-18-enoic acid (**143**) (0.090 g, 0.065 mmol), 2,3,4,2',3',4'-hexakis-O-(trimethylsilyl)-α,α'-trehalose (**144**) (0.022 g, 0.028 mmol) and powdered 4 A^o in dry dichloromethane (1 mL) at r. t. under nitrogen atmosphere. The mixture was stirred for 6 days at room temperature then diluted with CH_2Cl_2 (3 mL) and silica (5 g) was added then the solvent was evaporated. The residue was

purified by column chromatography on silica eluting with petroleum/ethyl acetate (20:1) to give the first fraction was the first title compound TDM (0.060 g, 26%), $[\alpha]_D^{22}$ = +19 (c 1.2, $CHCl_3$) {MALDI Found $[M + Na]^+$: 3496.4; $C_{212}H_{430}NaO_{17}Si_8$ requires: 3496.0]. This showed δ_H (400 MHz, $CDCl_3$): 5.35 (2H, dt, *J* 6.4, 15.3 Hz), 5.25 (2H, br. dd, *J* 7.4, 15.3 Hz), 4.85 (2H, br. d, *J* 3.0 Hz), 4.36 (2H, br. d, *J* 10.2 Hz), 4.01 (2H, br. tt, *J* 3.1, 10.8 Hz), 3.94 (2H, br. pent, *J* 5.1 Hz), 3.9 (2H, br. t, *J* 8.8 Hz), 3.52 (2H, br. t, J 9.0 Hz), 3.38 (2H, dd, *J* 2.9, 9.3 Hz), 3.34 (6H, s), 2.96 (2H, br. pent, *J* 4.2 Hz), 2.57-2.53 (2H, m), 2.03 (2H, br. pent, *J* 6.5 Hz), 1.96 (4H, br. q, *J* 6.7 Hz), 1.7-1.2 (292H, m), 1.13-1.07 (2H, m), 0.9 (6H, d, *J* 6.7 Hz), 0.89 (12H, t, *J* 6.6 Hz), 0.88 (18H, s), 0.16 (18H, s), 0.15 (18H, s), 0.14 (18H, s), 0.06 (12 H, s); δ_C (101 MHz, $CDCl_3$): 173.8, 136.5, 128.4, 94.8, 85.4, 73.5, 73.4, 72.8, 71.8, 70.7, 62.4, 57.7, 51.9, 37.3, 36.7, 35.3, 32.6, 32.4, 31.9, 30.5, 30.0, 29.95, 29.9, 29.7, 29.66, 29.6, 29.5, 29.4, 29.2, 27.6, 27.4, 26.2, 25.8, 22.7, 20.9, 18.0, 14.9, 14.1, 1.1, 0.9, 0.2, -4.5, -4.7; ν_{max}: 2924, 2853, 1743, 1466, 1377, 1251, 1163, 1100 cm^{-1}. The second compound was the title TMM (0.070 g, 50%), $[\alpha]_D^{22}$= +32 (c 1.1, $CHCl_3$) {MALDI Found $[M + Na]^+$: 2146.7; $C_{121}H_{250}NaO_{14}Si_7$ requires: 2146.7}. This showed δ_H (500 MHz, $CDCl_3$): 5.34 (1H, dt, *J* 6.4, 15.3 Hz), 5.24 (1H, dd, *J* 7.4, 15.3 Hz), 4.91 (1H, d, *J* 3.0 Hz), 4.84 (1H, d, *J* 3.0 Hz), 4.35 (1H, dd, *J* 2.0, 11.8 Hz), 4.08 (1H, dd, *J* 4.1, 11.8 Hz), 4.0 (1H, td, *J* 2.2, 9.5 Hz), 3.96-3.92 (2H, m), 3.89 (1H, dd, *J* 5.2, 8.9 Hz), 3.84 (1H, td, *J* 3.0, 9.4 Hz), 3.73-3.64 (2H, m), 3.5 (1H, dd, *J* 3.7, 9.0 Hz), 3.49 (1H, dd, *J* 3.7, 9.0 Hz), 3.47 (1H, dd, *J* 3.7, 9.0 Hz), 3.43 (1H, dd, *J* 3.0, 9.3 Hz), 3.4 (1H, dd, *J* 3.0, 9.3 Hz), 3.35 (3H, s), 2.96 (1H, br. pent, *J* 4.2 Hz), 2.56 (1H, ddd, *J* 3.36, 5.4, 9.7 Hz), 2.1-2.0 (1H, m), 1.96 (2H, br. q, *J* 6.7 Hz), 1.72 (1H, br. t, *J* 5.2, 6.9 Hz), 1.67-1.57 (3H, m), 1.5-1.15 (136 H, m), 1.3-1.07 (1H, m), 0.94 (3H, d, *J* 6.7 Hz), 0.89 (6H, t, *J* 6.6 Hz), 0.87 (9H, s), 0.85 (3H, d, *J* 7.0 Hz), 0.17 (9H, s), 0.16 (9H, s), 0.15 (9H, s), 0.148 (18H, s), 0.12 (9H, s), 0.06 (3H, s), 0.055 (3H, s); δ_C (101 MHz, $CDCl_3$): 174.1, 136.5, 128.4, 94.5, 94.4, 85.4, 73.4, 73.3, 72.9, 72.8, 72.7, 72.0, 71.4, 70.7, 62.5, 61.7, 57.7, 51.8, 37.3, 36.7, 35.3, 33.4, 32.6, 32.3, 31.9, 30.5, 30.0, 29.9, 29.8, 29.7, 29.66, 29.5, 29.4, 29.2, 28.1, 27.6, 27.4, 26.4, 26.2, 25.8, 24.8, 22.7, 20.9, 18.0, 14.9, 14.1, 1.1, 1.0, 0.9, 0.85, 0.2, 0.04, -4.5, -4.7; ν_{max}: 3608, 2925, 2854, 1743, 1466, 1251, 1100, 1077, 844 cm^{-1}.

Experiment 60: ((2*R*,2'*R*,4S,4'*S*,5*R*,5'*R*,6*R*,6'*R*)-Oxybis(3,4,5-trihydroxytetrahydro-2*H*-pyran-6,2-diyl))*bis*(methylene)(2*R*,2'*R*,3*R*,3'*R*,17*R*,17'*R*,18*E*,18'*E*,39*S*,39'*S*,40*S*,40'*S*)-*bis*(3-((*tert*-butyldimethylsilyl)oxy)-39-methoxy-17,40-dimethyl-2-tetracosyloctapentacont-18-enoate) (147)

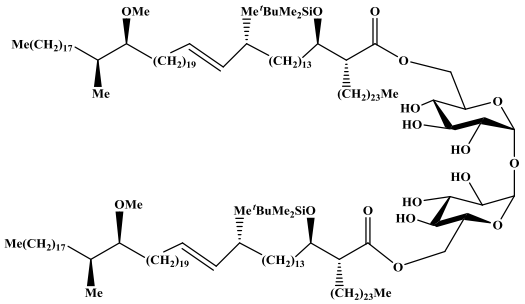

Tetrabutylammonium fluoride (0.1 mL, 0.1 mmol, 1 M) was added to a stirred solution of TDM (**145**) (0.06 g, 0.017 mmol) in dry THF (5 mL) at 5 ^{o}C under nitrogen atmosphere. The mixture was allowed to reach r. t. and stirred for 1 h. The solvent was evaporated under reduced pressure and the residue was purified by column chromatography on silica eluting with $CHCl_3$/MeOH (10:1) to give the title compound (0.035 g, 67.3%), $[\alpha]_D^{22}$= +19.5 (c 0.50, $CHCl_3$) {MALDI Found $[M+Na]^+$: 3063.9; $C_{194}H_{382}NaO_{17}Si_2$ requires: 3063.8}. This showed δ_H (500 MHz, $CDCl_3$ + few drops of CD_3OD): 5.27 (2H, dt, *J* 6.5, 15.3 Hz), 5.18 (2H, dd, *J* 7.4, 15.3 Hz), 5.04 (2H, d, *J* 3.4 Hz), 4.3 (2H, br. dd, *J* 3.8, 12.0 Hz), 4.2 (2H, br. d, *J* 10.84 Hz), 3.91 (2H, br. d, *J* 9.4 Hz), 3.85 (2H, br. q, *J* 5.0 Hz), 3.76 (2H, br. t, *J* 9.3 Hz), 3.44 (2H, dd, *J* 3.4, 9.6 Hz), 3.32 (2H, br. m), 3.3 (6H, s), 2.94-2.91 (2H, m), 2.53-2.48 (2H, m), 1.97 (2H, br. pent, *J* 6.3 Hz), 1.91 (2H, br. q, *J* 6.8 Hz), 1.57-1.1 (292H, m), 1.07-1.0 (2H, m), 0.88 (6H, d, *J* 6.7 Hz), 0.84 (12H, t, *J* 6.3 Hz), 0.81 (18H, s), 0.8 (6H, d, *J* 7.3 Hz), -0.003 (6H, s), - 0.023 (6H, s); δ_C (101 MHz, $CDCl_3$ + few drops of CD_3OD): 175.2, 136.4, 128.3, 93.5, 85.5, 73.2, 73.1, 71.6, 70.2, 69.9, 62.9, 57.6, 51.59, 37.1, 36.57, 35.2, 33.5, 32.5, 32.3, 31.8, 30.4, 29.83, 29.8, 29.7, 29.63, 29.6, 29.57, 29.4, 29.2, 29.0, 27.7, 27.4, 27.3, 26.9, 26.0, 25.7, 25.6, 24.1, 22.6, 20.8, 17.8, 14.7, 13.9, -4.6, -5.0. ν_{max}: 3400, 2924, 2853, 1742, 1464, 1100 cm^{-1}.

Experiment 61: ((2*R*,4*S*,5*R*,6*R*)-3,4,5-Trihydroxy-6-(((2*R*,3*R*,4*S*,6*R*)-3,4,5-trihydroxy-6-(hydroxymethyl)tetrahydro-2*H*-pyran-2-yl)oxy)tetrahydro-2*H*-pyran-2-yl)methyl-(2*R*, 3*R*,17*R*,39*S*,40*S*,*E*)-3-((*tert*-butyldimethylsilyl)oxy)-39-methoxy-17,40-dimethyl-2-tetra cosylocta- pentacont-18-enoate (148)

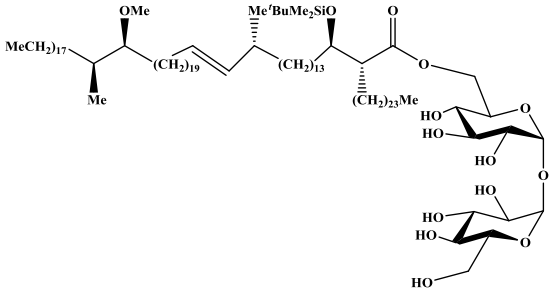

Tetrabutylammonium fluoride (0.16 mL, 0.16 mmol, 1M) was added to a stirred solution of TMM (**146**) (0.058 g, 0.027 mmol) in dry THF (2 mL) at 5 ^{o}C under nitrogen atmosphere. The mixture was allowed to reach r. t. and stirred for 1 h. The mixture was worked up and purified as before to give the title compound (0.030, 65%) as a colourless oil, $[\alpha]_D^{22}$= +39.5 (c 0.75, $CHCl_3$) {MALDI Found [M + Na]$^+$: 1714.2; $C_{103}H_{202}NaO_{14}Si$ requires: 1714.4}. This showed δ_H (500 MHz, $CDCl_3$ + few drop of CD_3OD): 5.28 (1H, dt, *J* 6.5, 15.5 Hz), 5.19 (1H, br. dd, *J* 7.6, 15.5 Hz), 5.05 (2H, br. t, *J* 3.5 Hz), 4.3 (1H, dd, *J* 4.6, 12.3 Hz), 4.23 (1H, dd, *J* 2.3, 12.3 Hz), 3.9 (1H, multi doublet, *J* 8.3 Hz), 3.87-3.84 (1H, m), 3.81-3.71 (4H, m), 3.65 (1H, dd, *J* 5.2, 11.6 Hz), 3.47 (1H, dd, *J* 3.9, 5.9 Hz), 3.46 (1H, dd, *J* 5.9, 9.7 Hz), 3.3 (3H, s), 2.93-2.91 (1H, m), 2.6-2.48 (1H, m), 1.99-1.95 (1H, m), 1.91 (2H, br. q, *J* 7.0 Hz), 1.6-1.55 (1H, m), 1.45-1.15 (150 H, m), 1.07-1.03 (1H, m), 0.89 (3H, d, *J* 6.7 Hz), 0.83 (6H, t, *J* 7.0 Hz), 0.81 (9H, s), 0.8 (3H, d, *J* 7.0 Hz), -0.003 (3H, s), -0.024 (3H, s); δ_C (101 MHz, $CDCl_3$ + few drop of CD_3OD): 174.9, 136.4, 128.3, 93.5, 93.4, 85.5, 73.2, 72.2, 71.7, 70.7, 70.3, 70.0, 62.7, 62.0, 58.7, 57. 6, 52.1, 51.7, 50.1, 37.2, 36.6, 35.2, 32.5, 32.3, 31.8, 30.4, 29.8, 29.8, 29.7, 29.7, 29.6, 29.5, 29.4, 29.2, 29.0, 27.4, 27.3, 26.0, 25.7, 25.1, 23.8, 22.6, 20.8, 20.0, 19.6, 17.9, 14.7, 14.0, 13.4, 13.38, -4.6, -5.0; ν_{max}: 3903.1, 3368.1, 2917.6, 2850.21, 1733.4, 1467.5, 1378.0, 1252.6, 1148.1, 1102.4, 1078.1, 1051.0, 992.4, 940.5, 836.4, 775.3, 720.8 cm^{-1}.

Experiment 62: ((2*R*,2'*R*,4*S*,4'*S*,5*R*,5'*R*,6*R*,6'*R*)-Oxy*bis*(3,4,5-trihydroxytetrahydro-2*H*-pyran-6,2-diyl))bis(methylene)-(2*R*,2'*R*,3*R*,3'*R*,17*R*,17'*R*,18*E*,18'*E*,39*S*,39'*S*,40*S*,40'*S*)-bis(3-hydroxy-39-methoxy-17,40-dimethyl-2-tetracosyloctapentacont-18-enoate) (44)

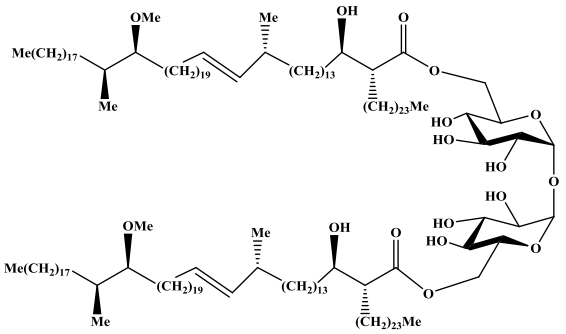

A dry polyethylene vial equipped with a rubber septum was charged with compound (**147**) (0.022 g, 0.007 mmol) and pyridine (0.05 mL) in dry THF (1.3 mL) and stirred at r. t. under argon. To it was added hydrogen fluoride-pyridine complex as ~70% hydrogen fluoride (0.2 mL). The mixture was stirred at 43 ^{o}C for 17 h. then neutralized by pouring slowly into sat. aq. $NaHCO_3$ until no more CO_2 was liberated. The product was extracted with chloroform (3 × 50 mL), then the combined organic layers were dried, evaporated to give a residue which was purified by chromatography eluting with $CHCl_3$/MeOH (10:1) to give the title compound (0.015, 75%), $[\alpha]_D^{22}$ = +18 (c 1.0, $CHCl_3$) {Found $[M+Na]^+$: 2835.6751; $C_{182}H_{354}NaO_{17}$ requires: 2835.6728}. This showed δ_H (500 MHz, $CDCl_3$ + few drops of CD_3OD): 5.3 (2H, dt, *J* 6.2, 15.6 Hz), 5.21 (2H, dd, *J* 7.2, 15.6 Hz), 5.0 (2H, br. d, *J* 3.4 Hz), 4.68 (2H, br. d, *J* 11.9 Hz), 4.23 (2H, br. t, *J* 9.4 Hz), 4.0-3.94 (2H, m), 3.74 (2H, br. t, *J* 9.3 Hz), 3.67-3.62 (2H, m), 3.5 (2H, dd, *J* 2.8, 9.6 Hz), 3.32 (6H, s), 3.21 (2H, t, *J* 9.3 Hz)), 2.96-2.93 (2H, m), 2.4-2.30 (2H, m), 1.97-2.02 (2H, m), 1.93 (4H, br. q, *J* 6.7 Hz), 1.65-1.01 (294H, m), 0.91 (6H, d, *J* 6.7 Hz), 0.86 (12H, t , *J* 6.7 Hz), 0.82 (6H, d, *J* 7 Hz); δ_C (101 MHz, $CDCl_3$ + few drops of CD_3OD): 175.2, 136.2, 128.2, 94.0, 85.5, 72.8, 72.3, 71.3, 70.6, 69.8, 63.5, 57.4, 52.4, 37.0, 36.5, 35.1, 34.6, 32.3, 32.1, 31.7, 30.2, 29.7, 29.6, 29.6, 29.4, 29.3, 29.3, 29.2, 29.1, 29.0, 28.9, 27.2, 27.1, 27.1, 25.8, 25.1, 22.4, 20.6, 14.5, 13.8; ν_{max} 3584, 3395, 2923, 2853, 1732, 1464, 1376 cm^{-1}.

Experiment 63: (2*R*,3*R*,17*R*,39*S*,40*S*,*E*)-((2*R*,3*S*,4*S*,5*R*,6*R*)-3,4,5-Trihydroxy-6-(((2*R*,3*R*,4*S*,5*S*,6*R*)-3,4,5-trihydroxy-6-(hydroxymethyl)tetrahydro-2*H*-pyran-2-yl) oxy) tetrahydro-2*H*-pyran-2-yl)methyl3-hydroxy-39-methoxy-17,40-dimethyl-2-tetracosyl octapentacont-18-enoate (45)

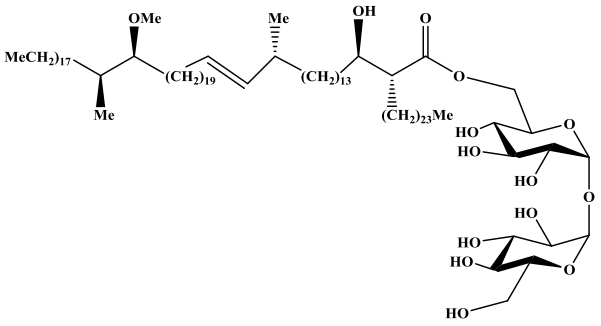

A dry polyethylene vial equipped with a rubber septum was charged with compound (**148**) (0.025 g, 0.015 mmol) and pyridine (0.05 mL) in dry THF (3 mL) and stirred at r. t. under argon. To it was added hydrogen fluoride-pyridine complex as ~70% hydrogen fluoride (0.25 mL). The mixture was stirred at 43 ^{o}C for 17 h. then worked up and purified as above to give of the title compound (0.015, 65.2%), $[\alpha]_D^{22}$ = + 34 (c 0.52, $CHCl_3$) {Found $[M+Na]^+$: 1600.3879; $C_{97}H_{188}NaO_{14}$ requires: 1600.3897}. This showed δ_H (400 MHz, $CDCl_3$): 5.26 (1H, dt, *J* 6.6, 15.2 Hz), 5.17 (1H, br. dd, *J* 7.4, 15.2 Hz), 5.03 (1H, d, *J* 3.2 Hz), 4.98 (1H, d, *J* 3.3 Hz), 4.61 (1H, br. d, *J* 11 Hz), 4.18 (1H, br. t, *J* 7.9 Hz), 3.95 (1H, dd, *J* 7.8, 12.0 Hz), 3.87-3.82 (1H, m), 3.79-3.71 (2H, m), 3.62-3.55 (2H, m), 3.5 (1H, dd, *J* 3.2, 9.8 Hz), 3.44 (1H, dd, *J* 3.3, 9.8 Hz), 3.32 (8H, br. s), 3.28 (3H, s), 3.23 (1H, br. t, *J* 9.5 Hz), 3.18 (1H, br. t, *J* 9.6 Hz), 2.93-2.89 (1H, m), 2.38-2.33 (1H, m), 1.99-1.94 (1H, m), 1.9 (2H, br. q, *J* 6.8 Hz), 1.57-1.10 (H, m), 1.06-0.98 (1H, m), 0.87 (3H, d, *J* 6.7 Hz), 0.81 (6H, t, *J* 6.4 Hz), 0.78 (3H, d, *J* 7.1 Hz). δ_C (101 MHz, $CDCl_3$): 175.4, 136.3, 128.3, 94.6, 85.5, 72.6, 72.4, 72.3, 71.5, 71.2, 71.1, 70.8, 69.9, 64.2, 62.3, 62.1, 57.5, 52.3, 37.1, 36.5, 35.2, 34.6, 32.4, 32.2, 31.8, 30.3, 29.8, 29.7, 29.7, 29.5, 29.4, 29.3, 29.2, 29.0, 27.3, 27.2, 27.1, 25.9, 25.1, 22.5, 20.7, 14.6, 13.9; ν_{max}: 3364, 2918, 2850, 1728, 1467, 1148, 992 cm^{-1}.

Experiment 64: (*S*)-2,3-Bis(benzyloxy)propyl (2*R*,3*R*,17*R*,39*S*,40*S*,*E*)-3-hydroxy-39-methoxy-17,40-dimethyl-2-tetracosyloctapentacont-18-enoate (150)

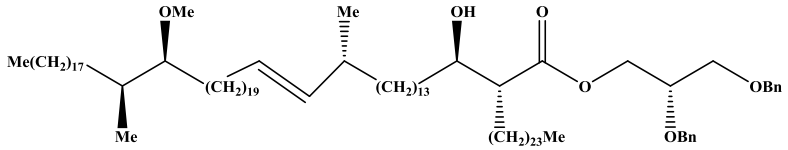

Cesium hydrogencarbonate (0.061 g, 0.313 mmol) was added to a stirred solution of (S)-2,3-bis(benzyloxy)propyl4-methylbenzenesulfonate (**149**) (supplied by Dr Mohsin Mohammed, 0.030 g, 0.067 mmol) and (2*R*,3*R*,17 *R*, 39*S*,40*S*,*E)*-3-hydroxy-39-methoxy-17,40-dimethyl-2-tetracosyloctapentacont-18-enoic acid (**43**) (0.056 g, 0.044 mmol) in dry DMF:THF (1:5, 2 mL) at r. t. and the mixture was stirred at 70 ^{o}C for two days. The suspension was diluted with ethyl acetate (20 mL) and water (10 mL). The organic layer was separated and the aqueous layer was re-extracted with ethyl acetate (3 × 10 mL). The combined organic layers were washed with water (10 mL) and brine (10 mL), dried over $MgSO_4$, filtered and evaporated to give a thick oil residue. The residue was purified by column chromatography on silica eluting with hexane/ethyl acetate (10:1) to give the title compound (0.060, 89%) {MALDI Found $[M+Na]^+$: 1530.3; $C_{102}H_{186}NaO_6$ requires: 1530.4}. This showed δ_H (400 MHz, $CDCl_3$): 7.4-7.28 (10H, m), 5.34 (1H, dt, *J* 6.4, 15.3 Hz), 5.25 (1H, dd, *J* 7.4, 15.3 Hz), 4.7 (1H, d, *J* 12.0 Hz), 4.65 (1H, d, *J* 12.0 Hz), 4.6 (2H, br. s), 4.44 (1H, dd, *J* 4, 11.6 Hz), 4.23 (1H, dd, *J* 5.4, 11.6 Hz), 3.84 (1H, br. pent, *J* 5.4 Hz), 3.64-3.57 (3H, m), 3.36 (3H, s), 2.99-2.96 (1H, m), 2.5 (1H, br. d, *J* 5.9 Hz), 2.44 (1H, br. td, *J* 5.4, 9.8 Hz), 2.1-2.03 (1H, m), 1.98 (2H, br. q, *J* 6.7 Hz), 1.73-1.2 (142H, br. m), 1.15-1.07 (1H, m), 0.96 (3H, d, *J* 6.7 Hz), 0.9 (6H, t, *J* 6.7 Hz), 0.87 (3H, d, *J* 6.9 Hz); δ_C (101 MHz, $CDCl_3$): 175.4, 138.0, 137.9, 136.5, 128.4, 128.35, 127.73, 127.7, 127.6, 85.4, 75.8, 73.5, 72.3, 72.1, 69.6, 63.5, 57.7, 51.4, 37.2, 36.7, 35.5, 35.3, 32.6, 32.4, 31.9, 30.5, 30.0, 29.9, 29.8, 29.7, 29.66, 29.6, 29.5, 29.44, 29.4, 29.1, 27.6, 27.5, 27.4, 26.2, 25.8, 22.7, 20.9, 14.9, 14.1; ν_{max}: 3474, 2924, 2853, 1735, 1466, 1370, 1100, 968, 908 cm^{-1}.

Experiment 65: ((2*R*,4*S*,5*R*,6*S*)-3,4,5,6-Tetrakis(benzyloxy)tetrahydro-2*H*-pyran-2-yl) methyl-(2*R*,3*R*,17*R*,39*S*,40*S*,*E*)-3-hydroxy-39-methoxy-17,40-dimethyl-2-tetra cosylocta-pentacont-18-enoate (152)

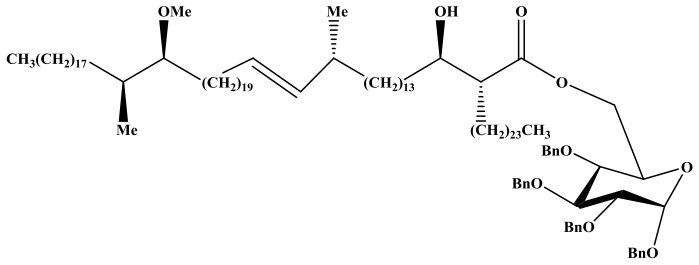

(2*R*,3*R*,17*R*,39*S*,40*S*,*E)*-3-Hydroxy-39-methoxy-17,40-dimethyl-2-tetracosyloctapentacont-18-enoic acid (**43**) (0.054 g, 0.043 mmol) was dissolved in mixture of THF and DMF (THF-DMF, 5:1, 1.5 mL) at r. t. then warmed very gently until all mycolic acid been dissolved. Dry cesium hydrogen carbonate (0.072 mg, 0.371 mmol) was added to a stirred solution and the mixture was left at r. t. for 1 h. Tosylate (**151)** (supplied by Dr K. Baols, 0.33 g, 0.047 mmol) was added. The mixture was stirred at 70 ^{o}C for 18 hs then quenched with water (5 mL). The product was extracted with CH_2Cl_2 (3 × 60 mL), dried over $MgSO_4$, filtered and evaporated. The product was purified by column chromatography over silica gel, eluting with petroleum/ethyl acetate (10:1) to give the title compound (0.056, 70%), $[\alpha]_D^{22}$= +15 (c 1.1, $CHCl_3$) {MALDI Found [M + Na] $^{+}$: 1798.6; $C_{119}H_{202}NaO_9$ requires: 1798.5}. This showed δ_H (400 MHz, $CDCl_3$): 7.4-7.26 (20H, m), 5.34 (1H, dt, *J* 6.4, 15.4 Hz), 5.24 (1H, dd, *J* 7.4, 15.4 Hz), 4.97 (1H, d, *J* 11.0 Hz), 4.95 (1H, d, *J* 11.0 Hz), 4.93 (1H, d, *J* 11.0 Hz), 4.9 (1H, d, *J* 12.0 Hz), 4.78 (1H, d, *J* 11.0 Hz), 4.71 (1H, d, *J* 11.0 Hz), 4.64 (1H, d, *J* 12.0 Hz), 4.61 (1H, d, *J* 11 Hz), 4.56 (1H, br. d, *J* 11.0 Hz), 4.54 (1H, d. *J* 7.6 Hz), 4.22 (1H, dd, *J* 4.6, 11.0 Hz), 3.67 (2H, br. t, *J* 8.7 Hz), 3.54-3.47 (3H, m), 3.35 (3H, s), 2.96 (1H, br, pent, *J* 4.2 Hz), 2.5-2.46 (2H, m), 2.06-2.01 (1H, m), 1.97 (2H, br. q, *J* 6.7 Hz), 1.8-1.7 (1H, m), 1.68-1.55 (3H, m), 1.5-1.2 (146H, m), 1.15-1.05 (1H, m), 0.94 (3H, d, *J* 6.7 Hz), 0.89 (6H, t, *J* 7 Hz), 0.85 (3H, d, *J* 6.7 Hz); δ_C (101 MHz, $CDCl_3$): 175.2, 138.4, 138.2, 137.7, 137.1, 136.5, 128.5, 128.4, 128.35, 128.1, 128.0, 127.97, 127.9, 127.85, 127.7, 102.3, 85.4, 84.5, 82.3, 77.8, 75.8, 75.1, 74.9, 72.8, 72.3, 71.1, 62.9, 57.7, 51.3, 37.2, 36.7, 35.6, 35.3, 32.6, 32.3, 31.9, 30.5, 30.0, 29.9, 29.8, 29.7, 29.66, 29.6, 29.58, 29.53, 29.5, 29.4, 29.1, 27.6, 27.5, 27.4, 26.2, 25.9, 22.7, 20.9, 14.9, 14.1; ν_{max}: 3487, 2920, 2851, 1738, 1466, 1072, 727, 696 cm^{-1}.

Experiment 66: (*S*)-2,3-Dihydroxypropyl (2*R*,3*R*,17*R*,39*S*,40*S*,*E*)-3-hydroxy-39-methoxy-17,40-dimethyl-2-tetracosyloctapentacont-18-enoate (46)

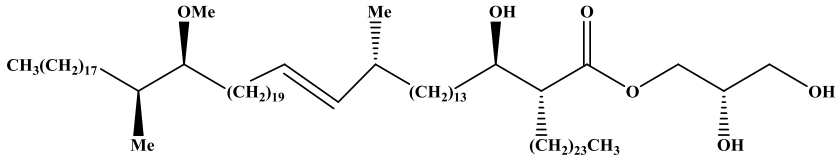

Liquid ammonia (100 mL) was decanted into a 250 mL 2-necked flask under a liquid nitrogen –methylated spirit condenser protected by a soda lime guard tube. Sodium (~50 mg) was added until the blue colour of the solution persisted. A sample of (*S*)-2,3-bis(benzyloxy)propyl (2*R*,3*R*,17*R*,39*S*, 40*S*,*E*)-3-hydroxy-39-methoxy-17,40-dimethyl-2-tetracosyloctapentacont-18-enoate (**150**) (52 mg, 0.034 mmol) in 1,4-dioxane (2 mL) was added; the mixture was stirred for 4-5 min, when the blue colour disappeared, followed by quenching with NH_4Cl (5 mL) and ether (30 mL). The ammonia was allowed to evaporate and the organic layer was separated and the aqueous layer was re-extracted with ether (2 × 30 mL). The combined organic layers were dried and evaporated. The residue was purified by column chromatography on silica, eluting with $CHCl_3$/ MeOH (10:1) to give the title compound (18 mg, 40%) {Found $[M + Na]^+$: 1350.3215; $C_{88}H_{174}NaO_6$ requires: 1350.3203}. This showed δ_H (400 MHz, $CDCl_3$ + few drops of CD_3OD): 5.33 (1H, dt, *J* 6.4, 15.3 Hz), 5.23 (1H, dd, *J* 7.4, 15.3 Hz), 4.27 (1H, dd, *J* 4.2, 11.5 Hz), 4.21 (1H, dd, *J* 6.4, 11.5 Hz), 3.96-3.91 (1H, m), 3.71-3.65 (2H, m), 3.61 (1H, br, dd, *J* 5.5, 11.5 Hz), 3.34 (3H, s), 2.97-2.94 (1H, br, m), 2.48-2.42 (1H, m), 2.06-2.01 (1H, m), 1.96 (2H, br. q, *J* 6.6 Hz), 1.71-1.05 (146 H, m), 0.93 (3H, d, *J* 6.7 Hz), 0.88 (6 H, t, *J* 6.6 Hz), 0.84 (3H, d, *J* 6.9 Hz); δ_C (101 MHz, $CDCl_3$+ few drops of CD_3OD): 175.5, 136.4, 128.3, 85.5, 72.6, 69.8, 65.1, 63.0, 57.6, 52.5, 37.1, 36.6, 35.2, 35.0, 32.5, 32.3, 31.8, 30.4, 29.9, 29.8, 29.7, 29.6, 29.55, 29.52, 29.5, 29.4, 29.3, 29.25, 29.0, 27.4, 27.36, 27.3, 26.0, 25.3, 22.6, 20.8, 14.7, 14.0; ν_{max}: 3434, 2922, 2853, 1722, 1465, 1099 cm^{-1}. Starting material (10 mg) was recovered.

Experiment 67: ((2*R*,4*S*,5*R*,6*S*)-3,4,5,6-Tetrahydroxytetrahydro-2*H*-pyran-2-yl)methyl (2*R*, 3*R*, 17*R*,39*S*,40S,*E*)-3-hydroxy-39-methoxy-17,40-dimethyl-2-tetracosyl octa pentacont-18-enoate (47)

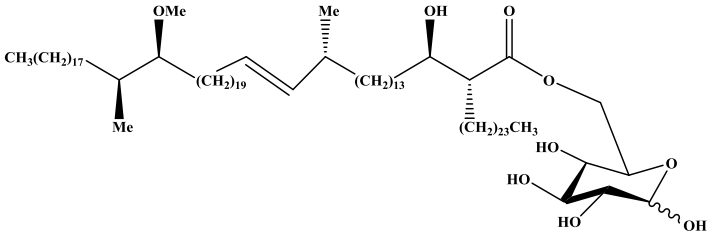

Liquid ammonia (100 mL) was decanted into a 250 mL 2-necked flask under a liquid nitrogen –methylated spirit condenser protected by a soda lime guard tube. Sodium (~50 mg) was added until the blue colour of the solution persisted. Compound (**152**) (48 mg, 0.027 mmol) in 1,4-dioxane (2 mL) was added, then the reaction mixture was stirred for 4-5 min, when the blue colour disappeared, followed by quenching with NH_4Cl (5 mL) and ether (30 mL). The ammonia was allowed to evaporate and the organic layer was separated and the aqueous layer was re-extracted with ether (2 × 30 mL). The combined organic layers were dried and evaporated. The residue was purified by column chromatography on silica, eluting with $CHCl_3$/MeOH (10:1) to give a mixture of (α, β)-(**47**) in ratio (0.6:0.4) (18 mg, 47%), $[\alpha]_D^{22}$= +28 (c 0.50, $CHCl_3$) {Found $[M + Na]^+$: 1438.3385; $C_{91}H_{178}NaO_9$ requires: 1438.3363}. This showed δ_H for α, β in ratio 0.6:0.4 (400 MHz, $CDCl_3$ + few drops of CD_3OD): 5.28 (1H, dt, *J* 6.4, 15.2 Hz), 5.18 (1H, br. dd, *J* 7.4, 15.2 Hz), 5.1 (0.6H, d, *J* 3.8 Hz, H-1α), 4.46 (0.4H, d, *J* 7.8 Hz, H-1β), 4.4 (1H, br. d, *J* 11.8 Hz, H-6α,β), 4.24 (1H, br. dd, *J* 5.8, 11.8 Hz, H-6 α,β), 3.96-3.92 (0.6H, ddd, *J* 2.2, 5.8, 9.8 Hz, H-5α), 3.67-3.58 (1.6H, m, H-4α + CH-OH mycolic acid), 3.48-3.44 (0.4H, ddd, *J* 2.2, 5.8, 9.8 Hz, H-5β), 3.43-3.26 (5H, H-2,3α, H-3,4β and a singlet at 3.3 for the methoxy group), 3.17 (0.4H, br. t, *J* 8.4 Hz H-2β), 2.95-2.91 (1H, m), 2.41-2.34 (1H, m), 2.0-1.95 (1H, m), 1.9 (2H, br. q, *J* 6.7 Hz), 1.62-1.1 (155H, m), 1.07-1.0 (2H, m), 0.88 (3H, d, *J* 6.7 Hz), 0.83 (6H, t, *J* 6.6 Hz), 0.8 (3H, d, *J* 7 Hz); δ_C for α, β isomers (400 MHz, $CDCl_3$ + few drops of CD_3OD): 175.1, 136.4, 128.2, 96.6 (C-1β), 92.2 (C-1α), 85.5, 76.1, 74.4, 73.6, 73.5, 72.4, 72.1, 70.4, 70.2, 69.1, 63.5, 63.4, 57.5, 52.7, 52.5, 37.1, 36.6, 35.2, 35.0, 32.4, 32.2, 31.8, 30.4, 29.8, 29.76, 29.7, 29.6, 29.5, 29.41, 29.4, 29.3, 29.2, 29.1, 29.0, 27.4, 27.2, 26.0, 22.5, 20.8, 14.7, 13.9; ν_{max}: 3400, 2923, 2852, 1720, 1466, 1376, 1100 cm^{-1}. Starting material (12 mg) was recovered.

Experiment 68: ((2*R*,3*R*,4*S*,5*S*)-3,4-Bis(benzyloxy)-5-methoxytetrahydrofuran-2-yl)methyl (2*R*,3*R*,17*R*,39*S*,40*S*,*E*)-3-hydroxy-39-methoxy-17,40-dimethyl-2-tetracosyloctapentacont-18-enoate (154)

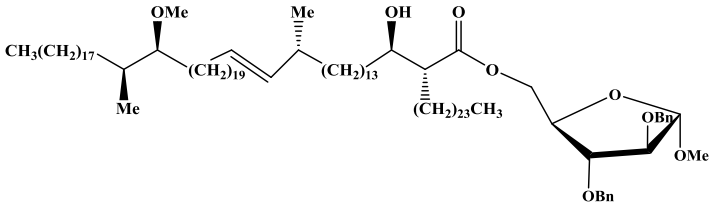

Acid (**43**) (0.056 g, 0.044 mmol) was dissolved in a mixture of THF and DMF (THF-DMF, 5:1, 1.5 mL) at room temperature, then warmed very gently until all mycolic acid been dissolved. Dry cesium hydrogen carbonate (0.061 g, 0.313 mmol) was added to a stirred solution and the mixture left at r. t. for 1 h, then (2*R*,3*R*,4*S*,5*S*)-3,4-bis(benzyloxy)-5-methoxytetrahydrofuran-2-yl)methyl 4-methyl benzene sulfonate (**153**) (supplied by Dr Mohsin Mohammed, 0.033g, 0.066 mmol) in THF/DMF (0.5 mL) was added. The mixture was stirred at 70 ^{o}C for 18 h. then quenched with water (3 mL). The product was extracted with CH_2Cl_2 (3 × 30 mL), dried over $MgSO_4$, filtered and evaporated. The crude product was purified by column chromatography over silica, eluting with petroleum/ethyl acetate (10:1) to give the title compound (0.049 g, 71%) as a colourless thick oil, $[\alpha]_D^{22}$ = + 21 (c 0.51 $CHCl_3$) {MALDI Found $[M + Na]^+$: 1602.3; $C_{105}H_{190}NaO_8$ requires: 1602.4}. This showed δ_H (400 MHz, $CDCl_3$): 7.4-7.28 (10H, m), 5.34 (1H, dt, *J* 6.3, 15.4 Hz), 5.25 (1H, dd, *J* 7.4, 15.4 Hz), 4.92 (1H, br. s), 4.57 (1H, d, *J* 12 Hz), 4.56 (1H, d, *J* 11.8 Hz), 4.5 (1H, d, *J* 12.0 Hz), 4.48 (1H, d, *J* 11.8 Hz), 4.33-4.26 (2H, m), 4.24-4.2.0 (1H, m), 3.99 (1H, d, *J* 2.1 Hz), 3.84 (1H, dd, *J* 2.6, 6.5 Hz), 3.65-3.62 (1H, m), 3.37 (3H, s), 3.35 (3H, s), 2.98-2.94 (1H, m), 2.43 (1H, tt, *J* 5.5, 9.1 Hz), 2.06-2.02 (1H, m), 1.97 (2H, br. q, *J* 6.7 Hz), 1.7-1.5 (5H, m), 1.45-1.2 (137H, m), 1.11-1.04 (2H, m), 0.94 (3H, d, *J* 6.7 Hz), 0.89 (6H, t, *J* 6.6 Hz), 0.85 (3H, d, *J* 6.9 Hz); δ_C (101 MHz, $CDCl_3$): 175.0, 137.4, 137.2, 136.4, 128.5, 128.46, 128.4, 128.0, 127.9, 127.86, 107.2, 87.8, 85.4, 83.7, 79.4, 72.4, 72.2, 72.1, 63.5, 57.7, 54.9, 51.5, 37.2, 36.7, 35.5, 35.3, 32.6, 32.3, 31.9, 30.5, 30.0, 29.9, 29.7, 29.6, 29.5, 29.4, 29.35, 29.1, 27.6, 27.4, 27.36, 26.2, 25.8, 22.7, 20.9, 14.9, 14.1; ν_{max}: 2923, 2853, 1738, 1465, 1100 cm^{-1}.

Experiment 69: ((2*R*,3*S*,4*S*,5*S*)-3,4-Dihydroxy-5-methoxytetrahydrofuran-2-yl)methyl (2*R*,3*R*,17*R*,39*S*,40*S*,*E*)-3-hydroxy-39-methoxy-17,40-dimethyl-2-tetracosyl octa pentacont-18-enoate (48)

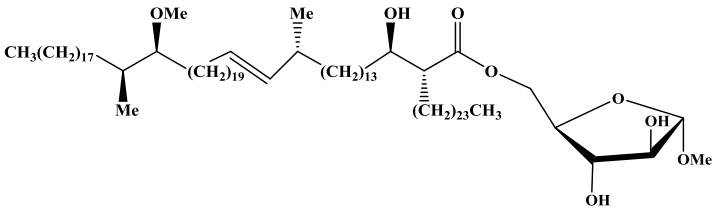

Liquid ammonia (100 mL) was decanted into a 250 mL 2-necked flask under a liquid nitrogen –methylated spirit condenser protected by a soda lime guard tube. Sodium (∼50 mg) was added until the blue colour of the solution persisted. Compound (**154**) (42 mg, 0.026 mmol) in 1,4-dioxane (2 mL) was added; then the mixture was stirred for 4-5 min, when the blue colour disappeared, then quenched with sat. solution of NH_4Cl (5 mL) and ether (30 mL). The ammonia was allowed to evaporate and the organic layer was separated and the aqueous layer was re-extracted with ether (2 × 30 mL). The combined organic layers were dried and evaporated. The residue was purified by column chromatography on silica, eluting with $CHCl_3$/MeOH (10:1) to give of the title compound as a thick oil (21 mg, 57%), $[\alpha]_D^{22}$ = + 26 (c 0.70 $CHCl_3$) {Found $[M + Na]^+$: 1422.3430; $C_{91}H_{178}NaO_8$ requires: 1422.3414}. This showed δ_H (400 MHz, $CDCl_3$ + few drops of CD_3OD): 5.28 (1H, dt, *J* 6.4, 15.2 Hz), 5.2 (1H, dd, *J* 7.4, 15.2 Hz), 4.78 (1H, br. s), 4.33 (1H, dd, *J* 4.6, 11.7 Hz), 4.28 (1H, dd, *J* 5, 11.7 Hz), 4.08 (1H, br. q, *J* 4.9 Hz), 3.96 (1H, dd, *J* 1.3, 2.8 Hz), 3.85 (1H, dd, *J* 2.8, 5.0 Hz), 3.65-3.60 (1H, m), 3.35 (3H, s), 3.3 (3H, s), 2.95-2.93 (1H, m), 2.39 (1H, ddd, *J* 4.8, 7.4, 10.2 Hz), 2.01-1.96 (1H, m), 1.91 (2H, br. q, *J* 6.6 Hz), 1.62-1.03 (145H, m), 0.89 (3H, d, *J* 6.7 Hz), 0.84 (6H, t, *J* 6.6 Hz), 0.8 (3H, d, *J* 7.0 Hz); δ_C (101 MHz, $CDCl_3$ + few drops of CD_3OD): 175.0, 136.4, 128.3, 108.8, 85.5, 81.9, 81.2, 78.0, 72.4, 63.4, 57.6, 55.0, 52.6, 37.1, 36.6, 35.2, 34.9, 32.4, 32.2, 31.8, 30.4, 29.8, 29.78, 29.7, 29.6, 29.5, 29.48, 29.4, 29.3, 29.2, 20.0, 27.4, 27.3, 27.2, 26.0, 25.3, 22.6, 20.8, 14.7, 14.0; ν_{max}: 3400, 2925, 2854, 1724, 1466, 1215, 1094 cm^{-1}. Starting material (10.2 mg) was recovered.

Chapter 7

7. ELISA experiments

7.1 Reagents

Phosphate buffered saline (PBS)

The stock solution of 20x PBS was prepared by dissolving NaCl (160.0 g), KCl (4 g), KH_2PO_4 (4.0 g) and Na_2HPO_4 (23.0 g) in (900) mL of double distilled de-ionised water ($dddH_2O$). The solution was then made up to a final volume of (1 L) using $dddH_2O$ and filtered through a (0.22 µL) membrane filter.

Casein/PBS buffer (0.5%)

20x PBS stock solutions (100 mL) was added to (1.4 L) of double distilled de-ionised water ($dddH_2O$) in (2 L) beaker, and casein (carbohydrates and fatty acid free) (10.0 g) was added. This solution was stirred for two hours at 37 ºC and then stored overnight at 4 ºC. The next day the pH was adjusted to 7.4 with sodium hydroxide NaOH (1.0 M) and the volume made up to 2 L with ddd H_2O.

TSST buffer solution

To wash the plates before starting, the TSST buffer was prepared one day before starting. Tris (hydroxymethyl)amino-methane (3 g) was added to (200 mL) of double distilled de-ionised water ($dddH_2O$) in (2 L) beaker and the pH was adjusted to 8.5 with HCl (1 M) and then the sucrose (12.5 g), NaCl (1.13 g) and Tween (125 µL) were added to the solution mixture and leave stirred until dissolved.

Tween and PBS buffer

To use in automatic washer to wash the plates during the test, the PBS buffer (100 mL) and Tween (1 mL) was added to the double distilled de-ionised water ($dddH_2O$) (1.8 L) and transferred to (2 L) volumetric flask.

To dilute serum samples and Secondary antibody, The PBS buffer (5 mL), albumin (1 g), pluronic (0.1 g) and Tween (50 µL) were added to the double distilled de-ionised water ($dddH_2O$) (100 mL) and leave stirred until dissolve and use as a fresh .

Secondary antibody (Goat anti-human IgG peroxidise conjugate)

Secondary antibody (10 µL) was added to 10 mL of 0.5 % casein / PBS. This solution was prepared 5 minutes before use.

Secondary antibody (Goat anti- bovine IgG and IgG Fc specific)

The conjugate was prepared by adding {(10 μL of peroxidase conjugate to 10 ml of 0.5% Casein/PBS) it means (10 μL in 10,000 μL) in order to (1 in 1000 dilution in Casein)}. This was prepared 5 minutes prior to use.

Secondary antibody (10 μL) was added to 10 mL of 0.5 % casein / PBS. This solution was prepared 5 minutes before use.

Citrate Buffer (0.1 M)

Citric acid solution (450 mL, 0.1 M) was added to tri-sodium citrate solution (450 mL, 0.1 M) until a pH of 4.5.

O-phenylenediamine dihydrochloride (OPD) substrate

OPD (10.0 mg) and H_2O_2 (8.0 mg) was added to citrate buffer (0.1 M, 10 mL). The substrate was prepared 5 minutes prior to use.

Natural mixture of TDM

Trehalose-6,6-dimycolate extracted from *M. Tuberculosis* and *M. bovis* was purchased from Aldrich.

Natural mixture of wax ester

Natural wax ester extracted from *M. avium* was purchased from Aldrich.

Synthetic antigens

Synthetic antigens were dissolved in hexane to give an antigen solution of concentration 62.5 μg/mL.

The serum

Human serum used in this work was provided by the WHO from its sample bank. In this case, all the patients had presented at a hospital with the symptoms of TB. Some were diagnosed as positive using the standard WHO protocols, others as negative. Another set of human serum was collected as part of a Welsh study of E. coli; an additional ethical approval was obtained to use the samples for this work.

Cattle serum for all experiments except the time study were provided by Prof M. Vordermeier of the VLA (now AHVLA). The serum for the time study was provided by Dr J. Mc Nair (AFBI, Belfast).

7.2 The ELISA assay experiments

All absorbances were measured at three different wavelengths (450, 492 and 630 nm).

All measurements were taken as four replicates unless otherwise stated. These were averaged and a standard deviation recorded.

Results are presented in the body of the thesis without standard deviations (which were small); the full results for each experiment, together with details of the serum samples are provided on a cd.

References

[1] Alkamo, I. E. (1994). *Fundamental of Microbiology* (4th Edi., pp. 203–208). New York.

[2] Davies, P., Barnes, P. and Gordon, S. (2008). *Clinical Tuberculosis* (4th Edi., pp. 163–188). London : Hodder Arnold.

[3] (a) Elder, N. C. (1992). Extrapulmonary tuberculosis. A review. *Archives of family medicine*, 1, 91–8. (b) Baydur, A. (1977). The spectrum of extrapulmonary tuberculosis. *West. J. Med.*, *126*, 253–262.

[4] Golden, M. P., and Vikram, H. R. (2005). Extrapulmonary tuberculosis: An overview. *Am. Fam. Phys.*, *72*, 1761–1768.

[5] Sandgren, A., Hollo, V. and van der Werf, M. J. (2013). Extrapulmonary tuberculosis in the European union and European economic area, 2002 to 2011. *Euro Surveill.*, *18*, 1–9.

[6] (a) Brennan, P.J. and Nikaido, H. (1995). The envelope of mycobacteria. Annu. Rev. Biochem., 64, 29–63. (b) Qureshi, N., Takayama, K., Jordi, H. C. and Schnoes, H. K. (1978). Characterization of the purified components of a new homologous series of α-mycolic acids from *Mycobacterium tuberculosis* H37Ra. J. *Biol. Chem.*, *253*, 5411–5417. (c) Daffé, M. and Draper, P. (1998). The envelope layers of mycobacteria with reference to their pathogenicity. *Adv. Microb. Physiol.*, *39*, 131–203. (d) Minnikin, D. E., Kremer, L., Dover, L. G. and Besra, G. S. (2002). The methyl-branched fortifications of *Mycobacterium tuberculosis*. *Chem. Biol.*, *9*, 545–553.

[7] Lawn, S. D. and Zumla, A. I. (2011). Tuberculosis. *Lancet*, *378*, 57–72.

[8] Kumar, V., Abbas, A. K., Fausto, N. and Mitchell, R. N. (2007). *Robbins Basic Pathology* (8th Edi., pp. 516–522). California San Francisco.

[9] Richard, E. C. and N. A. M. (2014). Tuberculosis in Africa — Combating an HIV-Driven Crisis. *N. Engl. J. Med.*, *358*, 1089–1092.

[10] Baydur, A. (1977). The spectrum of extrapulmonary tuberculosis. *West. J. Med.*, *126*, 253–262.

[11] Playfair, J. H. (2004). *Living with germs : in sickness and in health* (pp. 251–255). Oxford.

[12] DeFranco AL, Locksley RM, R. M. (2007). Immunity: The Immune Response to Infectious and Inflammatory Disease. *Yale J. Biol. Med.*, *80*, 5–6.

[13] Corbett, E. L., Watt, C. J., Walker, N., Maher, D., Williams, B. G., Raviglione, M. C. and DPhil, D. C. (2003). The Growing Burden of Tuberculosis. *Arch. Intern. Med.*, *163*, 1009–1021.

[14] Ritacco, V. (2011). The Situation of HIV/*Mycobacterium tuberculosis* Co-Infection in South America. *The Open Infect. Dis. J.*, *5*, 81–88.

[15] Hayman, J. (1984). *Mycobacterium* ulcerans: an infection from Jurassic time. *Lancet*, *2*, 1015–6.

[16] (a) Cave, A. J. (1939). The evidence for the incidence of tuberculosis in ancient Egypt. *Br. J. Tuberc.*, *33*, 142–152; (b) Nerlich, A. G. and Lösch, S. (2009). Paleopathology of human tuberculosis and the potential role of climate. *J. Archaeol. Sci.*, *23*, 789–798.

[17] Ahmad, T. (2014). History of Tuberculosis*: A short note*, *1*, 18–19.

[18] Daniel, T. M. (2006). The history of tuberculosis. *Respir. Med.*, *100*, 1862–1870.

[19] Daniel, T. M. (2000). The origins and precolonial epidemiology of tuberculosis in the Americas: can we figure them out? *Int. J. Tuberc. Lung Dis.*, *4*, 395–400.

[20] Roberts C. A. and Buikstra, J. E. (2003). *The bioarchaeology of tuberculosis: a global view on a reemerging disease* (pp. 344). Florida.

[21] Sakamoto, K. (2012). The Pathology of *Mycobacterium tuberculosis* Infection. *Vet. Pathol.*, *49*, 423–439.

[22] Grigg, E. (1958). The arcana of tuberculosis with a brief epidemiologic history of the disease in the U.S.A. IV. *Am. Rev. Tuberc.*, *78*, 583–603.

[23] Koch, R. (1884). The etiology [Koch's of tuberculosis postulates.]Die Aetiologie der Tuberkulose. Mittbeihgen aus dem Kaiserlichen Gesundbeitsamte. *The Germ Theor. Dis.*, *2*, 1–88.

[24] Koch, R. (1891). Continuation of communications on a cure for tuberculosis. *Ger. Med. Wochenschr.*, *17*, 101–102.

[25] Von Piquet, C. (1907). Frequency of tuberculosis in childhood. *J. AMA.*, *52*, 675–678.

[26] (a) Edwards, L. B., Acquaviva, F. A., Livesay, V. T., Cross, F. W. and Palmer, C. E. (1969). An atlas of sensitivity to tuberculin, PPDB, and histoplasmin in the United States. *Am. Rev. Respir. Dis., 99*, 1–132.

[27] Calmette, A. (1928). On preventive vaccination of the new-born against tuberculosis by B.C.G. *Brit. J. Tuberc., 22*, 161–165.

[28] Bryder, L. (1999). BCG vaccination in Scandinavia, Britain and the USA. *Soc. Sci. Med., 49*, 1157–1167.

[29] Feldberg, G. D. (1995). *Health and Medicine in American Society*. New Brunswick.

[30] (a) Menut, P. (2001). The Lübeck catastrophe and its consequences for anti-tuberculosis BCG-vaccination. In: Moulin AM, Cambrosio A, editors. Singular selves: historical issues and contemporary debates in immunology. Paris: Elsevier, 202–210. (b) Brimnes, N. (2011). Another vaccine, another story : BCG vaccination against tuberculosis in India, 1948 to 1960. *Cien. Saude Colet., 16*, 397–407.

[31] Rosenthal, S. R. (1980). Host response. In: BCG vaccination against tuberculosis, cancer. Boston. *Little Brown and Co.*, 76–98.

[32] Bonah, C. (2005). "The 'experimental stable' of the BCG Vaccine: Safety, Efficacy, Proof, and Standards, 1921–1933," Studies in History and Philosophy of *Biological and Biomedical Sciences, 36*, 696–721.

[33] Wallgren, A. (1948). BCG Inoculation and BCG Vaccination. *Am. J. Dis. Child., 76*, 485–491.

[34] Wallgren, A. (1949). Zur Frage der Tuberkulose-Schutzimpfung. *Beitr. Klin. Tuberk. Spezif. Tuberkuloseforsch., 101*, 296–315.

[35] Wilson, G. S. (1947). The value of B.C.G. vaccination in control of tuberculosis. *Br. Med. J., 2*, 855–859.

[36] W.H.O. (1948). Report of the expert commitee on tuberculosis. Bull. *WHO, 1*, 205–212.

[37] Archives, U. (1956). UNICEF-WHO Joint Commitee on health policy, ninth session. UN Archives JC9/UNICEF-WHO/Min/1.

[38] W.H.O. (1959). Review of BCG Vaccination Programmes. *Official Records of the WHO, 96*, 19–50.

[39] W.H.O. (1963). Justification and design for the undertaking of a large-scale BCG trial in India. WHO Archives, TB/Int./50; 60.

[40] W.H.O. (1977). Report on the ICMR Consultative Commitee on the Tuberculosis Prevention Trial. WHO Archives, T9/157/B/5; 20.

[41] W.H.O. (1980). Vaccination against tuberculosis: report of an ICMR/WHO scientific group. *WHO Technical Report Series, 651*, 1–21.

[42] W.H.O. (1983). The Executive Board. Summary records: Sixteenth meeting. WHO Archives, EB71/1983/REC/2; 63.

[43] W.H.O. (2009). Global Tuberculosis Control. Geneva: world Health Organization, http://whqlibdoc.who.int/publications/2009/9789241.

[44] W.H.O. (2010). Global tuberculosis control. Geneva: world Health Organization, http://whqlibdoc.who.int/publication/2010/97892415.

[45] W.H.O. (2011). Global Tuberculosis Control. Geneva: world Health Organization, http://whqlibdoc.who.int/publications/2011/9789241.

[46] W.H.O. (2013). Global Tuberculosis Report 2013. World Health Organization, 306. doi:10.3917/spub.092.0139.

[47] Phillips, I., and K. P. S. (1997). Aminoglycosides and aminocyclitols, 164–201. In F. O'Grady, H. P. Lambert, R. G. Finch, and D. G. (ed. (1997). *Antibiotic and chemotherapy* (7th Edi.). Churchill Livingstone, New York.

[48] Janin, Y. L. (2007). Antituberculosis drugs: ten years of research. *Bioorg. Med. Chem., 15*, 2479–2513.

[49] (a) Gilman, A. G., Rall, T. W., Nies, A. S. and Tylor, P. (1991). *Basis of Therapeutics* (8th Edi.). New. York. (b) Streicher, E. M., Bergval, I., Dheda, K., Böttger, E. C., Gey Van Pittius, N. C., Bosman, M., Coetzee, G., Anthony, R. M., Van Helden, P. D., Victor, T. C. and Warren, R. M. (2012). *Mycobacterium tuberculosis* population structure determines the outcome of genetics-based second-line drug resistance testing. *Antimicrob. Agents Chemother., 56*, 2420–2427.

[50] Iseman, M. D. (2002). Tuberculosis therapy: past, present and future. *Eur. Respir. J.. Supplement, 36*, 87s–94s.

[51] W.H.O. (2009). WHO Report 2009 Global Tuberculosis Control. Geneza: WHO. Retrieved from http://www.pubmedcentral.nih.gov/articlerender.fcgi.

[52] Vareldzis, B. P., Grosset, J., de Kantor, I., Crofton, J., Laszlo, A., Felten, M., Raviglione, M. C. and Kochi, A. (1994). Drug-resistant tuberculosis: laboratory issues. World Health Organization recommendations. *Tuber. Lung. Dis., 75*, 1–7.

[53] Espinal, M. A. (2003). The global situation of MDR-TB. *Tuber. Lung. Dis.*, *83*, 44–51.

[54] Shimao, T. (1987). Drug resistance in tuberculosis control. *Brit. Tuberc. Assoc.*, *68*, 5–18.

[55] Dye, C., Espinal, M. A., Watt, C. J., Mbiaga, C. and Williams, B. G. (2002). Worldwide incidence of multidrug-resistant tuberculosis. *J. Infect. Dis.*, *185*, 1197–1202.

[56] Vibol, I., Silaphet, S., Yves, B., Nicolas, S., Franck, B., Monique, C., Phannasinh, S., Phouratsamy, N., Alain, R., Jean-Luc, B. and Phimpha, P. (2013). Resistance of Mycobacterium tuberculosis to antibiotics in Lao PDR: first multicentric study conducted in 3 hospitals. *BMC Infect Dis.*, *13*, 275.

[57] Raviglione, M. C. (2010). *Lung Biology in Health and Disease* (4th Edi.). (World Health Organization, Geneva).

[58] Blöndal, K. (2007). A systematic review of inequalities in the use of maternal health care in developing countries. *Bulletin of the WHO*, *85*, 812 – 819.

[59] Neel, R. G., Anthony, M. A., Willem, S., Robert, P., Thiloshini, G., Umesh, L., Kimberly, Z., Jason, A. and Gerald, F. (2006). Extensively drug-resistant tuberculosis as a cause of death in patients co-infected with tuberculosis and HIV in a rural area of South Africa. *Lancet*, *368*, 1575 – 1580.

[60] Kumar, V., Abbas, A. K., Fausto, N. and Mitchell, R. N. (2007). *Robbins Basic Pathology* (8th Edi., pp. 516–522). California San Francisco.

[61] Cole, S. T., Brosch, R., Parkhill, J., Garnier, T., Churcher, C., Harris, D., Gordon, S. V., Eiglmeier, K., Gas, S., Barry III, C. E., Tekaia, F., Badcock, K., Basham, D., Brown, D., Chillingworth, T., Connor, R., Davies, R., Devlin, K., Feltwell, T., Gentles, B. G. (1998). Deciphering the biology of *Mycobacterium tuberculosis* from the complete genome sequence. *Nature*, *393*, 537–544.

[62] (a) Brennan, P.J. and Nikaido, H. (1995). The envelope of mycobacteria. *Annu. Rev. Biochem.*, *64*, 29–63. (b) Patterson, J. H., Waller, R. F., Jeevarajah, D., Billman-Jacobe, H., & McConville, M. J. (2003). Mannose metabolism is required for mycobacterial growth. *The Biochem. J.*, *372*, 77–86.

[63] http://www.turbosquid.com/3d-models/3d-mycobacterium-tuberculosis-model /683 10 5, accessed 07-08-2014.

[64] Betty, A. F., Daniel, F. S. and Alice, S. (2007). *Bailey & Scott's Diagnostic Microbiology* (12th Edi., pp. 93–119). Housto.

[65] Flowers, T. (1995). Quarantining the noncompliant TB patient: Catching the “red snapper.” *J. Health Hosp. Law*, *28*, 95–105.

[66] Awah-Ndukum, J., Kudi, A. C., Bradley, G., Ane-Anyangwe, I., Titanji, V. P., Fon-Tebug, S. and Tchoumboue, J. (2012). Prevalence of bovine tuberculosis in cattle in the highlands of Cameroon based on the detection of lesions in slaughtered cattle and tuberculin skin tests of live cattle. *Vet. Med.*, *57*, 59–76.

[67] Brosch, R., Gordon, S. V., Marmiesse, M., Brodin, P., Buchrieser, C., Eiglmeier, K., Garnier, T., Gutierrez, C., Hewinson, G., Kremer, K., Parsons, L. M., Pym, A. S., Samper, S., van Soolingen, D. and Cole, S. T. (2002). A new evolutionary scenario for the *Mycobacterium tuberculosis* complex. *Proc. Natl. Acad. Sci. U S A*, 99, 3684–3689.

[68] Garnier, T., Eiglmeier, K., Camus, J. C., Medina, N., Mansoor, H., Pryor, M., Duthoy, S., Grondin, S., Lacroix, C., Monsempe, C., Simon, S., Harris, B., Atkin, R., Doggett, J., Mayes, R., Keating, L., Wheeler, P. R., Parkhill, J., Barrell, B. G. and Cole, S. (2003). The complete genome sequence of *Mycobacterium bovis*. *Proc. Natl. Acad. Sci. U S A*, *100*, 7877–7882.

[69] Gordon, A. H. and Hart, P. D. (1994). Stimulation or inhibition of the respiratory burst in cultured macrophages in a mycobacterium model: Initial stimulation is followed by inhibition after phagocytosis. *Infect. Immun. 62*, 4650–4651.

[70] Lamhamedi-Cherradi, S., de Chastellier, C. and Casanova, J. L. (1999). Growth of *Mycobacterium bovis* bacille Calmette-Guerin, within human monocytes-macrophages cultured in serum-free medium. *J. Immunol. Methods, 225*, 75–86.

[71] Ayele, W. Y., Neill, S. D., Zinsstag, J., Weiss, M. G. and Pavlik, I. (2004). Bovine tuberculosis: an old disease but a new threat to Africa. *Int. J. Tuberc. Lung Dis.* , *8*, 924–37.

[72] Tanja K., Rimma A., Abigail W., Galimzhan R., Sabine, R. G. and S. N. (2006). *Mycobacterium bovisIsolates* with M. tuberculosis Specific Characteristics. *Emerg. Infect. Dis.*, *12*, 5–7.

[73] Prasad, H. K., Singhal, A., Mishra, A., Shah, N. P., Katoch, V. M., Thakral, S. S., Singh, D. V., Chumber, S., Bal, S., Aggarwal, S., Padma, M. V., Kumar, S., Singh, M. K. and Acharya, S. K. (2005). Bovine tuberculosis in India: potential basis for zoonosis. *Tuberculosis*, *85*, 421–8.

[74] Sharma, N., Sachan, S. K., Rai, R., Shukla, A., Nehra, A., Yadav, S. and Nautiyal, R. (2014). DNA Profiling Patterns of *Mycobacterium tuberculosis* and *Mycobacterium bovis*- A Review. *BMR Gene & Genome Biology, 1*, 1–17.

[75] https://www.google.co.uk/search/ M. bovis BCG, Identifiers J07AN01 accessed 20-12-2014.

[76] O'Reilly, L. M. and Daborn, C. J. (1995). The epidemiology of *Mycobacterium bovis* infections in animals and man: a review. *Tuber. Lung. Dis.*, *76*, 1–46.

[77] Wobeser, G. (2009). Bovine tuberculosis in Canadian wildlife: an updated history. *Can. Vet. J.*, *50*, 1169–1176.

[78] Gutiérrez, M., Tellechea, J. and G. M. J. (1998). Evaluation of cellular and serological diagnostic tests for the detection of *Mycobacterium bovis*-infected goats. *Vet. Microbiol.*, *62*, 281–290.

[79] Michel, A. L., Cooper, D., Jooste, J., de Klerk, L. M. and Jolles, A. (2011). Approaches towards optimising the gamma interferon assay for diagnosing *Mycobacterium bovis* infection in African buffalo (Syncerus caffer). *Prev. Vet. Med.*, *98*, 142–151.

[80] Lilenbaum, W., Pessolani, M. C. and Fonseca, L. S. (2001). The Use of Ag85 Complex as Antigen in ELISA for the Diagnosis of Bovine Tuberculosis in Dairy Cows in Brazil. *J. Vet. Med.*, *48*, 161–6.

[81] Bennett, R. M. and Cooke, R. J. (2006). "Costs to farmers of a TB breakdown." *Vet. Record*, *158*, 429–432.

[82] Schaefer, W. B. (1952). Growth Requirements of Dysgonic and Eugonic strains of *Mycobacterium tb* VAR. Bovis. *J. Exp. Med.*, *96*, 207–219.

[83] Niemann, S., Richter, E. and Rüsch-Gerdes, S. (2000). Differentiation among members of the *Mycobacterium tuberculosis* complex by molecular and biochemical features: evidence for two pyrazinamide-susceptible subtypes of M. bovis. *J. Clin. Microbiol.* , *38*, 152–7.

[84] Mariam, S. H. (2009). Interaction between *lactic acid bacteria* and *Mycobacterium bovis* in Ethiopian fermented milk: Insight into the fate of M. bovis. *Applied and Environ. Microbiol.*, *75*, 1790–1792.

[85] Newbold, C. J. and Wallace, R. J. (1988). Effects of the ionophores monensin and tetronasin on simulated development of ruminal lactic acidosis in vitro. *Applied and Environ. Microbiol.*, *54*, 2981–2985.

[86] Russell, J. B., Cotta, M. A. and Dombrowski, D. B. (1981). Rumen bacterial competition in continuous culture: *Streptococcus bovis* versus Megasphaera elsdenii. *Applied and Environ. Microbiol.*, *41*, 1394–1399.

[87] Le Dantec, C., J. P. Duguet, A. Montiel, N. Dumoutier, S. Dubrou, and V., & Vincent. (2002). Chlorine disinfection of atypical mycobacteria isolated from a water distribution system. *Appl. Environ. Microbiol.*, *68*, 1025–1032.

[89] Griffith, D. E., Aksamit, T., Brown-Elliott, B. A., Catanzaro, A., Daley, C., Gordin, F., Holland, S. M., Horsburgh, R., Huitt, G., Iademarco, M. F., Iseman, M., Olivier, K., Ruoss, S., von Reyn, C. F., Wallace, R. J. and Winthrop, K. (2007). An Official ATS/IDSA Statement: Diagnosis, Treatment, and Prevention of Nontuberculous Mycobacterial Diseases. *Amer. J. Resp.Crit.Care Med. 175*, 367–416.

[90] Moore, J. E., Kruijshaar, M. E., Ormerod, L. P., Drobniewski, F. and Abubakar, I. (2010). Increasing reports of non-tuberculous *mycobacteria* in England, Wales and Northern Ireland, 1995-2006. *BMC Public Health, 10*, 612.

[91] Theodore, K. M., Pamela, C., Alicia, M. Y. and Frances, J. (2007). Isolation prevalence of pulmonary non-tuberculous mycobacteria in Ontario, 1997–2003. *Can. Resp. J., 62*, 661–666.

[92] Won-Jung, K., Kwon, O. J. and Lee, K. S. (2005). Diagnosis and treatment of nontuberculous mycobacterial pulmonary diseases: A Korean perspective. *J. Korean Med. Sci., 20*, 913–925.

[93] Maugein, J., Dailloux, M., Carbonnelle, B., Vincent, V. and Grosset, J. (2005). Sentinel-site surveillance of Mycobacterium avium complex pulmonary disease. *Eur. J. Resp. Dis., 26*, 1092–6.

[94] Timpe, A. and Runyon, E. H. (1954). The relationship of atypical acid-fast bacteria to human disease; a preliminary report. *J. Lab. Clin. Med., 44*, 202–9.

[95] Runyon, E. H. (1959). Anonymous mycobacteria in pulmonary disease. *The Medical Clinics of North America., 43*, 273–90.

[96] Hnatko, S. I. (1953). The isolation of bacteriophages for mycobacteria with reference to phage typing of the genus. *Med. Clin. North Am., 31*, 462–73.

[97] Schaefer, W. B. (1965). Serologic identification of the atypical *mycobacteria* and its value in epidemiologic studies. *Am. Rev. Respir. Dis., 92*, 85–93.

[98] Parlitt, R. and Youmans, G. P. (1958). Antigenic relationship between ninety-eight strains of *mycobacteria* using gel-diffusion precipitation techniques. *Am. Rev. Tuberc., 77*, 450–461.

[99] Thoen, O., Karlson, G. and Himes, M. (1981). Mycobacterial infections in animals. *Rev. Infect. Dis., 3*, 960–972.

[100] Wayne, L. G. and Sramek, H. A. (1992). Agents of newly recognized or infrequently encountered mycobacterial diseases. *Clin. Microbiol. Rev., 5*, 1–25.

[101] Thorel, M. F., Krichevsky, M. and Lévy-Frébault, V. V. (1990). Numerical taxonomy of mycobactin-dependent mycobacteria, emended description of *Mycobacterium avium*, and description of *Mycobacterium avium* subsp. avium subsp. nov., *Mycobacterium avium* subsp.

paratuberculosis subsp. nov., and Mycobacterium avium subsp.s. *Int. J. Syst Bacteriol., 40*, 254–60.

[102] http://pl.wikipedia.org/wiki/*Mycobacterium_avium*_complex accessed 20-12-2014.

[103] Aberg, J. A., Yajko, D. M. and Jacobson, M. A. (1998). Eradication of AIDS related disseminated *Mycobacterium avium* complex after twelve months anti-mycobacterial therapy combined with highly active antiretroviral therapy. *J. Infect. Dis., 178*, 1446 –1449.

[104] Cinti, S. K., Kaul, D. R., Sax, P. E., Crane, L. R. and Kazanjian, P. H. (2000). Recurrence of *Mycobacterium avium* infection in patients receiving highly active antiretroviral therapy and antimycobacterial agents. *Clin. Infect. Dis., 30*, 511–514.

[105] Corbett, E. L., Churchyard, G. J., Hay, M., Herselman, P., Clayton, T., Williams, B., Hayes, R., Mulder, D. and De Cock, K. M. (1999). The impact of HIV infection on *Mycobacterium kansasii* disease in South African gold miners. *Amer. J. Resp.Crit.Care Med. 160*, 10–4.

[106] Huang, J. H., Kao, P. N., Adi, V. and Ruoss, S. J. (1999). Mycobacterium avium-intracellulare pulmonary infection in HIV-negative patients without preexisting lung disease: Diagnostic and management limitations. *Chest, 115*, 1033–1040.

[107] Arsenault, R. J., Li, Y., Bell, K., Doig, K., Potter, A., Griebel, P. J., Kusalik, A. and Napper, S. (2012). *Mycobacterium avium* subsp. Paratuberculosis inhibits gamma interferon-induced signaling in bovine monocytes: Insights into the cellular mechanisms of Johne's disease. *Infect. Immun. 80*, 3039–3048.

[108] Karen, S., Julio, A., Douwe, B., Franck, B., Lucia, de J., Susan, D., Zoi, D., Karen, D., Gerald, F. G., Ian, H., Marketa, K., Linda, M., Ivo Pavlik, J., Michael, S., Virginie, C. T., Peter, W., Ruth, N. Z. and Alastair, G. (2009). Occurrence of Mycobacterium avium subspecies paratuberculosis across host species and European countries with evidence for transmission between wildlife and domestic ruminants. *BMC Microbiology, 9*, 212.

[109] Good, M., Clegg, T., Sheridan, H., Yearsely, D., O'Brien, T., Egan, J. and Mullowney, P. (2009). Prevalence and distribution of paratuberculosis (Johne's disease) in cattle herds in Ireland. *Irish Vet. J., 62*, 597–606.

[110] Whittington, R. J. and Sergeant, E. S. (2001). Progress towards understanding the spread, detection and control of *Mycobacterium avium* subsp. paratuberculosis in animal populations. *Australian Vet. J., 79*, 267–278.

[111] Kennedy, D. J., & Benedictus, G. (2001). Control of *Mycobacterium avium* subsp. paratuberculosis infection in agricultural species. *Rev. Sci. Tech. (International Office of Epizootics), 20*, 151–179.

[112] Masala, S., Cossu, D., Pacifico, A., Molicotti, P. and Sechi, L. A. (2012). Sardinian Type 1 diabetes patients, Transthyretin and *Mycobacterium avium* subspecies paratuberculosis infection. *Gut Pathog.*, *4*, 24.

[113] Johnson-Ifearulundu, Y., Kaneene, J. B. and Lloyd, J. W. (1999). Herd-level economic analysis of the impact of paratuberculosis on dairy herds. *J. Am. Vet. Med. Assoc., 214*, 822–825.

[114] Horsburgh, C. R. and Selik, R. M. (1989). The epidemiology of disseminated nontuberculous mycobacterial infection in the acquired immunodeficiency syndrome (AIDS). *Am. Rev. Respir. Dis., 139*, 4–7.

[115] Nachamkin, I., Macgregor, R. R., Staneck, J. L., Tsang, A. Y., Denner, J. C., Willner, M. and Barbagallo, S. (1992). Niacin-positive *Mycobacterium kansasii* isolated from immunocompromised patients. *J. Clin. Microbiol. , 30*, 1344–1346.

[116] Valainis, G. T., Cardona, L. M. and Greer, D. L. (1991). The spectrum of Mycobacterium kansasii disease associated with HIV-1 infected patients. *J. Acquir. Immune Defic. Syndr., 4*, 516–520.

[117] Griffith, D. E. (2002). Management of disease due to Mycobacterium kansasii. *Clin. Chest. Med., 23*, 613–621.

[118] https://www.google.co.uk/search M. kansasii, bacterioweb.univ-fcomte accessed 07-08-2014.

[119] Steadham, J. E. (1980). High-catalase strains of Mycobacterium kansasii isolated from water in Texas. *J. Clin. Microbiol. , 11*, 496–498.

[120] Engel, H.W., Berwald, L. G. and Havelaar, A. H. (1980). The occurrence of Mycobacterium kansasii in tapwater. *Tubercle., 61*, 21–6.

[121] Lillo, M., Orengo, S., Cernoch, P. and Harris, R. L. (1990). Pulmonary and disseminated infection due to Mycobacterium kansasii: a decade of experience. *Rev. Infect. Dis., 12*, 760–767.

[122] Waters, W. R., Palmer, M. V., Thacker, T. C., Payeur, J. B., Harris, N. B., Minion, F. C., Greenwald, R., Esfandiari, J., Andersen, P., McNair, J., Pollock, J. M. and Lyashchenko, K. P. (2006). Immune responses to defined antigens of Mycobacterium bovis in cattle experimentally infected with Mycobacterium kansasii. *Clin. Vaccine Immunol., 13*, 611–619.

[123] Al-Anazi, K. A., Al-Jasser, A. M. and Al-Anazi, W. K. (2014). Infections Caused by Non-Tuberculous Mycobacteria in Recipients of Hematopoietic Stem Cell Transplantation. *Front. Oncol.*, *4*, 311.

[124] Foti, C., Sforza, Vi., Rizzo, C., De Pascale, G., Bonamonte, D., Conserva, A., Tarantino, A., Stella, C., Cantore, S., Grassi, R. F., Ballini, A., De Vito, D. and Angelini, G. (2009). Cutaneous manifestations of *Mycobacterium gordonae* infection described for the first time in Italy: a case report. *Cases J.*, *2*, 6828.

[125] http://www.snipview.com/q/*Mycobacterium*%20gordonae accessed 14-02-2015.

[126] Bagarazzi, M. L., Watson, B., Kim, L. K., Hogarty, M. and McGowan, K. L. (1996). Pulmonary *Mycobacterium gordonae* infection in a two-year-old child: case report. *Clin. Infect. Dis.*, *22*, 1124–1125.

[127] Weinberger, M., Berg, S. L., Feuerstein, I. M., Pizzo, P. A. and Witebsky, F. G. (1992). Disseminated infection with *Mycobacterium gordonae*: report of a case and critical review of the literature. *Clin. Infect. Dis.*, *14*, 1229–39.

[128] Jarikre, L. N. (1992). *Mycobacterium gordonae* genitourinary disease. *Genitourin. Med.*, *68*, 45–46.

[129] Gengoux, P., Portaels, F., Lachapelle, J. M., Minnikin, D. E., Tennstedt, D. and Tamigneau, P. (1987). Skin granulomas due to *Mycobacterium gordonae*. *Int. J. Dermatology*, *26*, 181–184.

[130] Moore, M. B., Newton, C. and Kaufman, H. E. (1986). Chronic keratitis caused by *Mycobacterium gordonae*. *American Journal of Ophthalmology*, *102*, 516–521.

[131] Busillo, C. P. (1992). Multidrug resistant *Mycobacterium tuberculosis* in patients with human immunodeficiency virus infection. *Chest J.*, *102*, 797.

[132] Vogiatzakis, E., Stefanou, S., Skroubelou, A., Anagnostou, S., Marinis, E. and Matsiota-Bernard, P. (1993). Molecular markers for the investigation of Mycobacterium gordonae epidemics. *Clin. Infect. Dis.*, *16*, 463–471.

[133] Bonnet, E., Massip, P., Bauriaud, R., Alric, L. and Auvergnat, J.-C. (1996). "Disseminated Mycobacterium gordonae infection in a patient infected with human immunodeficiency virus,." *Clin. Infect. Dis.*, *23*, 644–645.

[134] Barber, T. W. (1991). M gordonae: A Possible Opportunistic Respiratory Tract Pathogen. *Chest*, *100*, 716–720.

[135] Kirschner, P. and Bottger, E. C. (1992). Letter to the Editor Microheterogeneity within rRNA of Mycobacterium gordonae. *J. Clin. Microbiol.* , *30*, 1049–1050.

[136] Walton, D. T. and Valesco, M. (1991). Identification of Mycobacterium gordonae from culture by the Gen-Probe Rapid Diagnostic System: Evaluation of 218 isolates and potential sources of false-negative results. *J. Clin. Microbiol. , 29*, 1850–1854.

[137] Smith, M. B., Schnadig, V. J., Boyars, M. C. and Woods, G. L. (2001). Clinical and pathologic features of *Mycobacterium fortuitum* infections: An emerging pathogen in patients with AIDS. *Am. J. Clin. Pathol., 116*, 225–232.

[138] Brown, T. H. (1985). The rapidly growing mycobacteria--*Mycobacterium fortuitum* and *Mycobacterium chelonei*. *Infect. Control., 6*, 283–288.

[139] Heidarieh, P., Shojaei, H., Feizabadi, M. M., Havaei, A., Hashemi, A., Ataei, B. and Naser, A. D. (2010). Molecular Identification and Conventional Susceptibility Testing of Iranian Clinical *Mycobacterium fortuitum* Isolates. *Iran. J. Basic. Med. Sci. , 13*, 210–215.

[140] Wallace, R. J., Silcox, V. A., Tsukamura, M., Brown, B. A., Kilburn, J. O., Butler, W. R. and Ony, G. (1993). Clinical significance, biochemical features, and susceptibility patterns of sporadic isolates of the *Mycobacterium chelonae*-like organism. *J. Clin. Microbiol. , 31*, 3231–3239.

[141] Ingram, C. W., Tanner, D. C., Durack, D. T., Kernodle, G. W. and Corey, G. R. (1993). Disseminated infection with rapidly growing mycobacteria. *Clin. Infect. Dis., 16*, 463–471.

[142] http://www.superstock.com/stock-photography/*Mycobacterium+fortuitum* accessed 20-12-2014.

[143] Subcommittee, T. (2000). Management of opportunist mycobacterial infections: Joint Tuberculosis Committee guidelines 1999. *Thorax, 55*, 210–218.

[144] Diagnosis and treatment of disease caused by nontuberculous mycobacteria. This official statement of the American Thoracic Society was approved by the Board of Directors, March 1997. Medical Section of the American Lung Association. (1997). *Amer. J. Resp.Crit.Care Med.* 156, S1–S25.

[145] Gillespie, S. H., Basu, S., Dickens, A. L., O'Sullivan, D. M. and McHugh, T. D. (2005). Effect of subinhibitory concentrations of ciprofloxacin on *Mycobacterium fortuitum* mutation rates. *J. Antimicrob. Chemother., 56*, 344–348.

[146] Lim, Amanda and Dick, T. (2001). Plate-based dormancy culture system *for Mycobacterium smegmatis* and isolation of metronidazole-resistant mutants. *FEMS Microbiol. Letts., 200*, 215–219.

[147] Smeulders, M. J., Keer, J., Speight, R. A. and Williams, H. D. (1999). Adaptation of *Mycobacterium smegmatis* to Stationary Phase Adaptation of *Mycobacterium smegmatis* to Stationary Phase. *J. Bacteriol., 181*, 270–283.

[148] Brown-Elliott, B. A. and Wallace, R. J. (2002). Clinical and taxonomic status of pathogenic nonpigmented or late-pigmenting rapidly growing *mycobacteria. Clin. Microbiol. Rev., 15*, 716–746.

[149] Syed, H. A., Khalid, A., Sikander, K. S., Nazia, B. and Shahana, U. K. (2014). Detection of *Mycobacterium Smegmatis* Biofilm and its Control by Natural Agents. *Int. J. Curr. Microbiol. Appl. Sci., 3*, 801–812.

[150] https://www.google.co.uk/search *M. smegmatis* accessed 20-12-2014.

[151] Cayabyab, M. J., Hovav, A. H., Tsungda, K., Georgia R. L., Michelle, A., Gorgone, Darci, A., Fennelly, G. J., Haynes, B. F., Jacobs, W. R. and Letvin, N. L. (2006). Generation of CD8 ♀ T-Cell Responses by a Recombinant Nonpathogenic Mycobacterium smegmatis Vaccine Vector Expressing Human Immunodeficiency Virus Type 1 Env. *Society, 80*, 1645–1652.

[152] Bartram, J., Cotruvo, J., Exner, M., Fricker, C. and Glasmacher, A. (2003). Heterotrophic plate counts and drinking-water safety. *World Health Organization: The Significance of HPCs for Water Quality and Human Health*, 271.

[153] Reyrat, J. M., Kahn, D. (2001). *Mycobacterium smegmatis*: an absurd model for tuberculosis. *Trends Microbiol., 9*, 472–474.

[154] Tyagi, J. S. and Sharma, D. (2002). *Mycobacterium smegmatis* and tuberculosis. *Trends Microbiol., 10*, 68–9.

[155] Garrait, V., Cadranel, J., Esvant, H., Herry, I., Morinet, P., Mayaud, C. and Israël-Biet, D. (1997). Tuberculosis generates a microenvironment enhancing the productive infection of local lymphocytes by HIV. *J. Immunol., 159*, 2824–2830.

[156] Haraguchi, S., Day, N. K., Kamchaisatian, W., Beigier-Pompadre, M., Stenger, S., Tangsinmankong, N., Sleasman, J. W., Pizzo, S. V. and Cianciolo, G. J. (2006). LMP-420, a small-molecule inhibitor of TNF-alpha, reduces replication of HIV-1 and *Mycobacterium tuberculosis* in human cells. *AIDS Res. Ther., 3*, 8.

[157] Audu, R. A. (2005). Possible Impact of Co-Infections of Tuberculosis and Malaria on The CD4+ Cell Counts of HIV Patients in Nigeria. *Ann. Afr. Med., 4*, 10–13.

[158] Padmapriyadarsini, C., Narendran, G. and Swaminathan, S. (2011). Diagnosis & treatment of tuberculosis in HIV co-infected patients. *Indian J. Med. Res., 134*, 850–865.

[159] Kremer, L. and Besra, G. S. (2002). Re-emergence of tuberculosis: strategies and treatment. *Expert Opin. Investig., 11*, 153–157.

[160] Asselineau, J. and Lanéelle, G. (1998). Université Paul Sabatier (Toulouse 3) 1 and Institut de Pharmacologie et de Biologie Structurale du CNRS, 205 route de Narbonne, 31077 Toulouse, Cedex, France. *Front. Biosci, 3*, 164–174.

[161] Dye, C., Watt, C. J., Bleed, D. M., Hosseini, S. M. and Raviglione, M. C. (2005). Evolution of tuberculosis control and prospects for reducing tuberculosis incidence, prevalence, and deaths globally. *J. AMA., 293*, 2767–2775.

[162] Viviana Ritacco, M. G. M. and L. F. G. (2011). The Situation of HIV/Mycobacterium tuberculosis Co-Infection in South America. *The Open Infect. Dis. J., 5*, 81–88.

[163] Ortalo-Magné, A., Dupont, M. A., Lemassu, A., Andersen, A. B., Gounon, P. and Daffé, M. (1995). Molecular composition of the outermost capsular material of the tubercle bacillus. *Microbiology, 141*, 1609–1620.

[164] Lederer, E. (1971). The mycobacterial cell wall. *Pure and Applied Chemistry, 25*, 135–165.

[165] Liu, J., Barry III, C. E. and Nikaido, H. (1998). Cell wall: physical structure and permeability. *Mycobacteria: Molecular Biology and Virulence*, 1–44. Retrieved from Ratledge, C., and Dale, J.W. (eds). Philadelphia, PA: Chapman & Hall.

[166] Brennan, P. J. (2003). Structure, function, and biogenesis of the cell wall of Mycobacterium tuberculosis. *Tuberculosis, 83*, 91–97.

[167] Brennan, P.J. and Nikaido, H. (1995). The envelope of *mycobacteria*. *Annu. Rev. Biochem., 64*, 29–63.

[168] Minnikin, D. E. (1982). In The Biology of the *Mycobacteria*. *Academic, 1*, 95–184. Edited by C. Ratledge and J. L. Stanford. Retrieved from London: Academic Press.

[169] http://image.slidesharecdn.com/mycobacteriumtuberculosis-110228130131-phpapp 02/95 / *mycobacterium-tuberculosis*-13-728.jpg? cb=1423765369 accessed 20-12-2014.

[170] Black, M. T. and Bruton, G. (1998). Inhibitors of bacterial signal peptidases. *Curr. Pharm. Des., 4*, 133–154.

[171] Nikaido, H. (1994). Prevention of drug access to bacterial targets: permeability barriers and active efflux. *Science, 264*, 382–388.

[172] Barry III, C. E. and Mdluli, K. (1996). Drug sensitivity and environmental adaptation of mycobacterial cell wall components. *Trends Microbiol., 4*, 275–281.

[173] McNeil, M., Daffe, M. and Brennan, P. J. (1991). Location of the mycolyl ester substituents in the cell walls of mycobacteria. *J. Biol. Chem., 266*, 13217–13223.

[174] Anderson, R. J. (1941). Structural peculiarities of acid-fast bacterial lipids. *Chem. Rev., 29*, 225–243.

[175] Barry III, C. E., Lee, R. E., Mdluli, K., Sampson, A. E., Schroeder, B. G., Slayden, R. A. and Yuan, Y. (1998). Mycolic acids: structure, biosynthesis and physiological functions. *Prog. Lipid Res. , 37*, 143–179.

[176] Minnikin, D. E. and Polgar, N. (1967). Structural studies on the mycolic acids. *Chem. Commun., 7*, 312–314.

[177] Minnikin, D. E. and Polgar, N. (1966). Studies on the mycolic acids from human tubercle bacilli. *Tetrahedron Lett., 23*, 2643–2647.

[178] Minnikin, D. E. and Polgar, N. (1967). Mycolic Acids from Human and Avian Tubercle Bacilli. *Chem. Commun., 18*, 916–918.

[179] Minnikin, D. E. and Polgar, N. (1967). Methoxymycolic and ketomycolic acids from human Tubercle Bacilli. *Chem. Commun., 22*, 1172–1174.

[180] Watanabe, M., Aoyagi, Y., Ridell, M. and Minnikin, D. E. (2001). Separation and characterization of individual mycolic acids in representative mycobacteria. *Microbiology, 147*, 1825–37.

[181] Watanabe, M., Aoyagi, Y., Mitome, H., Fujita, T., Naoki, H., Ridell, M. and Minnikin, D. E. (2002). Location of functional groups in mycobacterial meromycolate chains; the recognition of new structural principles in mycolic acids. *Microbiology, 148*, 1881–902.

[182] Rastogi, N. (1991). Recent observations concerning structure and function relationships in the mycobacterial cell envelope: elaboration of a model in terms of mycobacterial pathogenicity, virulence and drug-resistance. *Res. Microbiol., 142*, 464–76.

[183] Xuan Hong and Hopfinger, A. J. (2004). Construction, Molecular Modeling, and Simulation of Mycobacterium tuberculosis Cell Walls. *Biomacromolecules, 5*, 1052–1065.

[184] Jackson, M., Raynaud, C., & Lanéelle, M. A., Guilhot, C., Laurent-Winter, C., Ensergueix, D., Gicquel, B. and Daffé, M. (1999). Inactivation of the antigen 85C gene profoundly affects the mycolate content and alters the permeability of the *Mycobacterium tuberculosis* cell envelope. *Mol. Microbiol., 31*, 1573–1587.

[185] Puech, V., Chami, M., Lemassu, A., Lanèelle, M.-A., Schiffler, B., Gounon, P., Bayan, N., Benz, R. and Daffé, M. (2001). Structure of the cell envelope of corynebacteria: importance of

the non-covalently bound lipids in the formation of the cell wall permeability barrier and fracture plane. *Microbiology, 147*, 1356–1382.

[186] Koza, G., Theunissen, C., Al Dulayymi, J. R., and Baird, M. S. (2009). The synthesis of single enantiomers of mycobacterial ketomycolic acids containing cis-cyclopropanes. *Tetrahedron, 65*, 10214–10229.

[187] Minnikin, D. E. (1993). An Integrated Procedure for the Direct Detection of Characteristic Lipids in Tuberculosis Patients. *Ann. Soc. Belg. Med. Trop. J., 73*, 13–24.

[188] Dobson, G., Minnikin, D. E., Minnikin, S. M., Parlett, J. H., Goodfellow, M. , Ridell, M. and Magnuson, M. (1985). Systematic analysis of complex mycobacterial lipids. *Chem. Methods in Bacterial Syst.*, 237–265.

[189] Minnikin, D. E., Minnikin, S. M., Parlett, J. H., Goodfellow, M. and Magnusson, M. (1984). Mycolic acid patterns of some species of *Mycobacterium. Arch. Microbiol., 139*, 225–231.

[190] Kaneda, K., Imaizumi, S., Mizuno, S., Baba, T., Tsukamura, M. and Yano, I. (1988). Structure and molecular species composition of three homologous series of alpha-mycolic acids from *Mycobacterium* spp. *J Gen. Microbiol., 134*, 2213–2229.

[191] Qureshi, N., Takayama, K., Jordi, H. C. and Schnoes, H. K. (1978). Characterization of the purified components of a new homologous series of alpha-mycolic acids from *Mycobacterium tuberculosis* H37Ra. *J. Biol. Chem., 253*, 5411–5417.

[192] Steck, P. A., Schwartz, B. A., Rosendahl, M. S. and Gray, G. R. (1978). Mycolic acids. A reinvestigation. *J. Biol. Chem., 253*, 5625–5629.

[193] Butler, W. R and Guthertz, L. S. (2001). Mycolic Acid Analysis by High-Performance Liquid Chromatography for Identification of *Mycobacterium* Species, *Clin. Microbiol. Rev., 14*, 704–726.

[194] Minnikin, D.E., Minnikin, S.M. and Goodfellow, M. (1982). The oxygenated mycolic acids of *Mycobacterium fortuitum, M. farcinogenes* and *M. senegalense*. *Biochim. Biophys. Acta., 712*, 616–620.

[195] Goodfellow, M., Minnikin, D. E. (1981). Identification of mycobacterium chelonei by thin-layer chromatographic analysis of whole-organism methanolysates. *Tubercle, 62*, 285–7.

[196] Minnikin, D. E., Minnikin, S. M., Goodfellow, M. and Stanford, J. L. (1982). The mycolic acids of *Mycobacterium chelonei*. *J Gen. Microbiol., 128*, 817–822.

[197] Lanéelle, M. A. and Lanéelle, G. (1970). Structure of mycolic acids and an intermediate in the biosynthesis of dicarboxylic mycolic acids. *Eur. J. Biochem., 12*, 296–300.

[198] Luquin, M., Roussel, J., Lopez-Calahorra, F., Lanéelle, G., Ausina, V. and Lanéelle, M. A. (1990). A novel mycolic acid in a *Mycobacterium* sp. from the environment. *Eur. J. Biochem., 192*, 753–759.

[199] Heym, B. and Cole, S. T. (1992). Isolation and characterization of isoniazid-resistant mutants of *Mycobacterium smegmatis* and M. aurum. *Res. Microbiol., 143*, 721–30.

[200] Quémard, A., Lanéelle, M. A., Marrakchi, H., Promé, D., Dubnau, E. and Daffé, M. (1997). Structure of a hydroxy mycolic acid potentially involved in the synthesis of oxygenated mycolic acids of the *Mycobacterium tuberculosis* complex. *Eur. J. Biochem., 250*, 758–63.

[201] Dubnau, E., Lanéelle, M. A., Soares, S., Bénichou, A., Vaz, T., Promé, D., Promé, J. C., Daffé, M. and Quémard, A. (1997). *Mycobacterium bovis* BCG genes involved in the biosynthesis of cyclopropyl keto- and hydroxy-mycolic acids. *Mol. Microbiol., 23*, 313–22.

[202] Toubiana, R., Berlan, J., Sato, H. and Strain, M. (1979). Three types of mycolic acid from Mycobacterium tuberculosis Brévanne: implications for structure-function relationships in pathogenesis. *J. Bacteriol., 139*, 205–211.

[203] Davidson, L. A., Draper, P. and Minnikin, D. E. (1982). Studies on the mycolic acids from the walls of *Mycobacterium microti*. *J Gen. Microbiol., 128*, 823–828.

[204] Laval, F., Lanéelle, M. A., Déon, C., Monsarrat, B. and Daffé, M. (2001). Accurate molecular mass determination of mycolic acids by MALDI-TOF mass spectrometry. *Anal. Chem., 73*, 4537–4544.

[205] Daffé, M., Lanéelle, M. A. and Valero Guillen, P. L. (1988). Tetraenoic and pentaenoic mycolic acids from *Mycobacterium thamnopheos*. Structure, taxonomic and biosynthetic implications. *Eur. J. Biochem. / FEBS, 177*, 339–344.

[206] Daffé, M. (1991). Further stereochemical studies of phthiocerol and phenol phthiocerol in mycobacteria. *Res. Microbiol., 142*, 405–410.

[207] Marrakchi, H., Lanéelle, M. A. and Daffé, M. (2014). Mycolic acids: Structures, biosynthesis, and beyond. *Chem. Biol., 21*, 67–85.

[208] Koza, G., and Baird, M. S. (2007). The first synthesis of single enantiomers of ketomycolic acids. *Tetrahedron Lett., 48*, 2165–2169.

[209] Moody, D. B., Guy, M. R., Grant, E., Cheng, T. Y., Brenner, M. B., Besra, G. S. and Porcelli, S. A. (2000). CD1b-mediated T cell recognition of a glycolipid antigen generated from mycobacterial lipid and host carbohydrate during infection. *J. Exp. Med., 192*, 965–976.

[210] Watanabe, R. Y., Yung C., Hata, K., Mitobe, M., Koike, Y., Nishizawa, M., Garcia, D. M., Nobuchi, Y., Imagawa, H., Yamada, H. and Azuma, I. (1999). Inhibitory effect of trehalose

dimycolate (TDM) and its stereoisometric derivatives, trehalose dicorynomycolates (TDCMs), with low toxicity on lung metastasis of tumour cells in mice. *Vaccine, 17*, 1484–1492.

[211] Dubnau, E., Chan, J., Raynaud, C., Mohan, V. P., Lanéelle, M. A., Yu, K., Quémard, A., Smith, I. and Daffé, M. (2000). Oxygenated mycolic acids are necessary for virulence of *Mycobacterium tuberculosis* in mice. *Mol. Microbiol., 36*, 630–7.

[212] Yuan, Y., Zhu, Y., Crane, D. D., Barry III, C. E. (1998). The effect of oxygenated mycolic acid composition on cell wall function and macrophage growth in *Mycobacterium tuberculosis*. *Mol. Microbiol., 29*, 1449–1458.

[213] Yuan, Y. and Barry III, C. E. (1996). A common mechanism for the biosynthesis of methoxy and cyclopropyl mycolic acids in *Mycobacterium tuberculosis. Proc. Natl. Acad. Sci. U S A, 93*, 12828–12833.

[214] Riley, L. W. (2006). Of mice, men, and elephants: *Mycobacterium tuberculosis* cell envelope lipids and pathogenesis. *J. Clin. Invest., 116*, 4–7.

[215] Dubnau, E., Lanéelle, M. A., Soares, S., Bénichou, A., Vaz, T., Promé, D., Promé, J. C., Daffé, M. and Quémard, A. (1997). *Mycobacterium bovis* BCG genes involved in the biosynthesis of cyclopropyl keto- and hydroxy-mycolic acids. *Mol. Microbiol., 23*, 313–322.

[216] Lacave, C., Laneelle, M. A., Daffé, M., Montrozier, H., Rols, M. P. and Asselineau, C. (1987). Etude structurale et mbtabolique des acides mycoliques de *Mycobacterium fortuitum*. *Eur. J. Biochem., 163*, 369–378.

[217] Daffé, M., Lanéelle, M. A., Lacave, C. (1991). Structure and stereochemistry of mycolic acids of Mycobacterium marinum and Mycobacterium ulcerans. *Res. Microbiol., 142*, 397–403.

[218] Marie-Antoinette, L., Charlotte, L., Mamadou, D. and Gilbert, L. (1988). Mycolic acids of *Mycobacterium aurum* Structure and biogenetic implications. *Eur. J. Biochem.y, 635*, 631–635.

[219] Al-Dulayymi, J. R., Baird, Mark S., Mohammed, Hayder, Roberts, Evan and Clegg, W. (2006). The synthesis of one enantiomer of the α-methyl-trans-cyclopropane unit of mycolic acids. *Tetrahedron, 62*, 4851–4862.

[220] Anderson R. J., Creighton, M. M. and R. L. P. (1940). Lipids of the Avian Tubercle Concerning the Firmly Bound Tubercle Bacilli: LX. The Chemistry of the lipids of Bacillus. *J. Biol. Chem., 133*, 675–693.

[221] Wang, L., Slayden, R. a., Barry, C. E. and Liu, J. (2000). Cell wall structure of a mutant of Mycobacterium smegmatis defective in the biosynthesis of mycolic acids. *J. Biol. Chem., 275*, 7224–7229.

[222] Liu, Jun, Barry, Clifton E., Besra, Gurdyal S. and Nikaido, H. (1996). Mycolic acid structure determines the fluidity of the mycobacterial cell wall. *J. Biol. Chem., 271*, 29545–29551.

[223] Glickman, M. S., Cox, J. S. and Jacobs, W. R. (2000). A novel mycolic acid cyclopropane synthetase is required for cording, persistence, and virulence of *Mycobacterium tuberculosis*. *Mol. Cell, 5*, 717–727.

[224] Grogan, D. W. and Cronan, J. E. (1997). Cyclopropane ring formation in membrane lipids of bacteria. *Microbiol. Mol. Biol. Rev., 61*, 429–441.

[225] Yuan, Y., Crane, Deborah C., Musser, J. M., Sreevatsan, S. and Barry III, C. E. (1997). MMAS-1, the Branch Point Between cis- and trans-Cyclopropanecontaining Oxygenated Mycolates in *Mycobacterium tuberculosis*. *The J. Biol. Chem., 272*, 10041–10049.

[226] Hasegawa, T. and Leblanc, R. M. (2003). Aggregation properties of mycolic acid molecules in monolayer films: a comparative study of compounds from various acid-fast bacterial species. *Biochim. Biophys. acta, 1617*, 89–95.

[227] Adam, B., David, A., Tania, D. P., Manon, G., Joses, J., Erwin, S., Jun, L., David, R. S. and Marcel, A. B. (2004). Impact of Methoxymycolic Acid Production by *Mycobacterium bovis* BCG Vaccines. *Infect. Immun. 72*, 2803–2809.

[228] Asselineau, C., Asselineau, J., Lanéelle, G. and Lanéelle, M. A. (2002). The biosynthesis of mycolic acids by *Mycobacteria*: current and alternative hypotheses. *Prog. Lipid Res. , 41*, 501–23.

[229] George, K. M., Yuan, Y., Sherman, D. R. and Barry, C. E. (1995). The biosynthesis of cyclopropanated mycolic acids in *Mycobacterium tuberculosis*: Identification and functional analysis of cmas-2. *J. Biol. Chem., 270*, 27292–27298.

[230] Danielson, S. J. and Gray, G. R. (1982). Structures of the two homologous series of dialkene mycolic acids from *Mycobacterium smegmatis*. *J. Biol. Chem., 257*, 12196–203.

[231] Wong, M. Y., Steck, P. A. and Gray, G. R. (1979). The major mycolic acids of *Mycobacterium smegmatis*. Characterization of their homologous series. *J. Biol. Chem., 254*, 5734–5740.

[232] Glickman, M. S., Cahill, S. M. and Jacobs, W. R. (2001). The *Mycobacterium tuberculosis* cmaA2 gene encodes a mycolic acid trans-cyclopropane synthetase. *J. Biol. Chem., 276*, 2228–2233.

[233] Minnikin, D. E. (1982). Lipids: complex lipids, their chemistry, biosynthesis and roles, p. 95–184.InC. Ratledge and J. Stanford (ed.), The biology of the mycobacteria, vol. 1. Physiology, identification and classification. Academic Press, Inc., London, United Kingdom.

[234] Draper, P. (1998). The Outer Parts of the Mycobacterial Envelope as Permeability Barriers. *Front. Biosci, 3*, 1253–1261.

[235] Villeneuve, M., Kawai, M., Watanabe, M., Aoyagi, Y., Hitotsuyanagi, Y., Takeya, K., Gouda, H., Hirono, S., Minnikin, D. E. and Nakahara, H. (2007). Conformational behavior of oxygenated mycobacterial mycolic acids from *Mycobacterium bovis* BCG. *Biochim. Biophys. acta, 1768*, 1717–1726.

[236] Hasegawa, T., Amino, S., Kitamura, S., Matsumoto, L., Katada, S. and Nishijo, J. (2003). Study of the Molecular Conformation of aplha- and Keto-Mycolic Acid Monolayers by the Langmuir-Blodgett Technique and Fourier Transform Infrared Reflection-Absorption Spectroscopy. *Langmuir, 19*, 105–109.

[237] Grant, E. P., Beckman, E. M., Behar, S. M., Degano, M., Frederique, D., Besra, G. S., Wilson, I. A., Porcelli, S. A., Furlong, S. T. and Brenner, M. B. (2002). Fine Specificity of TCR Complementarity-Determining Region Residues and Lipid Antigen Hydrophilic Moieties in then Recognition of a CD1-Lipid Complex. *J. Immunol. , 168*, 3933–3940.

[238] Villeneuve, M., Kawai, M., Kanashima, H., Watanabe, M., Minnikin, D. E. and Nakahara, H. (2005). Temperature dependence of the Langmuir monolayer packing of mycolic acids from Mycobacterium tuberculosis. *Biochim. Biophys. Acta, 1715*, 71–80.

[239] Hasegawa, T., Nishijo, J., Watanabe, M., Funayama, K. and Imae, T. (2000). Conformational characterization of α-mycolic acid in a monolayer film by the Langmuir–Blodgett technique and atomic force microscopy. *Langmuir, 16*, 7325–7330.

[240] Hoffmann, C., Leis, A., Niederweis, M., Plitzko, J. M. and Engelhardt, H. (2008). Disclosure of the mycobacterial outer membrane: cryo-electron tomography and vitreous sections reveal the lipid bilayer structure. *Proc. Natl. Acad. Sci. U S A, 105*, 3963–3967.

[241] Zuber, B., Chami, M., Houssin, C., Dubochet, J., Griffiths, G. and Daffé, M. (2008). Direct visualization of the outer membrane of *mycobacteria* and corynebacteria in their native state. *J. Bacteriol., 190*, 5672–5680.

[242] Groenewald, W., Baird, M. S., Verschoor, J. A., Minnikin, D. E. and Croft, A. K. (2014). Differential spontaneous folding of mycolic acids from *Mycobacterium tuberculosis*. *Chem. Phys. Lipids, 180*, 15–22.

[243] Villeneuve, M., Kawai, M., Watanabe, M., Aoyagi, Y., Hitotsuyanagi, Y., Takeya, K., Gouda, H., Hirono, S., Minnikin, D. E. and Nakahara, H. (2010). Differential conformational behaviors of View the MathML sourceα-mycolic acids in Langmuir monolayers and computer simulations. *Chem. Phys. Lipids, 163*, 569–579.

[244] Villeneuve, M., Kawai, M., Horiuchi, K., Watanabe, M., Aoyagi, Y., Hitotsuyanagi, Y., Takeya, K., Gouda, H., Hirono, S. and Minnikin, D. E. (2013). Conformational folding of mycobacterial methoxy- and ketomycolic acids facilitated by α-methyl trans-cyclopropane groups rather than cis-cyclopropane units. *Microbiology, 159*, 2405–2415.

[245] Villeneuve M. (2012). Characteristic conformational behaviors of representativemycolic acids in the interfacial monolayer. In: Cardona, P.-J. (Ed.), Under-standing Tuberculosis-Deciphering the Secret Life of the Bacilli. InTech – OpenAccess Publisher, Rijeka, Croatia, 317–334.

[246] Ryll, R., Kumazawa, Y. and Y. I. (2001). Immunological properties of trehalose dimycolate (cord factor) and other mycolic acid-containing glycolipids--a review. *Microbiol. Immunol., 45*, 801–811.

[247] Noll, H., Bloch, H., Asselineau, J. and Lederer, E. (1956). The chemical structure of the cord factor of *Mycobacterium tuberculosis*. *Biochim. Biophys. acta, 20*, 299–309.

[248] Verma, R. K. and Jain, A. (2007). Antibodies to mycobacterial antigens for diagnosis of tuberculosis. *Immunol. Med. Microbiol., 51*, 453–461.

[249] Chen, J. (2010). *Identifying Biosynthetic Pathways for Mycobacterial Cell Wall Components Using Transposon Mutagenesis degree of Doctor of Philosophy*. University of Birmingham.

[250] Al Dulayymi, J. R., Baird, M. S., Maza-Iglesias, M., Beken, S. V. and Grooten, J. (2009). The first unique synthetic mycobacterial cord factors. *Tetrahedron Lett., 50*, 3702–3705.

[251] Artman, M., Bekierkunst, A. and Goldenberg, I. (1964). Tissue metabolism in infection: Biochemical changes in mice treated with cord factor. *Arch. Biochem. Biophysics, 105*, 80–5.

[252] Fischer, K., Chatterjee, D., Torrelles, J., Brennan, P. J., Kaufmann, S. H. and Schaible, U. E. (2001). Mycobacterial lysocardiolipin is exported from phagosomes upon cleavage of cardiolipin by a macrophage-derived lysosomal phospholipase A2. *J. Immunol., 167*, 2187–2192.

[253] Allen, R. D., Francis, D. and R. Z. (1971). Suppression of Urethan-Induced Lung Adenomas in Mice Treated with Trehalose-6,6-Dimycolate (Cord Factor) and Living Bacillus Calmette Guerin. *Control, 174*, 1240–1242.

[254] Bekierkunst, A. (1968). Acute granulomatous response produced in mice by trehalose-6,6-dimycolate. *J. Bacteriol., 96*, 958–961.

[255] Morecki, S., Vilkas, E. and Lederer, E. (1971). Immune Response to Sheep Red Blood Cells in Mice Pretreated with Mycobacterial Fractions. *Microbiology, 4*, 256–263.

[256] Parant, M., Parant, F., Chedid, L., Drapier, J. C., Petit, J. F. and Wietzerbin, J. L. (1977). Enhancement of nonspecific immunity to bacterial infection by cord factor (6,6'-trehalose dimycolate). *J. Infect. Dis.*, *135*, 771–777.

[257] Parant, M., Audibert, F., Parant, F., Chedid, L., Soler, E., Polonsky, J. and Lederer, E. (1978). Nonspecific immunostimulant activities of synthetic trehalose-6,6'-diesters (lower homologs of cord factor). *Infect. Immun. 20*, 12–19.

[258] Ribi, E., Milner, K. C., Granger, D. L., Kelly, M. T., Yamamoto, K., Brehmer, W., Parker, R., Smith, R. F. and Strain, S. M. (1976). Immunotherapy with nonviable microbial components. *Ann. N. Y. Acad. Sci.*, *277*, 228–38.

[259] Yarkoni, E. and Bekierkunst, A. (1976). Nonspecific resistance against infection with Salmonella typhi and S. typhimurium induced in mice by cord factor (trehalose 6,6'-dimycolate) and its analogues. *Infect. Immun. 14*, 1125–1129.

[260] Indrigo, J., Hunter, R. L. and Actor, J. K. (2002). Influence of trehalose 6,6'-dimycolate (TDM) during mycobacterial infection of bone marrow macrophages. *Microbiology*, *148*, 1991–1998.

[261] Torrelles, J. B. and Schlesinger, L. S. (2011). Diversity in M. tuberculosis mannosylated cell wall dterminants impact adaptation to the host. *Tuberculosis*, *90*, 84–93.

[262] Yamasaki, S., Ishikawa, E., Sakuma, M., Hara, H., Ogata, K. and Saito, T. (2008). Mincle is an ITAM-coupled activating receptor that senses damaged cells. *Nature Immunol.*, *9*, 1179–1188.

[263] Arce, I., Martínez-Muñoz, L., Roda-Navarro, P. and Fernández-Ruiz, E. (2004). The human C-type lectin CLECSF8 is a novel monocyte/macrophage endocytic receptor. *Eur. J. Immunol.*, *34*, 210–220.

[264] Graham, L. M., Gupta, V., Schafer, G., Reid, D. M., Kimberg, M., Dennehy, K. M., Hornsell, W. G., Guler, R., Campanero-Rhodes, M. A., Palma, A. S., Feizi, T., Kim, S. K., Sobieszczuk, P., Willment, J. A. and Brown, G. D. (2012). The C-type lectin receptor CLECSF8 (CLEC4D) is expressed by myeloid cells and triggers cellular activation through syk kinase. *J. Biol. Chem.*, *287*, 25964–25974.

[265] Ishikawa, E., Ishikawa, T., Morita, Y. S., Toyonaga, K., Yamada, H., Takeuchi, O., Kinoshita, T., Akira, S., Yoshikai, Y. and Yamasaki, S. (2009). Direct recognition of the mycobacterial glycolipid, trehalose dimycolate, by C-type lectin Mincle. *J. Exp. Med.*, *206*, 2879–2888.

[266] Schoenen, H., Bodendorfer, B., Hitchens, K., Manzanero, S., Werninghaus, K., Nimmerjahn F., Agger, E. M., Stenger, S., Andersen, P., Ruland, J., Brown, G. D., Wells, C. and L. R. (2010). Cutting edge: Mincle is essential for recognition and adjuvanticity of the mycobacterial cord factor and its synthetic analog trehalose-dibehenate. *J. Immunol.*, *184*, 2756–2760.

[267] Kato, M. and Maeda, J. (1974). Isolation and biochemical activities of trehalose-6-monomycolate of Mycobacterium tuberculosis. *Infect. Immun. 9*, 8–14.

[268] Bekierkunst, A., Wang, L., Toubiana, R. and Lederer, E. (1974). Immunotherapy of cancer with nonliving BCG and fractions derived from mycobacteria: role of cord factor (trehalose 6,6' dimycolate) in tumor regression. *Infect. Immun. 10*, 1044–1050.

[269] Yarkoni, E., Wang, L. and Bekierkunst, A. (1974). Suppression of growth of Ehrlich ascites tumor cells in mice by trehalose-6,6'-dimycolate (cord factor) and BCG. *Infect. Immun. 9*, 977–984.

[270] Yano, K., Brown, L. F. and Detmar, M. (2001). Control of hair growth and follicle size by VEGF-mediated angiogenesis. *J. Clin. Invest., 107*, 409–417.

[271] Dover, L. G., Cerdeño-Tárraga, A. M., Pallen M. J., J. p. and B. G. S. (2004). Comparative cell wall core biosynthesis in the mycolated pathogens, *Mycobacterium tuberculosis* and Corynebacterium diphtheriae. *FEMS Microbiol. Rev., 28*, 225–250.

[272] Fujita, Y., Doi, T., & Sato, K. and Yano, I. (2005). Diverse humoral immune responses and changes in IgG antibody levels against mycobacterial lipid antigens in active tuberculosis. *Microbiology, 151*, 2065–2074.

[273] Rajni, R. N. and Meena, L. S. (2011). Biosynthesis and Virulent Behavior of Lipids Produced by Mycobacterium tuberculosis: LAM and Cord Factor. *An Overview. Biotechnol. Res. Int., 2011*, 2–7.

[274] Painter, T. J., Watkins, W. M. and Morgan, W. T. (1965). Serologically active fucose-containing oligosaccharides isolated from human blood-group A and B substances. *Nature, 206*, 594–597.

[275] Matsunaga, I., Naka, T., Talekar, R. S., McConnell, M. J., Katoh, K., Nakao, H., Otsuka, A., Behar, S. M., Yano, I., Moody, D. B. and Sugita, M. (2008). Mycolyltransferase-mediated Glycolipid Exchange in Mycobacteria. *J. Biol. Chem., 283*, 28835–28841.

[276] Thi Kim Anh, N., Koets, A. P., Santema, W. J., van Eden, W., Rutten, V. P. and Rhijn, I. V. (2009). The mycobacterial glycolipid glucose monomycolate induces a memory T cell response comparable to a model protein antigen and no B cell response upon experimental vaccination of cattle. *Vaccine, 27*, 4818–4825.

[277] Andersen S., Agger M., Rosenkrands I., Gomes M., Bhowruth V., Gibson J., Petersen V., Minnikin, D. E., Gurdyal, S. and Andersen, P. (2010). A Simple Mycobacterial Monomycolated Glycerol Lipid Has Potent Immunostimulatory Activity. *J. Immunol. , 182*, 424–432.

[278] Layre, E., Collmann, A., Bastian, M., Mariotti, S., Czaplicki, J., Prandi, J., Mori, L., Stenger, S., De Libero, G., Puzo, G. and Gilleron, M. (2009). Mycolic Acids Constitute a Scaffold for Mycobacterial Lipid Antigens Stimulating CD1-Restricted T Cells. *Chem. Biol.*, *16*, 82–92.

[279] Huijuan, Y., Jiajia, Z., Hirohide, T., William, Y., Yuki, S., Xiao, Y., Shige, H., Yoshimura, Y., Zhang, Y. L., Nerimiah, E., Vincent, B., Dongmei, W., Xia, D., Kunio, T., and Xebio, Y. (2014). Spatial control of proton pump H,K-ATPase docking at the apical membrane by phosphorylation-coupled ezrin-syntaxin 3 interaction. *The J. Biol. Chem.*, *277*, 50030–50035.

[280] Yang, Y., Kulka, K., Montelaro, C., Reinhart, A., Sissons, J., Aderem, A. and Ojha, K. (2014). A Hydrolase of Trehalose Dimycolate Induces Nutrient Influx and Stress Sensitivity to Balance Intracellular Growth of *Mycobacterium tuberculosis*. *Cell Host Microb.*, *15*, 153–163.

[281] Hattori, Y., Matsunaga, I., Komori, T., Urakawa, T., Nakamura, T., Fujiwara, N., Hiromatsu, K., Harashima, H. and Sugita, M. (2011). Glycerol monomycolate, a latent tuberculosis-associated mycobacterial lipid, induces eosinophilic hypersensitivity responses in guinea pigs. *Biochem. Biophys. Res. Commun.*, *409*, 304–307.

[282] Alderwick, L. J., Birch, H. L., Mishra, A. K., Eggeling, L. and Besra, G. S. (2007). Structure, function and biosynthesis of the *Mycobacterium tuberculosis* cell wall: arabinogalactan and lipoarabinomannan assembly with a view to discovering new drug targets. *Biochem. Soc. Trans.*, *35*, 1325–1328.

[283] Besra G. S., Khoo, K. H., McNeil, M. R., Dell, A., Morris, H. R. and Brennan, P. J. (1995). A new interpretation of the structure of the mycolyl-arabinogalactan complex of Mycobacterium tuberculosis as revealed through characterization of oligoglycosylalditol fragments by fast-atom bombardment mass spectrometry and 1H nuclear magnetic resonance. *Biochemistry*, *34*, 4257–4266.

[284] Daffe, M., Brennan, P. J. and McNeil, M. (1990). Predominant structural features of the cell wall arabinogalactan of *Mycobacterium tuberculosis* as revealed through characterization of oligoglycosyl alditol fragments by gas chromatography/mass spectrometry and by 1H and 13C NMR analyses. *J. Biol. Chem.*, *265*, 6734–43.

[285] McNeil, M. R., Robuck, K. G., Harter, M. and Brennan, P. J. (1994). Enzymatic evidence for the presence of a critical terminal hexa-arabinoside in the cell walls of *Mycobacterium tuberculosis. Glycobiology*, *4*, 165–173.

[286] Rombouts, Y., Brust, B., Ojha, A. K., Maes, E., Coddeville, B., Elass-Rochard, E., Kremer, L. and Guerardel, Y. (2012). Exposure of mycobacteria to cell wall-inhibitory drugs decreases production of arabinoglycerolipid related to mycolyl-arabinogalactan-peptidoglycan metabolism. *J. Biol. Chem.*, *287*, 11060–11069.

[287] McNeil, M., Wallner, S. J., Hunter, S. W. and Brennan, P. J. (1987). Demonstration that the galactosyl and arabinosyl residues in the cell-wall arabinogalactan of *Mycobacterium leprae* and *Mycobacterium tuberculosis* are furanoid. *Carbohydrate Res., 166*, 299–308.

[288] Mikusova, K., Slayden, R. A., Besra, G. S. and Brennan, P. J. (1995). Biogenesis of the mycobacterial cell wall and the site of action of ethambutol. *Antimicrob. Agents Chemother., 39*, 2484–2489.

[289] Azuma, I., Yamamura, Y. and Misaki, A. (1969). Isolation and characterization of arabinose mycolate from firmly bound lipids of mycobacteria. *J. Bacteriol., 98*, 331–333.

[290] Patterson, J. H., Waller, R. F., Jeevarajah, D., Billman-Jacobe, H. and McConville, M. J. (2003). Mannose metabolism is required for mycobacterial growth. *The Biochem. J., 372*, 77–86.

[291] De Libero, G. and Mori, L. (2005). Recognition of lipid antigens by T cells. *Nat. Rev. Immunol., 5*, 485–96.

[292] Moody, D. B., Zajonc, D. M. and Wilson, I. A. (2005). Anatomy of CD1-lipid antigen complexes. *Nat. Rev. Immunol., 5*, 387–399.

[293] Sköld, M. and Behar, S. M. (2005). The role of group 1 and group 2 CD1-restricted T cells in microbial immunity. *Microb. Infect., 7*, 544–551.

[294] Porcelli, S. A. (1995). The CD1 family: a third lineage of antigen-presenting molecules. *Adv. Immunol., 59*, 1–98.

[295] De la Salle, H., Mariotti, S., Angenieux, C., Gilleron, M., Garcia-Alles, L. F., Malm, D., Berg, T., Paoletti, S., Maître, B., Mourey, L., Salamero, J., Cazenave, J. P., Hanau, D., Mori, L., Puzo, G. and De Libero, G. (2005). Assistance of microbial glycolipid antigen processing by CD1e. *Science, 310*, 1321–4.

[296] Gilleron, M., Stenger, S., Mazorra, Z., Wittke, F., Mariotti, S., Böhmer, G., Prandi, J., Mori, L., Puzo, G. and De Libero, G. (2004). Diacylated sulfoglycolipids are novel mycobacterial antigens stimulating CD1-restricted T cells during infection with Mycobacterium tuberculosis. *J. Exp. Med., 199*, 649–659.

[297] Moody, D. B., Ulrichs, T., Mühlecker, W., Young, D. C., Gurcha, S. S., Grant, E., Rosat, J. P., Brenner, M. B., Costello, C. E., Besra, G. S. and Porcelli, S. A. (2000). CD1c-mediated T-cell recognition of isoprenoid glycolipids in *Mycobacterium tuberculosis* infection. *Nature, 404*, 884–888.

[298] Ulrichs, T., Moody, D. B., Grant, E., Kaufmann, S. H. and Porcelli, S. A. (2003). T-cell responses to CD1-presented lipid antigens in humans with *Mycobacterium tuberculosis* infection. *Infect. Immun. 71*, 3076–3087.

[299] Dascher, C. C., Hiromatsu, K., Xiong, X., Morehouse, C., Watts, G., Liu, G., McMurray, D. N., LeClair, K. P., Porcelli, S. A. and Brenner, M. B. (2003). Immunization with a mycobacterial lipid vaccine improves pulmonary pathology in the guinea pig model of tuberculosis. *Int. Immunol.*, *15*, 915–925.

[300] Strominger, J. L. (2010). An Alternative Path for Antigen Presentation: Group 1 CD1 Proteins. *J. Immunol. , 184*, 3303–3305.

[301] Kaufmann, S. H., Baumann, S. and Nasser, E. A. (2006). Exploiting immunology and molecular genetics for rational vaccine design against tuberculosis. *Int. J. Tuberc. Lung Dis. , 10*, 1068–1079.

[302] Montamat-sicotte, D. J., Millington, K. A., Willcox, C. R., Hingley-wilson, S., Hackforth, S., Innes, J., Kon, O. M., Lammas, D. A., Minnikin, D. E., Besra, G. S., Willcox, B. E. and Lalvani, A. (2011). A mycolic acid – specific CD1-restricted T cell population contributes to acute and memory immune responses in human tuberculosis infection. *J. Clin. Invest., 121*, 2493–2503.

[303] Beukes, M., Lemmer, Y., Deysel, M., Al Dulayymi, J. R., Baird, M. S., Koza, G., Iglesias, M. M., Rowles, R. R., Theunissen, C., Grooten, J., Toschi, G., Roberts, V. V., Pilcher, L., Van Wyngaardt, S., Mathebula, N., Balogun, M., Stoltz, A. C. and Verschoor, J. A. (2010). Structure-function relationships of the antigenicity of mycolic acids in tuberculosis patients. *Chem. Phys. Lipids, 163*, 800–808.

[304] Batuwangala, T., Shepherd, D., Gadola, S. D., Gibson, K. C., Zaccai, N. R., Fersht, A. R., Besra, G. S., Cerundolo, V. and Jones, E. Y. (2004). The crystal structure of human CD1b with a bound bacterial glycolipid. *J. Immunol., 172*, 2382–2388.

[305] Huang, C. C., Smith, C. V., Glickman, M. S., Jacobs, W. R. and Sacchettini, J. C. (2002). Crystal structures of mycolic acid cyclopropane synthases from *Mycobacterium tuberculosis*. *J. Biol. Chem., 277*, 11559–11569.

[306] Miller, D. J., Ouellette, N., Evdokimova, E., Savchenko, A., Edwards, A. and Anderson, W. F. (2003). Crystal complexes of a predicted S-adenosylmethionine-dependent methyltransferase reveal a typical AdoMet binding domain and a substrate recognition domain. Protein Science : *A Publication of the Protein Sci., 12*, 1432–1442.

[307] Gadola, S. D., Zaccai, N. R., Harlos, K., Shepherd, D., Castro-Palomino, J. C., Ritter, G., Schmidt, R. R., Jones, E. Y. and Cerundolo, V. (2002). Structure of human CD1b with bound ligands at 2.3 A, a maze for alkyl chains. *Nature Immunol.*, *3*, 721–726.

[308] Khan, A. A., Cheng, J. M., Stocker, L. B. and Timmer, M. S. (2010). Glycolipids and CD1 : The Crossroad between Chemistry and Immunology. *Chem. N.Z.*, *74*, 57–62.

[309] Moody, D. B., Reinhold, B. B., Guy, M. R., Beckman, E. M., Frederique, D. E., Furlong, S. T., Ye, S., Reinhold, V. N., Sieling, P. A., Modlin, R. L., Besra, G. S. and Porcelli, S. A. (1997). Structural requirements for glycolipid antigen recognition by CD1b-restricted T cells. *Science*, *278*, 283–286.

[310] Vogiatzakis, E., Stefanou, S., Skroubelou, A., Anagnostou, S., Marinis, E. and Matsiota-Bernard, P. (1998). Molecular markers for the investigation of *Mycobacterium gordonae* epidemics. *J. Hosp. Infect.*, *38*, 217–222.

[311] Wood, R. (2007). Challenges of TB diagnosis and treatment in South Africa: Roche Symposium, 3rd South African AIDS Conference, Durban. In Southern African. *J. HIV Med.*, *27*, 44–48.

[312] Bello, A. K. and Njoku, C. H. (2005). Tuberculosis: current trends in diagnosis and treatment. *Niger. J. Clin. Pract.*, *8*, 118–124.

[313] Dunlap E., Bass J., Fujiwara P., Hopewell P., Horsburgh R., S. M. and S. M. (2000). Diagnostic standards and classification of Tuberculosis in adults and children. *Amer. J. Resp.Crit.Care Med. 4*, 1376–1395.

[314] Pottumarthy, S., Morris, A. J., Harrison, A. C. and Wells, V. C. (1999). Evaluation of the tuberculin gamma interferon assay: Potential to replace the mantoux skin test. *J. Clin. Microbiol. , 37*, 3229–3232.

[315] Guerra, R. L., Baker, J. F., Alborz, R., Armstrong, D. T., Kiehlbauch, J. A., Conde, M. B., Dorman, S. E. and Hooper, N. M. (2008). Specimen dilution improves sensitivity of the amplified Mycobacterium tuberculosis direct test for smear microscopy-positive respiratory specimens. *J. Clin. Microbiol. , 46*, 314–316.

[316] Vlaspolder, F., Singer, P. and Roggeveen, C. (1995). Diagnostic value of an amplification method (Gen-Probe) compared with that of culture for diagnosis of tuberculosis. *J. Clin. Microbiol.*, *33*, 2699–2703.

[317] Anargyros, P., Astill, D. S. and Lim, I. (1990). Comparison of Improved BACTEC and Lawenstein-Jensen media for culture of *Mycobacteria* from Clinical Specimens. *J. Clin. Microbiol.*, *28*, 1288–1291.

[318] Yeager, H., Lacy, J., Smith, L. R. and LeMaistre, C. A. (1967). Quantitative studies of mycobacterial populations in sputum and saliva. *Am. Rev. Respir. Dis., 95*, 998–1004.

[319] Altman, G. and Bland, M. (1994). Diagnostic tests 3: receiver operating characteristic plots. *BMJ: Br. Med. J., 309*, 188.

[320] Morgan, M. A., Horstmeier, C. D., De Young, D. R. and Roberts, G. D. (1983). Comparison of a radiometric method (BACTEC) and conventional culture media for recovery of *mycobacteria* from smear-negative specimens. *J. Clin. Microbiol. , 18*, 384–388.

[321] Ichiyama S., S. K. and T. J. (1993). Comparative study of a biphasic culture system (Roche MB Check system) with a conventional egg medium for recovery of *mycobacteria*. Aichi Mycobacteriosis Research Group. *Tuber. Lung. Dis., 74*, 338–341.

[322] Steingart, K. R., Ng, V., Henry, M., Hopewell, P. C., Ramsay, A., Cunningham, J., Urbanczik, R., Perkins, M. D., Aziz, M. A. and Pai, M. (2006). NoSputum processing methods to improve the sensitivity of smear microscopy for tuberculosis: a systematic review Title. *Lancet Infect. Dis., 6*, 664–74.

[323] Harries, D., Maher, D. and Graham, S. (2004). *TB/HIV: A clinical manual, World Health Organisation*. (2nd Edi., pp. 75–100). Geneva.

[324] Golden, M. P. and Vikram, H. R. (2005). Extrapulmonary tuberculosis: An overview. *Am. Fam. Phys., 72*, 1761–1768.

[325] Masterson, L., Srouji, I., Kent, R. and Bath, A. P. (2011). Nasal tuberculosis--an update of current clinical and laboratory investigation. *J. Laryngol. Otol., 125*, 210–213.

[326] Hauck, F. R., Neese, B. H., Panchal, A. S. and El-Amin, W. (2009). Identification and management of latent tuberculosis infection. *Am. Fam. Phys., 79*, 879–886.

[327] Pai, M., Zwerling, A. and Menzies, D. (2008). Systematic review: T-cell-based assays for the diagnosis of latent tuberculosis infection: An update. *Annals of Intern. Med., 149*, 177–184.

[328] Chaparas D., Vandiviere M, Melvin I., K. G. and B. C. (1985). Tuberculin test. Variability with the Mantoux procedure. *Am. Rev. Respir. Dis., 132*, 175–177.

[329] Reichman, L. B. (1998). A scandalous incompetence...continued. *In Chest J., 113*, 1153–1154.

[330] Wang, L., Turner, M. O., Elwood, R. K., Schulzer, M. and FitzGerald, J. M. (2002). A meta-analysis of the effect of Bacille Calmette Guérin vaccination on tuberculin skin test measurements. *Thorax, 57*, 804–809.

[331] Menzies, R. and Vissandjee, B. (1992). Effect of Bacille Calmette-Guérin Vaccination on Tuberculin Reactivity. *Am. Rev. Respir. Dis., 145*, 621–625.

[332] Menzies, D. (1999). Interpretation of repeated tuberculin tests. Boosting, conversion, and reversion. *Amer. J. Resp.Crit.Care Med. 159*, 15–21.

[333] Kobashi Y, Mouri K., Yagi S., Obase Y., Fukuda M., Miyashita, N. and Oka, M. (2008). Usefulness of the QuantiFERON TB-2G test for the differential diagnosis of pulmonary tuberculosis. *Intern. Med., 47*, 237–243.

[334] Detjen, A. K., Keil, T., Roll, S., Hauer, B., Mauch, H., Wahn, U. and Magdorf, K. (2007). Interferon-gamma release assays improve the diagnosis of tuberculosis and nontuberculous mycobacterial disease in children in a country with a low incidence of tuberculosis. *Clin. Infect. Dis., 45*, 322–328.

[335] Brock, I., Weldingh, K., Leyten, E. M., Arend, S. M., Ravn, P. and Andersen, P. (2004). Specific T-Cell Epitopes for Immunoassay-Based Diagnosis of *Mycobacterium tuberculosis* Infection. *J. Clin. Microbiol. , 42*, 2379–2387.

[336] Mori T, Sakatani M, Yamagishi F, Takashima T, Kawabe, Y., Nagao, K., Shigeto, E., Harada, N., Mitarai, S., Okada, M., Suzuki, K., Inoue, Y., Tsuyuguchi, K., Sasaki, Y., Mazurek, G. H. and Tsuyuguchi, I. (2004). Specific detection of tuberculosis infection: an interferon-gamma-based assay using new antigens. *Amer. J. Resp.Crit.Care Med. 170*, 59–64.

[337] Lee, J. Y., Choi, H. J., Park, I. N., Hong, S. B., Oh, Y. M., Lim, C. M., Lee, S. D., Koh, Y., Kim, W. S., Kim, D. S., Kim, W. D. and Shim, T. S. (2006). Comparison of two commercial interferon-gamma assays for diagnosing *Mycobacterium tuberculosis* infection. *Eur. Respir. J., 28*, 24–30.

[338] Louise, R. S., Oettinger, T., Rosenkrands, I., Ravn, P., Brock, I., Jacobsen, S. and Andersen, P. (2000). Comparative Evaluation of Low-Molecular-Mass Proteins from *Mycobacterium tuberculosis* Identifies Members of the ESAT-6 Family as Immunodominant T-Cell Antigens. *Infect. Immun., 68*, 214–220.

[339] Dheda, K., van Zyl Smit, R., Badri, M. and Pai, M. (2009). T-cell interferon-gamma release assays for the rapid immunodiagnosis of tuberculosis: clinical utility in high-burden vs. low-burden settings. *Curr. Opin. Pulm. Med., 15*, 188–200.

[340] Kang, Y. A., Lee, H. W., Yoon, H. I., Cho, B., Han, S. K., Shim, Y. S. and Yim, J. J. (2005). Discrepancy between the tuberculin skin test and the whole-blood interferon gamma assay for the diagnosis of latent tuberculosis infection in an intermediate tuberculosis-burden country. *J. AMA., 293*, 2756–61.

[341] Mazurek, G. H., Jereb, J., Lobue, P., Iademarco, M. F., Metchock, B. and Vernon, A. (2005). Guidelines for using the QuantiFERON-TB Gold test for detecting *Mycobacterium tuberculosis* infection, United States. *MMWR. Recomm. Rep., 54*, 49–55.

[342] Ferrara, G., Losi, M., Meacci, M., Meccugni, B., Piro, R., Roversi, P., Bergamini, B. M., D'Amico, R., Marchegiano, P., Rumpianesi, F., Fabbri, L. M. and Richeldi, L. (2005). Routine hospital use of a new commercial whole blood interferon-gamma assay for the diagnosis of tuberculosis infection. *Amer. J. Resp.Crit.Care Med. 172*, 631–5.

[343] Brock, I., Munk, M. E., Kok-Jensen, A. and Andersen, P. (2001). Performance of whole blood IFN-gamma test for tuberculosis diagnosis based on PPD or the specific antigens ESAT-6 and CFP-10. *Int. J. Tuberc. Lung Dis., 5*, 462–467.

[344] Soysal, A., Torun, T., Efe, S., Gencer, H., Tahaoglu, K. and Bakir, M. (2008). Evaluation of cut-off values of interferon-gamma-based assays in the diagnosis of *M. tuberculosis* infection. *Int. J. Tuberc. Lung Dis., 12*, 50–56.

[345] Jafari, C., Ernst, M., Kalsdorf, B., Greinert, U., Diel, R., Kirsten, D., Marienfeld, K., Lalvani, A. and Lange, C. (2006). Rapid diagnosis of smear-negative tuberculosis by bronchoalveolar lavage enzyme-linked immunospot. *Amer. J. Resp.Crit.Care Med. 174*, 1048–1054.

[346] Ichiyama, S., Iinuma, Y., Tawada, Y., Yamori, S., Hasegawa, Y., Shimokata, K. and Nakashima, N. (1996). Evaluation of Gen-Probe Amplified *Mycobacterium Tuberculosis* Direct Test and Roche PCR-Microwell Plate Hybridization Method (Amplicor Mycobacterium) for Direct Detection of Mycobacteria. *J. Clin. Microbiol. , 34*, 130–133.

[347] Catanzaro, A. (1997). Rapid Diagnostic Tests for Tuberculosis. *Amer. J. Resp.Crit.Care Med. 155*, 1804–1814.

[348] Sloutsky, A, Han, L. L. and Werner, B. G. (2004). Rapid Diagnostic Tests for Tuberculosis. *Diagnostic. Microbiol. Infect. Dis., 50*, 109–11.

[349] Mothershed, E. A. and Whitney, A. M. (2006). Nucleic acid-based methods for the detection of bacterial pathogens : Present and future considerations for the clinical laboratory. *Clin. Chim. Acta, 363*, 206–220.

[350] Dinnes, J., Deeks, J., Kunst, H., Gibson, A., Cummins, E., Waugh, N., Drobniewski, F. and Lalvani, A. (2007). A systematic review of rapid diagnostic tests for the detection of tuberculosis infection. *Health Technol. Assess. , 11*, 1–196.

[351] Chedore, P. and Jamieson, F. B. (1999). Routine use of the Gen-Probe MTD2 amplification test for detection of *Mycobacterium tuberculosis* in clinical specimens in a large public health mycobacteriology laboratory. . *Diagn. Microbiol. Infect. Dis., 35*, 185–191.

[352] O'Sullivan, C. E., Miller, D. R., Schneider, P. S. and Roberts, G. D. (2002). Evaluation of Gen-Probe Amplified *Mycobacterium tuberculosis* Direct Test by using respiratory and nonrespiratory specimens in a tertiary care center laboratory. *J. Clin. Microbiol. , 40,* 1723–1727.

[353] Thanyani, S. T., Roberts, V., Siko, D. G., Very, P. and Verschoor, J. A. (2008). A novel application of affinity biosensor technology to detect antibodies to mycolic acid in tuberculosis patients. *J. Immunol. Methods, 332,* 61–72.

[354] Somonney, N., Labrousse, H., Ternynch, T. and Lagrange, P. H. (1996). Recycling of ELISA plates for the serological diagnosis of tuberculosis using a *Mycobacterium tuberculosis*-specific glycolipid antigen. *J. Immunol. Methods, 199,* 101–105.

[355] Nassau, E., Parsons, E. R. and Johnson, G. D. (1976). The detection of antibodies to *Mycobacterium tuberculosis* by microplate enzyme-linked immunosorbent assay (ELISA). *Tubercle, 57,* 67–70.

[356] Lequin, R. M. (2005). Enzyme Immunoassay (EIA)/ Enzyme-Linked Immunosorbent Assay (ELISA). *Clin. Chem., 2418,* 2415–2418.

[357] Csorba, K., Schmidt, S., Florea, F., Ishii, N., Hashimoto, T., Hertl, M., Kárpáti, S., Bruckner-tuderman, L., Nishie, W. and Sitaru, C. (2011). Development of an ELISA for sensitive and specific detection of IgA autoantibodies against BP180 in pemphigoid diseases. *Orphanet J. Rare Dis., 6,* 31.

[358] Mosedale, D. E., Sandhu, M. S., Luan, J., Goodall, M. and Grainger, D. J. (2006). A new sensitive and specific enzyme-linked immunosorbent assay for IgD. *J. Immunol. Methods, 313,* 74–80.

[359] Okayama, T., Matsuno, Y., Yasuda, N., Tsukui, T., Suzuta, Y., Koyanagi, M., Sakaguchi, M., Ishii, Y., Olivry, T. and Masuda, K. (2011). Establishment of a quantitative ELISA for the measurement of allergen-specific IgE in dogs using anti-IgE antibody cross-reactive to mouse and dog IgE. *Vet. Immunol. Immunopathol., 139,* 99–106.

[360] Wang, B., Hak, L. J., Relling, M. V., Pui, C. H., Woo, M. H. and Storm, M. C. (2000). ELISA to evaluate plasma anti-asparaginase IgG concentrations in patients with acute lymphoblastic leukemia. *J. Immunol. Methods, 239,* 75–83.

[361] Sharief, M. K. and Thompson, E. J. (1990). A sensitive ELISA system for the rapid detection of virus specific IgM antibodies in the cerebrospinal fluid. *J. Immunol. Methods, 130,* 19–24.

[362] Janeway, C. A., Travers, P., walport, M. and Shlomchik, M. J. (2005). *Immuno Biology: the immune system in health and disease* (6th Edi., pp. 104–107). New York and London.

[363] Maekura, R., Okuda, Y. Nakagawa, M., Hiraga, T., Yokota, S., Ito, M., Yano, I., Kohno, H., Wada, M., Abe, C., Toyoda, T., Kishimoto, T. and Ogura, T. (2001). Clinical Evaluation of Anti-Tuberculous Glycolipid Immunoglobulin G Antibody Assay for Rapid Serodiagnosis of Pulmonary Tuberculosis. *J. Clin. Microbiol. , 39*, 3603–3608.

[364] Heath, R. J., White, S. W. and Rock, C. O. (2002). Inhibitors of fatty acid synthesis as antimicrobial chemotherapeutics. *Appl. Microbiol. Biotechnol., 58*, 695–703.

[365] Fujiwara, N., Oka, S., Ide, M., Kashima, K. and Honda, T. (1999). Production and Partial Characterization of Antibody to Cord Factor (Trehalose-6,6P-Dimycolate) in Mice. *Microbiol. Immunol., 43*, 785–793.

[366] Sekanka, G., Baird, M. S., Minnikin, D. E. and Grooten, J. (2007). Mycolic acids for the control of tuberculosis. *Expert Opin. Ther. Pat., 17*, 315–331.

[367] Shui, G., Bendt, A. K., Pethe, K., Dick, Thomas, W. and Markus, R. (2007). Sensitive profiling of chemically diverse bioactive lipids. *J. Lipid Res., 48*, 1976–1984.

[368] Pan, J., Fujiwara, N., Oka, S., Maekura, R., Ogura, T. and Yano, I. (1999). Anti-cord factor (trehalose 6,6'dimycolate) IgG antibody in tuberculosis patients recognizes mycolic acid subclasses. *Microbiol. Immunol., 43*, 863–869.

[369] Won-Jung, K., Kwon, O. J. and, & Lee, K. S. (2005). Diagnosis and treatment of nontuberculous mycobacterial pulmonary diseases: A Korean perspective. *J. Korean Med. Sci., 20*, 913–925.

[370] Schleicher, G. K., Feldman, C., Vermaak, Y. and Verschoor, J. A. (2002). Prevalence of anti-mycolic acid antibodies in patients with pulmonary tuberculosis co-infected with HIV. *Clin. Chem. and lab. Med., 40*, 882–887.

[371] Benadie, Y., Deysel, M., Siko, D. G., Roberts, V. V., Van Wyngaardt, S., Thanyani, S. T., Sekanka, G., Ten Bokum, A. M., Collett, L. A., Grooten, J., Baird, M. S. and Verschoor, J. A. (2008). Cholesteroid nature of free mycolic acids from *M. tuberculosis*. *Chem. Phys. Lipids, 152*, 95–103.

[372] Prendergast, M. M., Lastovica, A. J. and Moran, A. P. (1998). Lipopolysaccharides from Campylobacter jejuni O: 41 Strains Associated with Guillain-Barre´ Syndrome Exhibit Mimicry of GM 1 Ganglioside. *Infect. Immun. 66*, 3649–3655.

[373] Verschoor, J. a., Baird, M. S. and Grooten, J. (2012). Towards understanding the functional diversity of cell wall mycolic acids of *Mycobacterium tuberculosis*. *Prog. Lipid Res. , 51*, 325–339.

[374] Geva, M., Izhaky, D., Mickus, D. E., Rychnovsky, S. D. and Addadi, L. (2001). Baird Stereoselective Recognition of Monolayers of Cholesterol, ent-Cholesterol, and Epicholesterol by an Antibody. *Chembiochem., 2*, 265–271.

[375] Bíró, A., Cervenak, L., Balogh, A., Lorincz, A., Uray, K., Horváth, A., Romics, L., Matkó, J., Füst, G. and László, G. (2007). Novel anti-cholesterol monoclonal immunoglobulin G antibodies as probes and potential modulators of membrane raft-dependent immune functions. *J. Lipid Res., 48*, 19–29.

[376] Ojha, A. K., Baughn, A. D., Sambandan, D., Hsu, T., Trivelli, X., Guerardel, Y., Alahari, A., Kremer, L., Jacobs, W. R. and Hatfull, G. F. (2008). Growth of *Mycobacterium tuberculosis* biofilms containing free mycolic acids and harbouring drug-tolerant bacteria. *Mol. Microbiol., 69*, 164–174.

[377] Fujiwara, N., Pan, J., Enomoto, K., Terano, Y., Honda, T., & Yano, I. (1999). Production and partial characterization of anti-cord factor (trehalose-6,6'-dimycolate) IgG antibody in rabbits recognizing mycolic acid subclasses of *Mycobacterium tuberculosis* or *Mycobacterium avium*. *Immunol. Med. Microbiol., 24*, 141–149.

[378] Saleh, A. D. (2013). *Development of a Method for Detecting TB-antibodies in Patient Serum*. Ph.D, Bangor University.

[379] Al dulayymi, J. R., Baird, M. S., Robert, E., Deysel, M. and Verschoor, J. (2007). The first syntheses of single enantiomers of the major methoxy mycolic acid of *Mycobacterium tuberculosis*. *Tetrahedron*, *63*, 2571-2592.

[380] (a) Glenn, C. A., Thomas, C. C. and Bradley, E. B. (1981). Stereoselective, catalytic reduction of L-ascorbic acid: a convenient synthesis of L-gulono-1,4-lactone. *The J. Org. Chem., 46*, 2976–2977; (b) Hubschwerlen, C., Jean-Luc, S. and Higelin, J. (1995). *Org. Syntheses, 72*,1.

[381] Hubschwerlen, C. (1986). A Convenient Synthesis of L-(S)-Glyceraldehyde Acetonide from L-Ascorbic Acid. *Synthesis*, *1986*, 962-964.

[382] Koza, G. (2007). *Synthesis of Single Enantiomers of Ketomycolic Acids.* Bangor University.

[383] Al-Kremawi, Z. D. (2011). *Synthesis of Epoxy-Mycolic Acids*. Bangor University.

[384] Schultz, H. S.; Freyermuth, H. B.; Buc, S. R. *J.* (1963). New Catalysts for the Oxidation of Sulfides to Sulfones with Hydrogen Peroxide. *Org. Chem*., *28*, 1140–1142.

[385] Julia, M. and Paris, J.-M. (1973). Syntheses a L'aide de sulphones - methode de syntheses generale de doubles liaisons. *Tetrahedron Lett., 49*, 4833-4836.

[386] Philip, J., Kocienski, B. L. and Steven, R. (1978). Scope and Stereochemistry of an ... from β-Hydroxy-Sulfones. *J. Chem. Soc., Perkin Trans. 1*, 829–834.

[387] Selected recent examples: (a) Yu, S.; Pu, X., Cheng, T., Wang, R. and Ma, D. (2006). Total synthesis of clavepictines A and B and pictamine. *Org. Lett., 8*, 3179-3182; (b) Guba, S. K. and Koo, S. (2005). Sulfone Coupling and Double-Elimination Strategy for Carotenoid Synthesis. *J. Org. Chem.*, *70*, 9662-9665 (c) Fuwa, H., Okamura Y. and Natsugari, H. (2004). Synthetic studies on antascomicin A: Construction of the C18-C34 fragment. *Tetrahedron*, *60*, 5341-5352; (d) Zanoni, G.; Porta, Al. and Vidari, G. (2002). First total synthesis of A (2) isoprostane. *J. Org. Chem.*, 67, 4346-4351; (e) Marino, J. P.; McClure, M. S., Holub, D. P., Comasseto, J. V. and Tucci, F. C. (2002). Stereocontrolled Synthesis of (−)-Macrolactin A. *J. Am. Chem. Soc.*, *124*, 1664–1668.

[388] Baudin, J. B., Hareau, G., Julia, S. A. and Ruel, O. (1991). A direct synthesis of olefins by reaction of carbonyl compounds with lithio derivatives of 2-[alkyl- or (2′-alkenyl)- or benzyl-sulfonyl]-benzothiazoles. *Tetrahedron Lett.*, *32*, 1175–1178.

[389] Truce, W. E., Kreider, E. M. and Brand, W. W. (1970). The Smiles and Related Rearrangements of Aromatic Systems. *Org. Reactions*, *18*, 99.

[390] Blakemore, P. R. (2002). The modified Julia olefination: alkene synthesis via the condensation of metallated heteroarylalkylsulfones with carbonyl compounds. *J. Chem. Soc., Perkin Trans. 1*, 2563-2585.

[391] Blakemore, P. R., Cole, W. J., Kocieński, P. J. and Morley, A. (1998). A Stereoselective Synthesis of trans-1,2-Disubstituted Alkenes Based on the Condensation of Aldehydes with Metallated 1-Phenyl-1H-tetrazol-5-yl Sulfones. *Synlett*, *1998*, 26-28.

[392] Baudin, L. B., Hareau, G., Julia, S. A. and Ruel O. (1993). A short and efficient Julia–Kocienski olefination protocol. *Bull. Soc. Chim. Fr.*, *130*, 336-357.

[393] (a) Mori, K. and Maemoto, S. (1987). Synthetic microbial chemistry, XV. Synthesis of (2E,4R,5S,11R)-(−)-Cladospolide A, a Phytotoxic Macrolide from Cladosporium cladosporioides. *Liebigs Annalen der Chemie*, *10*, 863; (b) Greene, T. W. and Wuts, P. G. (1991). *Protective Group in Organic Synthesis* (2nd Edi. p 126). Wiley, New York.

[394] Kang, S.-K., Kim, W.-S. and Moon, B.-H. (1985). An Effective Method for the Preparation of ω-Bromoalkanols from α,ω-Diols. *Synthesis*, *1985*, 1161-1162.

[395] Lermer, L., Neeland, E. G., Ounsworth, J. P. , Sims, R. J., Tischler, S. A. and Weiler L. (1992). The synthesis of β-keto lactones via cyclization of β-keto ester dianions or the cyclization of Meldrum's acid derivatives. *Can. J. Chem.*, *70*, 1427-1445.

[396] Baldwin, J. E., Adlington, R. M. and Ramcharitar, S. H. (1992). Free radical macrocyclisation via propiolate esters. *Tetrahedron*, *48*, 3413-3428.

[397] Rowles, R. (2010). *The synthesis of mycolic acids*. PhD Thesis Bangor University.

[398] Leonard, J., Mohialdin, S. and Swain, P. (1989). Efficient Procedures for in situ Trapping of (R)- and (S)-Glyceraldehyde acetonides by Stabilized Wittig Reagents. *Synth. Commun.*, *19*, 3529-3534.

[399] Takano, S., Kurotaki, A., Takahashi, M. and Ogasawara, K. (1986). Practical Synthesis of Some Versatile Chiral Building Blocks from (D)-Mannitol. *Synthesis*, *1986*, 403-406.

[400] Leonard, J., Mohialdin, S., Reed, D., Ryan, G. and Swain, P. A. (1995). Stereoselective conjugate addition of organolithium and organocopper reagents to gamma-oxygenated alpha,beta-unsaturated carbonyl systems dervied from glyceraldehyde acetonide. *Tetrahedron*, *51*, 12843-12858.

[401] Frick, J. A., Klassen, J. B., Bathe, A., Abramson, J. M. and Rappoport, H. (1992). An Efficient Synthesis of Enantiomerically Pure (*R*)-(2-Benzyloxyethyl) oxirane from (*S*)-Aspartic Acid. *Synthesis*, *1992*, 621-623.

[402] Majewski, M., Clive, D. L. and Anderson, P. C. (1984). Synthetic studies related to compactin and mevinolin: A new synthesis of the lactone system. *Tetrahedron Lett.*, *25*, 2101-2104.

[403] Su, Q., Dakin, L. A. and Panek, J. S. (2007). [4 + 2]-Annulations of Chiral Organosilanes: Application to the Total Synthesis of Leucascandrolide A. *J. Org. Chem.*, *72*, 2-24.

[404] Travis, B. R., Narayan, R. S. and Borhan, B. (2002). *J. Amer. Chem. Soc.*, *124*, 3824-3825.

[405] Fräter, G., Müller, U. and Günther, W. (1984). The stereoselective α-alkylation of chiral β-hydroxy esters and some applications thereof. *Tetrahedron*, *40*, 1269-1277.

[406] Fräter, G. (1981). On the stereoselectivity of the α-alkylation of β-hydroxy esters. Enantioselective synthesis of 4,4- and 6,6-disubstituted cyclohex-2-en-1-ones. *Tetrahedron Lett.*, *22*, 425-428.

[407] Yu, W.; Mei, Y.; Kang, Y.; Hua, Z.; Jin, Z. (2004). Improved procedure for the oxidative cleavage of olefins vy OsO4 - NaIO4. *Org. Lett.*, 6, 3217-3219.

[408] Koza, G., Rowles, R., Theunissen, C., Al dulayymi, J. R. and Baird, M. S. (2009). The synthesis of single enantiomers of *trans*-alkene-containing mycolic acids. *Tetrahedron Lett.*, *50*, 7259-7262.

[409] Al-Kremawi, Z. D., Al dulayymi, J. R. and Baird, M. S. (2010). *Tetrahedron Lett.*, *2*, 1698-1701.

[410] Sarabia, F., Miguel G.-C. and Chammaa, S. (2005). Synthesis of [13]-membered macrocyclic stevastelins via a transesterification reaction as the key step: total synthesis of stevastelin C3. *Tetrahedron Lett.*, *46*, 7695-7699.

[411] Al-Kremawi, Z. D., Al dulayymi, J. R. and Baird, M. S. (2014). Synthetic epoxy-mycolic acids. *Tetrahedron*, *70*, 7322-7335.

[412] Katz, Y., Lebas, F. X., Medley, H. V., Robson, R. (1998). Fluticasone propionate 50 micrograms BID versus 100 micrograms BID in the treatment of children with persistent asthma. Fluticasone Propionate Study Group. *Clin. Ther.*, *20*, 424-437.

[413] Stewart, T. G., Gibson, G. A. (1896). Asthma. *Twentieth century practice: an international encyclopedia of modern medical science by leading authorities of Europe and America; Stedman, T.L.; New York: William Wood and Co.*, 6, 585-617.

[414] Quémard A., Laneelle, M.-A., Marrakchi, H., Prome D., Dubnau E. and Daffe M. (1997). Structure of a Hydroxymycolic Acid Potentially Involved in the Synthesis of Oxygenated Mycolic Acids of the *Mycobacterium Tuberculosis* Complex. *Eur. J. Biochem.*, *250*, 758-763.

[415] Mohammed, M. O. (2014). *Synthesis of Glycolipid Fragments from Mycobacterium Tuberculosis.* Bangor University.

[416] Al Dulayymi, J. R., Baird, M.S. and Roberts, E. (2005). The synthesis of a single enantiomer of a major a-mycolic acid of M.tuberculosis. *Tetrahedron*, *61*, 11939-11951.

[417] Fujita, Y., Doi, T., Maekura, R., Ito, M. and Yano, I. (2006). Differences in serological responses to specific glycopeptidolipid-core and common lipid antigens in patients with pulmonary disease due to *Mycobacterium tuberculosis* and *Mycobacterium avium* complex. *J. Med. Microbiol.*, *55*, 189-199.

[418] Yuan, Y. and Barry III, C. E. (1996). A common mechanism for the biosynthesis of methoxy and cyclopropyl mycolic acids in *Mycobacterium tuberculosis*. *Proc. Natl. Acad. Sci. USA*, *93*, 12828-12833.

[419] Feng, X., Yang, X., Xiu, B., Qie, S., Dai, Z., Chen, K., Zhao, P., Zhang, L., Nicholson, R., Wang, G., Song, X. and Zhang, H. (2014). IgG, IgM and IgA antibodies against the novel polyprotein in active tuberculosis. *BMC Infect Dis.*, *14*, 336.

[420] Coleman, R. M., Lombard M. F. and Sicard R. E. (1992). *Fundamental Immunology* (2nd. Edi., pp. 58).United States of America.

[421] Torres, M. and Casadevall, A. (2008). The immunoglobulin constant region contributes to affinity and specificity. *Trends Immunol.*, *29*, 91-97.

[422] Gatfield, J. and Pieters, J. (2000). Essential role for cholesterol in entry of *mycobacteria* into macrophages. *Science*, *288*, 1647–1650.

[423] De Chastellier, C. and Thilo, L. (2006). Cholesterol depletion in *Mycobacterium avium*-infected macrophages overcomes the block in phagosome maturation and leads to the reversible sequestration of viable mycobacteria in phagolysosome-derived autophagic vacuoles. *Cell. Microbiol*., *8*, 242–256.

[424] Stephen, D. N., William, D. C., Fred, M. G., Paul, M. S., David, L. C., Richard, E. C., Lawrence, J. E., Paula, D. S., Bernard, B., David, L. K., John, J. S., Daniel, D. P., Winkler, G. W., Anthony, L. and Frederick, P. S. (1993). Two Controlled Trials of Rifabutin Prophylaxis against *Mycobacterium avium* Complex Infection in AIDS. *N. Engl. J. Med.*, *329*, 828-833.

[425] Wendland, T., Herren, S., Yawalkar, N., Cerny, A. and Pichler, W. J. (2000). Strong αβ and γδ TCR response in a patient with disseminated *Mycobacterium avium* infection and lack of NK cells and monocytopenia. *Immunol Lett.*, 72, 75–82.

[426] Hesseling, A. C., Johnson, L. F., Jaspan, H., Cotton, M. F., Whitelaw, A., Schaaf, H. S., Fine, P. E., Eley, B. S., Marais, B. J., Nuttall, J., Beyers, N. and Godfrey-Faussett, P. (2009). Disseminated bacille Calmette-Guerin disease in HIV-infected South African infants. *Bull WHO*, *87*, 505–511.

[427] Matsunaga, I. and Moody, D. B. (2009). Mincle is a long sought receptor for mycobacterial cord factor. *J. Exp. Med.*, *206*, 0-3.

[428] Orme, I. M. and Collins, F. M. (1984). Efficacy of *Mycobacterium bovis* BCG vaccination in mice undergoing prior pulmonary infection with atypical *mycobacteria*. *Infect. Immun. 44*, 28-32.

[429] Collins, F. M. (1971). Immunogenicity of various mycobacteria and the corresponding levels of cross-protection developed between species. *Infect. Immun*., *4*, 688-696.

[430] Roth, A., Fischer, M., Hamid, M. E., Michalke, S., Ludwig, W. and Mauch, H. (1998). Differentiation of phylogenetically related slowly growing *mycobacteria* based on 16S-23S rRNA gene internal transcribed spacer sequences. *J. Clin. Microbiol. ,* 36, 139–147.

[431] Evans, S. A., Colville, A., Evans, A. J., Crisp, A. J. and Johnston, I. D. (1996). Pulmonary *Mycobacterium kansasii* infection: comparison of the clinical features, treatment and outcome with pulmonary tuberculosis. *Thorax*, *51*, 1243–1247.

[432] Cayabyab, M. J., Hovav, A.-h., Hsu, T., Krivulka, G. R., Lifton, M. A., Gorgone, D. A., Fennelly, G. J., Haynes, B. F., Jacobs, W. R. and Letvin, N. L. (2006). Generation of CD8 ∂ T-Cell Responses by a Recombinant Nonpathogenic *Mycobacterium smegmatis* Vaccine Vector Expressing Human Immunodeficiency Virus Type 1 Env. *J. Virol.* , 80, 41645–1652.

[433] Tima, G., Romano, M. and Huygen, K., Institute for Infection Diseases, Brussels.

[434] Yokoyama, H., Otaya, K., Kobayashi, H., Miyazawa, M., Yamaguchi, S. and Hirai Y. (2000). Palladium (II)-Catalyzed Cyclization of Urethanes and Total Synthesis of 1-Deoxymannojirimycin. *Org. Lett.*, *2*, 2427-2429.

[435] Nilsson, K. and Ullenius, C. (1994). Stereoselectivity in the 1,4-addition reaction of organocopper reagents to ethyl 3-[(*S*)-2,2-dimethyl-1,3-dioxolan-4-yl]propenoate. *Tetrahedron*, *50*, 13173-13180.

[436] Jung, M. E. and Shaw T. J. (1980). Total synthesis of (R)-glycerol acetonide and the antiepileptic and hypotensive drug (-)-.gamma.-amino-.beta.-hydroxybutyric acid (GABOB): use of vitamin C as a chiral starting material. *J. Am. Chem. Soc.*, *102*, 6304–6311.

[437] Koza, G., Muzael, M., Schubert-Rowles, R. R., Theunissen, C., Al Dulayymi, J. R. and Baird, M. S. (2013). The synthesis of methoxy and keto mycolic acids containing methyl-trans-cyclopropanes. *Tetrahedron*, *69*, 6285-6296.